MONITORING AND INTELLIGENT CONTROL FOR COMPLEX CURVATURE FRICTION STIR WELDING

Tao Hua

COPYRIGHT STATEMENT

MONITORING AND INTELLIGENT CONTROL FOR COMPLEX CURVATURE FRICTION STIR WELDING

by

Tao Hua

A dissertation submitted in compliance with the full requirements for the

Doctor Technologiae: Engineering

In the

Faculty of Engineering,
The Built Environment and Information Technology

Nelson Mandela Metropolitan University

January 2006

Promoters

Prof T.I. van Niekerk (PrEng)

Prof D.G. Hattingh (PrTech)

Author's Declaration

Tao Hua hereby declares that:

- At no time during the registration for the degree of Doctor Technologiae has the author been registered for any other university degree;
- The work done in the dissertation is his own; and
- All sources used or referred to have been documented and recognized.

Acknowledgements

I want to acknowledge the contribution by the following people and institution:

- My promoters, Profs Theo van Niekerk and Daniel Hattingh, for their support, guidance and encouragement;
- All the team members, the other research students in the Manufacturing Technology Research Centre, and staff in the workshop for their assistance;
- The Faculty of Engineering, the Built Environment and Information Technology for giving me the opportunity of pursuing my studies at the Nelson Mandela Metropolitan University;
- South African National Research Foundation for providing funding towards this research; and
- My girlfriend, Yanchen, Liu, and my parents for their love and support throughout the duration of my research.

Abstract

A multi-input multi-output system to implement on-line process monitoring and intelligent control of complex curvature friction stir welding was proposed. An extra rotation axis was added to the existing three translation axes to perform friction stir welding of complex curvature other than straight welding line. A clamping system was designed for locating and holding the workpieces to bear the large force involved in the process between the welding tool and workpieces. Process parameters (feed rate, spindle speed, tilt angle and plunge depth), and process conditions (parent material and curvature), were used as factors for the orthogonal array experiments to collect sensor data of force, torque and tool temperature using multiple sensors and telemetry system.

Using statistic analysis of the experimental data, sensitive signal features were selected to train the feed-forward neural networks, which were used for mapping the relationships between process parameters, process conditions and sensor data. A fuzzy controller with initial input/output membership functions and fuzzy rules generated on-line from the trained neural network was applied to perceive process condition changes and make adjustment of process parameters to maintain tool/workpiece contact and energy input. Input/output scaling factors of the fuzzy controller were tuned on-line to improve output response to the amount and trend of control variable deviation from the reference value. Simulation results showed that the presented neuro-fuzzy control scheme has adaptability to process conditions such as parent material and curvature changes, and that the control variables were well regulated. The presented neuro-fuzzy control scheme can be also expected to be applied in other multi-input multi-output machining processes.

Table of Contents

Abbreviations

ACC	Adaptive Control Constraints
ACO	Adaptive Control Optimization
AE	Acoustic Emission
AI	Artificial Intelligence
ANN	Artificial Neural Network
ANOVA	Analysis of Variance
CC	Cutter Contact Points
CL	Cutter Location Points
EC	Evolutionary Computation
ES	Expert Systems
FL	Fuzzy Logic
FLC	Fuzzy Logic Controller
FI	Fuzzy Inference
FSW	Friction Stir Welding
GA	Genetic Algorithms
GUI	Graphic User Interface
GUIDE	Graphical User Interface Development Environment
MIMO	Multi-input and Multi-output
MSE	Mean Sum of Squares
NMMU	Nelson Mandela Metropolitan University

List of Figures

List of Tables

Glossary

A

Adaptive Control: When the parameters of a system are slowly time-varying or uncertain, adaptive control is used to sense such conditions and adjust control signals to give reliable performance. It does not need *prior* information about the bounds on the uncertain or time-varying parameters.

Artificial Intelligence: Artificial intelligence is defined as intelligence exhibited by an artificial entity. Artificial intelligence forms a vital branch of computer science, dealing with intelligent behavior (control, planning and scheduling), learning and adaptation in machines.

B

Back-propagation Learning: A learning rule in which weights and biases are adjusted by error-derivative vectors back-propagated through the network. Back-propagation is commonly applied to feed-forward multi-layer networks.

C

Centre of Area: The point in an area where the entire area could be concentrated and produce the same density resultant as for the area itself.

Clamping System: The device used to hold, locate and prevent the workpiece from moving during the large force involved in the FSW process.

Correlation Coefficient: A numeric measure of the strength of linear relationship between two random variables. In general statistical usage, correlation refers to the departure of two variables from independence.

D

Defuzzification: The process of transforming a fuzzy output of a fuzzy inference system into a crisp output.

Degree of Membership: The output of a membership function, this value is always limited to between 0 and 1.

E

Encoder: A transducer used to convert linear or rotary position to digital data.

Expert System: System in which human expertise is held in the form of rules, which enable the system to diagnose situations without the human expert being present.

F

Feed-forward Network: A layered network in which each layer only receives inputs from previous layers.

Feedback: The signal or data sent to the control system from a controlled machine or process to denote its response to the command signal.

Friction Stir Welding: A process utilises frictional heating and a stirring motion to break down the interface between two workpieces yielding a solid, fully consolidated weldment. A rotating tool with a protruding pin is forced into the joint until a larger concentric shoulder rests on the surface. The spinning tool is advanced along the joint

line providing frictional heating which softens the material. The spinning pin and shoulder help mix and reconsolidate the material, respectively.

Fuzzification: The process of generating membership values for a fuzzy variable using membership functions.

Fuzzy Logic: Fuzzy logic is an extension of Boolean logic dealing with the concept of partial truth. Whereas classical logic holds that everything (statements) can be expressed in binary terms (0 or 1, black or white, yes or no), fuzzy logic replaces Boolean truth values with degrees of truth.

Fuzzy Rule Base: A group of fuzzy 'if-then' rules using linguistic variables for representing the knowledge of a system.

Fuzzy Set: Fuzzy sets are an extension of classical set theory. In classical set theory the membership of elements in relation to a set is assessed in binary terms according to a crisp condition (either belongs or does not belong to the set). Fuzzy set permits the gradual assessment of the membership of elements in relation to a set; this is described with the aid of membership function.

G

Generalization: An attribute of a network whose output for a new input vector tends to be close to outputs for similar input vectors in its training set.

Genetic Algorithms: A search technique used to find approximate solutions to optimization and search problems. Genetic algorithms are a particular class of evolutionary algorithms that use techniques inspired by evolutionary biology such as inheritance, mutation, natural selection and recombination.

Graphical User Interface: A type of user interface where the user controls the operation of a piece of software by interacting with graphical elements on the display.

H

Hierarchical system: A system of ranking and organizing things, where each element of the system (except for the top element) is subordinate to a single other element.

I

Implication: The process of shaping the fuzzy set in the consequent based on the results of the antecedent in a Mamdani-type fuzzy inference system.

Intelligent Control: All control techniques that use various soft computing approaches such as neural networks, Bayesian probability, fuzzy logic, machine learning, evolutionary computation and genetic algorithms can be put into the class of intelligent control.

Intelligent System: A system designed with the capabilities for evolution, adaptation, and learning to recognize the environment, make decisions and take action.

Interface: A shared boundary which might be a mechanical or electrical connection between two devices; it might be a portion of computer storage accessed by two or more programs; or it might be a device for communication with a human operator.

Inverter: A term commonly used for an AC adjustable frequency drives. An inverter is also a term used to describe a particular section of an AC drive.

K

Knowledge: Knowledge is information combined with experience, context, interpretation, and reflection. It is a high-value form of information that is ready to apply to decisions and actions.

L

Learning: Learning is a process of autonomous acquisition and integration of knowledge from experience, analytical observation, and other means, that results in a system that can continuously self-improve and thereby offer increased efficiency and effectiveness.

Linear Interpolation: A computer function automatically performed in the control that defines the continuum of points in a straight line based on only two taught coordinate positions. All calculated points are automatically inserted between the taught coordinate positions upon playback.

M

Machine Intelligence: The study of how to make machines learn and reason to make decisions, as humans do.

Mamdani-type inference: A type of fuzzy inference in which the fuzzy sets from the consequent of each rule are combined through the aggregation operator and the resulting fuzzy set is defuzzified to yield the output of the system.

Membership Function: A function that specifies the degree to which a given input belongs to a set or is related to a concept.

Multi-axis Machining: Two or more axes on a single machine work independently or move simultaneously to allow machining of multiple sides in one setup. Multi-axis machining is used more often for complex contour work.

N

Neural Network: An artificial neural network is an interconnected group of artificial neurons that uses a mathematical or computational model for information processing based on a connectionist approach to computation.

Neuro-fuzzy: Neuro-fuzzy refers to hybrids of artificial neural network and fuzzy logic. It is used to describe configurations such as realization of a fuzzy system through connectionist networks, fuzzy logic based tuning of neural network training parameters, fuzzy logic criteria for increasing a network size, representing fuzzy inference through multi-layered feed-forward connectionist networks, realizing fuzzy membership through clustering algorithms in neural networks and deriving fuzzy rules from trained RBF networks.

Non-linear System: A system whose behavior is not expressible as a sum of the behaviors of its descriptors.

O

Orientation: The consistent movement or manipulation of an object into a controlled position and attitude in space.

Orthogonal Array: The efficient experimental method developed by Taguchi minimizes the number of tests, represents all factors equally and investigates some combinations of

factors and factor levels. Influence of each experimental factor on experimental results is investigated in an orthogonal array experiment.

P

Path: A series of positions in space that a object moves through.

Path Interpolation: The process of converting tool paths obtained from a tool path planning system into time-dependent commands for driving the servo control system of a multi-axis machine.

R

Real-time: An operation within a larger dynamic system is called a real-time operation if the combined reaction and operation time of a task is shorter than the maximum delay that is allowed, in view of circumstances outside the operation. The task must also occur before the system to be controlled becomes unstable.

Reasoning: A process of applying general rules, equations and relationships to an initial collection of data, facts, and so on, to deduce a result or decision.

Recognition: The act of taking in raw data and classifying data based on either a *priori* knowledge or on statistical information extracted from the patterns.

Regularization: It involves modifying the performance function, which is normally chosen to be the sum of squares of the network errors on the training set, by adding some fraction of the squares of the network weights.

Robotics: The science of designing, building, and applying robots.

S

Sensing: The feedback from the environment of the robot which enables the robot to react to its environment. Sensory inputs may come from a variety of sensor types including proximity switches, force sensors, tactile sensors, and machine vision systems.

Sensitive Feature: Features extracted from sensor signals which are sensitive to variables selected as control targets.

Sensor: A device such as a transducer that detects a physical phenomenon and relays information to a control device.

Sensor Fusion: Sensor fusion is a method of integrating signals from multiple sources. It allows extracting information from several different sources to integrate them into a single signal or information.

Servo-Control: An actuator which is equipped with a control system, in which the control computer issues motion commands to the actuators, internal measurement devices measure the motion and signal the results back to the computer. The process continues until the actuator reaches the desired position.

Signal Processing: Signal processing is the processing, amplification and interpretation of signals and deals with the analysis and manipulation of signals.

T

Table-tilting: In a multi-axis machine, the workpiece is mounted on the table that is rotated about the rotational axis during machining.

Tool Path Planning: In multi-axis machining, both the tool position and tool orientation need to be determined in tool path generation. Hence the task of tool path planning is twofold, namely tool position path planning and tool orientation path planning.

Translation: A movement such that all axes remain parallel to where they were (i.e. without rotation).

V

Variance: In probability theory and statistics, the variance of a random variable is a measure of its statistical dispersion, indicating how far from the expected value its values typically are. The variance of a real-valued random variable is its second central moment. The variance of a random variable is the square of its standard deviation.

Void Formation: In FSW areas where improper consolidation of the plasticized material occurred, cavities can be left along the surface of the weld.

Chapter 1 Introduction

Friction Stir Welding (FSW) has recently emerged as a solid-joining technology for welding of high strength aluminium alloys (Thomas, *et al*., 1991). Currently, industrial application of FSW is mostly limited to straight seam welding. When welding workpieces with complex curvature (circle, triangle, square, etc.), a robotic or multi-axis system for complex shaped weld is needed. One of the difficulties for robotic FSW is the large force involved in the welding process and thus the large spindle drive motor size (Hirano, *et al*., 2001).

FSW involves large forces between the welding head and workpiece. For complex shape FSW, the maintenance of correct contact between the tool and workpiece and energy into the welding is a requirement to perform a quality weld. A multi-axis welding system must provide large mechanical stiffness and precision positioning needs to be developed and applied to complex shape joints welding.

When welding workpieces with complex curvature, the process conditions may change dynamically, thus it is necessary to maintain process performance during the welding. The on-line process status must be transferred to the control system, and the control system must make decisions and act to adapt to the changing environment in real-time.

The welding quality of FSW is determined by material properties, tool design and the synthesized effect of the process parameters. The proper description of welding quality, the selection of control variables characterizing process conditions, and the relation between control variables and process parameters must be established.

1.1 Aim

To perform FSW joints of complex shapes with good weld quality and surface integrity, a multi-axis system with the ability of sensor-based monitoring and intelligent process control must be established.

1.2 Objectives

The following objectives were accordingly specified for this project:

- To design a multi-axis mechanical system providing large force and precise orientation and position control on the platform of a three-axis milling machine to perform complex curvature FSW.

- To develop interpolation algorithms to generate the speed, direction, and distance of each axis from programmed positions, error compensation, and preset process parameters. Encoders are needed to provide position feedback.

- To perform experiment design and obtain experimental data by varying welding parameters and to evaluate weld performance (weldability, tensile strength, bending strength, and fatigue) by relevant measurement.

- To identify signals characterizing tool/workpiece contact condition and welding quality from the multi-sensor data, and hence to select control variables for process monitoring.

- To develop an intelligent welding system that is able to control the process parameters for maintaining the control variables within acceptable limits.

- To propose and implement hardware architecture and software components to perform multi-axis control and multi-sensor data processing.

- To test the performance of the intelligent control system using welding process simulation and experiments.

1.3 Hypodissertation

An extra rotary axis can be added to the three-axis milling machine tool to implement FSW for complex curvature such as a circle, triangle, or square. Based on the present control system for plate FSW, the intelligent monitoring and control for complex curvature may be achieved through the integration of multi-sensor data processing and multi-axis machine control with available sensor technology and motion control. Computational intelligent methods such as fuzzy logic (FL) and neural networks (NN) can be applied to realize the intelligence (Fukuda and Kubota, 1997).

1.4 Methodological Justification

In order to accomplish the research, a study will be done on the methods used for monitoring and intelligent control for complex curvature FSW:

- **Table-tilting Multi-axis Machining**

In a typical table-tilting type multi-axis machine, there are several translational axes and one rotational axis, and the part is mounted on the table that rotates about the rotational axis during machining. In complex curvature FSW, the workpiece is mounted on the rotating worktable. At each welding segment through two consecutive CC (cutter contact)

points, motions of welding tool and worktable vary linearly from the start to the end positions. The workpiece is rotated linearly from the start to the end orientations. Hence, the complex curvature FSW can be achieved through the simultaneous motion control of the translational axes and the rotational axis (Hwang, 2000).

- **Fuzzy Logic Control**

Fuzzy logic (FL) is a powerful tool for control of mathematically complex, uncertain systems. Performance of a FL controller is a function of the quality of its embedded expert knowledge rather than a highly accurate mathematical model (Akbarzadeh-T, 2000). For complex shape FSW that is non-linear and involves multiple input and output parameters, FL reasoning can be applied to generate suggestion for modifying the weld parameters in order to maintain weld performance parameters within acceptable limits. The deployment of fuzzy rules can be set based on past experience and trial result of operations. This will realize intelligent machining and enable quality control.

- **Neural Network**

The main characteristic of neural network (NN) is to recognize patterns and to adapt themselves to dynamic environments by learning. NN can be applied to learn the relationship among input and output data sets through training process. When welding a workpiece with complex curvature, trained NN can be used to induce the modification of process parameters (feed rate, spindle speed, and plunge depth) if a new set of control variables (force, torque, temperature, etc.) is available. The induced information can be used to generate ‘if-then’ fuzzy rules for fuzzy inferencing process, which results in the generation of new process parameters for enhancing machine intelligence of a parameter-

based control situation. Thus, NN can be used to recognize process status and predict process parameter modification from a *prior* knowledge and sensory information.

1.5 Delimitations

This research will focus on monitoring and intelligent control of FSW for 2-dimensional complex curvature. An additional axis will be added to the present three-axis machine for plate FSW. The intelligent algorithms with which intelligent control can be carried out will be developed. The intelligent monitoring and control system will be limited to the process of FSW.

1.6 Significance of Research

Within the University

- Expanding the research of FSW in NMMU based on the former research of Friction Stir Welding for straight line, this project will initiate the research of FSW for complex curvature.

General

- Complex curvature FSW will greatly expand the industrial application of FSW.
- The intelligent monitoring and control system can realize on-line quality control and flexible automation of FSW.

1.7 Organization of Dissertation

Chapter 1 introduces the objective, hypodissertation, delimitations, and significance of this research project.

Chapter 2 presents the relevant theoretical concepts, corresponding components, related technologies, and the state-of-the-art in the field of FSW, FL, NN, monitoring, and intelligent machining. It also proposes a logical framework that shows and connects all system components for monitoring and intelligent control for complex curvature FSW.

Chapter 3 describes the overall system setup and experimental design, including mechanical device design, implementation of sensor and motor control equipment, hardware and software architecture to perform on-line monitoring and control for complex curvature FSW. Process simulation is also implemented to demonstrate the on-line intelligent control algorithms.

Chapter 4 provides a detailed description of experimental data analyzing, weld quality characterising, NN building and training for on-line process monitoring, and fuzzy rule generation.

Chapter 5 provides a detailed explanation of the structure of the neuro-fuzzy based intelligent control scheme for complex curvature FSW. Process simulations are also carried out to demonstrate the performance of the intelligent monitoring and control system, and discuss its adaptability to process condition (parent material and curvature) changes.

Chapter 6 is the conclusion, which includes a discussion on future research and development.

Appendix A provides the experimental data recorded during experiments of flat plate and round tube FSW.

Appendix B provides some MATLAB M functions, M scripts and figures referenced in the chapters of the dissertation.

Appendix C provides design drawings of mechanical equipment, which was used for experiment implementation.

Chapter 2 Relevant Concepts of Monitoring and Intelligent Control for Complex Curvature FSW

FSW is a technique developed by TWI in 1991 joining aluminium and aluminium alloys (Thomas, *et al*., 1991). In FSW, a cylindrical tool which consists of a profiled pin under a wider shoulder rotates about its own axis and the pin is slowly plunged into the joint of the sheets or plates. Material in the joint is plasticized by frictional heating between the tool and the workpiece. The welding head is moved along the weld joint when the material has been sufficiently plasticized. The plasticized material is transported around the rotating pin and is pressed together, forming a solid joint on cooling. To provide a stable welding process the presence of a backing plate and side clamping forces are essential. Figure 2.1 shows the principle and microstructure of FSW.

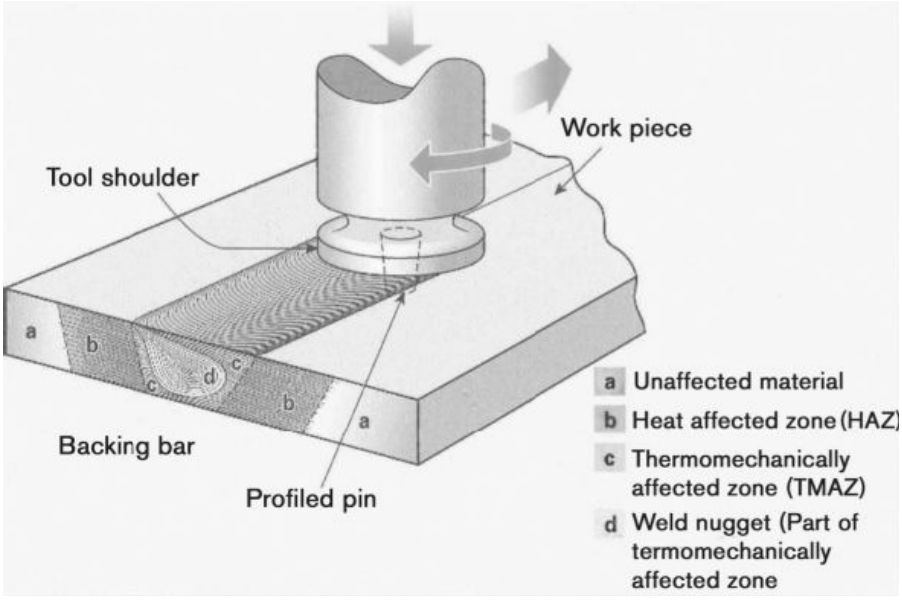

Figure 2.1: Friction stir welding principle and microstructure (Nicholas and Kallee, 2000)

In the microstructure of FSW plate, a well-developed nugget is visible at the centre of the weld, as schematically shown in Figure 2.1. Outside the nugget there is a thermomechanically affected zone, which has been severely plastically deformed and shows some areas of partial grain refinement (Threadgill, 1997).

The process advantages result from the fact that FSW process takes place in the solid phase below the melting point of the materials to be joined. The benefits therefore include low distortion, excellent mechanical properties, environmentally friendly, etc. The main limitations of FSW are the moderately slow welding speed, rigid clamping device and backing bar needed because of the large force involved and keyhole at the end of the welds.

2.1 Complex Curvature FSW

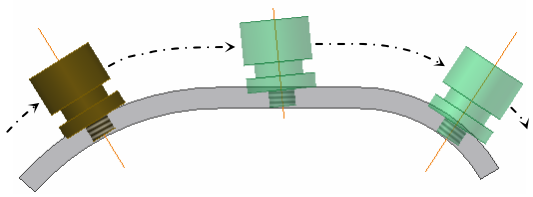

Figure 2.2: FSW of workpiece with complex curvature

Figure 2.2 shows a typical workpiece with complex curvature for FSW. Using existing and readily available machine tool technology, FSW is suitable for automation and adaptable for robot use. A robotic or multi-axis system can be applied to complex curvature FSW. A multi-axis system is preferred due to the large force involved in the process for which a large size spindle motor is needed (Hirano, *et al*., 2001; Arbegast and Skinner, 2002).

FSW involves multi-input and multi-output (MIMO). Inputs of FSW include process parameters (feed rate, spindle speed, plunge depth and tilt angle), and process conditions (tool geometry, parent material and thickness). Outputs generated from FSW process include downward force Fz, forward force Fx, side force Fy, spindle torque, temperature, tool power, etc.. During complex curvature FSW, the relative motion between tool and workpiece causes sufficient forces and torque for cutting, stirring and pressing the material to generate material flow and friction heat. Figure 2.3 shows the process parameters, process conditions, process outputs and the coordinate system of complex curvature FSW.

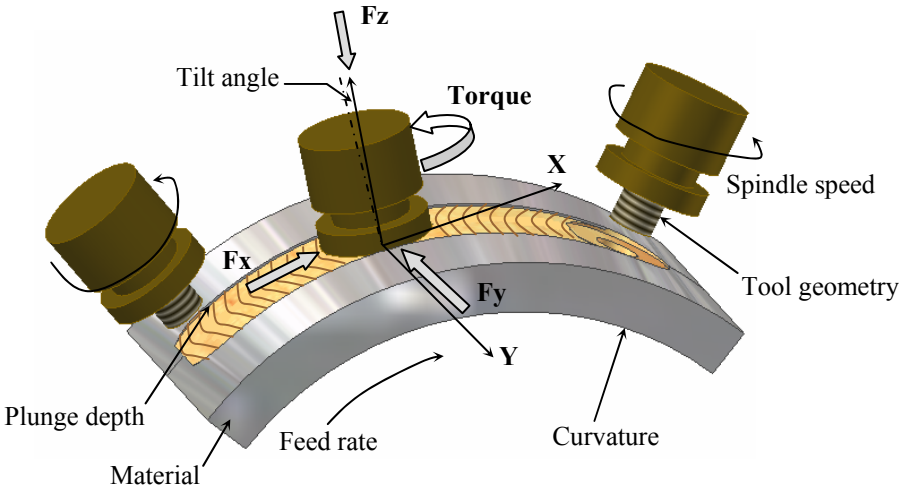

Figure 2.3: Process inputs and outputs of complex curvature FSW

During complex curvature FSW, many variables must be controlled in order to avoid welding defects such as void formation and excessive flashes, which are often combined with microstructural changes and even tool breakage, as shown in Figure 2.4. In order to properly control the process, the influences of process parameters, process conditions and process outputs on weld quality and their relationships need to be investigated.

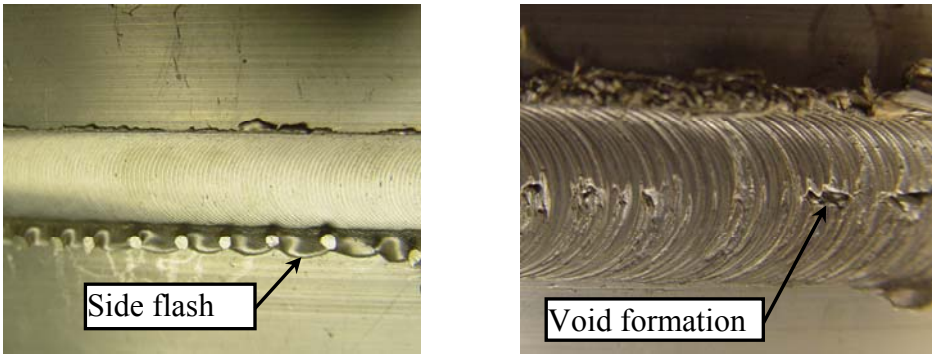

Figure 2.4: Typical welding defects of excessive side flash and void formation

2.1.1 Process Parameters

- **Feed Rate**

It has been reported that the mechanical and fatigue properties of FSW decrease as feed rate of welding increase in a specific range (Ericsson and Sandström, 2003; James, *et al*., 2003). It has been also observed that the maximum Fx and Fy in one tool revolution and vertical force Fz increase as feed rate increases.

- **Spindle Speed**

The rotation speed must be large enough to generate sufficient heat to soften the material to prevent void formation and tool fracture. For a thicker material, the rotation speed has to be increased to match the increased heat conduction away from the weld zone. It had been shown that there are few voids in the weld zone if the rotational speed and welding speed are optimised (Liu, *et al*., 1997). The rotation speed is considered as a most significant process parameter (North, *et al*., 2000).

- **Tilt Angle**

Tool tilt angle is used to improve the forging of the back edge of the tool shoulder. In this way, it may be possible to eliminate sub-surface voids. It has been shown that in aluminium welds, a tilt angle from 0° to 2° gives a dramatic change in the microstructure development and material flow. A larger tilt angle gives a tighter weld, and a more uniform material flow (Shinoda, *et al*., 2001).

- **Plunge Depth**

A plunge depth of tool shoulder into parent material is necessary to obtain tool/workpiece contact and thus generate sufficient friction heat and vertical force for plasticizing and pressing the material. With other process parameters and conditions constant, deeper plunge results in higher forces, torque and temperature. Excessive plunge depth can cause lower tensile- and bend strength due to excessive side flashes.

2.1.2 Process Condition

- **Parent material**

Different parent materials result in different welding performance due to their difference in chemical composition and mechanical properties. Figure 2.5 shows the torque, temperature, and Fz of 3mm Al 6061 and Al 5251 aluminium alloy welded with the same process parameters: feed rate 100 mm/min, spindle speed 500 rpm, tilt angle 1° and plunge depth 0.2 mm. It shows that when welded with the same process parameters and thickness, the sensor data of bending force, which characterizes co-effect of Fx and Fy, torque, temperature and Fz of Al 6061, are higher than those of Al 5251.

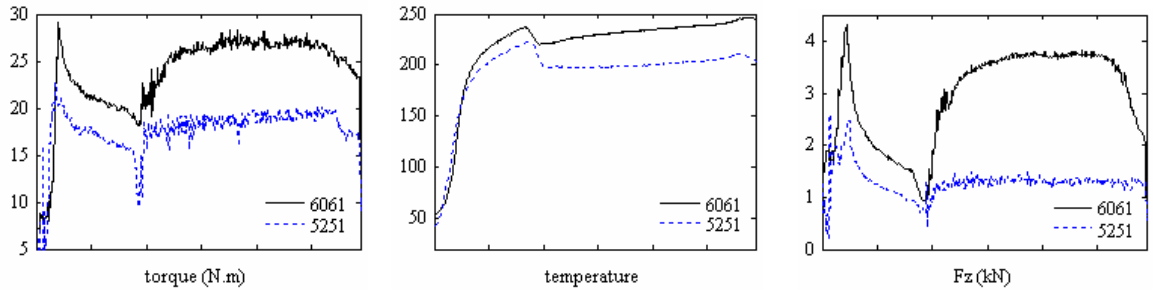

Figure 2.5: Sensor data of different materials welded with same process parameters

- **Tool Geometry**

The tool geometry influences the heat generation, plastic flow and the stirring action in the weld. It had been tested that with a spiral scroll on the underside of the shoulder, the material flow can be improved with reduced extruded surface flash. Threads are often machined on tool pin to force down the stirred material and assist material rotation. The purpose of the intense stirring action is to close voids and provide a large rubbing surface to generate heat rapidly (Midling, *et al*., 1994). Figure 2.6 shows TWI's new generation of Whorl^{TM} type FSW tools designed with specific shape to provide enhanced flow and adequate stirring action, and thereby reduce or eliminate the presence of voids.

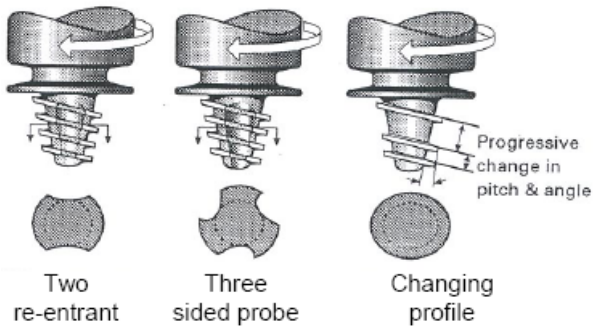

Figure 2.6: TWI's Whorl^{TM} type FSW tools for welding thick workpieces (Nicholas and Kallee, 2000)

2.1.3 Force, Torque and Temperature

- **Fz**

The downward force Fz significantly depends on the tool penetration depth (Satoshi, *et al*., 2001). It has been observed that insufficient downward force Fz generates insufficient heat at the tool/workpiec interface, while excessive Fz results in excessive shoulder penetration into the material, which causes excessive flash at the edges of the shoulder (Midling, *et al*., 1994). The influence of Fz on surface texture and fatigue performance of FSW was also reported in (Haagensen, *et al*., 1995).

- **Fy**

The side force Fy from the clamping system holds and prevents workpieces from being pushed apart by the force generated by the rotating tool. The force Fy increases with the thickness of the plates because the dimensions of the tool pin increases at the same time. It has been observed that insufficient Fy causes void formation below the surface on the advancing side of the weld (Andrews, 1999).

- **Heat input and Temperature**

The energy input during FSW is generally considered to be from the friction heat between the rotating tool and workpieces, and the "cold work" during plastic deformation of material in the vicinity of the tool (Chen and Kovacevic, 2003). A certain fraction of the heat is dissipated through the backing plate and through the tool.

According to Song and Kovacevic (2003), the heat generated at the tool shoulder/workpiece interface is assumed frictional work, and can be calculated as:

$$q_{shoulder} = \int_{r_P}^{r_S} 2\pi\mu F_z r\omega dr \tag{2.1}$$

Where r is the distance from the calculated point to the axis of the rotating tool, ω is the rotational speed of the tool, Fz is the downward force, r_p is pin radius, r_s is shoulder radius, and μ is local friction coefficient.

The heat generated by the tool pin, consisting of heat generated by shearing of the material and friction on threaded surface and vertical surface of the pin, can be express by the following equation (Colegrove, 2000):

$$q_{pin} = 2\pi r_p h k\tau \frac{V_m}{\sqrt{3}} + \frac{2\mu k\tau\pi r_p V_{rp}}{\sqrt{3(1+\mu^2)}} + \frac{4F_P \mu V_m \cos\theta}{\pi} \tag{2.2}$$

The calculations of θ, V_m, V_{rp}, and V_p are given:

$$\theta = 90^\circ - \lambda - \tan^{-1}(\mu) \tag{2.3}$$

$$V_m = \frac{\sin\lambda}{\sin(180^\circ - \theta - \lambda)} v_p \tag{2.4}$$

$$V_{rp} = \frac{\sin\theta}{\sin(180^\circ - \theta - \lambda)} v_p \tag{2.5}$$

$$V_p = r_p \omega \tag{2.6}$$

Where r_p is the radius of the tool pin, h is the thickness of the workpiece, τ is the average shear stress of the material, F_p is the translation force during the welding, and λ is the helix angle of the thread.

Deformation together with high temperature generates re-crystallization which results in a complex microstructure in the weld zone. The temperature decreases as a function of the distance from the centre of the weld. Based on Fourlier's equation, the temperature can be calculated from the generated heat between tool and parent material (Chen and Kovacevic, 2003):

$$\rho c \frac{dT}{dt} = div(k \cdot gradT) + q \qquad (\Omega) \tag{2.7}$$

Where q is the heat generated by friction between the tool and the top of the workpiece and by the plastic deformation work of the central weld zone, T is the temperature, k is the conductivity, ρ is the material density, and c is the heat capacity.

- **Tool Torque**

Tool torque is mainly dependent on tool rotation speed and tool/workpiece contact area, which is governed more by the size of the tool's shoulder. Its value is almost constant at a particular rotation speed with specific tool size. Khandkar, *et al*. (2003) presented that the input torque measured during FSW of aluminium plates is correlated with the heat input at interfaces, and the total torque including interfaces at tool shoulder, pin bottom, and vertical pin surface was given as:

$$M = \int_0^{r_s} (\tau r)(2\pi r)dr + (\tau r_p)2\pi r_p h \tag{2.8}$$

Where r is the radial distance from the tool centre, r_p is the pin radius, r_s is the shoulder radius, h is the pin length, and τ is the assumed uniform shear stress.

2.1.4 FSW Machine Tool

For complex curvature FSW, the changing curvature of the joint requires the multi-axis mechatronic system to provide large force, precise orientation and position control. The workpiece should be firmly held, located and supported by the fixture to prevent it from collapsing or undergoing undesired changes in shape, as shown in Figure 2.7.

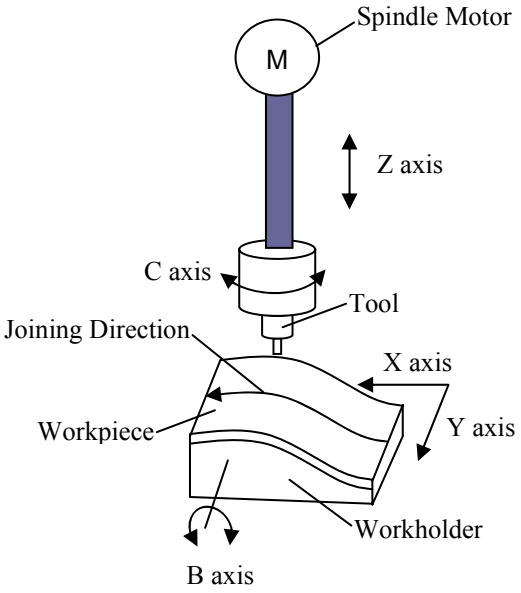

Figure 2.7: Multi-axis structure for complex curvature FSW (Satoshi, *et al*., 2001)

Complex curvature FSW is a non-linear process involving multi-input and multi-output (MIMO). Due to the changing process condition of workpiece curvature, process outputs of forces, torque and temperature may change more frequently in complex curvature FSW than in straight line welding. Except for workpiece curvature, other process conditions such as parent material, tool geometry and thickness also play an important

role in weld quality. To perform reconfigurable manufacturing of non-linear process such as complex curvature FSW, it is necessary for the system to recognize process condition changes and make decision to effectively control process outputs towards desired reference values for maintaining constant weld quality.

2.2 Intelligent Control overview

Intelligence of a control system is the integration of knowledge and feedback into a sensory-interactive goal-directed control system that can make plans, and generate effective, purposeful action directed toward achieving the goal (Antsaklis, 1993). Intelligent control systems require capabilities for evolution, adaptation, and learning. Artificial intelligence (AI) is to describe and build an intelligent agent, which has the ability to sense the environment, to make decisions and to take action (Fukuda and Kubota, 1997; Brezocnika *et al*., 2003).

AI techniques such as genetic algorithms (GA), evolutionary computation (EC), expert systems (ES), FL and NN have been widely applied to control systems, especially in milling and turning (Haber *et al*., 2002; Liu *et al*., 1999; Liu and Wang, 1999; Lin and Lee, 1999). They provide the controller with the following features (Stephanopoulos and Han, 1996):

- Using logic, sequencing, and reasoning in addition to numerical algorithms;
- Dealing with non-linear process autonomy; and
- Emulating paradigms assumed to be in action of human/biological systems in representational forms and decision-making procedures.

2.2.1 Fuzzy Logic Control

Its tolerance for imprecision, uncertainty and partial truth, and its ability to model non-linear functions of arbitrary complexity, make FL control an ideal tool for machining process control (Liang, *et al*, 2003). FL is aimed at treating problems affected by imprecision due to lack of sharp criteria for deciding set membership, rather than to the presence of random variables and stochastic processes. In fuzzy process control, expertise is encapsulated into a system in terms of linguistic descriptions of knowledge, and knowledge about the process states and input-output relationships (D'Errico, 2001).

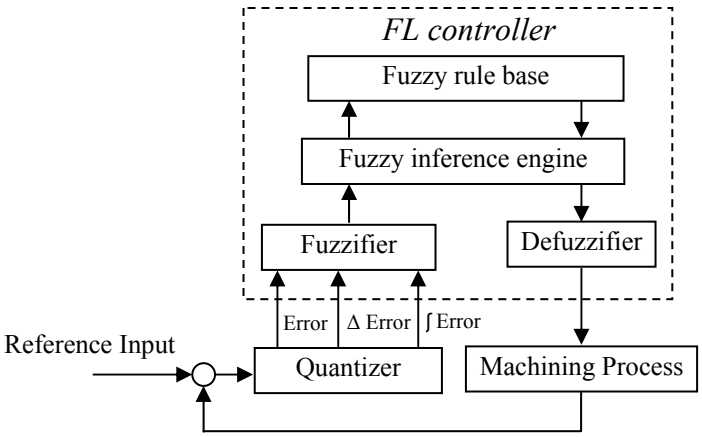

Figure 2.8: Structure of a typical fuzzy logic controller (Carvajal, *et al*., 2000)

Figure 2.8 shows a typical FL controller and its interface to machining process. A FL controller mainly consists of four components: a fuzzy rule base built on general observations and knowledge of the problem, a fuzzifier transforming a numerical input signal into some fuzzy values, a defuzzifier transforming final fuzzy value into an output signal, and a fuzzy inference engine performing decision-making (Carvajal, *et al*., 2000).

2.2.1.1 Fuzzifier

The fuzzifier is used to take numerical inputs and determine the degree to which they belong to each of the appropriate fuzzy sets via membership functions (MFs). A MF is a curve that defines how each point in the input discourse is mapped to a degree of membership between 0 and 1 (The MathWorks, 2004a). Figure 2.9 illustrates the linguistic terms "small", "middle" and "large" of an input with typical triangular MFs.

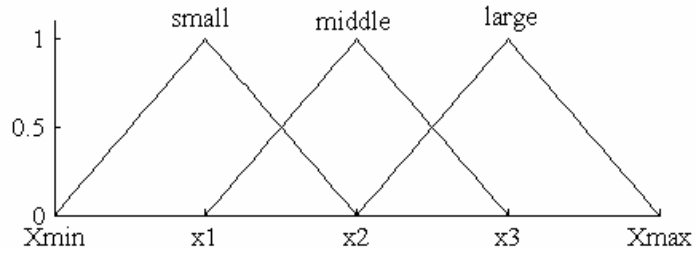

Figure 2.9: Triangular membership functions for fuzzy input

The mathematical computation for fuzzy term "small" is given as follows. The similar computation applies to the other two linguistic terms "middle" and "large".

$$\mu_{small} = \begin{cases} \dfrac{x - x_{\min}}{x1 - x_{\min}} & x_{\min} \le x \le x1 \\ \dfrac{x2 - x}{x2 - x1} & x1 \le x \le x2 \\ 0 & otherwise \end{cases} \tag{2.9}$$

Where μ_{small} is the membership value for the fuzzy term "small"; x_{min}, $x1$, $x2$ parameters determine the MF shape, and x is the numerical value of input.

Using equation (2.9), the fuzzifier computes to what degree the input belongs to the three linguistic terms. The fuzzified values for the numerical input x are thus computed as $\mu 1$, $\mu 2$ and 0 for "small", "middle" and "large" respectively, as shown in Figure 2.10.

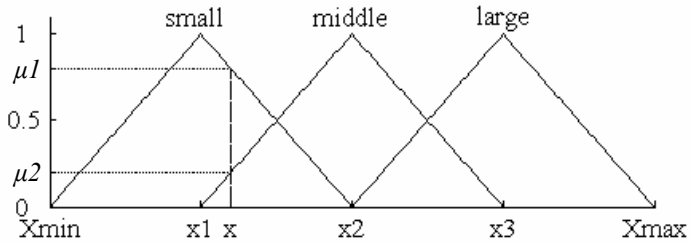

Figure 2.10: Fuzzified values of numerical input

For a FL controller with m inputs, the fuzzified results of the ith input with n MFs can also be expressed with following fuzzy set:

$$A_i = \{\mu_{Ai1}(x_1), \mu_{Ai2}(x_2), ..., \mu_{Ain}(x_n)\} \tag{2.10}$$

Where A_i is the fuzzy set for fuzzified ith input, and μ_{Ain} the value illustrating to what degree the ith input belongs to the nth linguistic term.

2.2.1.2 Fuzzy Rule Base and Inference Engine

Mamdani's fuzzy inference method is the most commonly used fuzzy methodology. Mamdani-type inference expects the output membership functions to be fuzzy sets. A fuzzy base consists of multiple fuzzy rules based on knowledge of the control problem. For a typical MIMO FL system, the linguistic expression of a fuzzy rule is given:

$$\begin{aligned} &\text{If} \quad input_1 \text{ is } A_1 \text{ AND } input_2 \text{ is } A_2 \ \ldots \text{ AND } input_m \text{ is } A_m, \\ &\text{Then} \quad output_1 \text{ is } B_1 \text{ AND } output_2 \text{ is } B_2 \ \ldots \text{ AND } output_n \text{ is } B_n \end{aligned} \tag{2.11}$$

Where A_i *(i=1* to *m)* and B_j *(j=1* to *n)* are linguistic values defined by fuzzy sets on the discourse of inputs and outputs, respectively.

Fuzzy inference (FI) is the process of formulating the mapping, which provides a basis for decision-making or pattern-discerning, from a given input to an output using FL. The FI process performs applying fuzzy operator and implication methods, and aggregating all outputs. The entire FI process mapping inputs to output, including fuzzification, fuzzy operator, implication, aggregation and defuzzification, is illustrated in Figure 2.11:

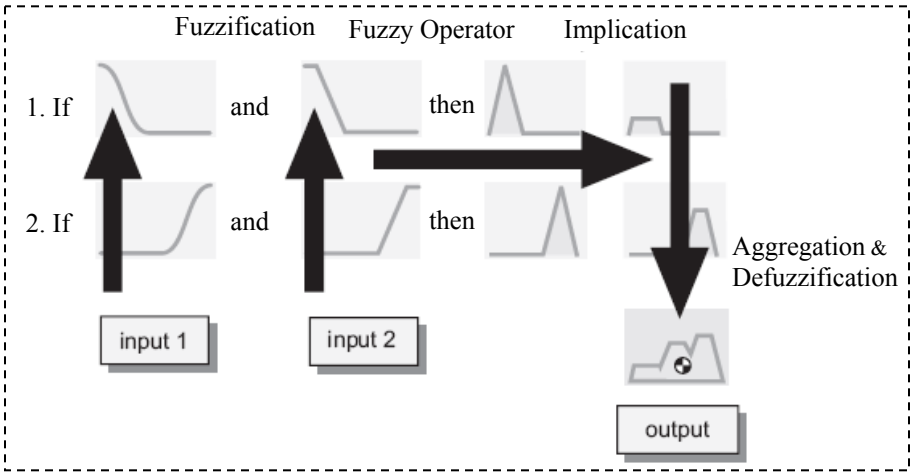

Figure 2.11: Interpreting diagram of fuzzy inference process (The MathWorks, 2004a)

Once the degree to which each part of the 'if-then' antecedent has been satisfied for each rule, and the antecedent of a given rule has more than one part, the fuzzy operator is applied to obtain one number that represents the result of the antecedent for that rule. In this study, the AND and OR operations for 'if-then' antecedents are given as:

$$\mu_A(AND) = \min[\mu_{A1}, \mu_{A2}, ...\mu_{Am}] \tag{2.12}$$

$$\mu_A(OR) = \max[\mu_{A1}, \mu_{A2}, ...\mu_{Am}] \tag{2.13}$$

Where μ_A is the value representing the result of the antecedent for the rule, μ_{Ai} ($i = 1$ to m) value of the MF for the ith part of antecedent.

The input for the implication process is a single number given by the antecedent, and the output is a fuzzy set representing consequent of each 'if-then' rule. In this study, the implication is performed by truncating the output fuzzy set:

$$\mu_B = \min[\mu_{B1}, \mu_{B2}, ...\mu_{Bn}] \tag{2.14}$$

Input of aggregation process is the list of truncated output functions returned by the implication process for each rule. Output of the aggregation process is one fuzzy set for each output variable. In this study, the aggregation method is given:

$$\mu_{OUT} = \max[\mu_{B,Rule(1)}, \mu_{B,Rule(1)}, ...\mu_{B,Rule(q)}] \tag{2.15}$$

Where $\mu_{AB,Rule(j)}$ ($j = 1$ to q) is the jth complication result for output variable, μ_{OUT} aggregation result of the output variable.

2.2.1.3 Defuzzifier

The defuzzifier resolves a single output value from the aggregate output fuzzy set. The centre of area defuzzification method is used in this study. The final crisp value for an output is given as follows:

$$V_{OUT} = \frac{\int x\mu_{OUT}(x)dx}{\int \mu_{OUT}(x)dx} \tag{2.16}$$

Where V_{OUT} is the final output value, x the output discourse, and $\mu_{OUT}(x)$ the MF value at point x.

2.2.1.4 Adaptive Fuzzy Control

To adjust control action with respect to the process environment changing, adaptation techniques, including MF tuning, fuzzy rule tuning and input/output tuning, have been applied in adaptive fuzzy control. Liang, *et al*. (2002) proposed an input/output scale factor tuning mechanism for fuzzy power control in end milling, as shown in Figure 2.12. The tuning mechanism is based on the idea that process parameters of feed rate and spindle speed are adaptively adjusted in response to both the amount and the trend of deviation from the control target. The results show that the system was adaptive to workpiece and tool changes, and cutting power was well regulated.

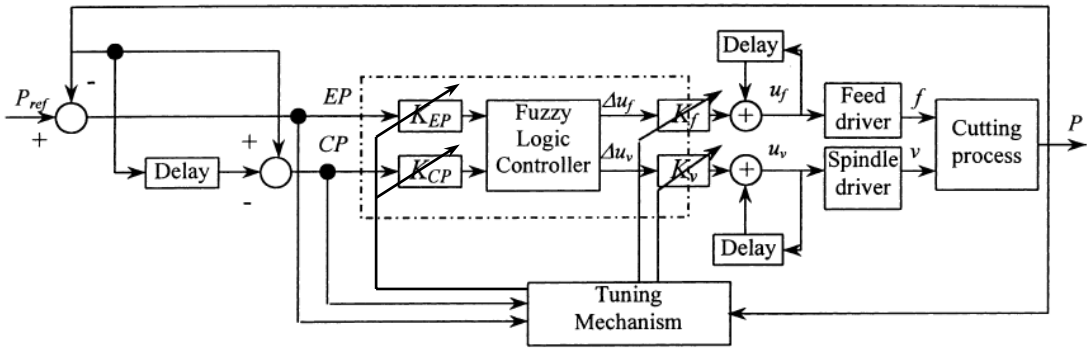

Figure 2.12: FL controller with input/output tuning mechanism (Liang, *et al*. (2002)

2.2.2 Neural network

Artificial Neural Networks (ANNs) are generally composed of numerous processing elements, termed nodes, which weight input signals and sum them together with a bias

through a non-linear transfer function, arranged in layers to form a network (Lennox, *et al*., 2001; Lisboa, 1992). Feed-forward ANN architecture consists of an input layer, one or more hidden layer(s) and an output layer. Figure 2.13 shows a feed-forward ANN with three layers connected by input weight matrix IW and layer weight matrix LW.

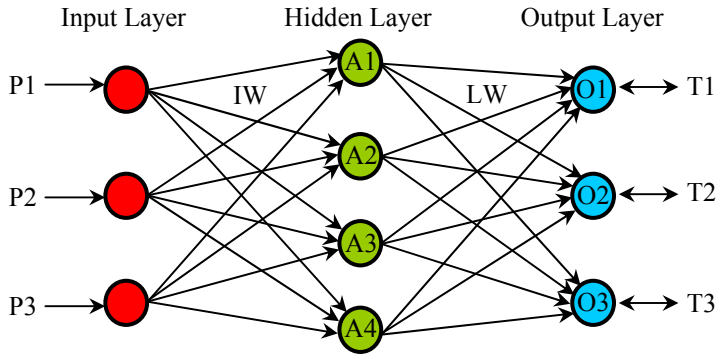

Figure 2.13: Architecture of a three layer feed-forward ANN

Figure 2.14 shows the classical transfer functions and bias for above ANN:

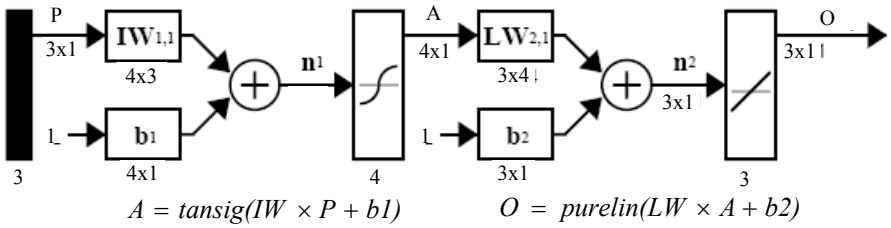

Figure 2.14: Transfer functions and bias of feed-forward ANN (The MathWorks, 2004b)

The final relationship between inputs and outputs can be expressed as:

$$O = pureline(LW \times (tansig(IW \times P + b1)) + b2) \qquad (2.17)$$

Where the transfer functions in the above equation are given as:

$$tansig(n) = \frac{2}{e^{-2n}} - 1 \qquad \text{and} \qquad purelin(n) = n \tag{2.18}$$

Back-propagation is a learning method to train networks by iteratively adjusting the weights and biases of the network to minimize network performance function. Levenberg-Marquardt algorithm is a back-propagation training method designed for fast training. One iteration of this algorithm can be written as (The MathWorks, 2004b; Funahashi, 1989):

$$W^{k+1} = W^k - \left[J^T J + \mu I\right]^{-1} J^T e \tag{2.19}$$

Where W^k is a vector of current weights and biases, J is the Jacobian matrix that contains first derivatives of the network errors with respect to the weights and biases, e is a vector of network errors, I is unit matrix, and μ is constant.

In order to prevent overfitting during NN training, Automated Regularization is often used to improve NN's generalization ability to new situations. This method modifies the performance function and automatically sets optimal regularization parameters to achieve the best generalization. The typical performance function used for training feed-forward NNs is the mean sum of squares of the network errors (MSE) (The MathWorks, 2004b).

$$F = mse = \frac{1}{N}\sum_{i=1}^{N}(e_i)^2 = \frac{1}{N}\sum_{i=1}^{N}(T_i - O_i)^2 \tag{2.20}$$

Where T_i is the ith element of target output, O_i is the ith element of NN output, and N is the size of NN output.

The performance function is modified by adding a term consisting of MSE of the network weights and biases. The modified performance function will cause the network to have smaller weights and biases, and thus force the network response to be smoother and less likely to overfit. The modified performance function is given as (The MathWorks, 2004b):

$$msereg = \gamma mse + (1-\gamma)(\frac{1}{n}\sum_{j=1}^{n}(W_j)^2) \tag{2.21}$$

Where W is a matrix of connection weights and biases, and γ is the performance ratio which is automatically estimated using statistical techniques with the distributions of the random NN weights and biases (MacKay, 1992).

Owing to its ability to learn and generalize from examples and experience, ANN has been applied to perform many different tasks, such as filtering, identification, process modelling, monitoring and control. Applications of NN in manufacturing areas in milling, turning, metal cutting, injection modelling, arc welding and spray painting were cited (Li, *et al*., 2003; Hoo, *et al*., 2002; Rafiq, *et al*., 2001; Zhang and Huang, 1995).

2.2.3 Neuro-fuzzy Control

The capabilities of NN and FL can be synergized through the formation of an integrated neuro-fuzzy model, which is useful in MIMO control situations with complex interactions among the input and output variables. In a neuro-fuzzy control system, FL inference is employed to deal with the complex control issues, while NN is used to generate 'if-then' fuzzy rules by learning input/output relationship through training and thus eliminate the knowledge acquisition bottleneck of FL (Ma, *et al*., 2001). Lau *et al*.

(2001) presented a neuro-fuzzy model consisting of a NN for acquiring the knowledge between input/output, and a FL reasoning mechanism for generating a more reliable suggestion to modify the induced output values from the trained NN. Figure 2.15 shows the flow diagram of the neuro-fuzzy model.

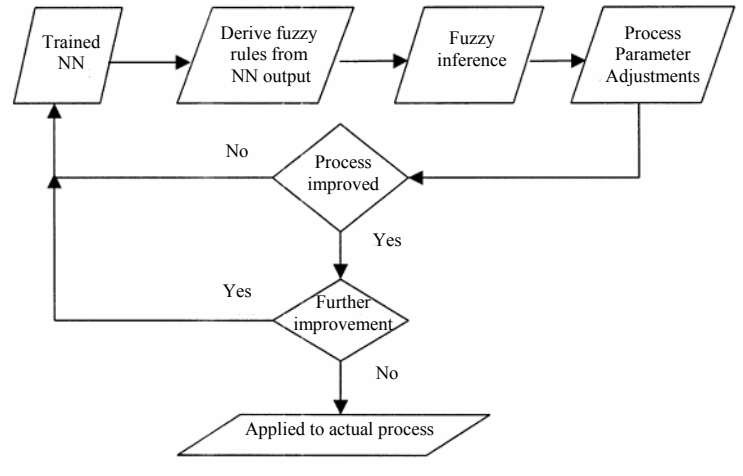

Figure 2.15: Flow diagram of neuro-fuzzy controller (Lau *et al*., 2001)

Much research has been done on different neuro-fuzzy hybrid systems and fuzzy rule extraction (Sun and Deng, 1996; Jin and Sendhoff, 2003; Kasabov, 1996; Suh and Kim, 1994; Suh and Kim, 2000; Kim and Yuh, 2002). Figure 2.16 shows the procedure of on-line fuzzy rule generation proposed by Lau *et al*. (2001). The rule generation is based on the idea that there should be no changes of control variables T_{ref} if process parameters P_{ref} remain unchanged. Thus if any changes of control variables occurred, the new values T of control variables are mapped into the input nodes of the trained NN. The outputs P from the trained NN suggest the deviations of process parameters that cause the changes of control variables.

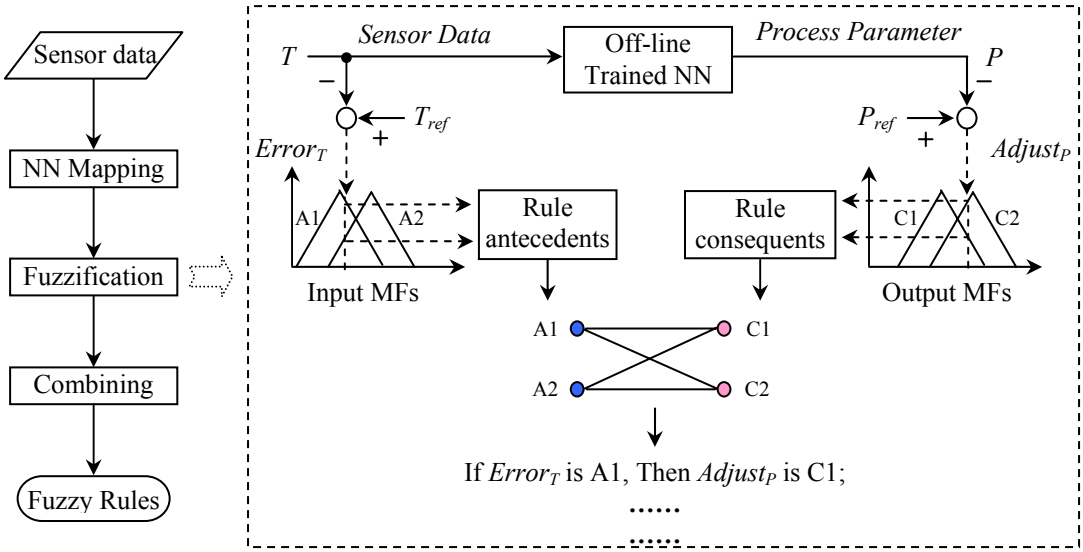

Figure 2.16: Procedure of fuzzy rule generation with NN approach

2.3 On-line Monitoring

The ultimate objective of monitoring systems for machining operations is to enhance the quality of manufactured products via detection of process state. The problem with machining processes is that they are complex, and create a unique design problem in every case. The main obstacles facing the designers of monitoring systems for machining operations are (Al-Habaibeh, *et al*., 2002):

- Selection of the number and type of sensors;
- Selection of effective signal processing methods associated with selected sensors;
- Design of an effective fusion model (i.e., the combination of sensors and signal processing methods which give an improved performance);

- Reduction in cost of machine and process monitoring systems without affecting the system's performance; and

- Automation of the design process.

Using on-line sensors in automatic process control is attractive mainly in that the manufacturing process can be monitored continually without interruption. Process monitoring has been widely researched for the theoretical development and industrial deployment of intelligent systems. Integration methods of AI tools (expert system, FL, NN, etc.) with statistical methods (hypodissertation testing, principal component analysis, etc.) have been utilised in process monitoring and analysis. A formal induction from measured sensor data to process conditions consists of the following three tasks (Stephanopoulos and Han, 1996):

- Extraction of pivotal, temporal features of process trends from sensory data;

- Learning of the relationship between the features and process parameters; and

- Adaptation of the relationship utilizing future operating data.

2.3.1 Multi-sensor System

An important capability of a multi-sensor system is the selection of a few reliable characteristic features from the large amount of signal data, which could be used for learning and decision making to implement a suitable monitoring and control methodology (Chung and Geddam, 2003). The application of multi-sensor systems for the monitoring of machining processes is becoming more common-place to improve

machining precision, productivity, automation and reliability (Dornfeld, *et al*., 1993; Noori-Khajavi and Komanduri, 1993).

The objectives of process monitoring are usually related to the performance of the machine tool, progression of tool wear, dimensional tolerances, surface roughness and other features of the workpiece. Measuring force, torque, power, temperature, and acoustic emission (AE) signals has been commonly used for the monitoring of turning, drilling and milling operations. Different types of sensors such as dynamometers, AE transducers, accelerometers and thermocouples have been commonly applied to sense a particular characteristic or a combination of characteristics such as tool wear, tool fracture, machine vibration, etc. (Chung and Geddam, 2003; Kang, *et al*., 2001).

2.3.2 Sensor Fusion

Sensor fusion is a method of integrating signals from multiple sources. Sensor fusion algorithms can be classified into three different groups (Sasiadek, 2002):

- Fusion based on probabilistic model methods such as Bayesian reasoning, evidence theory, robust statistics and recursive operators;
- Fusion based on least-squares techniques such as Kalman filtering, optimal theory, regularization and uncertainty ellipsoids; and
- Intelligent fusion methods such as FL and NN.

Research has been done in such areas as introducing NN and FL to intelligent monitoring of tool condition from signals of spindle power, spindle torque, and spindle current during processing (Tseng and Chou, 2002).

Azouzi and Guillot (1997) presented a systematic sensor selection and fusion method for surface finish and dimensional deviation prediction in turning. Shown in Figure 2.17 is the proposed procedure of sensor fusion. Statistical methods including orthogonal arrays (OAs), correlation and analysis of variance (ANOVA) were used to select the sensitive features to state variables, and NN was used to build a sensor model which represents the relationship between state variables and selected sensitive features.

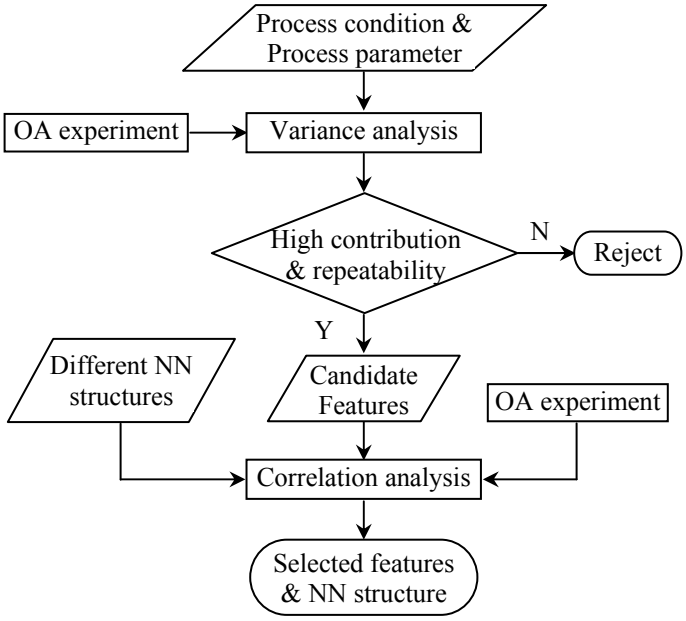

Figure 2.17: Procedure of sensor fusion with statistical analysis and NN

2.3.2.1 Statistical Analysis

Using an efficient testing strategy such as OA, process conditions and process parameters were designed for different levels of experiment action. Sensor data and state variables were recorded and measured for statistical analysis in order to select sensitive features.

The percentage contribution, which reflects the portion of the total variation observed in the experiment attributed to a factor. A factor (process parameter, process condition, or sensor data) with higher percentage contribution to a state variable indicates that this factor is more sensitive to that state variable. The calculation of percentage contribution of a factor is given as (Ross, 1995):

$$P_F = \frac{SS_F - V_e v_F}{SS_T} 100 \tag{2.22}$$

SS_F and SS_T are given as:

$$SS_F = \sum_{i=1}^{K_F} \frac{F_i^2}{n_{Fi}} - \frac{T^2}{N} \qquad \text{and} \qquad SS_T = \sum_{i=1}^{N} y_i^{\,2} - \frac{T^2}{N} \tag{2.23}$$

V_e is the variance due to the error and is given as:

$$V_e = \frac{SS_T - \sum_F SS_F}{N - 1 - \sum_F v_F} \tag{2.24}$$

Where:

v_F degree of freedom

K_F number of levels for the factor

n_{Fi} number of observations under level *i* of the factor

T sum of all observations

N total number of observations

Fi sum of observations under *i*th level of factor

Using additional repetition tests, factors with relative high percentage contribution and repeatability were used as candidates for further selection and expected to be used in sensor fusion.

2.3.2.2 Feature Selection and NN Sensor Fusion

Features selected from above statistical analyses were used together with different NN structures as further OA experimental factors for final feature selecting and sensor fusion. Each feature has two levels: level "0" indicates the feature is not used in the NN model; while level "1" indicates its presentation in NN model. The factors and levels for the OA experiment are shown in Figure 2.18 (Azouzi and Guillot, 1997).

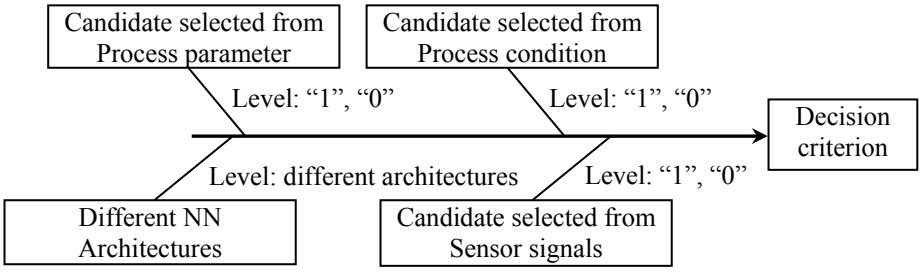

Figure 2.18: OA experiment for sensitive feature and NN structure selection

Correlation analysis is used to study the statistical relationship between the outputs of a model and experimental data. The correlation coefficient of the modeled values of a state variable to its measured values is given as follows (Azouzi and Guillot, 1997):

$$r^2 = \frac{\sum_i (Y_i^{\text{model}} - Y_{mean})^2}{\sum_i (Y_i^{\text{model}} - Y_{mean})^2 + \sum_i (Y_i^{measure} - Y_{mean})^2} \tag{2.25}$$

Where:

Y^{model} value of state variable Y from the NN model

Y_{mean} measured value of state variable Y

$Y^{measure}$ average value of state variable Y

With the correlation coefficients calculated, the features and NN architecture in the trained NN model, which provides the best correlation with measured values, are selected as final sensitive features and NN architecture for process monitoring.

2.3.3 Multi-sensor System for FSW Monitoring

A variety of intelligent monitoring systems based on multi-sensor have been presented for manufacturing processes of milling, turning, grinding, forging, etc. (Van Niekerk, 2001; Lezanski, 2001; Axinte and Gindy, 2003; Tseng and Chou, 2002; Kong and Nahavandi, 2002). Sensory systems, data mining, integrated media, AI (NN, FL, neuro-fuzzy, etc.), real-time control and signal processing were integrated to establish intelligent monitoring systems which perform data acquisition, feature extraction, pattern

recognition, multi-sensor integration and decision making (Kuo, 2000; HOU, *et al*., 2003; Al-Habaibeh, *et al*., 2002; Chang and Jiang, 2002; Lee, *et al*., 2003).

Currently, the research of monitoring and control of FSW is mainly focused on straight welds. Effects of process parameters such as feed rate, spindle speed and tool size on fatigue life, tensile strength, weld crack and residual stress of FSW welds have been investigated (James, *et al.*, 2003; Reynolds, *et al.*, 2003; Nakata, *et al.*, 2001; Ericsson and Sandström, 2003). It was also presented that the weld properties were dominated by the thermal input rather than the mechanical deformation by the tool, and the relationship between tensile strength and weld crack, and traverse speed and tool size is mentioned (Peel, *et al*., 2003). Khandkar *et al.* (2003) introduced an input torque based model of temperature distribution and thermal history prediction. Chen *et al.* (2003) presented a monitoring system using wavelet transform analysis of acoustic emission for Al 6061 aluminium FSW.

FSW involves in complex material flow and temperature distribution, together with a large force involved. Multiple process parameters and control variables need to be monitored during the process. Accurate mathematical or FEM models of FSW are difficult to acquire to describe the relationship among the multiple variables.

For complex curvature FSW monitoring, the signals acquired from multiple sensors contain many of the informative features related to the welding state. Sensor data of force, torque, temperature, position, temperature, etc., should be collected and processed in real-time. To integrate the information received from multi-sensor into meaningful signal or information that can be used in control systems, sensor fusion must investigate the non-

linear relationship between measurable variables (forces, torque, temperature, etc.) and process parameters (spindle speed, feed rate, tilt angle, plunge depth, etc.). ANN, together with statistical analysis can be employed to perform sensor fusion.

2.4 Intelligent Control for Complex Curvature FSW

Like other friction welding techniques, FSW has the advantage that many of the welding parameters, e.g. tool design, feed rate, spindle speed, tilt angle and plunge depth, can be controlled in a precise manner (Peel, *et al*., 2003). However, except the large force and complex material flow involved, the changing curvature introduces more uncertainty during complex curvature FSW. It is difficult to establish an accurate kinematic and dynamic model. Conventional control methods, including computed torque technique and non-linear feedback control, resort to non-linear compensation to eliminate the interactions. These methods are based on having full knowledge of the dynamic model. In the practice of complex curvature FSW, process conditions of the welding vary from a task to another, and hence, may not be precisely known in advance (Chan, 2003; Haber *et al*., 2003).

The complexity and non-linearity of processes like complex curvature FSW make intelligent systems technology a feasible option to classical control strategies. Intelligent methods such as NN and FL can be applied to control the non-linear and dynamically changing process. To be intelligent, the FSW system requires the ability of learning and planning. During complex curvature FSW, deviation of process status may occur due to the changes of process condition and process parameters. The intelligent control system must be able to perceive the changes, make decisions and act to adapt to the changing

process environment. During the perception→decision→action process, the intelligent system also learns from the sensing and command experience to updates the knowledge base inside (Fukuda and Kubota, 1997). Figure 2.19 shows the interaction of the proposed intelligent FSW system with its environment.

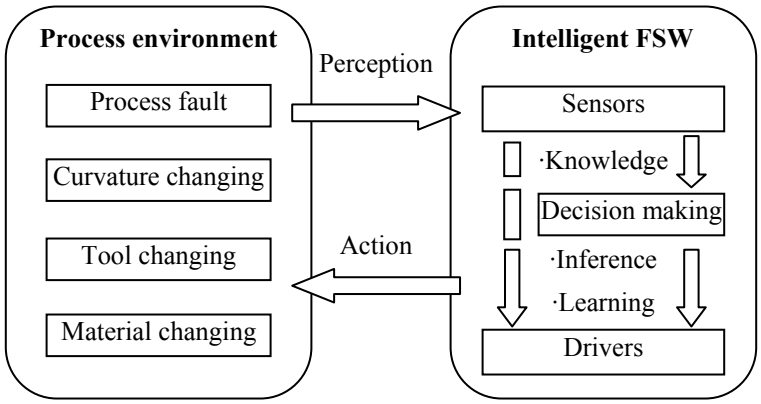

Figure 2.19: Interaction of intelligent FSW system with its environment

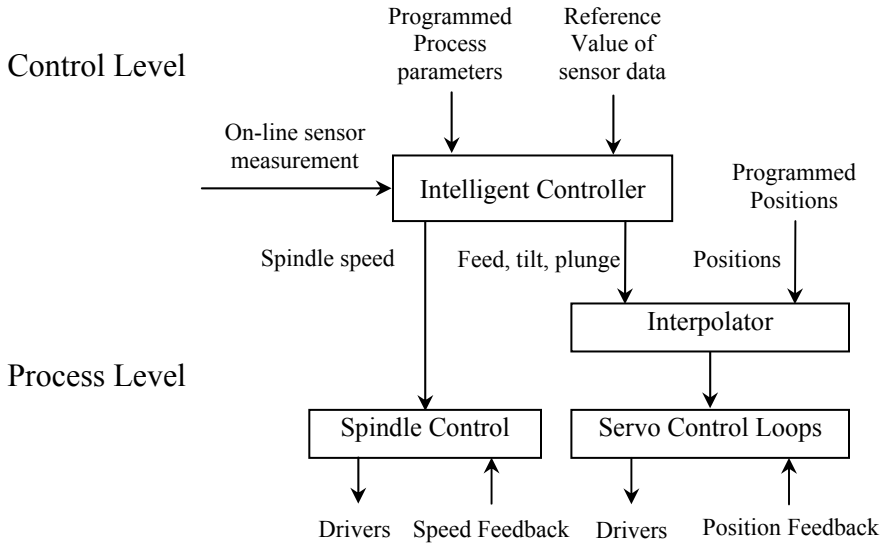

Figure 2.20: Hierarchical levels in the proposed intelligent FSW control system

As shown in Figure 2.20, to perform sensing, decision making and control action, the proposed intelligent system for complex curvature FSW consists of two hierarchical

levels: a control level which performs learning and decision making, and a process level which implements the control commands from the upper level (Fukuda and Kubota, 1997; Koren, 1997).

2.4.1 Control Level

Weld quality of FSW is determined by the combination of process condition and process parameters. To maintain weld quality in changing process conditions, the intelligent neuro-fuzzy controller at control level can be used to adapt to process condition changes. Sensitive features characterizing process conditions are selected from process outputs (e.g. temperature, torque, forces, etc.) and process parameters (e.g. feed rate, spindle speed, tilt angle, plunge depth, etc.). ANN can be used to learn the non-linear relationship between process condition and the selected sensitive features owing to its ability of approximating a random complex mathematical model.

FL control is feasible for the MIMO process of complex curvature FSW owing to its tolerance for imprecision, uncertainty and non-linearity. Tuning mechanism is used to tune the outputs from the FL controller to adapt to the dynamic machining conditions. Also, NN can be used to learn from previous knowledge to generate fuzzy rules for the FL controller (Liang, *et al*., 2003).

2.4.2 Process Level

In complex curvature FSW, the precise contact between the tool and workpiece is needed to maintain the energy into the workpiece, thus the system needs to provide large force and accurate orientation and position control. The fundamental issues of multi-axis

surface machining include tool path planning, optimization of machining process parameters, path interpolation and servo control (Xua, *et al*., 2003a).

- **Tool Path Planning**

In multi-axis machining, due to the additional rotation axes, both the cutter contact points (CC points) and cutter location points (CL points) need to be determined in tool path generation. Hence the task of tool path planning is twofold, namely tool position path planning and tool orientation path planning. Much contribution (Dragomatz and Mann, 1997; Choi and Jerard, 1998) has been made on tool position path planning. The methods of iso-planar curve (Bobrow, 1985), iso-parametric curve (Elber and Cohen, 1994), iso-scallop curve (Lin and Koren, 1996) and iso-phote curve (Han and Yang, 1999) are examples of such methods. Meanwhile there is an increasing focus (Lee, 1998; Lo, 1999; Rao, *et al*., 1997; Warkentin, 2000) on tool positioning strategies able to produce tool orientation paths, where an orientation path is constructed based on a planned position path.

Figure 2.21 shows the tool position in one cutting step for a table-tilting four-axis machine. During each cutting step, the cutting tool and the machined part are translated along three translational axes (from C_1 to C_2) and the part is rotated about the rotational axis (from $\beta+\varphi_1$ to $\beta+\varphi_2$). The corresponding position for arc centre O_{p2} and the tool corner centre A_2 (with tool corner radius ρ) are given as (Hwang, 2000):

$$O_{p2} = \begin{pmatrix} x_m \\ R_o cos(\beta + \varphi_2) \\ R_o sin(\beta + \varphi_2) \end{pmatrix} \quad \text{and} \quad A_2 = O_{p2} + (R_c + \rho) \begin{pmatrix} x_m \\ cos(\pi/2 + \alpha_2) \\ sin(\pi/2 + \alpha_2) \end{pmatrix} \qquad (2.26)$$

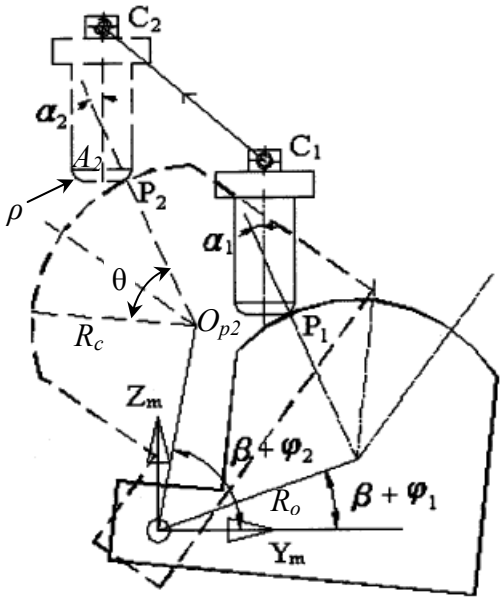

Figure 2.21: Tool position for table-tilting machine (Hwang, 2000)

- **Path Interpolation**

Path interpolation is concerned with converting tool paths obtained from a tool path planning system into time-dependent commands for driving the servo control system of a multi-axis machine (Xua, *et al*., 2003a). CNC interpolation is to convert the prescribed paths and feedrate information into time-dependent commands for driving the servo-motors of a CNC machine (Xua, *et al*., 2003b).

Linear interpolation is widely used for path interpolation in CNC systems. Once the machining tool paths are generated, line approximation schemes are used to discretize the tool paths into line segments for the generation of NC codes, as shown in Figure 2.22. Arc approximation schemes were proposed to improve the smoothness of machined surfaces. Qiu *et al*. (1997) proposed to use circular arc interpolation for tool path generation. Curve fitting with arc splines was suggested by Yeung and Walton (1994).

Biarcs were used to approximate complex tool paths in which line and arc segments were special cases of biarcs (Tseng and Chen, 2000).

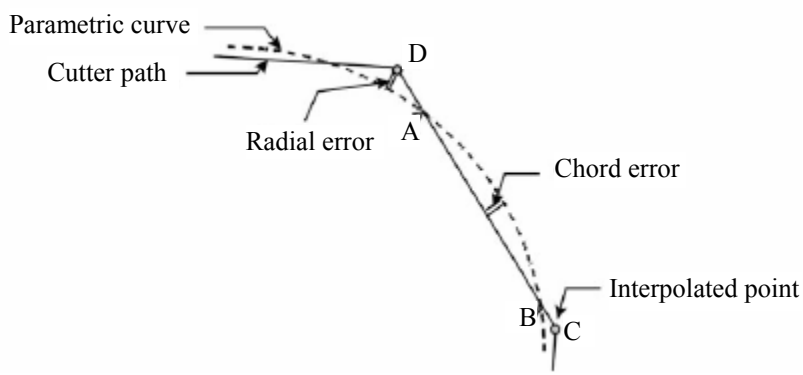

Figure 2.22: Errors in linear interpolation of tool path (Yeh and Hsu, 2002)

The disadvantages of the approximation approach, however, include significant contour and orientation errors, heavy communication loading and high memory requirement for the controller and considerable acceleration and deceleration for line segment executions (Shiptalni, 1994; Koren and Lin, 1995).

Real-time path approach has become a feasible alternative to the off-line path approximation schemes. In the real-time path approach, the machining system with built-in free-form curve interpolator inputs curve geometry parameters directly and generates motion commands in real-time.

Parametric curves represent the most important form of tool paths for surface machining, and good progress has been made in parametric curve interpolation (Lo, 1997; Lo, 1998; Farouki, *et al*., 1998). Implicit curves are another form in the representation of tool paths for surface machining. Recently there is increased interest in real-time interpolation for implicit curves (Tam, *et al*., 2002; Xu, *et al*., 2001). The iso-planar method is an

important approach to tool path planning and has been well investigated (Choi and Jerard, 1998). Tool paths can be generated by intersecting a part surface in a parametric form with a family of drive planes. A new method, called the bi-parameter curve method was also proposed (Xua, *et al*., 2003b). With the proposed bi-parameter curve method, the tool path is obtained by intersecting a parametric surface with an implicitly defined drive surface.

- **Servo Control**

To realize a specified tool path, a multi-axes machine uses independent motors to drive several translational and/or rotational axes in a coordinated manner. In multi-axis machining, the cutting tool not only translates along a curve with respect to a workpiece, but also rotates about a specific axis. Consequently, there exists two kinds of feedrates, namely linear feedrate (mm/min) and angular feedrate (rev/min) (Sarma and Rao, 2000; Xu, 2003). An angular feedrate defines the speed of rotational movement of the cutting tool while a linear feedrate defines the speed of its translation movement with respect to the workpiece. In fact, the angular feedrate also affects the dynamics of the machine tool and the quality of the machined product just as the linear feedrate (Xua, *et al*., 2003b).

2.5 Proposed System Framework for Advanced Monitoring and Intelligent Control of Complex Curvature FSW

Figure 2.23 shows a proposed system framework for the implementation of a sensor-based monitoring and intelligent control for complex curvature FSW. The overall system

implementation include multi-axis system setup, experimental work, NN training and FL controller configuration.

- **Multi-axis System**

To maintain correct tool/workpiece contact, an additional rotation axis, including electrical motor, motor driver and gearbox, is integrated into the existing three translation axes to provide a large force and precise orientation and position control. The clamping system is designed for workpiece locating and holding. Sensors for measuring tool force, torque and temperature, and encoders for axis position and speed are utilised to provide feedback information. The process information is fed into the intelligent controller through the DAQ card. Based on feedback information, the intelligent controller senses the environment, makes decisions and control actions to maintain certain variables within a limited range from the set point in order to maintain correct tool/workpiece contact and energy input.

- **Experimental Work**

Experiments are set up to acquire the data for NN training. The experiment factors include feed rate, spindle speed, plunge depth, tilt angle, parent material and curvature. Sensor data of torque, temperature, Fx, Fy and Fz are recorded in the welding process. From the experiments, the optimized process parameters related to the best weld quality and the corresponding reference value of sensor data, which are chosen as control variables, can be derived. The most sensitive sensor signals, which characterize tool/workpiece contact condition, can also be deduced using statistical analysis and selected as the control variables for tool/workiece contact condition monitoring.

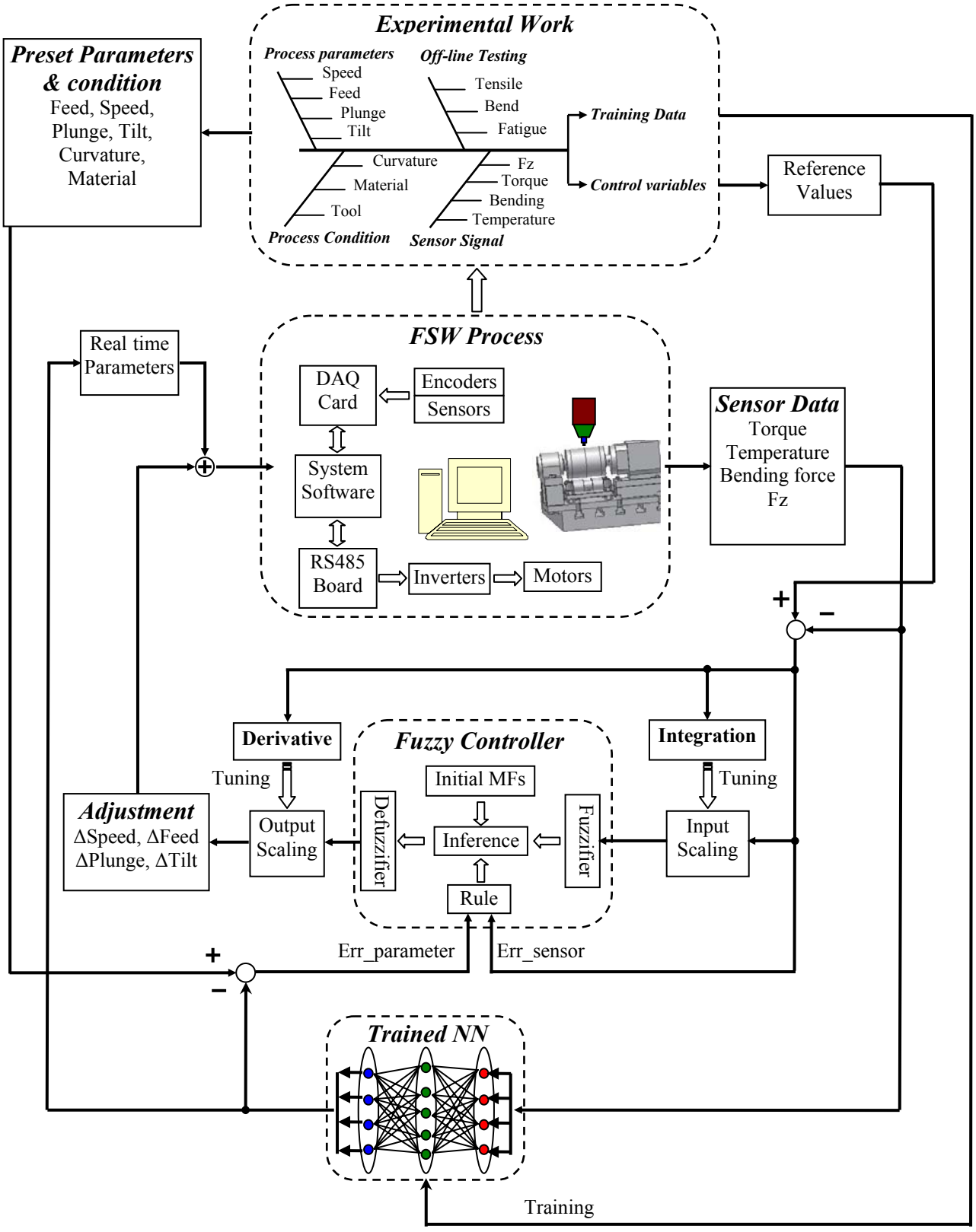

Figure 2.23: Framework for monitoring and intelligent control of complex curvature FSW

- **Trained Neural Networks**

Two kinds of MIMO NNs are trained for process condition detecting and process parameter deriving, respectively. Inputs to the NN for process condition detecting (or process parameter deriving) are selected sensor features and process parameters (or process conditions). Outputs from the NN are process conditions (or process parameters). The trained NNs have the ability to learn the relationship among sensor data, process parameters and process conditions. The training data and checking data for training are chosen that they can cover the ranges of process parameters in FSW process.

With on-line sensor data and current process parameters, the NN for process condition detecting is used to perceive process conditions such as material and curvature changes. With sensitive sensor features and detected process conditions, the NN for process parameter deriving recalls the relationship acquired during data training for 'inducing' the process parameters. When the new set of sensor data are fed into the NN, the outputs from the trained NN suggest the deviations of the process parameters that subsequently cause the inconsistency of the sensor data. This suggestion can be used to derive on-line fuzzy rules for further fuzzy control. The detailed description of NN training and on-line fuzzy rule generation can be seen in Chapters 4 and 5, respectively.

- **Fuzzy Controller**

The initial FL controller is built by presetting MFs for each input and output without fuzzy rules, which are generated on-line with the trained NNs. Inputs of the FL controller are errors between real sensor data and reference values. Outputs of the FLC are primary adjustments of process parameters.

Input and output scaling factors are adaptively tuned to suggest more reasonable adjustments of process parameters. Output scaling factors of the FLC are also set and on-line tuned in response to the changes in the welding process. With the tuning mechanism, the process parameters are adjusted not only on the amount of deviation of control variables from the target value, but also on the trend of the deviation. If the current condition is worse than before, namely, the trend is away from the reference level, more adjustment should be made. If the condition is better than before and the changing rate of deviation is high, then less adjustment of process parameter is preferred.

2.6 Summary

Backgrounds of FSW and complex curvature FSW, including process parameters, process conditions and process outputs and their influence on weld quality, were described in this chapter. A multi-axis system is preferred to a robotic system for complex curvature FSW due to the large force involved in the process. A table-tilting multi-axis system was selected to provide large force, and precise orientation and position control.

The MIMO process of FSW involves complex material flow and temperature distribution, which are determined by tool/workpiece contact conditions, material properties, and the interaction of process parameters. Thus it is difficult to establish accurate mathematical model for conventional model-based control methods. It is feasible to control the non-linear FSW process using an intelligent system owing to its ability to sense the environment; learn from the process; and make decisions based on the significant information from the process. The state-of-the-art AI methods such as NN, FL, neuro-

fuzzy and their application in on-line monitoring and intelligent control have been reviewed in this chapter.

A framework of multi-sensor based monitoring and intelligent control for complex curvature FSW is proposed. The detailed description of the proposed neuro-fuzzy monitoring and control scheme can be seen in Chapter 4 and Chapter 5.

Chapter 3 Experimental Setup: Multi-axis Control, Fixture Design, Sensors, Experimental Design and Software Components

The FSW system for workpieces with complex curvature was based on the existing FSW system for flat plate welding. To perform on-line monitoring and intelligent control, the system provides the ability to acquire measured sensory information and make on-line decisions and act quickly to maintain the desired process status and product quality.

To set up the system for complex curvature FSW described in the proposed framework in Section 2.6, system hardware components such as machine tool, sensors, fixtures and software components need to be seamlessly integrated to implement complex curvature FSW. This was implemented by adding new hardware such as the rotation axis and clamping system, additional software components for on-line monitoring and intelligent control to the existing FSW machine.

Experiments were designed to investigate the relationships among process parameters, sensor data, tool/workpiece contact condition and weld quality. Data obtained from the experiments were then used to train and configure the intelligent controller for process condition detecting and weld quality prediction.

To implement and simulate the performance of the intelligent system, software components were composed using MATLAB language with its graphical user interface (GUI), NN and FL toolboxes.

3.1 FSW System Hardware Description: Machine Tool, Multi-axis Control and Sensors

3.1.1 Brief Description of the FSW Machine

The FSW machine was converted from a conventional 3-axis F3UE milling machine built by NICOLAS CORREA SA. Three translational axes (X, Y and Z) for bed movements, one spindle axis and one rotational axis (R) for workpieces rotation were all driven by three-phase induction motors, which were controlled by inverters. The clamping system was designed for orientating and locating the workpieces on the machine worktable. Figure 3.1 shows a picture of the FSW machine used in this project.

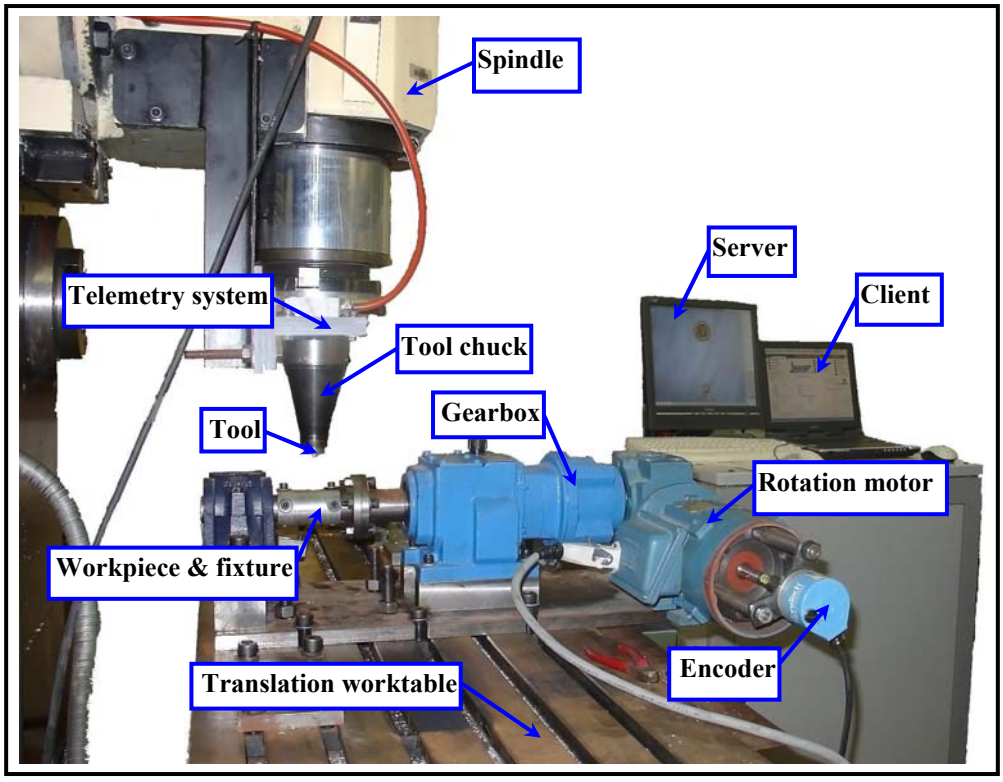

Figure 3.1: FSW machine with additional rotation axis implemented for this project

The hardware of the FSW machine provides the following functionalities for process monitoring and control (Kruger, 2003):

- Pre-setting the process parameters such as spindle speed, feed rate, tilt angle and plunge depth before the process, and adjusting them on-line without interrupting the machining process.

- Detecting and controlling the distance and speed of each axis, and thus providing commanded relative positions of tool and workpieces with required accuracy.

- Providing soft- and hard stop, home position, and position holding by clutches, brakes and limit switches, and interfacing them to computer.

- Recording and transferring process data including vertical force, horizontal force footprint, torque and temperature from the tool to the computer for further processing.

3.1.2 Multi-axis Control and the Client-Server Computer System

To realize a specified welding path for complex curvature workpieces, a multi-axis FSW machine uses independent motors to drive three translational axes, one spindle axis and one rotational axis in a coordinated manner (Hwang, 2000). Restricted by the response time and control accuracy of motors on the FSW machine, the weld path was interpolated before the welding process to convert the complex welding path into a series of time-dependent commands of distances and velocities for all motors, which were controlled by the corresponding inverters to operate simultaneously.

Each of the four motors is controlled by a Siemens Micromaster 440 inverter, which is used to protect, monitor and control the motor's operation to a user specified set point. The inverters use RS485 communication to interface to the computer system. RS485 allows multiple motor/inverter parameters to be written and read directly form the inverter by the computer. PCI RS485 4 Port Interface Card, and a 16550 USART chip on the computer connects each inverter with a dedicated RS485 cable to the computer (Siemens, 2001; Kruger, 2003).

The FSW machine was controlled by a client computer which is connected to the server computer using Ethernet. TCP/IP protocol was used in the communication between client computer and FSW machine server. When a client connects to the machine's server using a web browser, the server sends the GUI to the client. Requests for information and control messages are then continually sent between the client and server, until the client breaks the connection (Kruger, 2003).

3.1.3 Sensors and the Telemetry Monitoring System

To maintain the desired contact and energy into the tool/workpieces, the feedback from the multiple axes and the information of process variables need to be continuously recorded and fed into the controller for on-line decision-making when the tool is busy traversing along the weld path. Thus different types of sensors and sensor data transmitting system were installed on the FSW machine.

The spindle motor, feed motors (X and Z feed), and the motor for workpiece rotation were fitted with Leine and Linde 610/632 industrial incremental optical encoders with a resolution of 512 pulses per revolution. The feed motor encoders provide feedback

related to bed position and the spindle motor encoder allows more accurate spindle speed control by the inverter. A standard low backlash coupling was used to link the encoder shaft to the motor's rotor. The encoder is interfaced to the machine server through a PCI730 data acquisition card (Leine and Linde, 2002; Kruger, 2003).

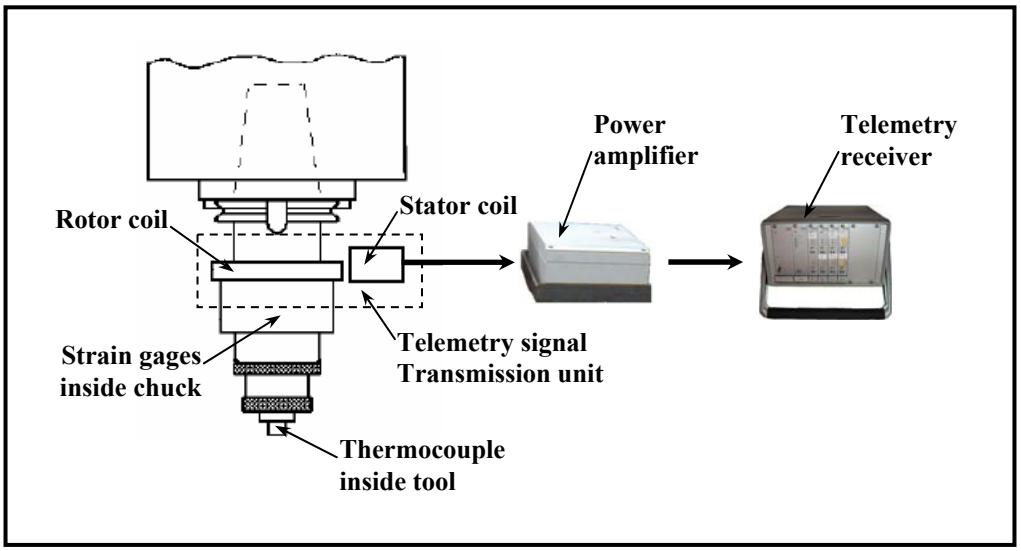

Figure 3.2: Telemetry monitoring system used in study

A telemetry system instrumented on the tool chuck was built to obtain on-line detailed information about process variables, as shown in Figure 3.2. The electronics mounted on the chuck were used to sample the required process variables. Raw sensor data was signal conditioned and then passed to a microprocessor, where it was prepared for transmission to the TS1000 interface. Electrical power is transferred to the chuck using induction and the sampled data is sent off the chuck in digital form using a capacitive technique. Strain gauges and thermal couple were fitted on the chuck and tool to detect horizontal forces, vertical force, torque exerted on the tool and the tool's pin temperature. When the

interface unit receives a request for data, it transfers the information via the RS232 serial interface to the computer (Blignault, 2005; Kruger, 2003).

Specifically arranged precision foil-type strain gauges were attached to a thin shell cylindrical element to measure forces and moment acting on the tool assembly. The sensing system was capable of measuring loads up to 60kN on z-axis, 8kN on x and y-axis and a torque of 400N.m. The strain gauges were applied on the outer surface of the elastic element and on a common centre line in full bridge configurations to compensate for unwanted superimposed stresses. Figure 3.3 shows the principal dimensions of the elastic element as well as the axial positioning and channel number of the strain gauge elements are illustrated in. The two bending channels Channel 1 and 2 measure bending in the x & y direction. Channel 3 measures the compression or tensile force in the axial direction while Channel 4 measures the shear load (Blignault, 2005).

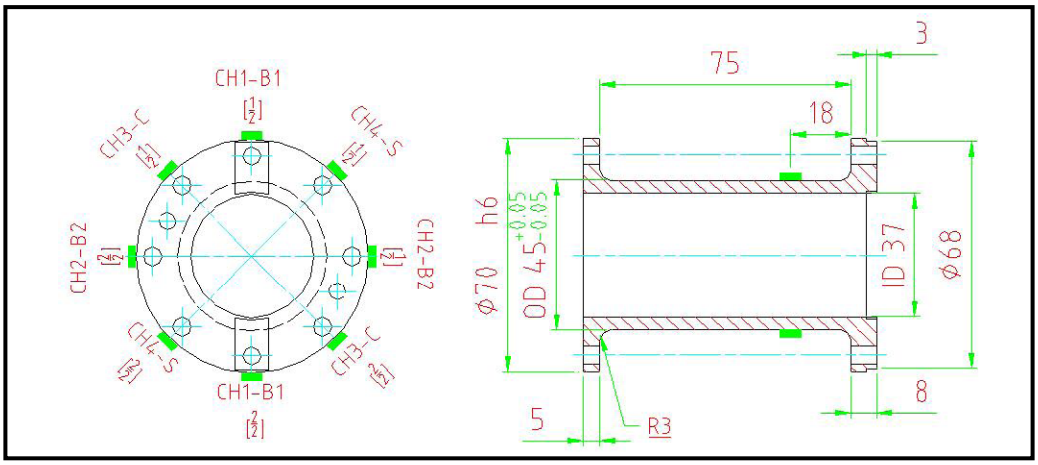

Figure 3.3: Principal dimensions of the elastic element and axial positioning of the strain gauge elements (Blignault, 2005)

A 0.5mm diameter embedded thermocouple probe (type K) was fitted into the 0.7mm diameter hole inside welding tool for measuring the interface temperature between the

tool pin and shoulder. Thermal paste with a high thermal conductivity was also applied on the probe to ensure good contact between the probe and tool interface (Blignault, 2005). The tool and thermocouple assembly was illustrated by Figure 3.4.

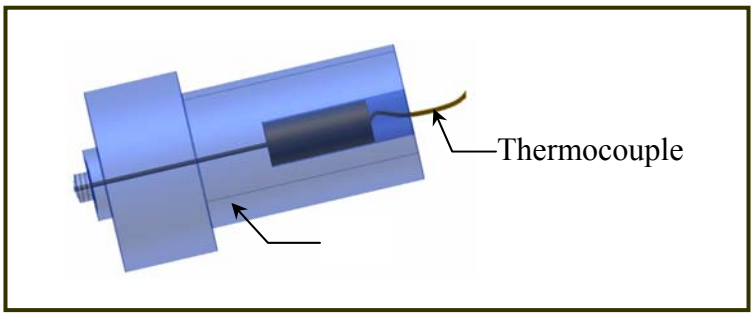

Figure 3.4: Tool and thermocouple assembly

The telemetry system and encoders provide real-time welding process information, which can be used to train and build the on-line monitoring and intelligent control system. The sufficiently high sample rate of process variables from the telemetry system and encoders allows acceptable response time for on-line monitoring and intelligent control of complex curvature FSW.

3.2 Experiment Design for the On-line Monitoring and Intelligent Control System for Complex Curvature FSW

To build a neuro-fuzzy controller for complex curvature FSW, an initial rule base was established by investigating the relationships among process parameters, sensor data and mechanical test. These relationships were revealed through NN training using the experimental data from flat and circular workpiece welding. The performance of the neuro-fuzzy controller was then evaluated through the welding of workpieces consisting of complex curves. A detailed description of NN training and FLC building is in Chapters

4 and 5.

The purpose of experiment design for complex curvature FSW was to select the appropriate experimental method, set up the necessary system hardware and analyse the experimental results. The detailed description of system hardware implementation is given in Section 3.3 and the software implementation is given in Section 3.4. The principles of the experimental design and method selection for complex curvature FSW are discussed in the following subsections.

3.2.1 Definition of the Complex Curvature

Due to the hardware limitation of the existing FSW machine, the complex curvature in this study is defined as two-dimensional convex curve representing the joint of two workpieces with the same dimension of vertical section, as shown in Figure 3.5 (c). In this study, this complex curvature can be considered as the connection of a series of simple curvatures such as straight line and circular arc, as shown in Figure 3.5 (a) and Figure 3.5 (b) respectively.

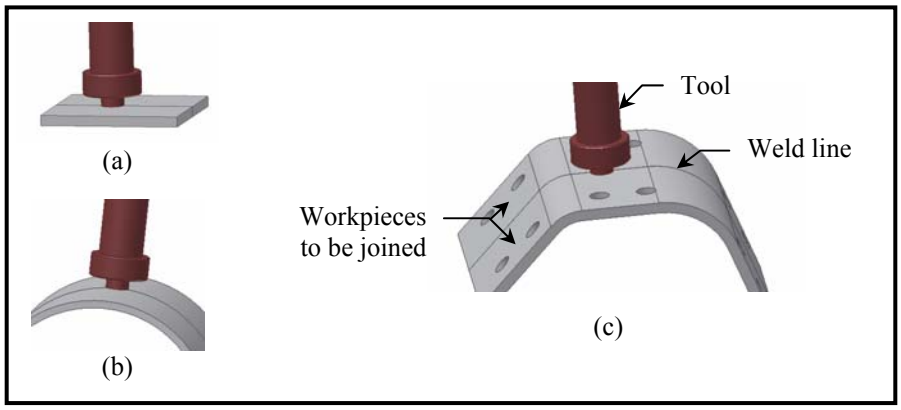

Figure 3.5: Workpieces of different curvature. (a) Flat (b) Circular (c) Complex curvature

At the connection of two segments in a complex welding curve, although full contact between tool shoulder and parent material can be obtained at each segment, it is impractical to maintain full contact when the tool is moving to the intersection corner of a sharp angle. The tool either inevitably loses part of contact with the workpieces or plunges into the backing piece in order to obtain full tool/workpiece contact, as shown in Figure 3.6 (a). The excessive plunging may cause tool and backing piece damage. On the contrary, when welding a round intersection corner with the same tool and material, full tool/workpiece contact can be obtained without damaging the tool and back piece, as shown in Figure 3.6 (b). Thus in this study, complex curvature can be further represented as a series of straight lines connected by round intersection corners of different radii.

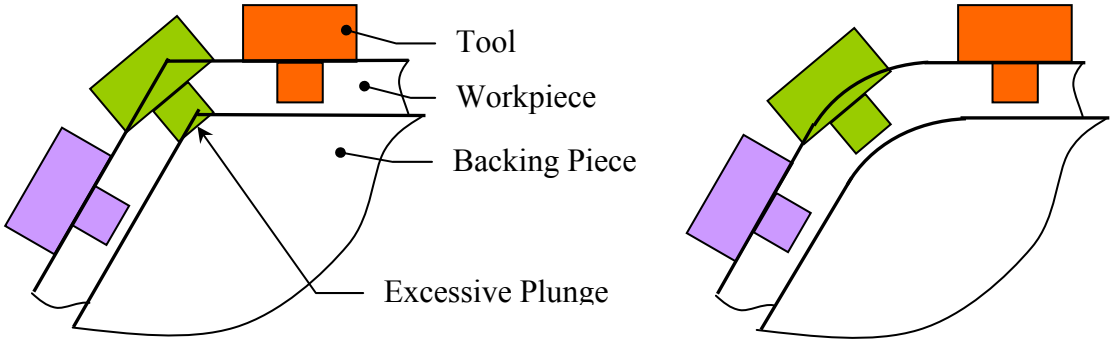

(a) Sharp corner (b) Round corner

Figure 3.6: Tool/workpiece contact when moving at the corner.

3.2.2 Tool/workpiece Contact Condition

For complex curvature FSW, except the process parameters (such as spindle speed, feed rate and plunge depth), the tool/workpiece contact condition also largely influences the quality of the welds. When the tool shoulder partly loses contact with the parent material,

the material stirred and extruded by the rotation pin may flow out and can not be pressed together by the shoulder, thus cause non-integrity in the welds. Whereas, if the tool plunges too deep into the material, not only excessive force and torque will be exerted to tool and workpiece, but also too much heat may be generated with the same feed rate and spindle speed. This may cause residual stress and distortion (Chen and Kovacevic, 2003). Thus it is critical to maintain full shoulder/material contact and the plunge depth within a certain range.

The tool/workpiece contact condition changes along with the changing curvature of the workpiece with the same plunge depth and tilt angle, especially on the connection corner of two segments. As can be seen in Figure 3.4, tool/workpiece contact is influenced by workpiece curvature and tool size. With larger curvature radius and smaller tool shoulder size, it is easier to maintain full tool/workpiece contact without plunging into the backing piece. The curvature radius of the workpiece other than flat plate in this study is restricted to the range of 15 to 47.5mm, and the design of tool size is discussed in detail in Section 3.3.4.

Even if the tool/workpiece positions have been well pre-planned to obtain contact adapt to changing curvatures, the predefined positions may be not maintained due to a disturbance during the process. Basically, the wrong contact condition, including excessive and insufficient contact may be caused by the wrong plunge depth, tilt angle of tool axis to workpiece surface normal, or the combination of these two, as shown in Figure 3.7.

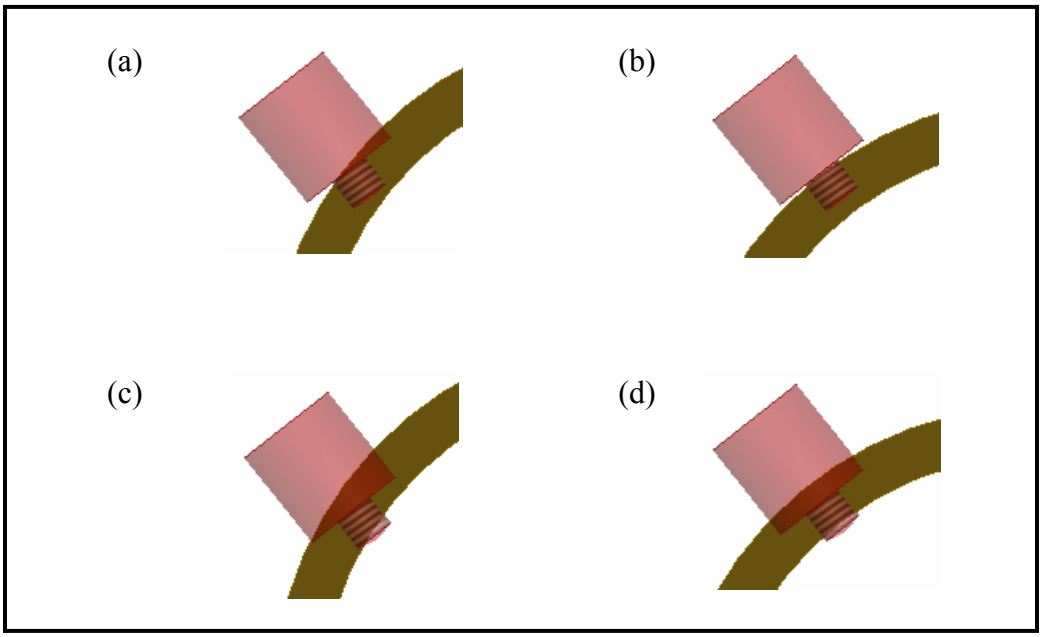

Figure 3.7: Examples of faulty tool/workpiece contact. (a) Insufficient contact due to tool tilt (b) Insufficient contact due to insufficient plunge depth (c) Excessive contact due to tool tilt (d) Excessive contact due to excessive plunge

The tool/workpiece contact condition has a direct relation to the sensor data such as force, torque and temperature. In order to detect the contact condition from the on-line sensor data, a rule base which represents the relationship between sensor data and tool/workpiece contact conditions was established. The establishing of this rule base is mentioned in section 3.4 and a detailed description is given in Chapter 4.

3.2.3 Process of System Setup

The following steps were followed setting up the on-line monitoring and intelligent control for complex curvature FSW:

- Mechanical design including the design of rotary axis, fixture and tool for workpieces with flat, circular and complex curvature. Detailed discussion can be seen in Section 3.3.

- Experiments of flat and circular samples for welding. Using OA analysis to find the most sensitive sensor signals, together with the mathematical relation of the sensor signals to tool/workpiece contact and welding quality, and develop experiments for these sensitive features to get more data. Initial optimised range of process parameters and corresponding sensor data are also derived for maintaining correct contact and high quality.

- Using the sensitive features derived from above experiments and corresponding process parameters to train and test NNs with different architecture. Using the best NN architecture to perform sensor fusion. Find out to what extend sensor fusions may be applied to predict mechanical quality within changes in curvature. Select appropriate sensor signals as control variables. Train and test the NN using the experimental data to find the relationship among process parameters, sensor data and weld quality. A detailed description can be seen in Chapter 4.

- Based on the information from experimental data and the trained NN, design initial structure of the FL controller. Establish performance criterion for tool/workpiece contact and welding quality. Use the trained NN and on-line sensor data to derive fuzzy rules for the FL controller, which is used to maintain preset control variables within dynamic changes in curvature by adjusting the process parameters. Detailed description can be seen in Chapter 5.

- Test the performance of the on-line monitoring and intelligent control system with workpieces with complex curvature. If possible, check the adaptability of the monitoring and control system to different tool, parent material and thickness.

3.3 Fixture Design for Flat Plate, Pipe and Complex Curvature Workpieces

To investigate the relationships among process parameters, sensor data and weld quality, experiments for flat plates, circular plates and plates with changing curvature were carried out to obtain necessary data for further building of the intelligent monitoring and control system. Basically, the two joint workpieces need to be firmly held, located, and supported by the fixture to prevent it collapsing or undergoing undesired changes in shape during the process of FSW. When welding workpieces with curvatures other than straight line, backing plates with the same shape as the workpieces and a clamping system for loading and unloading the workpieces are required. For this purpose, different fixtures were designed for workpieces with different curvatures.

3.3.1 Clamping System for Flat Plate FSW

Alminium 6061 and Al 5251 were selected as the material for FSW experiments. Workpieces with thickness of 3mm were used in straight line FSW. All workpieces were precisely cut into rectangular shape with three aligning holes, which were used to locate and mount the workpieces on the backing plate. A backing plate was also cut into the required shape to support and locate the two workpieces for straight line FSW. Six threaded holes and four through holes were used to fit the workpieces on the backing

plate and to mount the backing plate itself on the FSW machine worktable respectively, as shown in Figure 3.8.

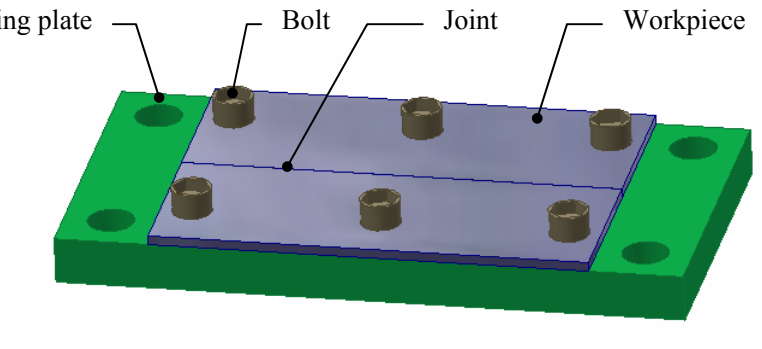

Figure 3.8: Clamping of flat plate workpieces

3.3.2 Clamping System for Pipe Welding

Aluminium pipes and circular arc segments with different radii were used in FSW experiments to study the effects of different curvature on the sensor data and mechanical tests. To perform pipe welding, an extra rotational axis was added to the existing three translational axes (X, Y and Z). A motor plus inverter and gearboxes were used to provide adjustable rotation speed of the workpieces.

Figure 3.9 shows the whole rotational system for pipe welding. To prevent the pipe from moving and deforming from radial and axial direction during welding, a clamping system including shaft, tapering collect, tapering bushing, locking nuts and bearings were installed on the machine worktable and connected to the output shaft of the gearbox. An

auxiliary supporting system including height adjusting screws and supporting rollers was also designed to bear the large Z force during welding.

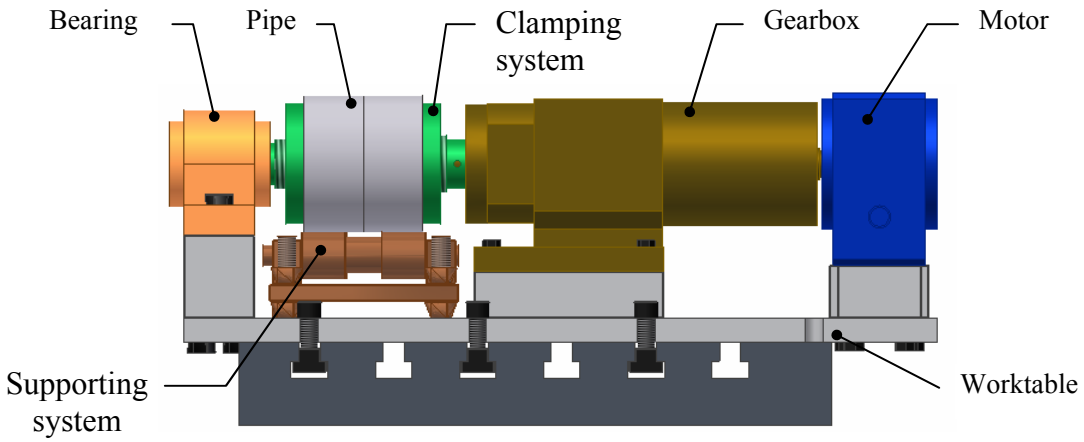

Figure 3.9: Rotational system for pipe welding

Similar clamping systems were also designed to support and hold the circular workpieces other than pipe with different radii. The clamping system consists of a central shaft, a coupling connected to the gearbox output shaft and axial bushings of different radii. Figure 3.10 shows the clamping system for the circular workpieces with an inside diameter of 70mm. The detailed design drawings of the clamping systems mentioned above can be seen in Appendix C.

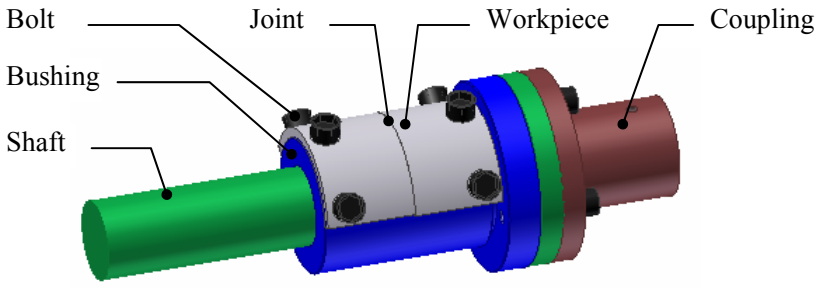

Figure 3.10: Clamping system for circular workpieces

3.3.3 Clamping System for Complex Curvature Workpieces

To check the performance of the intelligent monitoring and control system, experiments with workpieces of changing curvatures was carried out. A specific backing piece, which is locked onto the central shaft by a tapering bushing and nuts, was built to support workpieces with the same complex curvature during welding. The complex curvature workpieces and corresponding backing piece are shown in Figure 3.11. The detailed design drawings can be seen in Appendix C.

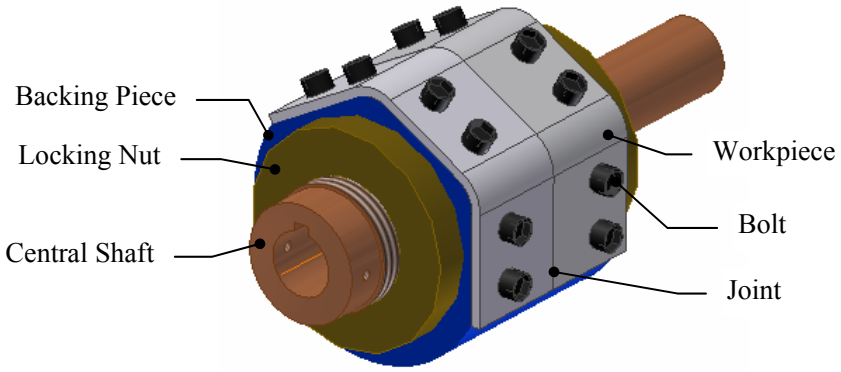

Figure 3.11 Workpieces with complex curvature

3.3.4 Tool Design

It was reported that during the FSW of thin sheets, the friction between the rotating tool shoulder and the material generates most of the heat, and the main function of the pin is to stir and control material flow around the tool at the weld joint to form a quality weld (Tomas *et al*., 2001).

Johnson indicated that heat input to the process is proportional to the tool area and tool rotation speed. He also concluded that shoulder diameter is proportional to the torque at a constant tool rotational speed, and that different pin diameters have virtually no effect on torque values (Johnson, 2001).

An adequate tool pin length was suggested for stirring up the oxide layers in the welds to prevent potential flaws (Kallee and Nicholas, 2002). Tool pin with a profiled surface was usually used to facilitate a downward auguring effect, which can be described as the tool gripping the plasticized material and pulling it in a downward direction (Blignault, 2005).

In practical tool design for complex curvature FSW, the size of the tool was also restricted by the following factors:

- Material thickness of the workpieces, which restricts the pin length, and

- The range of workpiece curvature radii, which restricts tool shoulder diameter in order to obtain full shoulder/workpiece contact.

Figure 3.12 shows the relative tool/workpiece position when the tool plunges into the material along the normal direction to the workpiece surface and full tool/workpiece contact is obtained. If the tool plunges into the material off the surface normal with the same plunge depth, reduced tool/workpiece contact can be expected.

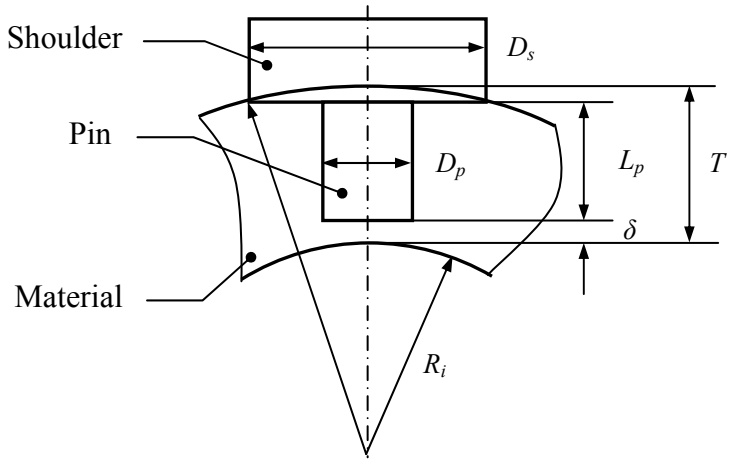

Figure 3.12: Relative position between tool and curving workpiece

Where:

D_s tool shoulder diameter

D_p tool pin diameter

T material thickness

L_p tool pin length

δ clearance between the top of tool pin and bottom of the workpiece

R_i workpiece curvature radius

The following expression can be inferred from Figure 3.10:

$$(R_i + T)^2 = \left(\frac{D_s}{2}\right)^2 + (L_p + \delta + R_i)^2 \tag{3.1}$$

Given the material thickness T, workpiece curvature radius R_i, clearance δ and pin length L_p, the maximum tool shoulder diameter with full tool/workpiece contact can be represented as

$$D_s = 2\sqrt{T^2 - (L_P + \delta)^2 + 2R_i(T - L_P - \delta)} \tag{3.2}$$

As can be seen, the tool shoulder diameter D_s increases with workpiece thickness T and curvature radius R_i, and decreases with clearance δ and pin length L_p. As mentioned in Chapter 2, if the tool pin is too short, insufficient material flow will be caused. The clearance δ is always held at a certain value to allow adequate plunge depth and prevent the tool from plunging into the back piece. Thus maximum tool shoulder diameter is mainly determined by the workpiece thickness and curvature radius.

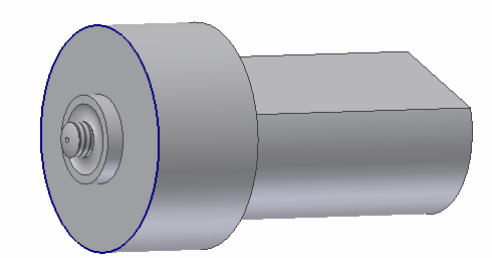

Figure 3.13: Tool designed for 3mm plates

Figure 3.13 shows the welding tool designed for 3mm thickness FSW. In this study, the material thickness is 3.18mm and 4.5mm and the range of workpiece curvature radii is from 15 to 47.5mm. When welding a workpiece with complex curvatures, the same tool was used to avoid tool changing. To make the effect of tool size and shape on weld quality consistent, the same tool was used in the experiment of workpieces with the same

thickness, but different curvature. Thus the smallest curvature radius of 15mm was used to determine the tool shoulder diameter for each workpiece thickness.

For 3.18mm thick material, the clearance δ and pin length L_p were chosen as 0.25mm and 2.3mm respectively. Using expression 3.2, the tool shoulder diameter was calculated as 10.73mm, which was rounded to 10mm. For 4.5mm material, the clearance δ and pin length L_p were chosen as 0.35mm and 3.5mm, thus the tool shoulder diameter was calculated as 10mm using equation (3.2). Thus 10mm was chosen as tool shoulder diameter for both material thicknesses. The ratio of shoulder diameter to pin diameter was chosen as 2.5, thus both pin diameters are 4 mm. Anti-clockwise threads was cut on the tool pin to enhance material flow during welding. The detailed tool drawings can be seen in Appendix C. Both of the tools were machined from W302 tool steel bar and then heat-treated according to certain procedures (Blignault, 2005).

3.4 Software Components for Complex Curvature FSW

In the real process of complex curvature FSW, the intelligent control system must respond quickly to the changing process conditions such as contact and energy into the tool/material. Additional software modules need to be integrated into the existing FSW software architecture.

Figure 3.14 shows the data flow in the proposed neuro-fuzzy controller for on-line monitoring and intelligent control. The on-line value of control variables $Y_{S(t)}$ at time t from the telemetry system and encoders are fed back and compared to the preset reference value $R_{S(t)}$. The error $E_{S(t)}$ were then mapped into the trained NN which presents the relationship between control variables and process parameters. The derived process

parameters were then compared to the preset process parameters $R_{U(t)}$, and the deviation of control variables and process parameters were then fuzzified into the FLC input and output MFs respectively to generate on-line fuzzy rules. The outputs from FLC were then scaled adapting to the trend of control variable deviation from the reference value to suggest a more reliable adjustment $\Delta_{U(t)}$ of process parameters. The sum of $R_{U(t)}$ and $\Delta_{U(t)}$ was used as the desired process parameters for the next time step. The whole neuro-fuzzy controller was integrated into the existing program to maintain the desired contact condition and energy into the tool/workpiece responding to the changing process environment. Chapters 4 and 5 describe the details of the implementation of the NN and FLC components.

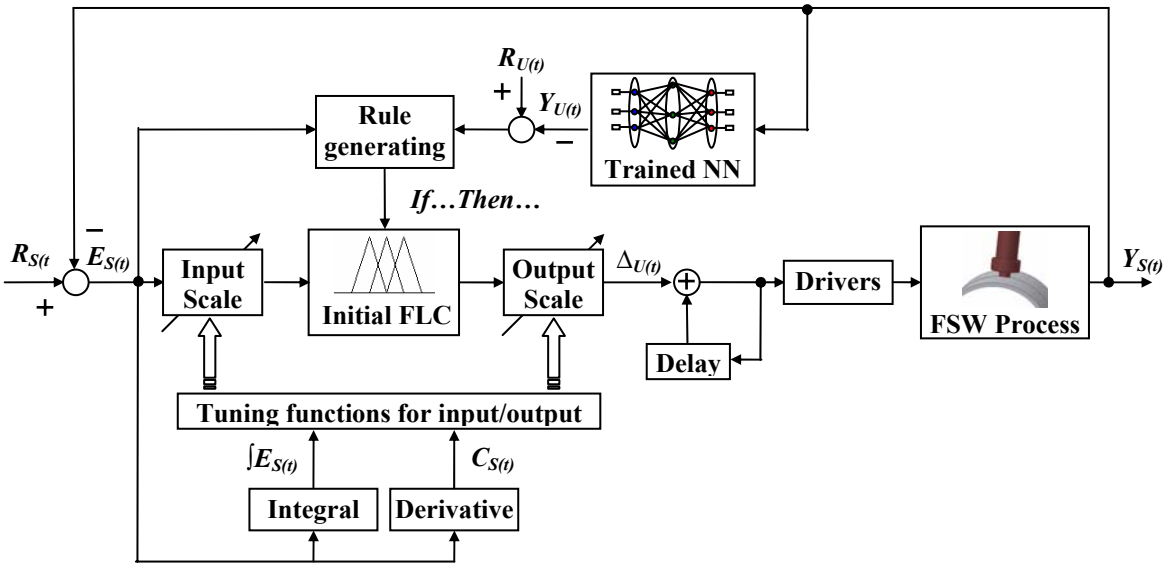

Figure 3.14: Data flow in the proposed intelligent controller for complex FSW

3.4.1 Brief Description of the Existing FSW Software Architecture

The existing FSW control software was developed in ANSI C and C++ programming language on the real-time operating system, QNX, and was designed based on Open

System Architecture principles. The QNX operating system supports the POSIX standard and allows each of the FSW software modules to be memory protected and scaleable. It provides various services for implementing the FSW software, including thread, signal, message-passing, synchronization, scheduling, timer, interrupt and process management. These advantages enable the existing FSW system to record process variables, obtain good response time, access recorded data, allow software modification and expansion, and be reliable (Kruger, 2003).

The existing FSW systems software is organized into a series of layers, each of which provides a set of services. Each layer defines an abstract machine whose machine language (services) is used to implement the next level of abstract machine. The layered architecture is changeable and portable, and supports incremental system development (Sommerville, 2001). The existing FSW system includes following layers (Kruger, 2003):

Layer 0: hardware Interface

Layer 1: Machine Level Control and Monitoring

Layer 2: Process Level Control and Monitoring

Layer 3: Network Distributed User Interface

3.4.2 On-line Monitoring and Intelligent Control Module

The proposed on-line monitoring and intelligent controller was developed using MATLAB together with its neural network, fuzzy logic and simulation toolboxes.

MATLAB was chosen as the developing environment for the following reasons (The MathWorks, 2004c):

- It is a powerful mathematical computing engine that includes an extensive catalogue of functions and toolboxes, an environment in which to develop customer functions and scripts, and the ability to import and export to many types of data files.

- MATLAB provides interfaces to external routines written in other programming languages such as C and Fortran, and for data that needs to be shared with external routines.

- MATLAB engine library is a set of C or Fortran routines that can be used to start or end the MATLAB process, send data to or from MATLAB and send commands to be processed in MATLAB. Instead of requiring that all of MATLAB be linked to a customer program, only a small engine communication library is needed.

The proposed software implementation of the on-line monitoring and intelligent controller and its interface to the existing FSW software are shown in Figure 3.15. The existing software coded in C and C++ was installed on the machine server on the QNX platform. The neuro-fuzzy intelligent controller was installed on the client on a Windows operation system. The FSW machine server was connected to and communicates with the client using Ethernet and the TCP/IP protocol. On-line sensor data from the welding process was sent from server to client for process status recognition; decisions made by

the neuro-fuzzy controller are called back to C programs in the FSW software of the server.

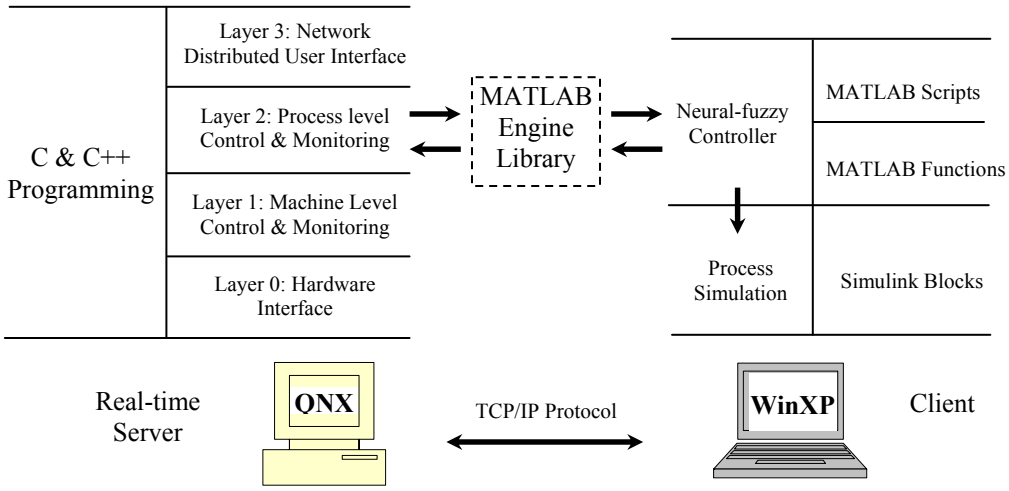

Figure 3.15: Proposed neural-fuzzy controller and its interface to existing FSW system

The intelligent neuro-fuzzy controller was developed with MATLAB 7 and corresponding toolboxes. M-File functions and M-File scripts were coded to implement the controller. Basic Simulink blocks, together with the Fuzzy Logic Toolbox and Neural Network blockset were used to model, simulate and analyse the dynamic process of complex curvature FSW.

MATLAB engine library was used to start and stop the MATLAB process, and send on-line data to the intelligent neuro-fuzzy controller by C programs in the FSW software system. FSW process condition is recognized by analyzing information sent from the server with MATLAB functions and scripts in the neuro-fuzzy controller. Recommended process parameters adjustments to maintain correct contact and energy into

tool/workpiece are then fed back to C & C++ programs in the FSW software with MATLAB engine library. The recommended process parameters adjustments were implemented by sending commands to the corresponding inverters and motors from the FSW software system. The information to and from the neuro-fuzzy controller was also sent to the Simulink model for simulating and displaying the FSW process for complex curvature.

3.4.3 Process Modelling and Simulation

To visualise and simulate the process of complex curvature FSW, a graphic user interface with process simulation was composed. MATLAB GUIDE, Simulink blocks and corresponding M functions and scripts were used to simulate the intelligent neuro-fuzzy controller and process condition. GUIDE, the MATLAB Graphical User Interface development environment, provided a set of tools for creating GUIs. GUIDE also automatically generated an M-file that controled how the GUI operated. The M-file initialised the GUI and contained a framework for all the GUI callbacks -- the commands that were executed when a user clicked a GUI component.

Figure 3.16 shows the GUI and its M-file created for starting process simulation of intelligent complex curvature FSW. The desired process parameters were preset in textbox of the GUI. In this example, the preset parameters are 600 rpm, 100 mm/min, 0.2mm and 0.5° for spindle speed, feed rate, plunge depth and tilt angle respectively. The reference values of sensor data are derived as 275 °C, 20 Nm, 1.75 kN and 335 N for temperature, torque, Fz and bending force respectively with NN mapping. Sensor data

acquired from manual input, recorded data or on-line process are then input into the model and compared to reference values for simulating and plotting the simulation result.

(a)

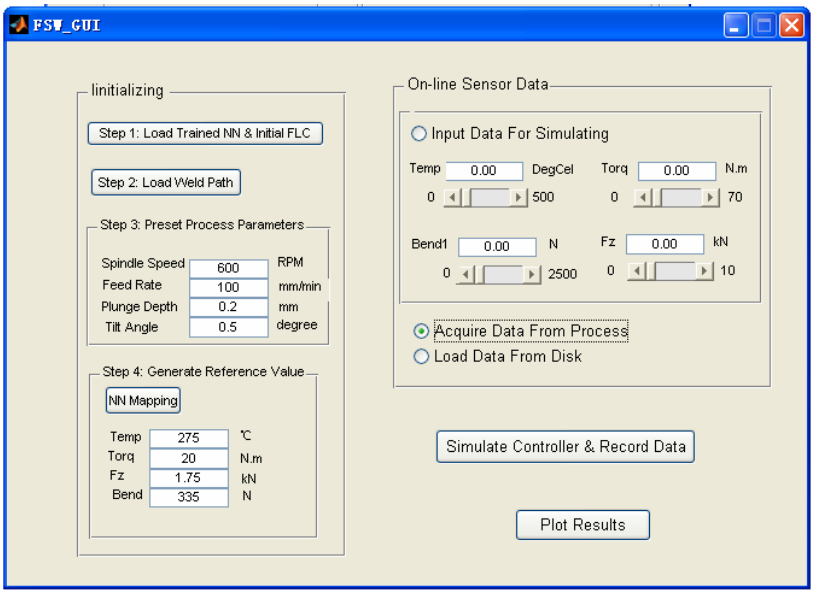

(b)

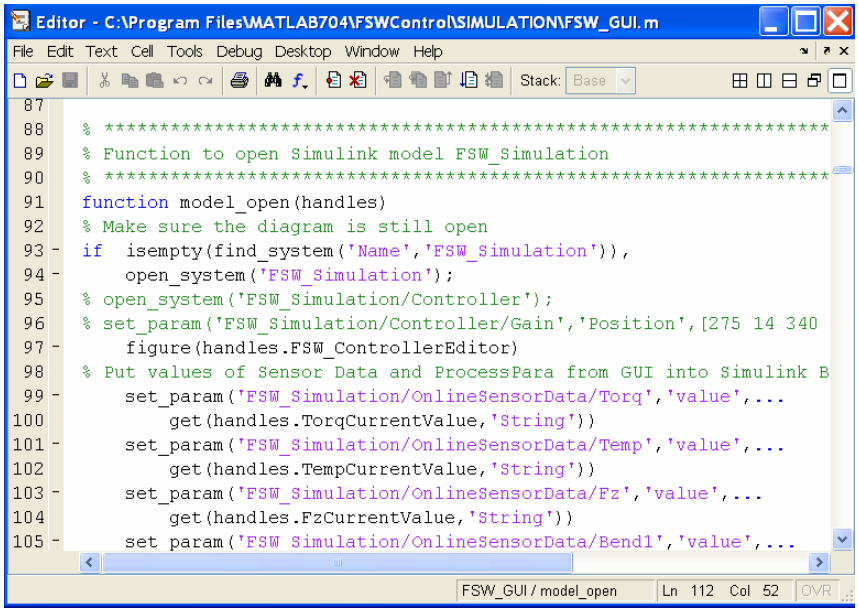

Figure 3.16: Graphical user interface for on-line FSW process simulation

Simulink is a software package for modelling, simulating, and analyzing dynamic systems. It supports linear and non-linear systems, modelled in continuous time, sampled

time, or a hybrid of the two. The simulation of FSW in this study is implemented with Simulink due to the following reasons (The MathWorks, 2004d):

- It is integrated with MATLAB, thus the model built can be interactively simulated, analysed, revised and visualised in either environment at any point;

- It provides a comprehensive block library of commonly used sinks, sources, and mathematic functions. Furthermore, it provides blocks in the Fuzzy Logic Toolbox and Neural Network Blockset to simplify the building of the neuro-fuzzy controller. Customized blocks can also be built to realize specific functions.

- The Simulink model is hierarchical, thus it can be built using both top-down and bottom-up approaches. This approach provides insight into how a model is organised and how its parts interact.

- Using scopes and other display blocks in the Simulink library, the simulation results can be visualised while the simulation is running. In addition, model and block parameters can be interactively changed to see the effects immediately.

Figure 3.17 shows the overall Simulink block diagram for FSW process simulation. The hierarchical model is composed of Simulink blocks and subsystems. Starting the simulation is controlled in the GUI shown in Figure 3.14. This model was built with Simulink blocks, Neural Network Blockset and Fuzzy Logic Toolbox. Two NN blocksets were used in process simulation: one for setting reference values of sensor data; the other for deriving fuzzy rules for the initialized FLCs. Data generated during simulating can be recorded in the workspace and used to implement process animation and result plotting.

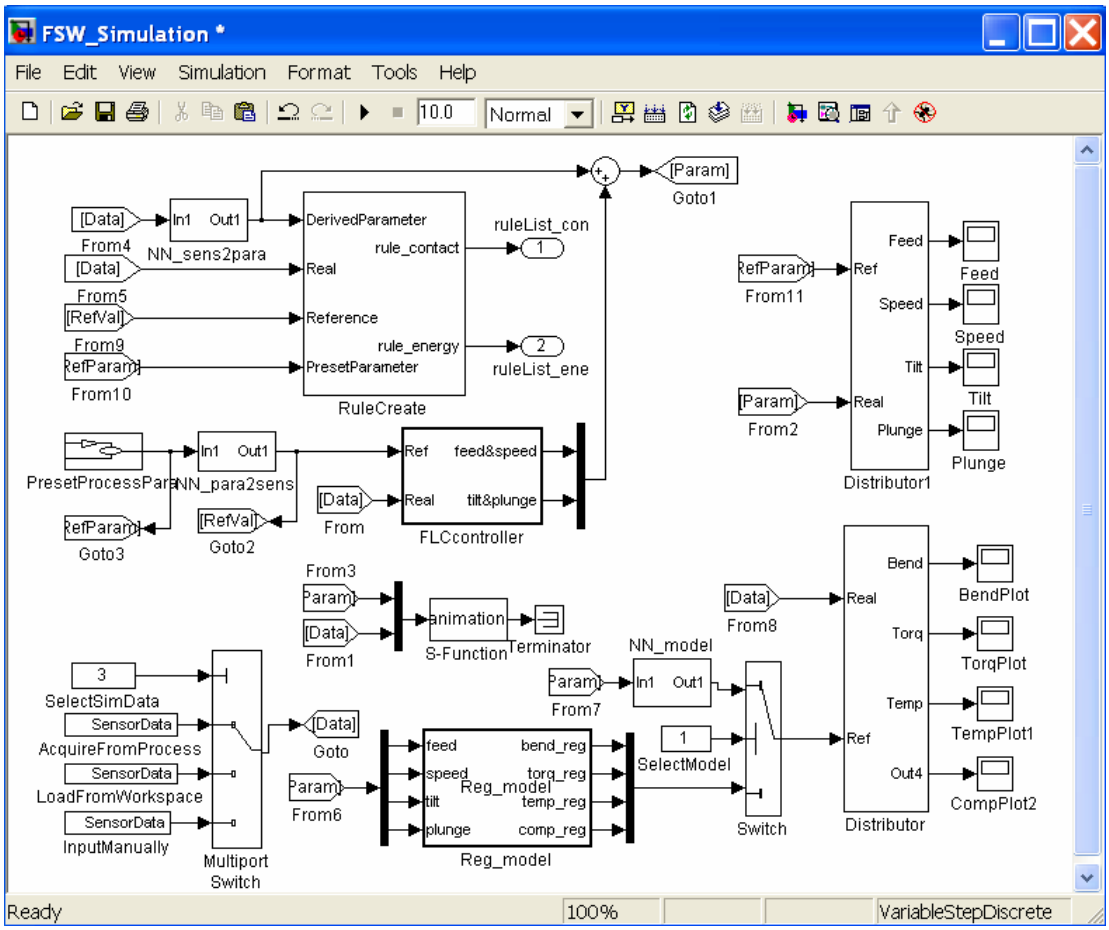

Figure 3.17: Simulink block diagram for on-line process simulation

3.4.3.1 Fuzzy Control Subsystem

The fuzzy control subsystem consists of two parallel-working FLCs, input normalising blocks and output scale tuning blocks. The two FLC blocks load the fuzzy inference systems from the workspace. The fuzzy inference systems in the workspace were updated on-line with new fuzzy rules which were generated from the fuzzy rule generation subsystem. Inputs to the FLCs were normalized into [-1 1] before being fed into the FLCs. Outputs from the FLCs were tuned on-line by the output scale tuning blocks adapted to

process trends. Figure 3.18 (a) and (b) shows the SIMULINK block diagram of the fuzzy control subsystem and the embedded M function for output tuning.

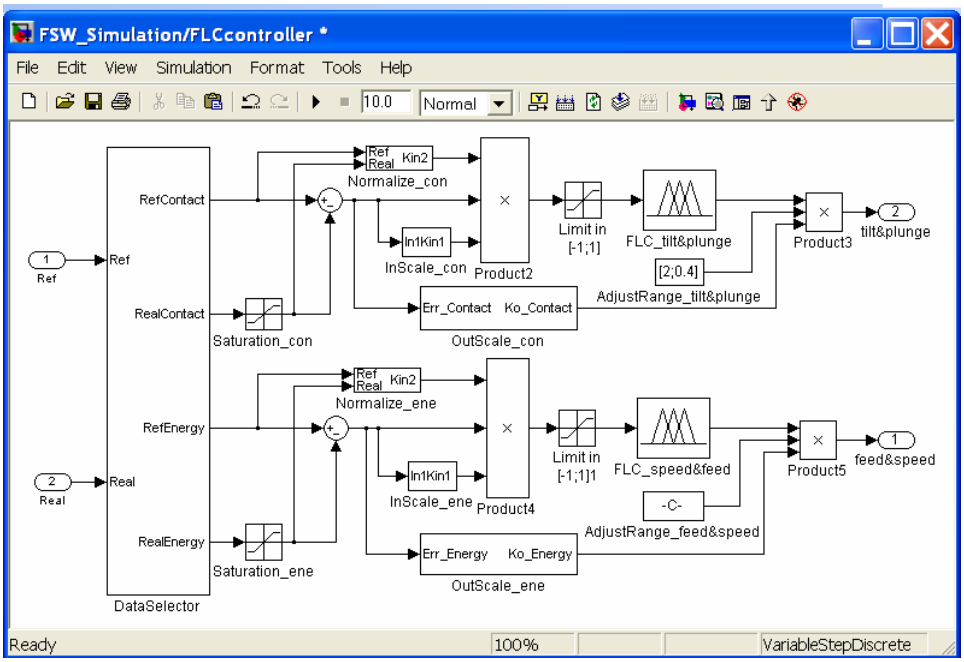

(a)

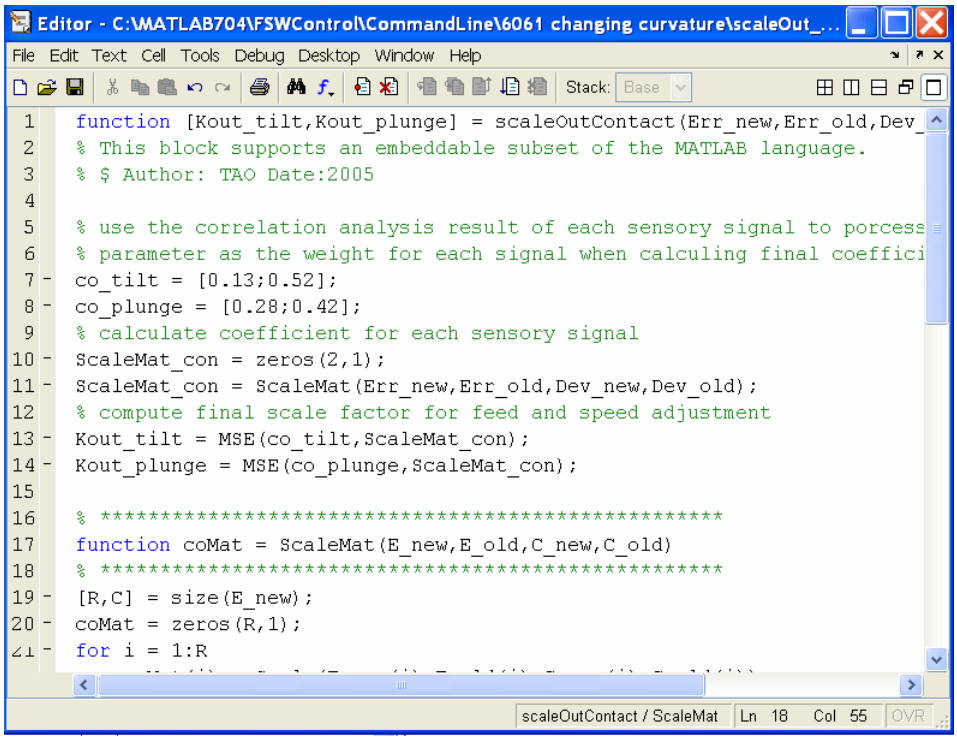

(b)

Figure 3.18: Simulink block diagram and M-file for fuzzy control subsystem

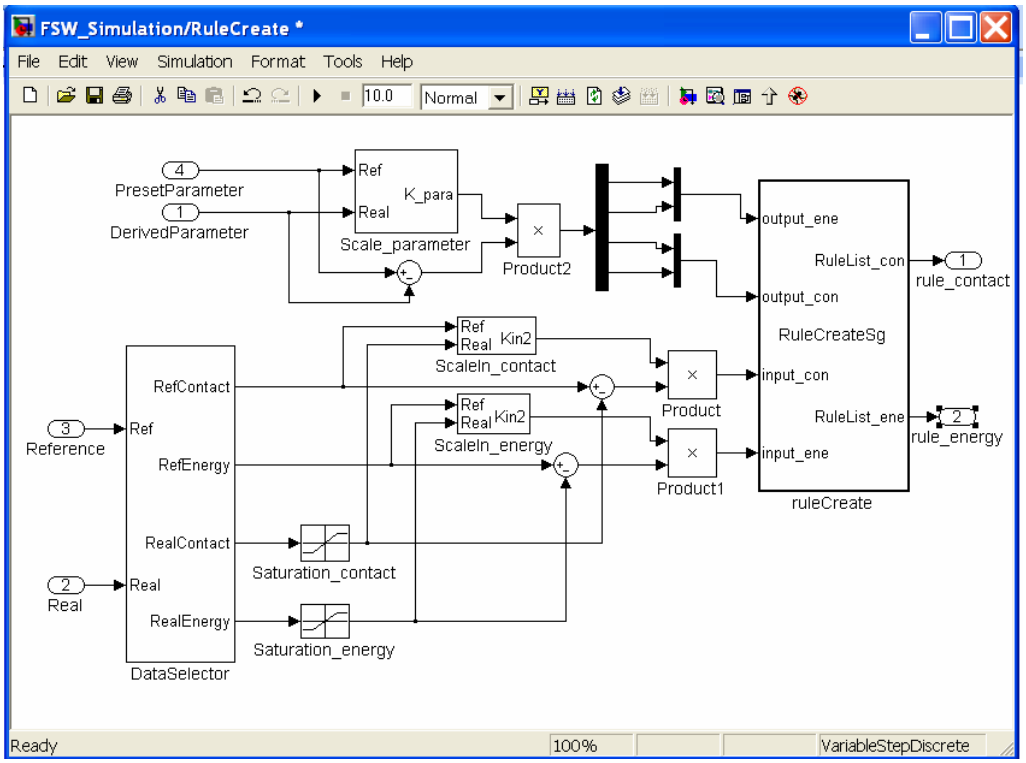

(a)

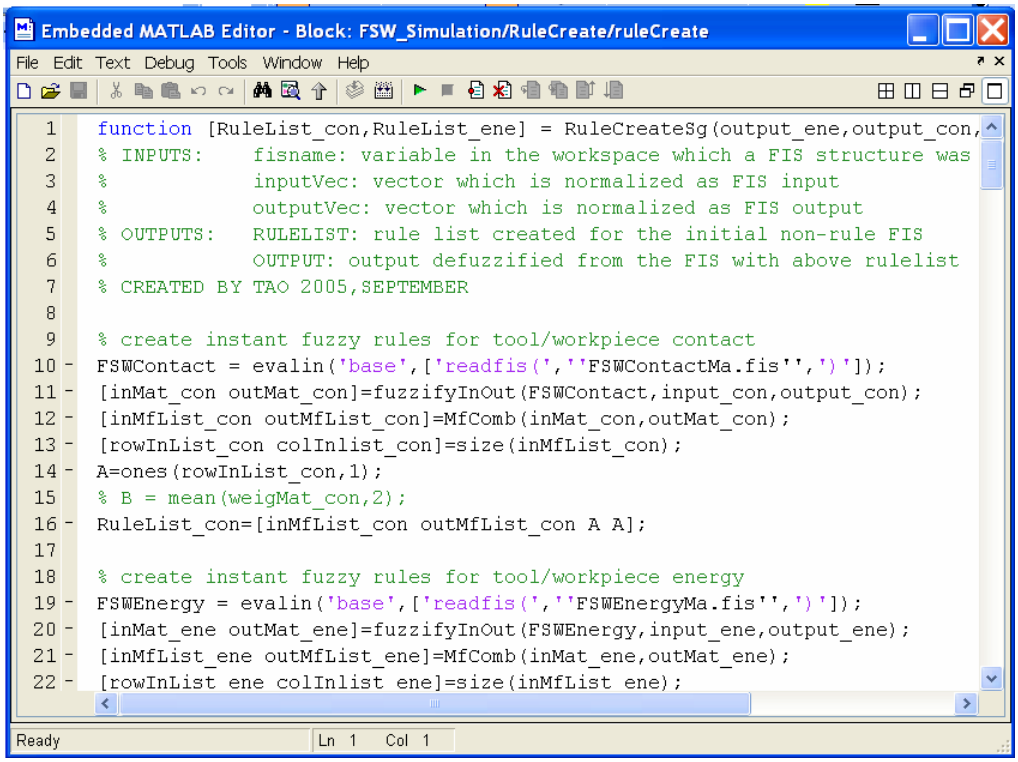

(b)

Figure 3.19: Simulink block diagram and M-file for fuzzy rule generation subsytem

3.4.3.2 Subsystem of Rule Create

Figure 3.19 shows the SIMULINK blocks (a) and the embedded M function (b) of the fuzzy rule generation subsystem. With the error of input on-line sensor data to their reference values and the difference between NN derived instant process parameters and preset process parameters, the subsystem is used to recommend 'if-then' fuzzy rules for the FLC blocks in fuzzy control subsystem.

3.5 Summary

The overall system hardware and software setup needed for the establishment of the proposed intelligent monitoring and control system for complex curvature FSW was described in this chapter. An additional rotational axis and clamping systems are designed for workpiece locating and holding. Software module for process monitoring and control and its interface to existing FSW software architecture is proposed.

A table-tilting multi-axis system for complex curvature FSW was established by integrating an additional rotation axis including electric motor, speed reducer, main shaft and encoder to the existing FSW machine. Clamping systems for flat plate, round tube and complex curvature workpiece were designed for holding and locating different curvature workpieces. A special tool and workpiece were also machined with analysis of complex curvature for experiments.

A neuro-fuzzy controller integrating non-linear fuzzy control, on-line rule generation and adaptive tuning mechanism for complex curvature FSW was proposed. MATLAB language was chosen as programming tool for the intelligent controller owing to its

powerful computing ability, external interface to external routines and availability of multiple toolboxes such as NN and FL. The MATLAB engine library was used to communicate between the intelligent neuro-fuzzy controller and C programs in the multi-layered FSW software architecture.

The GUI, SIMULINK model library, Fuzzy Logic Toolbox, Neural Network Blockset and M-files of MATLAB were integrated to perform simulation of the proposed neuro-fuzzy controller for complex curvature FSW.

Chapter 4 Multi-sensor Fusion Model for Tool/workpiece Contact and Energy Input Monitoring during Complex Curvature FSW

To measure and estimate process variables, a broad spectrum of on-line sensors, signal processing schemes and various model-based calculations have been proposed to retrieve information relevant to machining process conditions (Liang *et al*., 2004). During complex curvature FSW, process parameters and sensor signals may deviate from reference values due to curvature changing and other reasons. To maintain tool/workpiece contact and energy input, which dominates the weld properties (Peel, *et al*., 2003; Chen and Kovacevic, 2003), a multi-sensor fusion model is proposed for tool/workpiece contact condition and energy input monitoring, as shown in Figure 4.1. Using statistical analysis of experimental results, sensitive features that characterizing tool/workpiece contact and energy input were selected as NN training data for sensor fusion modelling and on-line fuzzy rule generation. Sensor features and process parameters may be also used as process control variable for FL controlling. The details of fuzzy rule generation and FL control are described in Chapter 5.

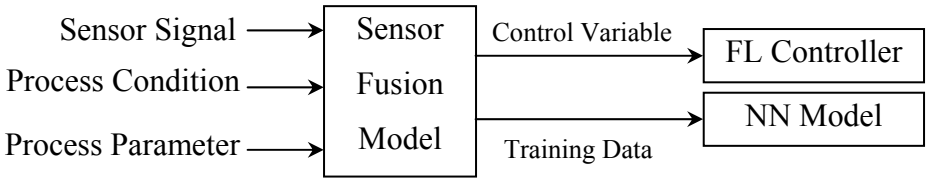

Figure 4.1: Sensor fusion model for tool/workpiece contact and energy input monitoring.

Section 4.1 introduces the methods used in FSW process monitoring and sensor fusion. Section 4.2 describes the process to perform sensor fusion by statistical analysis and NN training with experimental data. Section 4.3 explains the experimental design and data acquisition methods. Section 4.4 provides the details of sensor fusion modelling including sensitive feature selection and NN training with the MATLAB language (The MathWorks, 2004c). A summary of this chapter is given in section 4.5.

4.1 Introduction

Currently, the research of monitoring and control of FSW is mainly focused on straight welds. Effects of process parameters such as feed rate, spindle speed and tool size on fatigue life, tensile strength, weld crack and residual stress of FS welds in aluminum and other materials have been investigated (James, *et al*., 2003; Reynolds, *et al*., 2003; Nakata, *et al*., 2001; Ericsson and Sandström, 2003). An input torque based model of temperature distribution and thermal history prediction is introduced by Khandkar *et al*. (2003). Chen and Kovacevic (2003) presented both a heat transfer model and a mechanical model using a finite element method. Song and Kovacevic (2003) proposed a heat transfer model of FSW in a moving coordinate system. Chen *et al*. (2003) used wavelet transform analysis of acoustic emission in monitoring FSW of Al 6061 aluminium.

Tool/workpiece contact conditions play a critical role in thermal input between tool and workpiece, which dominates weld properties (Peel, *et al*., 2003; Chen and Kovacevic, 2003). During complex curvature FSW, physical condition changes dynamically due to complexity. The optimised process parameters for certain material and thickness need to be adaptable for different curvature. The relationship between sensor signals and

tool/workpiece contact and thermal input must be investigated, and a multi-sensor fusion model for tool/workpiece contact and energy input prediction needs to be built.

During FSW processing, various signals are emitted from the machine tool. Although these signals can provide useful information for process monitoring, some of them may include a significant amount of noise and are thus unsuitable for monitoring purposes (AI-Habaibeh, *et al*., 2002). In order to extract useful information from process sensor data, several stages of signal processing and data analysis are normally needed.

The measurement of tool/workpiece contact condition and energy input can be done by direct or indirect methods. Direct sensing method using contacting sensors are usually not effective due to wear, vibration and chip evacuation problems, while non-contacting direct sensing are impractical mainly due to the interference of chips and noise (Birla, 1980). Indirect sensing methods can use a mathematical model to estimate the value of investigated characteristics with on-line measured physical quantities. Sensor signals such as force, torque, temperature, power and vibrations etc., have been successfully applied in indirect sensing (Van Niekerk, 2001; Liang *et al*., 2004; O'Donnel *et al*., 2001; Chittayil *et al*., 1992; Jiaa and Dornfeld, 1998; Kuo, 2000; Rangwala and Dornfeld, 1987;Azouzi and Guillot, 1997).

Sensor fusion is a method of integrating signals from multiple sources to provide a robust prediction of one or more machining attributes with a fusion model (Sasiadek, 2002; Guillot, *et al*., 1994). Sensor fusion mainly consists of two components: selecting sensitive signals as good candidates and establishing proper relationships between the sensed variables and the investigated features. With sensor fusion, only basic sensors,

which reliably measure different variables in an industrial environment, are selected for on-line process monitoring (Azouzi and Guillot, 1997).

Azouzi and Guillot (1997) presented an exhaustive analysis to determine the most sensitive process parameters (feed, depth of cut, cutting velocity) and signals (AE, forces, vibration) to predict the surface roughness and the final diameter error in machining. In this study, on-line sensor signals of Fz, temperature, torque, bending force and the ratios between them were investigated to select candidates for sensor fusion modelling.

To establish the relationship between sensed variables and the investigated features, two distinct methods were used: theoretical and empirical. Theoretical techniques normally include a great deal of simplification because of the poor understanding of fundamental behavior of machining processes, which makes them difficult to implement in real industrial environments. Empirical modelling uses experimental work to evaluate process performance (Ulsoy and Koren, 1993; Mashimoto, *et al*., 1996). As recommended by Rangwala and Dornfeld (1987), easily available information during the operation of the process can be used to build the empirical fusion model. Various techniques such as multiple regression, the group method of data handling or neural networks are implemented in building sensor fusion models (Liang *et al*., 2004; Azouzi and Guillot, 1997). Neural network (NN), which has the ability to learn relationships among input and output data sets through a training process, was chosen in this study to 'induce' the investigated features if a new set of sensed variables were made available (The MathWorks, 2004b).

4.2 Process of Multi-sensor Modelling

Plunge depth and tilt angle of welding tool to workpieces co-operate to determine tool/workpiece contact conditions. For workpieces with uniform curvature, the well pre-planned tilt angle and plunge depth may not be maintained due to process disturbances. Figure 4.2 (a) shows that either insufficient or excessive plunge depth can cause either insufficient or excessive tool/workpiece contact. Figure 4.2 (b) shows that excessive tilt angle can cause either insufficient or excessive tool/workpiece contact. During complex curvature FSW, tilt angle and plunge depth need to be adaptive to changing curvature in order to maintain tool/workpiece contact. Figure 4.2 (c) shows that with the same tilt angle and plunge depth, tool/workpiece contact is partly lost when the tool is moving from a larger curvature radius zone towards a smaller curvature radius zone of a complex curvature workpiece.

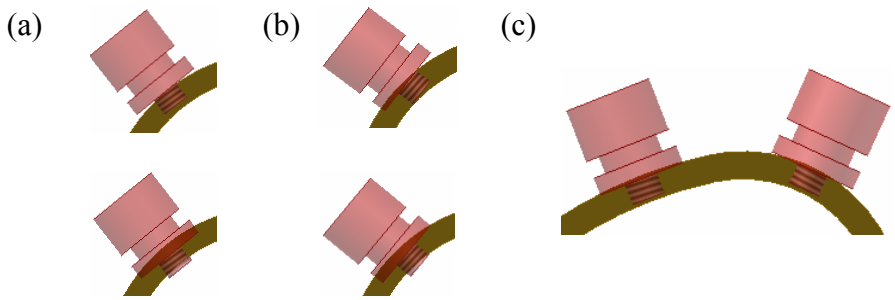

Figure 4.2: Incorrect tool/workpiece contact due to (a) incorrect plunge depth, (b) incorrect tilt angle and (c) changing curvature

Except plunge depth and tilt angle, spindle speed and feed rate have significant effects on tool/workpiece thermal input, which is manifested in the resulting temperature observed during welding (Nakata *et al*., 2001; Reynolds *et al*., 2003). Thus to monitor and maintain

tool/workpiece contact and energy input, a sensor fusion model which represents sensed variables and process parameters must be established.

Statistical tools and NN modelling techniques were used to select sensors and build a fusion model for on-line monitoring of complex curvature FSW. Experimental data including force, torque, bending force and temperature obtained under a variety of machining parameters and conditions were first used to select sensors with high sensitivity to tool/workpiece contact and energy input (Kuo, 2000). NNs with different structures with different training algorithms were trained and compared to select the one with smallest error between NN outputs and target values. Inputs for NN training are selected based on the orthogonal array (OA) experimental results. Both the statistical analysis and NN training were implemented in a MATLAB program. Figure 4.3 shows the proposed procedure for sensor selection and fusion.

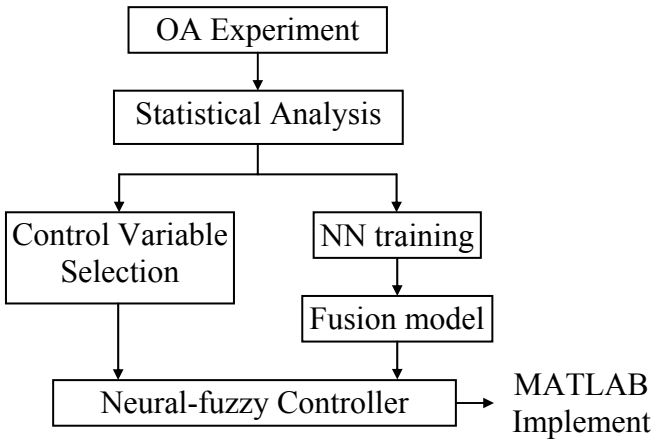

Figure 4.3: Process of sensor fusion modelling

4.3 Experimental Data Acquisition

Based on the existing FSW system, experiments of aluminium samples with flat bars and round tubes of different curvature were conducted to acquire sufficient information for sensitive feature selection and sensor fusion. Under different process conditions such as material, thickness, and curvature, various process parameters of feed rate, spindle speed, plunge depth and tilt angle were used to record on-line sensor data of torque, bending force, Fz and temperature. Tensile, bending and fatigue tests were usually used to evaluate the mechanical properties of weld samples. In this study only tensile test was carried out for flat bar samples. Figure 4.4 shows the welding cause-effect diagram.

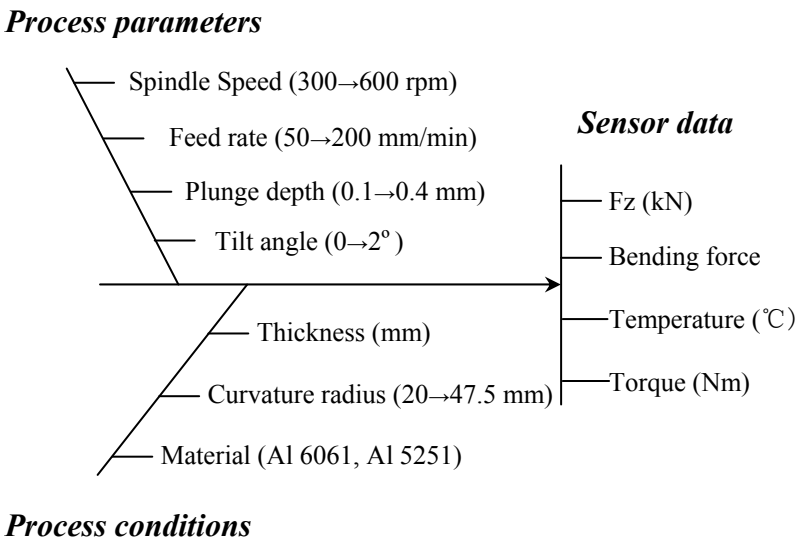

Figure 4.4: Cause-effect diagram of FSW

4.3.1 Material

Al 6061 flat bars and round tubes, and Al 5251 sheets were used for FSW. The thicknesses of Al 6061 flat bars and round tubes were both 3.18mm. The thicknesses of

Al 5251 flat bars were 3mm and 4.5mm respectively. The flat bars and tubes were commercially available, and their chemical compositions and mechanical properties are shown in Table 4.1 (Aluminium City, 1999) and Table 4.2 respectively (Malan and Paterson, 1987).

Table 4.1: Chemical composition limits of alloy Al 5251 and Al 6061(wt %)

Element	Si	Fe	Cu	Mn	Mg	Cr	Zn	Ti	Others
5251	0.40	0.50	0.15	0.1-0.5	1.7-2.4	0.15	0.15	0.15	0.15
6061	0.4-0.8	0.7	0.15-0.4	0.15	0.8-1.2	0.04-0.35	0.25	0.15	0.15

Table 4.2: Mechanical properties of alloy Al 5251 and Al 6061

Property	0.02% Proof Stress MPa	Ultimate Tensile Strength MPa	Elongation A_5 %	Brinell Hardness HB	Thermal Conductivity At 100 ˚C W/m˚C	Formability
5251	60 (100)	170(195)	14(20)	(40)	134	very good
6061	160 (250)	185(245)	7(13)	(63)	180-218	severe

4.3.2 FSW Condition

Efficient experimental method Orthogonal arrays (OAs) developed by Taguchi (Ross, 1995) was chosen to minimize the number of tests. Another advantage of OA design is its equal representation of all factors. Some combinations of factors and factor levels were also investigated. Influence of each experimental factor on experimental results, or in other words dependency of a result on an experimental factor, was investigated in OA design. In this study, L16_4_5 and L18_3_7 OA experiments were chosen for flat bars of

Al 5251 and Al 6061 alloy and round tubes of Al 6061 alloy respectively. The process parameter factor-level table for flat bars and round tubes is shown in Table 4.3.

Table 4.3: Process parameter factor-level table for FSW experiment

Factor & level		Feed rate (mm/min)	Spindle Speed (rpm)	Tilt angle (°)	Plunge depth (mm)	Tube diameter (mm)
Flat Bar	Level 1	50	300	0	0.1	
	Level 2	100	400	0.5	0.2	
	Level 3	150	500	1	0.3	
	Level 4	200	600	2	0.4	
Round Tube	Level 1	50	400	0	0.1	40
	Level 2	100	500	1	0.2	70
	Level 3	200	600	2	0.4	95

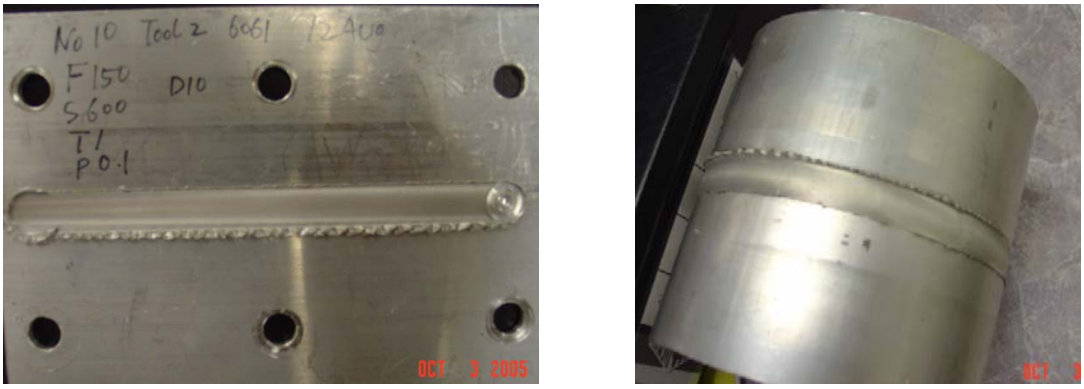

(a) Flat plate (b) Round tube

Figure 4.5: Aluminium flat plate and round tube welded at NMMU

Figure 4.5 shows the experimental samples welded in this study at NMMU. Sensor signals of temperature, torque, bending force, and Fz were acquired from the telemetry system with a sampling time of 0.001 second and then processed so that only the steady-state portions were kept and averaged. The sensor data of Al 5251 and Al 6061 alloy flat

bar welds is shown in Table A.1 and Table A.2 respectively in Appendix A. The processed sensor data of round tube is shown in Table A.3 in Appendix A.

4.4 Sensor Fusion Modelling for Tool/workpiece Contact and Energy Input

Sensor data acquired during OA experiments were first preprocessed to obtain the steady-state portion. The processed data were then analyzed with OA and additional statistical methods to select proper candidates which are sensitive to tool/workpiece contact and energy input. With NN training, the selected sensor features were finally used to establish the tool/workpiece contact and energy input fusion models, which were later used to generate on-line decision, in other words, on-line fuzzy rules of the FL controller.

Sensor data acquired during OA experiments include the complete welding period of plunging, dwelling, feeding and extracting. To obtain reliable sensor values under certain process parameters and condition, data recorded during plunging, dwelling, withdrawing, and the starting and ending portions of the feeding period were first eliminated from the data set. The rest of the data were then preprocessed by removing outliers greater than three standard deviations of the rest of the data. The average of the preprocessed data set was used as final sensor values for further sensitive feature selection.

Figure 4.6 shows the original and preprocessed torque data of one sample obtained under process parameters: feed 150mm/min, speed 400 rpm, tilt angle 0°, and plunge depth 0.3mm. The final value of torque for this sample is thus the average of preprocessed data 29.18 Nm.

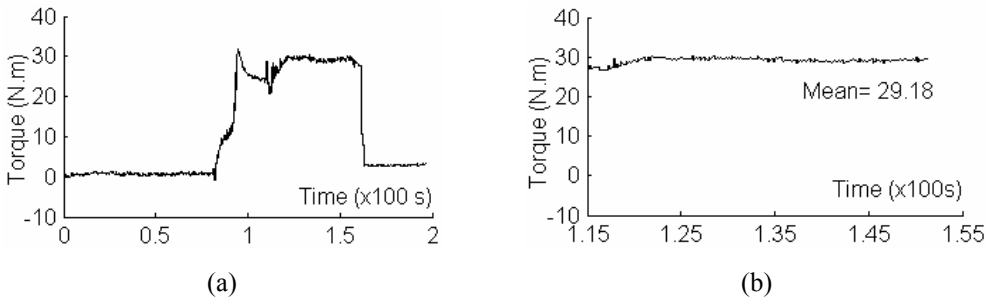

(a) (b)

Figure 4.6: Diagrams of (a) original torque data and (b) preprocessed torque data

4.4.1 Statistics Analysis

Data from OA experiments were analyzed using the following statistical tools: (1) the average effect of each factor level on sensor measurements, (2) the significance estimation of each factor under certain confidence levels and (3) the correlation between process parameters and sensor measurements.

Figure 4.7 shows the average effect of each factor level on sensor measurements with the data obtained from 3.18mm Al 6061 and Al 5251 alloy flat bar welds. The plotted points correspond simply to the average of all observations under each factor level. It can be concluded that all the sensor data are affected at different degrees by each process parameter. Temperature seems to be more sensitive to process parameter changes. In the process parameters, spindle speed seems to have stronger influence on sensor data than the other parameters. It also shows that for Al 6061 and Al 5251 alloy, most of the sensor measurements have the same changing trend with process parameter changes, while the averages bending force, torque, temperature and Fz from each factor level of Al 5251 alloy are significantly lower than Al 6061 alloy. This can be explained by their mechanical properties as shown in Table 4.2. Al 5251 alloy is a softer material with better

formability, thus lower force is caused during welding using the same process parameters, while Al 6061 alloy has better thermal conductivity. More heat is propagated from tool/workpiece contact area to the area to be welded whilst higher temperature is generated.

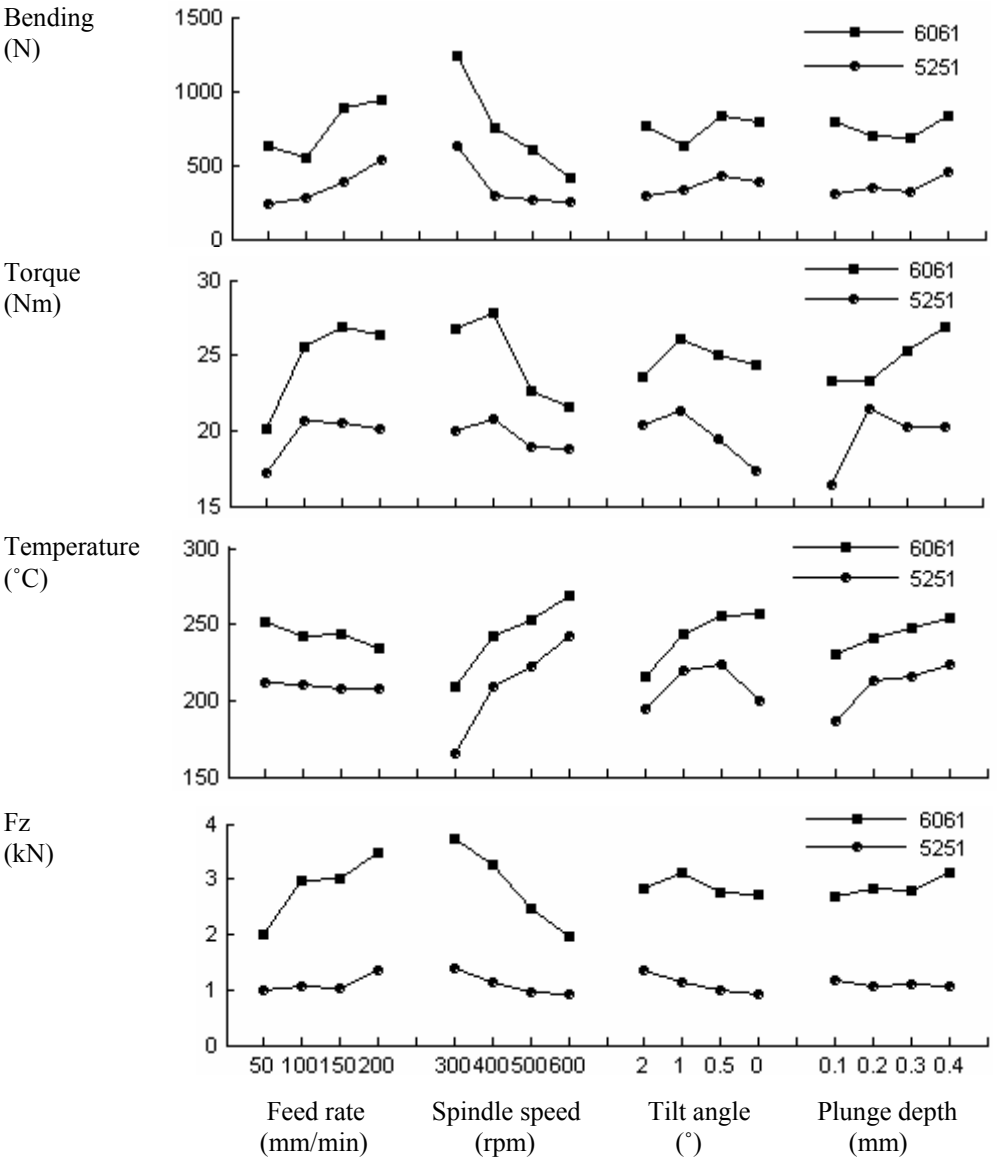

Figure 4.7: Effects of process parameters on sensor measurements of flat bar friction stir welds

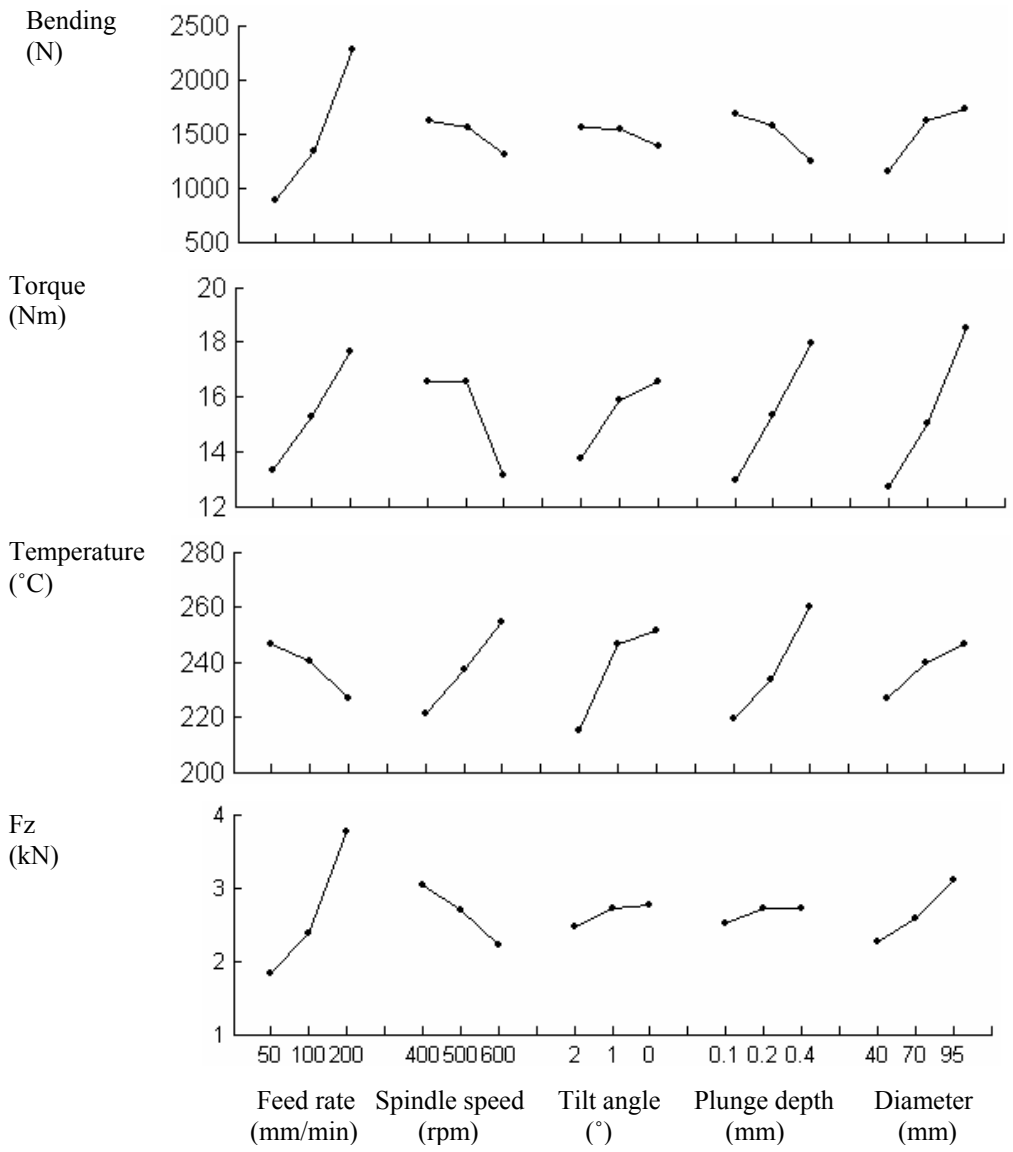

Figure 4.8: Effects of process parameters on sensor measurements of round tube friction stir welds

Figure 4.8 shows the average effect of each factor level on sensor measurements with the data from 3.18mm Al 6061 round tube welding. From the figure, it can be concluded that besides process parameters of feed, speed, tilt and plunge, the process condition of curvature radius also significantly affects sensor data. It is also shown that the temperature and all the forces increase with curvature diameter. This can be explained by

the tool/workpiece contact condition: with smaller curvature radius, less tool/workpiece contact is obtained, and thus less force and temperature are generated due to less friction between tool and workpieces during welding.

Using ANOVA of the OA experiment, the percentage contribution of each factor to each experimental measurement variance is calculated. F ratio is used to determine the significance level of a factor to an experimental measurement under a certain confidence level. The F ratio is the ratio of squares of deviation obtained from a factor to the squares of deviation generated from random error. Table 4.4 shows the percentage contribution and significance level of each process parameter on experimental measurements with F critical ratio 9.28 ($\alpha = 0.05$) of data collected from the OA experiments of Al 6061 and Al 5251 plate welds.

Table 4.4: Variance analysis of Al 6061 and Al 5251 alloy plate welds

Factors		Bending force		Torque		Temperature		Fz	
		Percentage	significance	Percentage	significance	Percentage	significance	Percentage	significance
6061	Feed	20.11%		38.50%		4.56%		35.05%	*
	Speed	69.46%	*	35.80%		55.05%	*	56.55%	*
	Tilt	4.29%		4.13%		30.85%	*	2.93%	
	Plunge	2.93%		11.89%		8.75%	*	3.17%	
	error	3.22%		9.68%		0.79%		2.29%	
5251	Feed	28.10%	*	20.27%		0.22%		25.86%	*
	Speed	56.23%	*	6.41%		64.74%	*	38.06%	*
	Tilt	5.57%		21.69%		12.22%		31.81%	*
	Plunge	7.19%		34.77%		16.39%		2.06%	
	error	2.91%		16.86%		6.42%		2.20%	

It can be seen from the table that Al 6061 and Al 5251 have similar variance distribution. Spindle speed is the most significant factor on all the sensor signals except torque. Temperature is the most sensitive signal to process parameters of Al 6061 plate welding, as it is significantly affected by spindle speed, tilt angle and plunge depth. Fz is the most sensitive signal to process parameters in Al 5251 plate welding, as it is significantly affected by feed rate, spindle speed and tilt angle in Al 5251 plate welding. It can be concluded that both temperature and Fz are good candidates for FSW process monitoring.

Table 4.5: Variance analysis of Al 6061 alloy round tube welds

Factors	Bending force		Torque	Temperature		Fz
	Percentage	significance	Percentage	Percentage	significance	Percentage
Feed	71.42%	*	16.61%	7.79%		68.52%
Speed	3.18%		13.69%	21.09%	*	11.34%
Tilt	1.58%		7.76%	30.16%	*	1.57%
Plunge	8.24%		22.67%	33.08%	*	0.89%
Curvature	14.10%		30.88%	7.38%		12.07%
error	1.48%		8.39%	0.50%		5.61%

Table 4.5 shows the percentage contribution and significance level of the process parameters (feed, speed, tilt angle and plunge depth) and the process condition (curvature diameter) on sensor data obtained in Al 6061 round tube welding experiments. It also shows that temperature is the most sensitive signal to spindle speed, tilt angle, and plunge depth. Thus temperature is chosen as the sensor signal for process monitoring.

Both the flat plate and round tube experimental data show that the error contributions associated with sensor signals are acceptable (less than 8%). This implies that the most important process conditions and parameters that influence these characteristics were included in the experiment (Azouzi and Guillot, 1997).

In order to further investigate relationships between process parameter and sensor data, correlation coefficient, a normalized measure of the strength of the linear relationship between two variables, was used in this study to investigate the dependency of a sensor signal, or the ratio of two sensor signals, on a process parameter (The MathWorks, 2004c). The correlation efficient *r(x, y)* of variable *y* to variable *x* is calculated as:

$$r(x,y) = \frac{\sum (x_i - \bar{x})(y_i - \bar{y})}{\sqrt{\sum (x_i - \bar{x})^2}\sqrt{\sum (y_i - \bar{y})^2}} \tag{4.1}$$

Where:

x_i the *i*th element of variable x

$\bar{x}$ the mean value of variable x

y_i the *i*th element of variable y

$\bar{y}$ the mean value of variable y

Table 4.6 shows the correlation coefficients of process parameters (e.g. feed, speed, tilt and plunge) and process condition (e.g. material) to sensor data obtained from Al 5251 flat plate and Al 6061 flat plate welds. To develop an intelligent monitoring and control system for FSW process, it is necessary to investigate the adaptability of the controller to material changes. Thus besides investigating correlation coefficients of sensor signals to process parameters of Al 5251 and Al 6061 plate respectively, additional correlation analysis was carried out by incorporating the data from two independent OA experiments of the two materials to investigate the influence of material on sensor data.

Table 4.6: Correlation coefficients of sensor signals to process parameters of Al 6061 flat plate and Al 5251 flat plate

experiment	*Sensor signal*	*Co_tilt*	*Co_plunge*	*Absolute sum*	*Co_feed*	*Co_speed*	*Absolute sum*	*Co_material*
6061 plate	bending force (N)	-0.0596	0.0315	0.0911	0.3875	-0.7994	**1.1869**	
	torque (Nm)	-0.0623	0.3279	**0.3902**	0.5084	-0.5234	1.0318	
	temperature (˚C)	-0.5382	0.2932	**0.8314**	-0.1984	0.7202	0.9186	
	Fz (kN)	0.0479	0.1582	0.2061	0.5512	-0.7471	**1.2983**	
5251 plate	bending force (N)	-0.2076	0.2127	0.4203	0.5117	-0.6244	**1.1361**	
	torque (Nm)	0.3343	0.3629	**0.6972**	0.3002	-0.1895	0.4897	
	temperature (˚C)	-0.1160	0.3707	0.4867	-0.0453	0.7794	0.8247	
	Fz (kN)	0.5580	-0.1135	**0.6715**	0.4164	-0.5878	**1.0042**	
5251 & 6061 plate	bending force (N)	-0.09	0.08	0.17	0.35	-0.60	**0.95**	0.08
	torque (Nm)	0.09	0.28	**0.37**	0.35	-0.31	0.66	0.28
	temperature (˚C)	-0.27	0.30	**0.57**	-0.10	0.67	**0.77**	0.30
	Fz (kN)	0.09	0.05	0.14	0.28	-0.38	0.66	0.05

In this study, the tool/workpiece contact is supposed to be controlled by means of tilt angle and plunge depth, thus it is important to select sensor signals with high correlation to tilt angle and plunge depth as control variables for tool/workpiece contact maintenance. It can be seen from table 4.6 that the sensor signal for torque has larger absolute sum of correlation coefficients to tilt angle and plunge depth in both Al 5251 and Al 6061 plates, thus was selected as a control variable for tool/workpiece contact control. It can be also seen temperature has larger absolute sum of correlation coefficients to tilt angle and plunge depth in the Al 6061 flat welding experiment, and combined experiment of Al 5251 and Al 6061, thus it was also selected as a control variable for tool/workpiece contact in the welding of Al 5251 and Al 6061 flat plate, as well as the flat plate with the combination of the two materials. The same conclusion can be drawn that bending force and Fz can be chosen as control variables for tool/workpiece energy input as they have larger absolute sum of correlation coefficients to feed rate and spindle speed.

To further study the sensitivity of sensor signals to process parameters, the ratios between the sensor signals were also investigated in correlation analysis. Table 4.7 shows the correlation coefficients of expanded sensor data to process parameters for Al 6061 flat plate welds. It can be seen that sensor signals of temperature, the ratio of temperature to Fz, and the ratio of torque to Fz, have larger correlation coefficients to tilt angle and plunge depth. Therefore, they were chosen as the control variables for tool/workpiece contact of Al 6061 alloy flat welds. Fz, the ratio of temperature to torque, and the ratio of torque to Fz were chosen as control variables for tool/workpiece energy input as they have larger absolute sum of correlation coefficients to feed rate and spindle speed.

Table 4.7: Correlation coefficients of expanded sensor signals to process parameters of Al 6061 flat weld

Sensor signal	*Co_tilt*	*Co_plunge*	*Absolute sum*	*Co_feed*	*Co_speed*	*Absolute sum*
bending force (N)	-0.0596	0.0315	0.0911	0.3875	-0.7994	1.1869
torque (Nm)	-0.0623	0.3279	0.3902	0.5084	-0.5234	1.0318
temperature (˚C)	-0.5382	0.2932	**0.8314**	-0.1984	0.7202	0.9186
Fz (KN)	0.0479	0.1582	0.2061	0.5512	-0.7471	**1.2983**
bending/torque	0.0974	-0.1559	0.2533	0.1506	-0.6877	0.8383
bending/temperature	0.0728	-0.0772	0.1500	0.2787	-0.8179	1.0966
bending/Fz	-0.0350	-0.0421	0.0771	-0.0865	-0.4362	0.5227
temperature/torque	-0.2789	0.0400	0.3189	-0.5024	0.7109	**1.2133**
temperature/Fz	-0.3322	0.1486	**0.4808**	-0.5208	0.6870	1.2078
torque/Fz	-0.3074	0.1546	**0.4620**	-0.4966	0.7180	**1.2146**

Similarly, Table 4.8 shows the correlation coefficients of expanded sensor data to process parameters for Al 5251 flat welds. It can be concluded that torque, the ratio of bending force to Fz, and the ratio of torque to Fz have the larger correlation coefficient absolute sum to tilt angle and plunge depth, and were thus chosen as the control variables for tool/workpiece contact of Al 5251 flat weld. It can also be seen that bending force, the

ratio of bending force to temperature, and the ratio of temperature to Fz, have larger correlation coefficient absolute sum to feed and speed, and were thus selected as control variables for tool/workpiece energy input.

Table 4.8: Correlation coefficients of expanded sensor signals to process parameters of Al 5251 flat welds

Sensor signal	*Co_tilt*	*Co_plunge*	*Absolute sum*	*Co_feed*	*Co_speed*	*Absolute sum*
bending force (N)	-0.2076	0.2127	0.4203	0.5117	-0.6244	**1.1361**
torque (Nm)	0.3343	0.3629	**0.6972**	0.3002	-0.1895	0.4897
temperature (˚C)	-0.1160	0.3707	0.4867	-0.0453	0.7794	0.8247
Fz (kN)	0.5580	-0.1135	0.6715	0.4164	-0.5878	1.0042
bending/torque	-0.2106	0.0787	0.2893	0.4179	-0.6241	1.0420
bending/temperature	-0.1361	0.0453	0.1814	0.3842	-0.7285	**1.1127**
bending/Fz	-0.4835	0.3743	**0.8578**	0.3535	-0.4079	0.7614
temperature/torque	-0.3998	0.0864	0.4862	-0.3089	0.7789	1.0878
temperature/Fz	-0.4277	0.2437	0.6714	-0.4352	0.6874	**1.1226**
torque/Fz	-0.3679	0.3266	**0.6945**	-0.3898	0.5396	0.9294

To develop an intelligent monitoring and control system for complex curvature FSW, relationships between sensor signals and different workpiece curvature radii is required to be investigated. Table 4.9 shows the correlation coefficients of process parameters and process condition curvature diameter to sensor signals of different diameter Al 6061 alloy round tube welds. It can be seen that torque and temperature were chosen as control variables for tool/workpiece contact, while bending force and Fz were selected as control variables for tool/workpiece energy input. The detailed description of tool/workpiece contact and energy input control can be found in Chapter 5.

Table 4.9: Correlation coefficients of sensor signals to process parameters of Al 6061 flat plate and Al 6061 round tube

experiment	*Sensor signal*	*Co_tilt*	*Co_plunge*	*Absolute sum*	*Co_feed*	*Co_speed*	*Absolute sum*	*Co_curvature*
6061 plate	bending force (N)	-0.0596	0.0315	0.0911	0.3875	-0.7994	**1.1869**	
	torque (Nm)	-0.0623	0.3279	**0.3902**	0.5084	-0.5234	1.0318	
	temperature (˚C)	-0.5382	0.2932	**0.8314**	-0.1984	0.7202	0.9186	
	Fz (kN)	0.0479	0.1582	0.2061	0.5512	-0.7471	**1.2983**	
6061 tube	bending force (N)	0.16	-0.24	0.40	0.72	-0.22	**0.940**	**0.40**
	torque (Nm)	-0.22	0.41	**0.63**	0.38	-0.32	0.70	**0.47**
	temperature (˚C)	-0.51	0.52	**1.03**	-0.28	0.48	0.76	0.27
	Fz (kN)	-0.05	0.03	0.08	0.73	-0.38	**1.11**	0.35
6061 plate & tube	bending force (N)	0.11	-0.17	0.28	0.47	-0.15	0.62	**0.30**
	torque (Nm)	-0.13	0.28	**0.41**	0.33	-0.45	0.78	**-0.75**
	temperature (˚C)	-0.52	0.42	**0.94**	-0.24	0.56	**0.80**	-0.17
	Fz (kN)	-0.02	0.09	0.11	0.66	-0.55	**1.21**	-0.26

4.4.2 Multi-sensor Modelling

A process condition monitoring system consists of three main elements: sensors for capturing process signals, signal processing methods to extract important information (sensory characteristic features (SCFs)) about the process, and a pattern recognition stage to interpret the sensory information for process condition classification **(**Al-Habaibeh and Gindy, 2001). Owing to the limitations of single sensor instrumentation, there is an increasing effort to use combinations of different sensors or transducers to monitor various variables. It has been proven that the three layer network with a sufficient number of nodes in the hidden layer is able to model any mathematical function (Rafalowicz, *et al*., 1998; Rowe, 1994). In this study, NN was used as a modelling tool for sensor fusion due to its ability to approximate random complex mathematical functions.

The experiment with Al 5251 round rube was not conducted in this study, therefore,

monitoring for process condition changing does not include curvature changing of Al 5251 plate. Thus, process condition changing was restricted to flat plate welding with changing material, and Al 6061 alloy welding with changing curvature. Figure 4.9 shows the procedure of process monitoring proposed in this study.

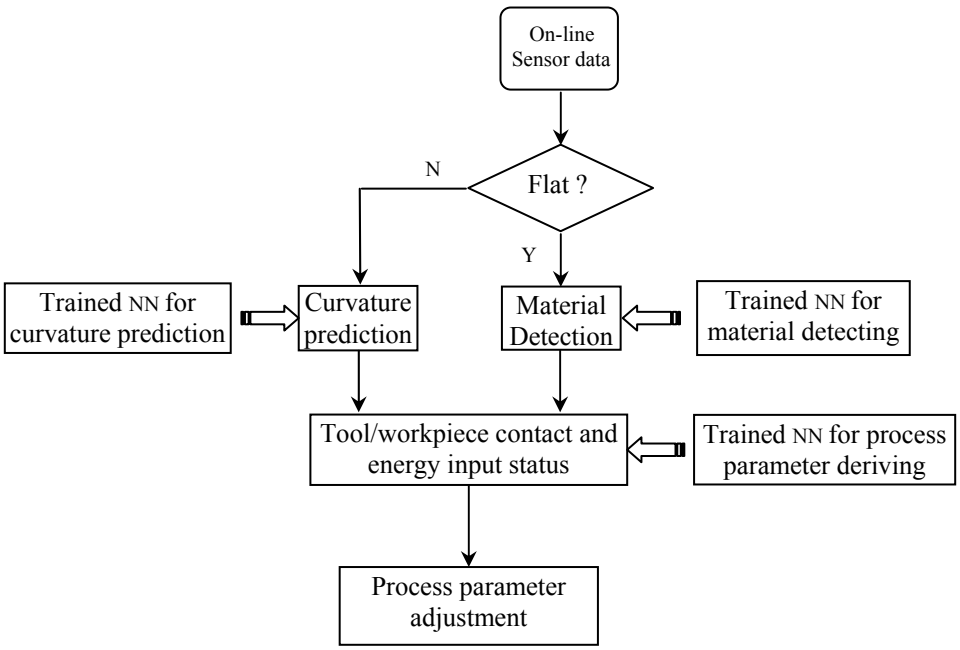

Figure 4.9: Procedure of process monitoring with trained NNs.

The sensor fusion work was done through application of different feed-forward back-propagation NNs. In this study, a control scheme with the adaptability to complex curvature needs to be established, thus different NNs for mapping the relationships of material changing, curvature changing and process parameters changing to sensor data changing were trained. The training and simulation results of the NNs are described in the following subsections.

4.4.2.1 NN Training for Curvature Prediction

In complex curvature FSW, process parameters of feed rate, spindle speed, tilt angle and plunge depth cooperate with workpiece curvature to determine the condition of tool/workpiece contact and energy input. To make correct decisions for process parameter adjustment, the changing of workpiece curvature radius needs to be detected from on-line sensor data. In this study, only Al 6061 material is investigated with complex curvature. Using the data obtained in previous Al 6061 flat plate and round tube experiments, a feed-forward back-propagation NN was trained. The NN architecture is shown as follows:

NN inputs: torque, temperature and Fz.

NN outputs: workpiece curvature (e.g. 1/20 for curvature radius of 20 mm).

NN structure: 3-6-1.

The Levenberg-Marquardt algorithm was used as a fast training method. The 16 flat plate welds and 18 round tube welds from the OA experiments, together with another five additional round tube welds were used as training and checking data. The M script for NN training can be seen in Appendix B.5. The comparison of NN outputs to experimental data, the final value of training performance function and the final NN architecture are shown in Figure 4.10 (a) to (c) respectively. The training result shows that good performance was achieved and that the NN can be used to predict workpiece curvature given on-line sensor data. The performance function *mse* was 0.0153772 after training 50 epochs and the error of NN outputs to target was restricted within a small band.

(a)

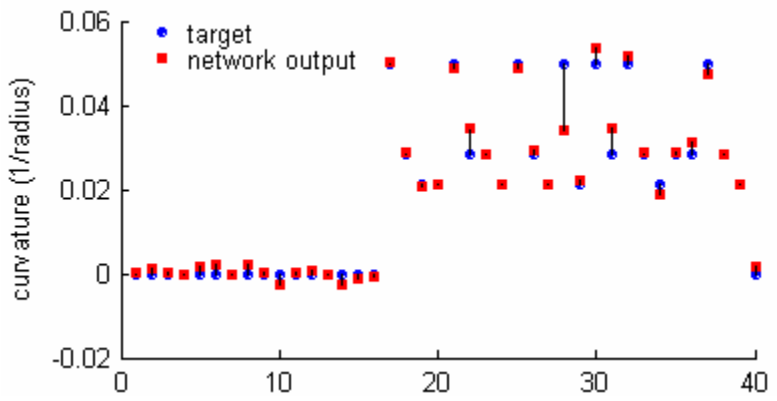

(b)

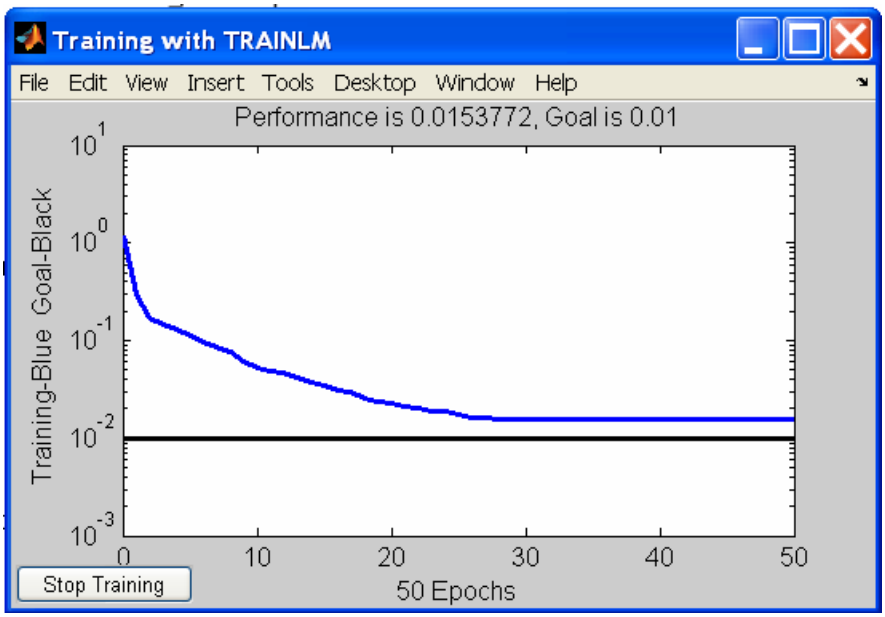

(c)

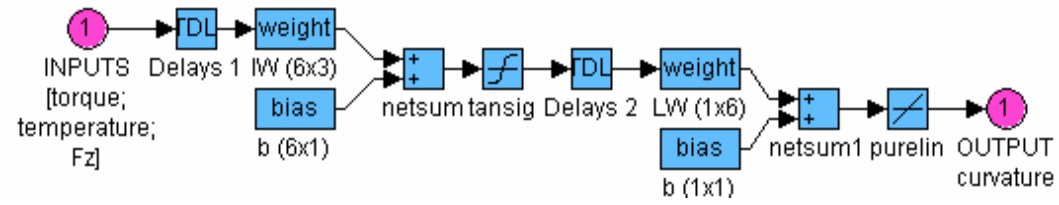

Figure 4.10: Training of NN for workpiece curvature prediction. (a) NN outputs vs targets, (b) NN performance function, and (c) NN structure

4.4.2.2 NN Training for Material Detection

When welding plates of different materials, different sensor data were obtained using the same process parameters, as can be seen in the factor-effect curve in Figure 4.7. Thus the intelligent monitoring system must 'tell' what kind of material is being welded before process adjustments for tool/workpiece energy input maintenance. In this study, the changing of material is limited in flat plates of Al 5251 and Al 6061 alloy. Using the data from the two OA experiment and additional test data, a 4-4-1 back-propagation NN was trained with the reduced memory Levenberg-Marquardt algorithm. After training, the system can 'tell' whether the material being welded was '0' (for Al 6061 alloy) or '1' (for Al 5251 alloy). The architecture of the NN is shown as follows:

NN inputs: tilt angle, plunge depth, torque and temperature.

NN outputs: parent material ("0" for Al 6061 alloy, "1" for Al 5251 alloy).

NN structure: 4-5-1.

The Levenberg-Marquardt algorithm was used as the training method. 16 flat welds of both Al 5251 and Al 6061 alloy plate welded from the OA experiments were used as training data. Another six additional flat welds were used as checking data. The final architecture, comparison of NN outputs to experimental data and final value of training performance function are shown in Figure 4.11 (a) to (c) respectively. The training result shows good performance with *mse* value 0.0874027 after 300 training epochs. It can be seen that the trained NN can be used to predict workpiece curvature given on-line sensor data and process parameters.

(a)

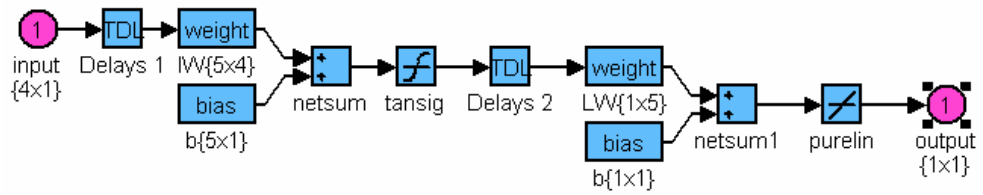

(b)

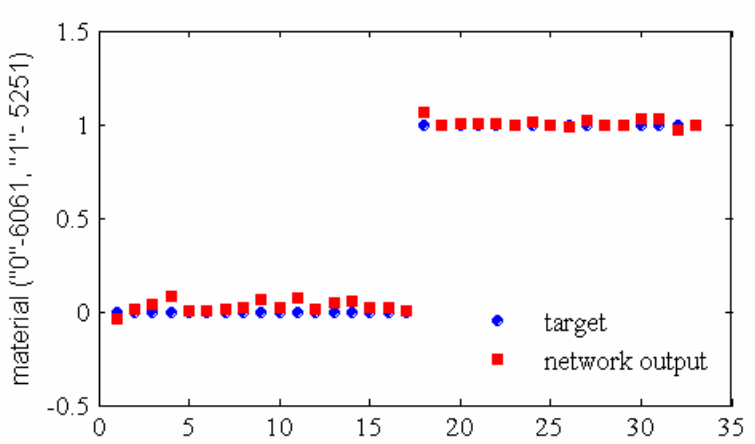

(c)

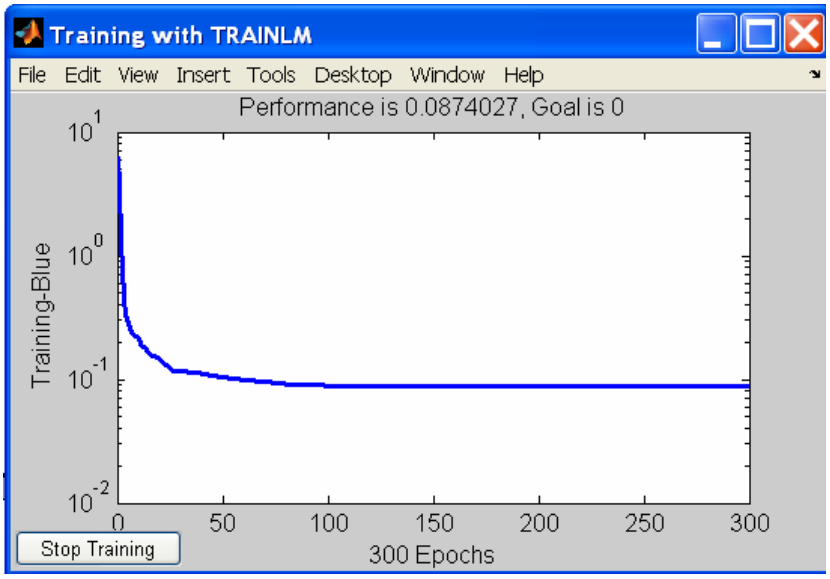

Figure 4.11: Training of NN for parent material detecting. (a) NN structure, (b) NN outputs vs targets and (c) NN performance function

4.4.2.3 NN Training for Mapping Sensor Data/Process Parameter Relationships

With the previous two NNs, when on-line sensor data was read, and the material and

curvature were recognized, the intelligent control system was able to derive on-line control decisions by recalling the relationships between process parameters and sensor data. This is achieved through two NN training: one for changing curvature Al 6061 workpiece welding, the other for changing material flat plate welding. Figures 4.12 (a) to (f) show the final architecture, value of training performance function and the comparison of NN outputs to experimental data of the trained NN for complex curvature FSW of Al 6061. The architecture of the trained NN is shown as follows:

NN inputs: curvature, torque, temperature and Fz.

NN outputs: feed rate, spindle speed, tilt angle and plunge depth.

NN structure: 4-9-4.

(a)

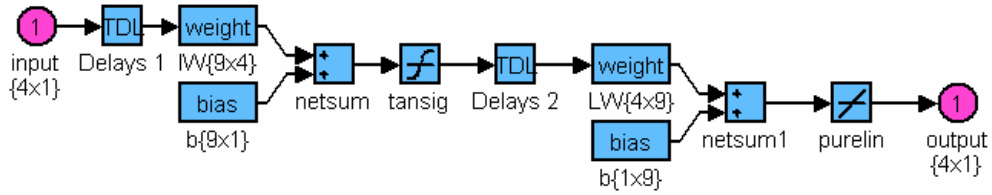

(b)

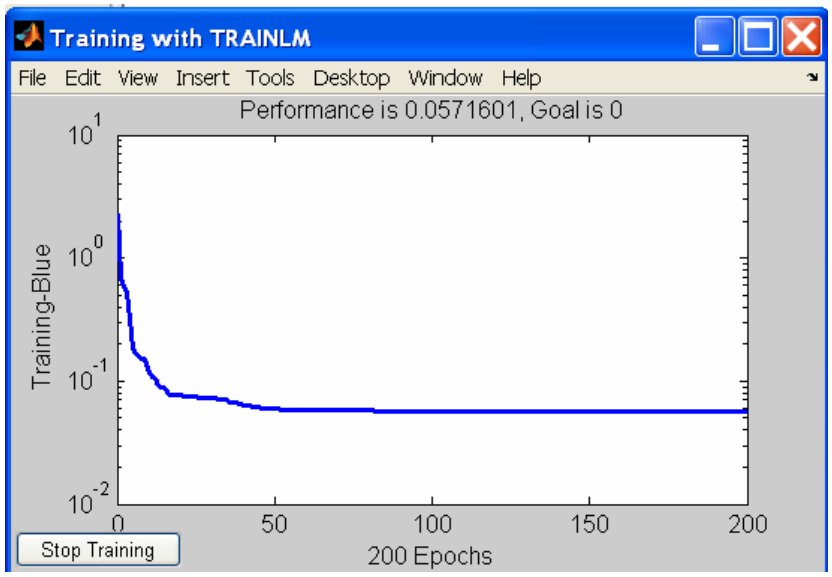

Figure 4.12: Training of NN for process parameter deriving. (a) NN architecture, (b) performance function

(c)

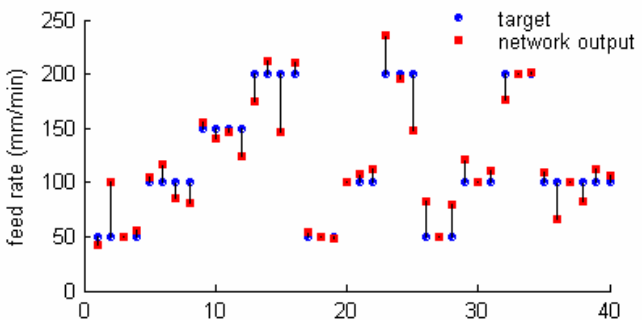

(d)

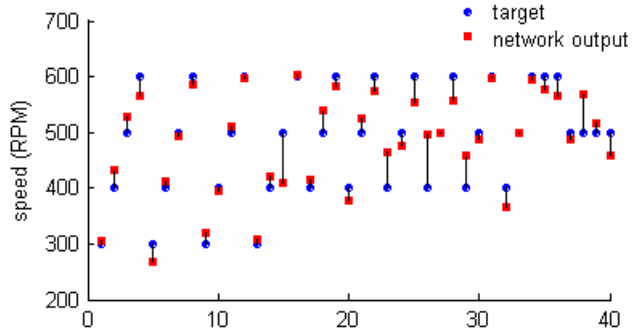

(e)

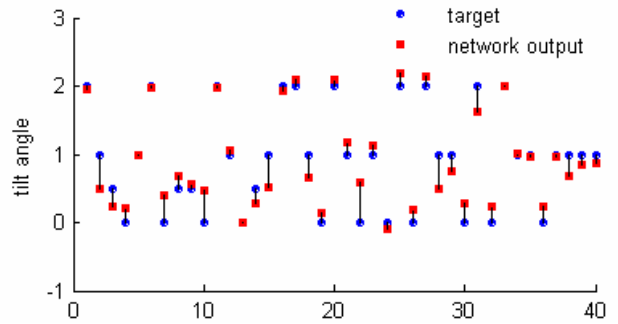

(f)

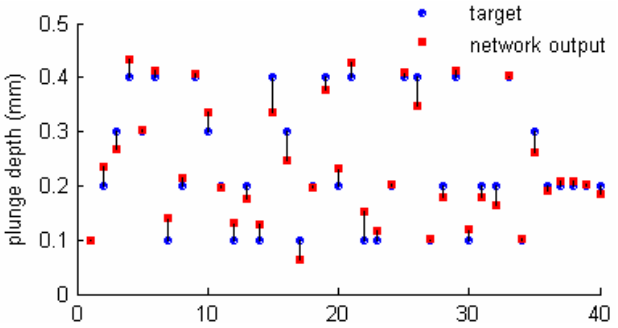

Figure 4.12 (cont): Training of NN for process parameter deriving. Comparison of NN outputs to target values of (c) feed rate, (d) spindle speed, (e) tilt angle and (f) plunge depth

The NN trained with the Levenberg-Marquardt algorithm training resulted in a *mse* value

of 0.0571601 after 200 training epochs. It can be used to derive instant process parameters given on-line sensor data and process conditions. The derived process parameters can be used for on-line fuzzy rule generating as described in Chapter 5.

4.4.2.4 NN Training for Mapping Process Parameter/Sensor Data Relationships

The non-linear relationships of sensor data to process parameters and process conditions can also be modeled by NN training for process simulation. Figures 4.13 (a) to (e) show the final value of the training performance function, the final architecture and comparison of NN outputs to experimental data of the trained NN for complex curvature FSW of Al 6061 alloy. The architecture of the trained NN is shown as follows:

NN inputs: feed rate, spindle speed, tilt angle, plunge depth and curvature.

NN outputs: torque, temperature and Fz.

NN structure: 5-7-3.

(a)

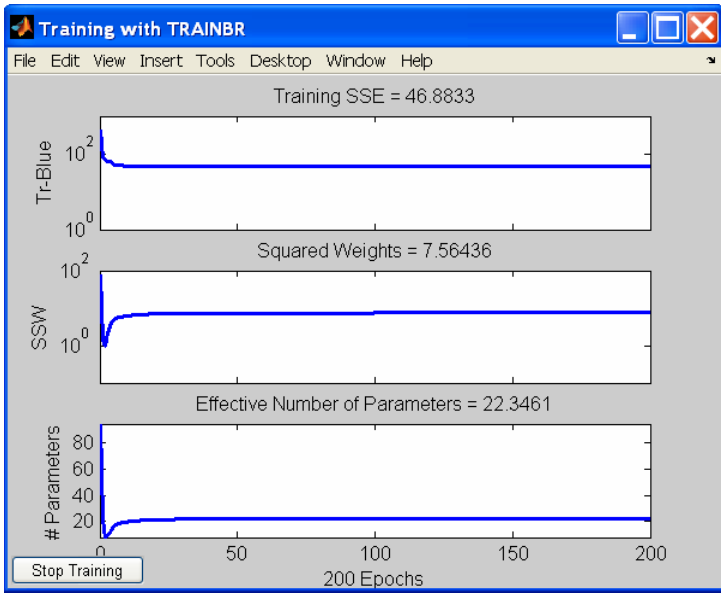

Figure 4.13: Training of NN for sensor data modelling. (a) Performance function

(b)

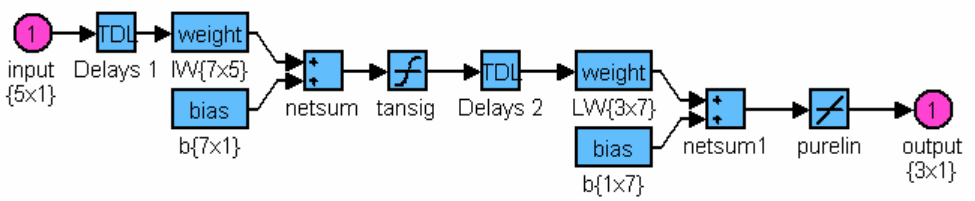

(c)

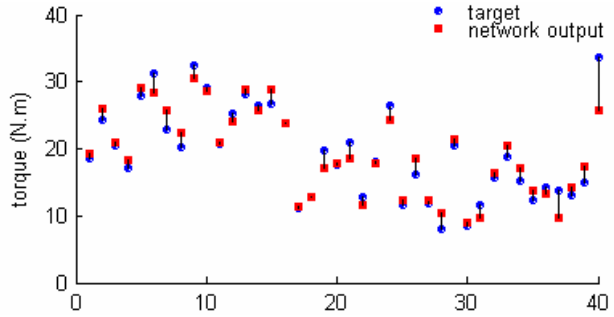

(d)

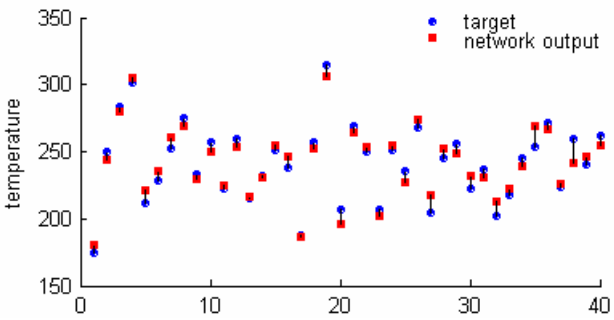

(e)

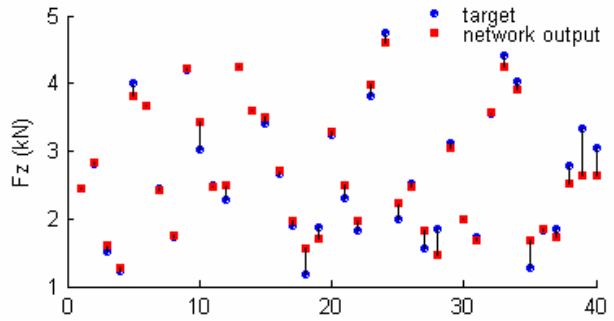

Figure 4.13 (cont): Training of NN for sensor data modelling. (b) NN structure, and comparison of NN outputs to target values of (c) toruqe, (d) temperature and (e) Fz

Automated Regularization was used as the training method as it can prevent the NN from overfitting and improve generalisation. One feature of this algorithm is that it provides a

measure of how many network parameters (weights and biases) are being effectively used by the network. In this case, the final trained network used approximately 20 parameters in the 5-7-3 network after approximately 40 training epochs. This effective number of parameters remained approximately the same during the rest of the 200 total epochs. This indicates that the network has been trained for a sufficient number of iterations to ensure convergence. The inputs and outputs of the training data were scaled in the range [-1 1] to obtain the best performance of the *Automated Regularization* algorithm (The MathWorks, 2004b). From the comparison of NN outputs to target values, it can be seen that the trained NN has a good ability to predict the expected sensor data given a set of process parameters and process conditions.

4.5 Summary

This chapter provides a systematic method for multi-sensor based sensitive feature selection and sensor fusion. OA experiment, statistical tools and NNs were used in experimental data acquisition, sensitive feature selection and sensor fusion.

OA experimental method was chosen to minimize the number of tests due to its ability to represents all factors equally and investigate some combinations of factors and factor levels. OA experiments were conducted by varying process parameters (feed rate, spindle speed, tilts angle and plunge depth) and process conditions (parent material and curvature) to acquire sensor data of bending force, torque, temperature and Fz.

The ANOVA, correlation analysis and percentage contributions were used to select sensitive sensor features as candidates for NN training and control variables for

intelligent system control. The average effect of each factor on sensor data (bending force, torque, temperature and Fz) was investigated. Both temperature and Fz showed high sensitivity to process parameter and process condition changes. Bending force was found to be the least sensitive. With further ANOVA, percentage contribution and correlation analysis, sensitive sensor features to tool/workpiec contact and energy input were selected for further sensor fusion.

Feed-forward back-propagation NNs were trained to perform sensor fusion for process condition detecting, tool/workpiece contact and energy input monitoring. Different inputs and outputs were designed for different NNs with a specific modelling target. All the simulation results showed that the errors of NN outputs to target values were well controlled within a limited range after NN training. Using the trained NNs, the intelligent system can detect curvature and material changes during complex curvature FSW of Al 5251 and Al 6061. The trained NNs can be also used to generate on-line 'if-then' fuzzy rules. The details of on-line fuzzy rule generation with trained NN can be seen in Chapter 5. All the NN training and statistical analyses were performed with MATLAB and related toolboxes.

The systematic method of statistical analysis and NN training for sensitive feature selection and sensor fusion can be expanded to new inputs and outputs. Given new process condition (e.g. tool geometry, etc.) and sensor signal (e.g. power, AE, etc.), the sensitive feature selection and NN training can be easily upgraded.

The statistical analysis and NN models are useful in describing a steady-state response given certain input parameters. Because only steady-state values were utilised in the

analysis, these models do not describe the transient portions of welds. Additional signal processing methods, both in the time domain and frequency domain would be required for further testing and analysis.

Process parameters for the OA experiments were selected within a certain range of the FSW machine. Further experiments with process parameters outside the selected range, different workpiece thickness, and more material types should be carried out to expand the range of the monitoring system applications.

Chapter 5 Neural-fuzzy Control Scheme during Complex Curvature FSW

Complex curvature FSW is a dynamic process which is controlled via multiple process parameters of feed rate, spindle speed, tilt angle and plunge depth. These variables cooperate to determine the dependent variables such as tool temperature, torque, and Fz. To obtain constant values of such dependent variables, it is desirable to maintain well-matched feed rate, spindle speed, plunge depth and tilt angle. However, during complex curvature, process condition such as workpiece curvature changes dynamically. To maintain tool/workpiece contact and energy input, it is inevitable to have to consistently adjust process parameters adapting to the changing environment. An intelligent control system which has the ability to detect process condition changes and make on-line response to the environment is needed.

5.1 Introduction

To machine parts with complex geometry which involves multi-inputs and multi-outputs, a wide spectrum of on-line controllers have been developed in the manufacturing industry. AI techniques have roused great interest in the scientific community and have been applied to machining, especially in milling and turning. Tarng and Cheng (1993) presented a fuzzy control of feed rate in end milling. Neural networks have been used in process control of turning and milling (Tarng, *et al*., 1994; Chiang, *et al*., 1995; Haber, *et al*., 2002; Liu and Wang, 1999). Direct intelligent adaptive control was applied in a milling process (Altintas, 1994; Liu *et al*., 1999).

Fuzzy logic control is an ideal tool for multi-input multi-output machining process control due to its tolerance of imprecise data and ability to model non-linear functions of arbitrary complexity. It can also be blended with conventional control techniques (The MathWorks, 2004a). Liang *et al*., (2003) presented a tuning mechanism, including an input scale factor tuned with the integration of torque error and an output scale factor tuned by the change of torque error, to strengthen or weaken the fuzzy control of CNC machine spindle torque by adjusting spindle speed and feed rate.

The fuzzy rules of most fuzzy controllers are set based on past experience. However, when facing a complex MIMO process which involves non-linear relationships between inputs and outputs, a more efficient fuzzy rule generating method is needed for the fuzzy controller to make instant decisions with on-line sensor signals. In this respect, NN has the ability to learn relationships among input and output data sets through a training process, thus is able to 'induce' output data if a new set of input data is made available (Zahedi, 1991). This can be utilised to solve the 'bottleneck' problem of rule extraction of a fuzzy controller. Sun and Deng, (1996) presented a control structure with fuzzy neural network which is composed of an antecedent network to match the premises of the fuzzy rules, and a consequent network to implement the consequences of the rules. Lau *et al*. (2001) proposed an integrated neural-fuzzy model using neural network to generate 'if-then' fuzzy rules.

The MIMO and non-linear process of FSW makes intelligent systems technology a feasible option to classical control strategies. A neuro-fuzzy control scheme was proposed in this study for tool/workpiece contact control of complex curvature FSW. The

proposed controller incorporates the advantages of neural network and fuzzy logic, and utilises a tuning mechanism for adapting the control action to process condition changes.

5.2 Proposed System Structure

Figure 5.1 shows the overall structure of the proposed neuro-fuzzy control scheme. Inputs $E_{S(t)}$ to the control system are errors of on-line control variables $Y_{S(t)}$ to their reference values $R_{S(t)}$. Outputs from the control system are proposed process parameter adjustments $\Delta_{U(t)}$. Two trained NNs were used to detect process condition changes and derive instant process parameters $Y_{U(t)}$. A rule-generating module for fuzzy rule generation used control variable errors $E_{S(t)}$, and process parameter error $E_{U(t)}$ between preset value $R_{U(t)}$ and derived instant value $Y_{U(t)}$ to generate on-line fuzzy rules. A fuzzy controller with predefined input/output membership functions was used to generate primary commands for process parameters adjustment, which are further tuned by a tuning module to strengthen or weaken control actions in response of the dynamic process changes. The design details and simulation are described in the following sections.

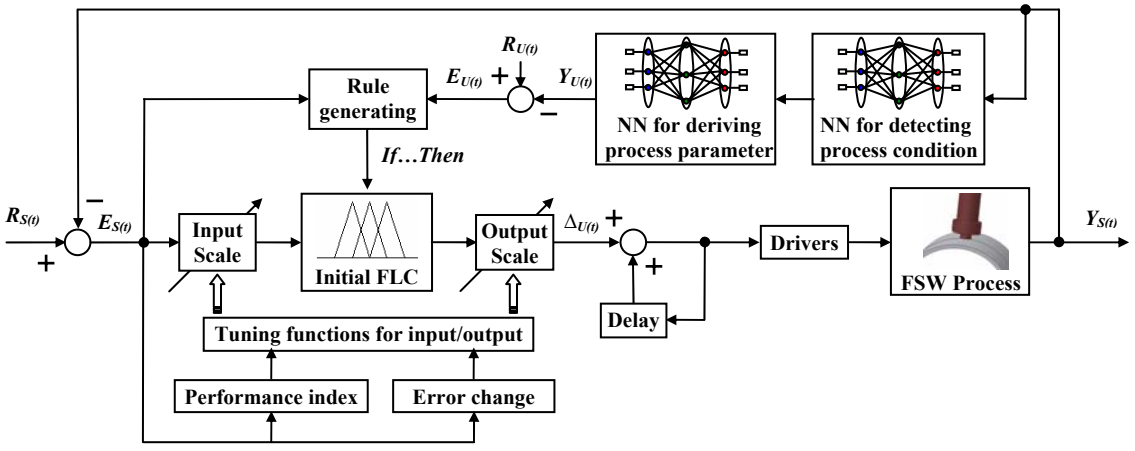

Figure 5.1: Structure of the proposed neuro-fuzzy scheme for process control

5.3 The Neuro-fuzzy Control Scheme

The neuro-fuzzy control scheme is mainly composed of a basic FLC, a fuzzy rule generating module, and a fuzzy input/output tuning mechanism. The integrated neuro-fuzzy control scheme performs the intelligent monitoring and control of tool/workpiece contact and energy input for complex curvature FSW.

5.3.1 The Basic Fuzzy Controller

The main part of the control system consists of two parallel-working FLCs, which perform the basic fuzzy control of tool/workpiece contact and energy input respectively. The basic Mamdani type fuzzy controller consists of a fuzzifier, a fuzzy inference engine, a defuzzifier and membership functions. The fuzzy rules are however not preset, but generated on-line for the controller in this study. Using the example of neuro-fuzzy control of Al 6061 alloy flat plate FSW, the details of the basic fuzzy controller are described in the following subsections.

5.3.1.1 Inputs and Normalising

The control variables of the tool/workpiece contact FLC, which recommends on-line adjustments of tilt angle and plunge depth, are temperature, the ratio of temperature to Fz, and the ratio of torque to Fz. The control variables of the tool/workpiece energy input FLC, which recommends on-line adjustments of feed rate and spindle speed, are Fz, the ratio of temperature to torque, and the ratio of torque to Fz. The statistical analysis of control variable selection was covered in Chapter 4. Each of the control variables is compared to a reference value. This yields three inputs to the tool/workpiece contact FLC,

the temperature error (ERR_{Temp}), the temperature/Fz error ($ERR_{Temp/Fz}$) and the torque/Fz error ($ERR_{Torq/Fz}$). At the same time, besides the same control variable $ERR_{Torq/Fz}$, two new inputs to the tool/workpiece energy input FLC are obtained as the Fz error (ERR_{Fz}) and the temperature/torque error ($ERR_{Temp/Torq}$). At each sampling time i, all the five errors are respectively calculated as:

$$ERR_{Temp}(i) = Temp_{ref} - Temp(i) \tag{5.1}$$

$$ERR_{Temp/Fz}(i) = \frac{Temp_{ref}}{Fz_{ref}} - \frac{Temp(i)}{Fz(i)} \tag{5.2}$$

$$ERR_{Torq/Fz}(i) = \frac{Torq_{ref}}{Fz_{ref}} - \frac{Torq(i)}{Fz(i)} \tag{5.3}$$

$$ERR_{Fz}(i) = Fz_{ref} - Fz(i) \tag{5.4}$$

$$ERR_{Temp/Torq}(i) = \frac{Temp_{ref}}{Torq_{ref}} - \frac{Temp(i)}{Torq(i)} \tag{5.5}$$

Where,

$Temp_{ref}$ Reference value of temperature;

$Torq_{ref}$ Reference value of torque;

Fz_{ref} Reference value of Fz;

$Temp(i)$ Temperature value at sample time i;

$Torq(i)$ Torque value at sample time i;

$Fz(i)$ Fz value at sample time i.

Each of the errors is normalised into [-1 1] before being fed into the controller by multiplying the corresponding normalising coefficient (Liang *et al*., 2003).

$$err_{Temp}(i) = ERR_{Temp}(i) \times K_{Temp}(i) \tag{5.6}$$

$$err_{Fz}(i) = ERR_{Fz}(i) \times K_{Fz}(i) \tag{5.7}$$

$$err_{Temp/Fz}(i) = ERR_{Temp/Fz}(i) \times K_{Temp/Fz}(i) \tag{5.8}$$

$$err_{Torq/Fz}(i) = ERR_{Torq/Fz}(i) \times K_{Torq/Fz}(i) \tag{5.9}$$

$$err_{Temp/Torq}(i) = ERR_{Temp/Torq}(i) \times K_{Temp/Torq}(i) \tag{5.10}$$

The normalising coefficient for input normalising is separately considered in the zones above and below the reference value to ensure both sides from the reference value (zero error point) have the same number and shapes of membership functions.

The normalising coefficient for error of temperature is calculated as follows. The same rule is applied for the other errors.

If $Temp(i) \geq Temp_{ref}$

$$K_{Temp}(i) = 1/(Temp_{\max} - Temp_{ref})$$

Else $K_{Temp}(i) = 1/(Temp_{ref} - Temp_{\min})$

Where,

$K_{Temp}(i)$ Temperature normalising coefficient;

$Temp_{\max}$ Maximum temperature;

$Temp_{\min}$ Minimum temperature.

5.3.1.2 Membership Functions

All the inputs and outputs of the fuzzy controller use the same triangular membership function due to its computation efficiency. Each fuzzy input or output has nine MFs: NX (extra negative), NL (negative large), NM (negative middle), NS (negative small), ZE (zero error), PS (positive small), PM (positive middle), PL (positive large), and PX (extra positive). In order to regulate the system output to a desired output, more accurate control actions are taken near the reference value (Kim and Yuh, 2002). Therefore, finer fuzzy sets are placed near the reference value. Figure 5.2 shows the membership functions of input err_{Temp}. It can be seen that the fuzzy values are dense when near zero but sparse when far from zero.

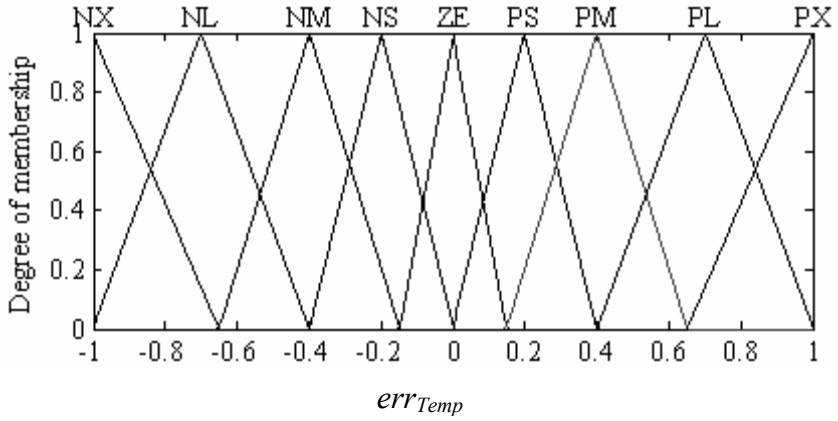

Figure 5.2 Membership functions of fuzzy input err_{Temp}

5.3.2 Tuning Mechanism

Three parts of a fuzzy controller including membership functions, fuzzy rule and input/output scale factors can be tuned to make the controller adaptable. In this study, the membership functions are preset, and the fuzzy rules are generated on-line. Thus to enhance the control actions, inputs and outputs of the controller are tuned by changing the gain of input and output scale factors.

5.3.2.1 Performance Index and Input Scale Factor

As can be seen in Figure 5.1, the integration of errors of control variables to their reference values are used for input tuning. A performance index is also established to evaluate process quality using integration of the error of control variable to its reference value. The error of a control variable to its reference value in current and the last two sample times are used to calculate the performance index.

Equation (5.11) calculates the performance index for temperature. The calculation method applies for the other inputs as well.

$$Perform_{Temp}(i) = \sqrt{\frac{\sum_{i-2}^{i} (err_{Temp}(i))^2}{3}} \tag{5.11}$$

A small value of performance index indicates that a control variable is well controlled by the fuzzy controller. In practice, it is expected to maintain a performance value within a narrow tolerance zone. To adaptively strengthen or weaken control actions in response to on-line signals, the performance index value is used to tune the input scale factor. The tuneable input scale factor for temperature error at sampling time *i* is calculated as shown in equation (5.12). The other two fuzzy inputs are also tuned by similar input scale factors (Liang *et al*., 2003).

$$Kin_{Temp}(i) = \left(\frac{Perform_{Temp}(i)}{\varepsilon_{Temp}} \right)^{0.16} \tag{5.12}$$

where,

ε_{Temp} Bandwidth of the tolerance zone;

$Kin_{Temp}(i)$ Temperature error scale factor.

Thus the final inputs to the FLCs are calculated as follows:

$$err_{Temp}(i) = err_{Temp}(i) \times Kin_{Temp}(i) \tag{5.13}$$

$$err_{Fz} = err_{Fz}(i) \times Kin_{Fz}(i) \tag{5.14}$$

$$err_{Torq/Fz} = err_{Torq/Fz}(i) \times Kin_{Torq/Fz}(i) \tag{5.15}$$

$$err_{Temp/Fz} = err_{Temp/Fz}(i) \times Kin_{Temp/Fz}(i) \tag{5.16}$$

$$err_{Temp/Torq} = err_{Temp/Torq}(i) \times Kin_{Temp/Torq}(i) \tag{5.17}$$

5.3.2.2 Output Scale Factors and Coefficient

Defuzzified outputs from the tool/workpiece contact FLC are recommended changes of tilt angle $Fuzzyout_{tilt}$ and plunge depth $Fuzzyout_{plunge}$. Defuzzified outputs from the tool/workpiece energy input FLC are recommended changes of feed rate $Fuzzyout_{feed}$ and spindle speed $Fuzzyout_{speed}$. Each output variable falls in the preset input range [-1 1]. They need to be multiplied by an adjustment step to obtain primary adjustment. The primary adjustments of tilt angle Δ_{tilt}, plunge depth Δ_{plunge}, feed rate Δ_{feed} and spindle speed Δ_{speed} are calculated as follows with the adjustment steps selected from simulation.

$$\Delta_{tilt} = Fuzzyout_{tilt} \times 1(^{\circ}) \tag{5.18}$$

$$\Delta_{plunge} = Fuzzyout_{plunge} \times 0.2(mm) \tag{5.19}$$

$$\Delta_{feed} = Fuzzyout_{feed} \times 50(mm/\min) \tag{5.20}$$

$$\Delta_{speed} = Fuzzyout_{speed} \times 100(rpm) \tag{5.21}$$

The primary adjustments of tilt angle, plunge depth, feed rate and spindle speed are further tuned by corresponding output scale factors according to the trend of control variable deviation from its reference value. Thus the derivatives of deviations, or in other words the change of the errors are used to calculate the output scale factor.

As all three fuzzy inputs have influence on each fuzzy output in one FLC, the output scale factor for each output is calculated by taking the correlation coefficients of the three inputs to the output into account. The following shows the equation for tilt angle adjustment scale factor. The same equation is applied to the other three output scale factors.

$$Kout_{Tilt} = \sqrt{\frac{\sum_{i=1}^{3} Co_{Tilt}(i) \times (K_{Tilt}(i))^2}{\sum_{i=1}^{3} Co_{Tilt}(i)}} \tag{5.22}$$

Where,

$Co_{Tilt}(i)$ Correlation efficient of the ith control variable to tilt angle. The coefficient of temperature, temperature/Fz, and torque/Fz to tilt angle is 0.8314, 0.4808, and 0.4620 respectively, as can be seen in Table 4.7 of Chapter 4.

$K_{Tilt}(i)$ Scale factor calculated from the ith control variable.

The calculation of the scale factor from the first control variable deviation (temperature error) is shown as follows (Liang *et al*., 2003). The same calculation applies to the other control variable errors:

$$\text{If} \quad \frac{\nabla_{Temp}(i)}{\nabla_{Temp}(i-1)} < 0 \quad \&\& \quad \left| \frac{\nabla_{Temp}(i)}{\nabla_{Temp}(i-1)} \right| > 1$$

$$\text{If} \quad \frac{ERR_{Temp}(i)}{ERR_{Temp}(i-1)} > 1, \qquad K_{Tilt}(1) = \left| \frac{\nabla_{Temp}(i)}{\nabla_{Temp}(i-1)} \right|^{\alpha};$$

If $0 < \frac{ERR_{Temp}(i)}{ERR_{Temp}(i-1)} < 1$, $K_{Tilt}(1) = \left| \frac{\nabla_{Temp}(i-1)}{\nabla_{Temp}(i)} \right|^{\alpha}$;

If $\frac{\nabla_{Temp}(i)}{\nabla_{Temp}(i-1)} > 0$ && $\left| \frac{\nabla_{Temp}(i)}{\nabla_{Temp}(i-1)} \right| > 1$

If $\left| \frac{ERRTemp(i)}{ERRTemp(i-1)} \right| > 1$, $K_{Tilt}(1) = \left| \frac{\nabla_{Temp}(i)}{\nabla_{Temp}(i-1)} \right|^{\alpha}$;

If $\left| \frac{ERRTemp(i)}{ERRTemp(i-1)} \right| < 1$, $K_{Tilt}(1) = \left| \frac{\nabla_{Temp}(i-1)}{\nabla_{Temp}(i)} \right|^{\alpha}$;

Else $K_{Tilt}(1) = 1$

Where,

$K_{Tilt}(1)$ Output scale factor for tilt angle from the first input temperature error.

α Constant in [-1 1]. In this study it was chosen as 0.1 through simulation.

$$\nabla_{Temp}(i) = ERR_{Temp}(i) - ERR_{Temp}(i-1) \tag{5.23}$$

$$\nabla_{Temp}(i-1) = ERR_{Temp}(i-1) - ERR_{Temp}(i-2) \tag{5.24}$$

The output scale factor utilises the value of error and its change trend to tune the controller. If the absolute value of current error is bigger, in other words the process condition is worse, and the change of error is faster than before, then a larger adjustment

of the process parameter is desired. Accordingly, the output scale factor should be set larger than 1. Whereas if the absolute value of error is smaller, in other words the process condition is better, and the change of error is slower than before, then a smaller adjustment of the process parameter is preferred, accordingly the output scale factor should be set smaller than 1. Appendix B.6 shows the M function for output scaling.

With the output scale factors and coefficients, the final adjustment of tilt angle, plunge depth, feed rate, and spindle speed from the two parallel-working FLCs are given:

$$\Delta_{tilt} = Fuzzyout_{tilt} \times Kout_{Tilt} \times 1 \qquad (^{\circ}) \tag{5.25}$$

$$\Delta_{plunge} = C_{plunge} \times Kout_{Plunge} \times 0.2 \qquad (mm) \tag{5.26}$$

$$\Delta_{feed} = C_{feed} \times Kout_{feed} \times 50 \qquad (mm/\min) \tag{5.27}$$

$$\Delta_{speed} = C_{speed} \times Kout_{speed} \times 100 \qquad (rpm) \tag{5.28}$$

5.3.3 Fuzzy Rule Generation

As mentioned earlier, the rule base for the initial fuzzy controller is generated on-line using on-line signals of control variables and the trained neural network. The details of the fuzzy rule generating are described in the following procedure (Lau *et al*. 2001).

5.3.3.1 Trained NN

Technically, for FSW with the same process condition (material, curvature, tool, etc.), if the predefined process parameters are well maintained during welding, there should not

be big changes in the sensor signal. In reality, there can be many reasons for process parameters and sensor signals changing. The trained NNs were used to detect process conditions and derive the instant process parameters from the on-line sensor signals, using the relationships established during training. With new inputs of bending force, torque, temperature and Fz, the process conditions can be detected first for FSW with changing process condition. Using the detected process condition, together with on-line sensor data, instant values of process parameters can be derived. Similarly, given reference values of sensor signals and original process conditions, the desired process parameters can be derived and used as preferred values at the start of the process. The preset and instant tilt angle, plunge depth, feed rate and spindle speed derived from the NN with the original process conditions (material Al 6061) are shown in Table 5.1.

Table 5.1: On-line sensor signal and reference values, instant process parameters and preset values

Sensor signal & process parameter		Reference value	On-line value
NN inputs	Bending force (N)	1070	980
	Torque (Nm)	27	20
	Temperature (°C)	230	200
	Fz (kN)	3.6	3
NN outputs	Feed rate (mm/min)	191.41	77.613
	Spindle Speed (rpm)	398.56	323.91
	Tilt angle (°)	0.55472	0.83998
	Plunge depth (mm)	0.17666	0.10163

The difference between on-line process parameters derived from NN and preferred process parameters suggests that the deviations of tilt angle, plunge depth, feed rate and

spindle speed from their preferred values cause the deviation of sensor signals from their reference values. It also indicates to what extend the sensor signals and process parameters have deviated from their reference and preferred values.

5.3.3.2 Fuzzify Input

Each error between reference value and on-line value of sensor signals is fuzzified with the preset membership functions of corresponding fuzzy input of the two basic FLCs. The inputs to the fuzzy controller are the errors of temperature, Fz, temperature/Fz and torque/Fz, temperature/torque compared to their reference values. The five errors are then normalized into [-1 1] with equations (5.6) to (5.10) as the five inputs of the two FLCs. Using the reference and on-line sensor signal values listed in Table 5.1, the five errors and their normalized value are given in Table 5.2:

Table 5.2: Errors and normalized values of control variables

Control variable	Reference value	On-line value	Error	Normalized value
Temperature	230	200	30	0.5403
Fz	3.6	3	0.6	0.2532
Temperature/Fz	63.89	66.67	-2.78	-0.0153
Torque/Fz	7.5	6.67	0.83	0.2402
Temperature/Torque	8.52	10	-1.48	-0.1621

The normalized values are then mapped into the basic FLCs for fuzzification. Each input is fuzzified with predefined fuzzy input membership functions to acquire the name and value of the membership functions it falls into. Figure 5.3 shows the fuzzification results of the five inputs.

(a)

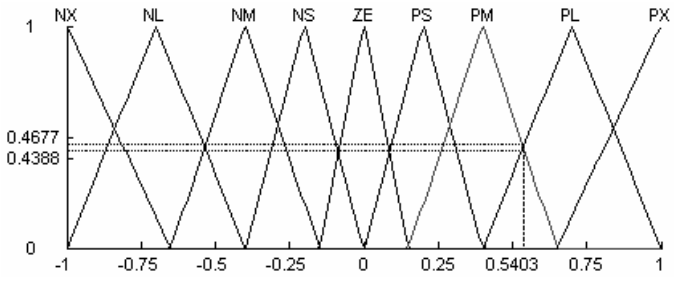

(b)

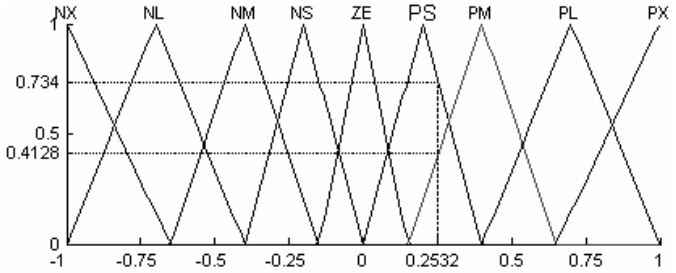

(c)

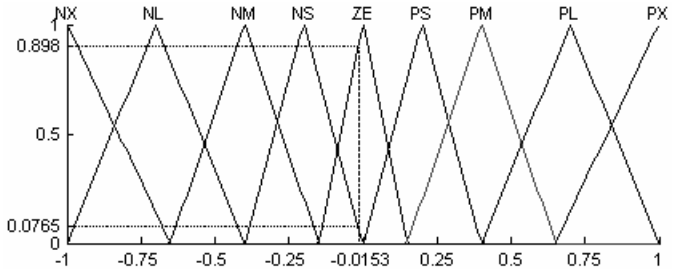

(d)

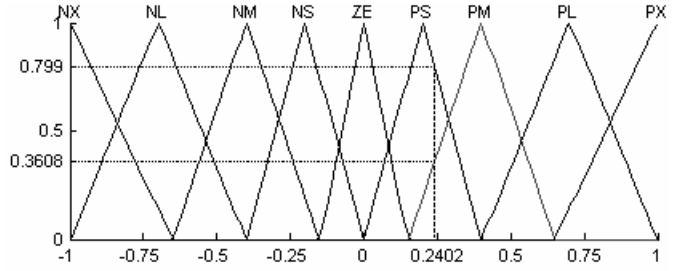

(e)

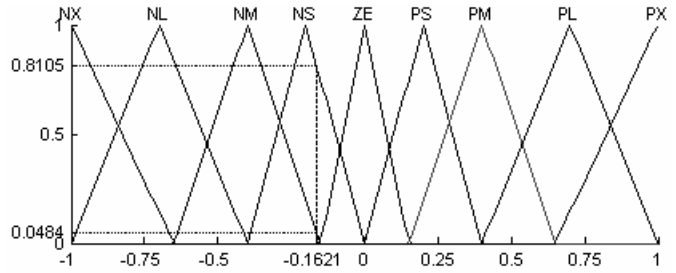

Figure 5.3: Membership function name and value of fuzzified input: (a) error of temperature, (b) error of Fz, (c) error of temperature/Fz, (d) error of torque/Fz, and (e) error of temperature/torque

5.3.3.3 Fuzzify Output

The errors between the preferred and instantly derived values of process parameters are also fuzzified with the preset membership functions of the basic FLCs.

Using the same normalization method, the errors of tilt angle, plunge depth, feed rate and spindle speed are normalized into [-1 1]. Using the reference and on-line values of feed rate, spindle speed, tilt angle and plunge depth listed in Table 5.1, the four errors and their normalized values are given in Table 5.3:

Table 5.3: Errors and normalized values of process parameters

Process	Preferred value	On-line value	Error	Normalized value
Feed rate	191.41	77.613	113.897	0.8047
Spindle speed	398.56	323.91	74.650	0.7574
Tilt angle	0.55472	0.83998	-0.285	-0.1974
Plunge depth	0.17666	0.10163	0.075	0.9787

The normalized values are also mapped into the basic FLCs. Each of the normalized values is fuzzified with the predefined output membership functions to acquire the name and value of the membership functions it falls into. Figure 5.4 shows the fuzzification results of (a) adjustment of feed rate, (b) adjustment of spindle, (c) adjustment of tilt angle, and (d) adjustment of plunge depth.

(a)

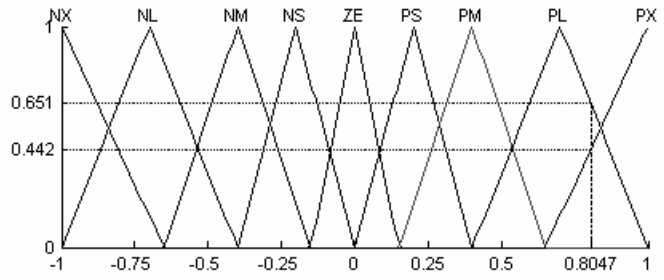

(b)

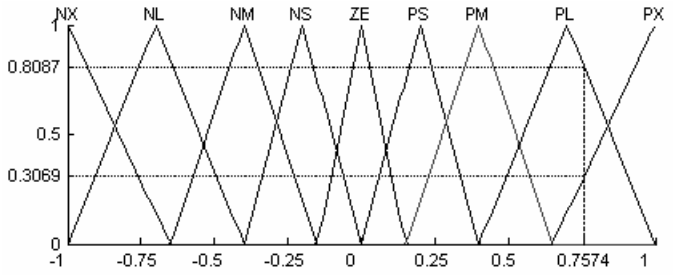

(c)

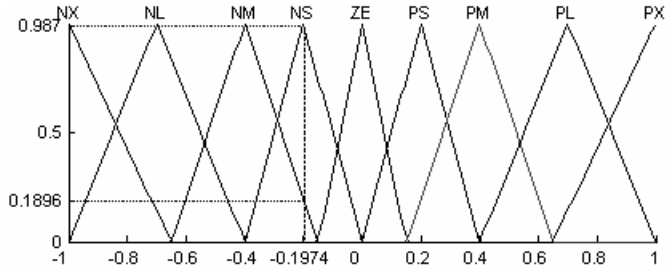

(d)

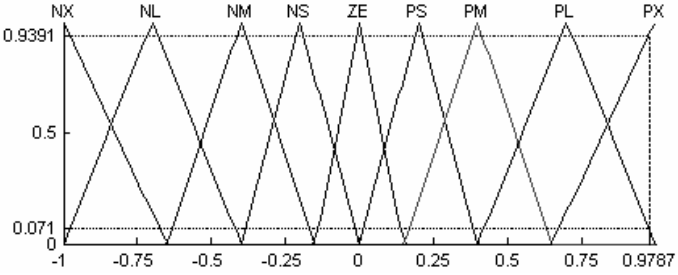

Figure 5.4: Membership function name and value of fuzzified outputs: (a) feed adjustment, (b) speed adjustment, (c) tilt adjustment, and (d) plunge adjustment

5.3.3.4 Rule Generation

The fuzzified inputs and outputs from previous procedures are used to generate on-line fuzzy rules for the FLCs. Membership function names of the fuzzified inputs are used as fuzzy rule antecedents; while the membership function names of fuzzified outputs are

used as fuzzy rule consequents. The antecedents and consequents of the on-line fuzzy rules generated from the example are shown in Table 5.4.

Table 5.4: Fuzzy rule antecedents and consequents

Fuzzy rule antecedents & consequents			Membership function
Tool/workpiece contact FLC	Antecedents	err_{Temp}	*PM, PL*
		$err_{Temp/Fz}$	*NS, ZE*
		$err_{Torq/Fz}$	*PS, PM*
	Consequents	Δ_{Tilt}	*NM, NS*
		Δ_{Plunge}	*PL, PX*
Tool/workpiece energy input FLC	Antecedents	err_{Fz}	*PS, PM*
		$err_{Temp/Torq}$	*NM, NS*
		$err_{Torq/Fz}$	*PS, PM*
	Consequents	Δ_{Feed}	*PL, PX*
		Δ_{Speed}	*PL, PX*

The on-line fuzzy rule is thus generated from the full combination of the antecedents and consequents. For this example, there are 2x2x2x2x2 = 32 fuzzy rules generated on-line for the tool/workpiece contact FLC, and 2x2x2x2x2 = 32 fuzzy rules generated on-line for the tool/workpiece energy input FLC respectively. The linguistic expression of the 32 fuzzy rules for the tool/workpiece contact FLC is listed in Appendix B.1. The first rule is shown as follows:

IF error of temperature is PM && error of temperature/Fz is NS

&& error of torque/Fz is PS,

THEN tilt angle adjustment is NM && plunge depth adjustment is PL.

The linguistic expression of the 32 fuzzy rules for the tool/workpiece energy input FLC can be seen in Appendix B.2. The first rule is listed as follows:

IF error of Fz is PS && error of temperature/torque is NM &&

error of torque/Fz is PS,

THEN feed rate adjustment is PL && spindle speed adjustment is PL.

With this method, when each set of on-line sensor data is collected from the welding process, the rule generation module automatically generates the on-line fuzzy rules. The two basic FLCs are then updated with the fuzzy rules and perform fuzzy inference. The MATLAB for rule generation can be seen in Appendix B.7. The visualised fuzzy rules for tool/workiece contact and energy input are shown in Appendix B.3 and B.4 respectively, using the MATLAB fuzzy rule viewer.

5.4 Simulations

To test the performance and adaptability of the proposed neuro-fuzzy control scheme, four examples need to be demonstrated: (1) 3mm Al 6061 flat plate weld, (2) 3mm Al 6061 round tube weld, (3) 3mm flat plate with material changing from Al 6061 to Al 5251 and (4) 3mm thickness Al 6061 alloy with curvature changing from a diameter of 70mm to flat and a diameter of 40mm. The simulation results were compared to the data recorded in the experiments of the old welding system. Figure 5.5 shows the workpieces to be welded in the four demonstrations.

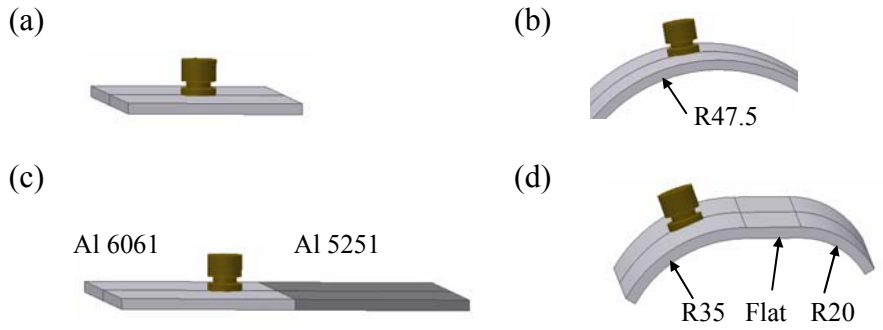

Figure 5.5: FSW workpieces of (a) Al 6061 flat plate weld, (b) Al 6061 round tube weld, (c) flat plate with changing material and (d) Al 6061 plate with changing curvature.

5.4.1 FSW of Al 6061 Flat Plate

The recorded sensor data of a sample welded with process parameters: feed rate 100 mm/min, spindle speed 600 rpm, tilt angle 0.5° and plunge depth 0.2 mm, in the OA experiment were compared to the simulation results from the proposed neuro-fuzzy controller. The average value of the recorded sensor data: bending force 335.95 N, torque 20.33 Nm, temperature 275.2 ˚C, and Fz 1.74 kN were used as the reference value for the neuro-fuzzy controller. Using the trained NN, the preferred process parameters of the weld were derived as: feed rate 103.53 mm/min, spindle speed 595.4 rpm, tilt angle 0.52˚ and plunge depth 0.19 mm.

Figure 5.6 shows the comparison of bending force, torque, temperature, and Fz between recorded value of the welded sample and the simulation results from the proposed controller. The simulated process parameter adjustments by the controller were also shown in Figures 5.6 (a) to (d).

(a)

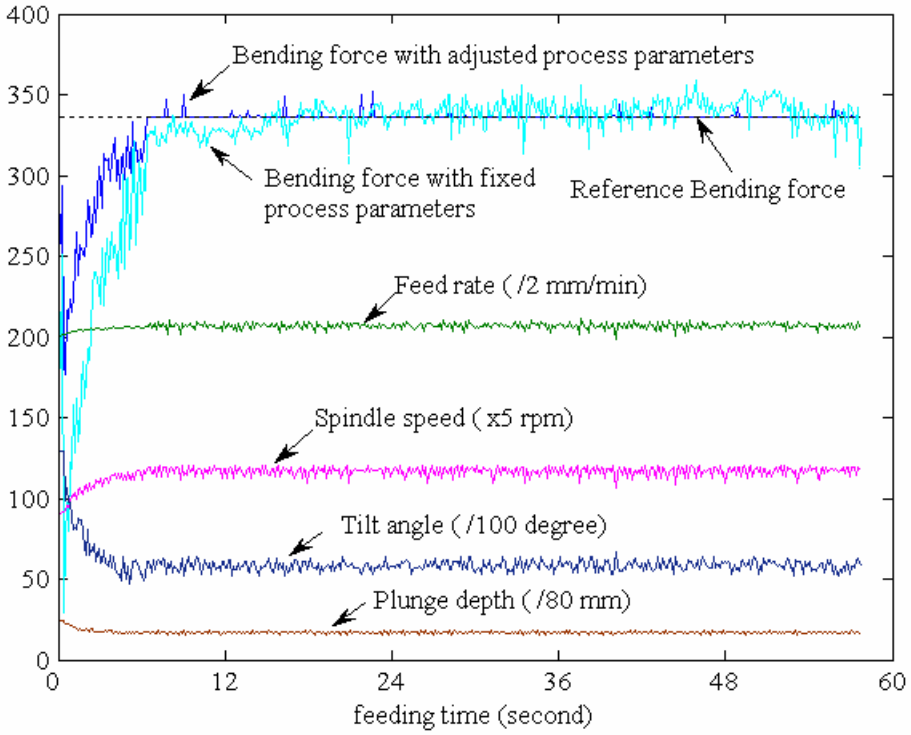

(b)

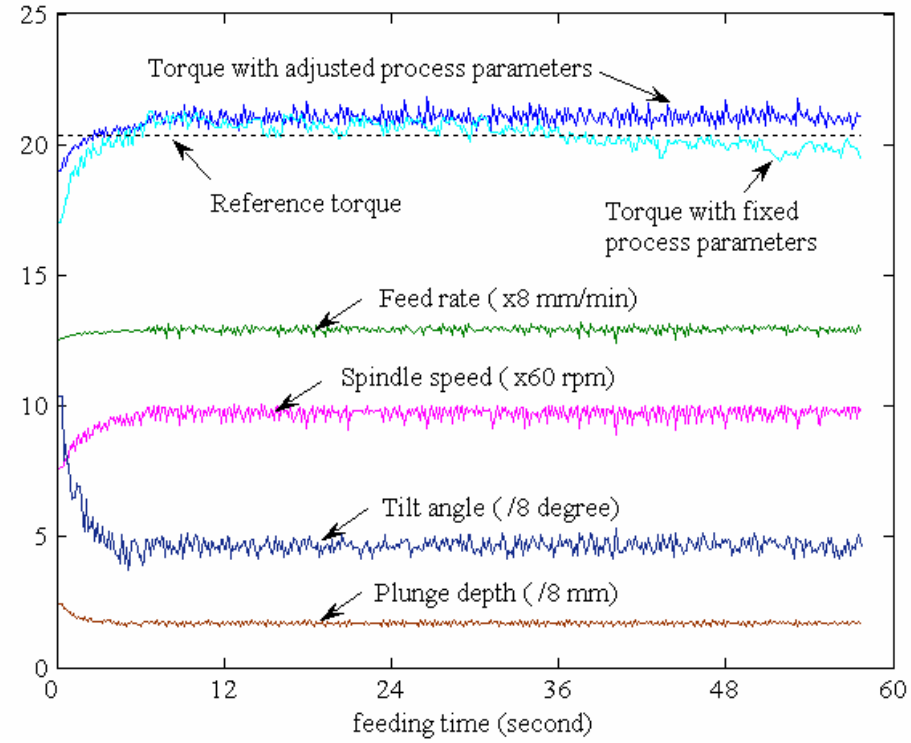

Figure 5.6: Comparison of (a) bending force and (b) torque between sample weld and simulation results of Al 6061 flat plate.

(c)

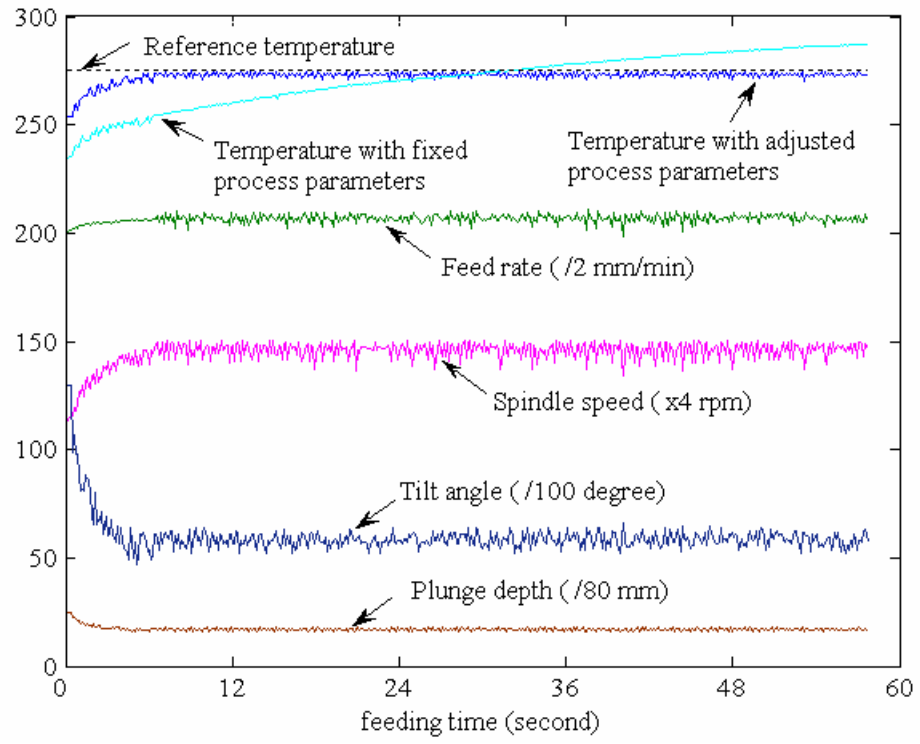

(d)

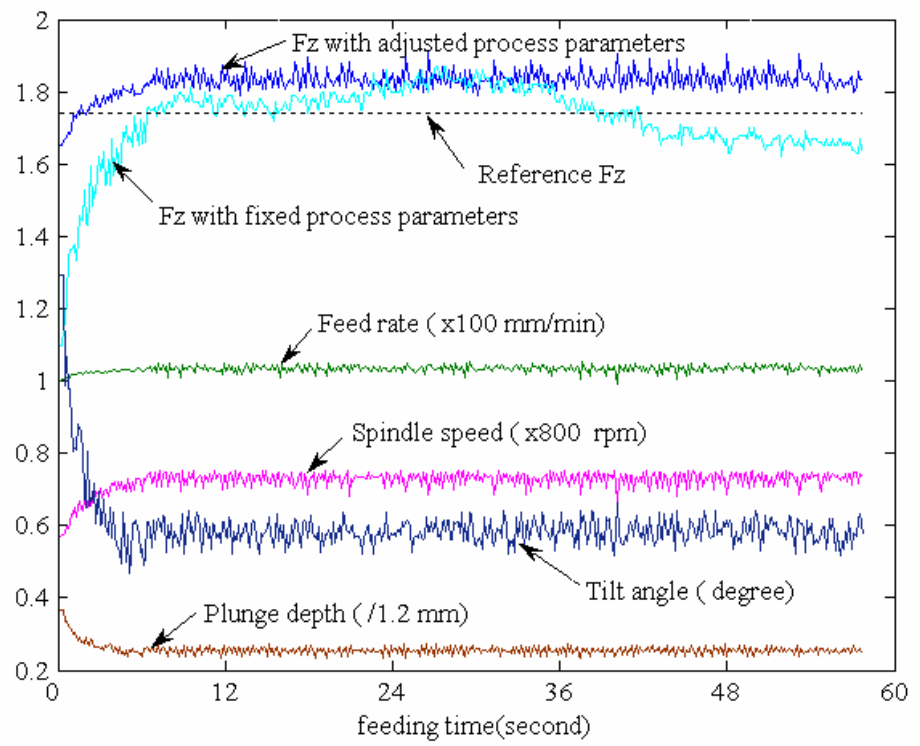

Figure 5.6 (cont): Comparison of (c) temperature, and (d) Fz between sample weld and simulation results of Al 6061 flat plate.

It can be seen that sensor data of the experimental sample were well controlled, as in flat plate welding of uniform material, process condition and parameters can be well maintained. It also shows that even the process parameters were well predefined; there are still small deviations of sensor data from their reference values in the sample welding. The simulation results of bending force, torque, temperature and Fz from the neuro-fuzzy controller are better maintained toward their reference value than the sample weld, except that torque and Fz of the simulation results are a little bit higher than their reference values. This can be explained by the training error of the NNs representing the relationship between process parameters and sensor data. It can be also seen that process parameters of tilt angle and plunge depth are adjusted on-line by analyzing on-line sensor data to maintain tool/workpiece contact.

5.4.2 FSW of Al 6061 Round Tube with Constant Curvature

During welding of round tubes with constant curvature, the real tool/workpiece contact changed due to the deviations of tilt angle and plunge depth from the predetermined condition, which were caused by workpiece and clamping system machining errors together with process disturbance by the large force involved. Thus, to maintain the desired tool/workpiece contact and energy input, on-line sensor data of temperature, torque and Fz are fed back to the control system for analyzing and making on-line process parameter adjustments.

Using the proposed neuro-fuzzy control scheme, on-line value of control variables (torque, temperature, and Fz) are fed into the controller as inputs, while feed rate, spindle speed and plunge depth are adjusted on-line by the controller.

Figures 5.7 (a) to (c) show the comparisons of sensor data between a sample round tube weld and simulation results of the controller. The sample was welded on the machine with process parameters: feed rate 100 mm/min, spindle speed 500 rpm, tilt angle 1 ° and plunge depth 0.2 mm. The four process parameters and the process condition curvature radius of 47.5 mm were used as inputs of the trained NN to derive reference values of torque, temperature and Fz; which are 15 Nm, 240 °C and 3.34 kN. The tilt angle was considered as constant, as it changes very little during welding once the workpiece was firmly clamped. The curvature radius, tilt angle, reference values of torque, temperature and Fz were fed into another trained NN to derive the preferred process parameters of feed rate (101.47 mm/min), spindle speed (500.98 rpm) and plunge depth (0.20mm).

(a)

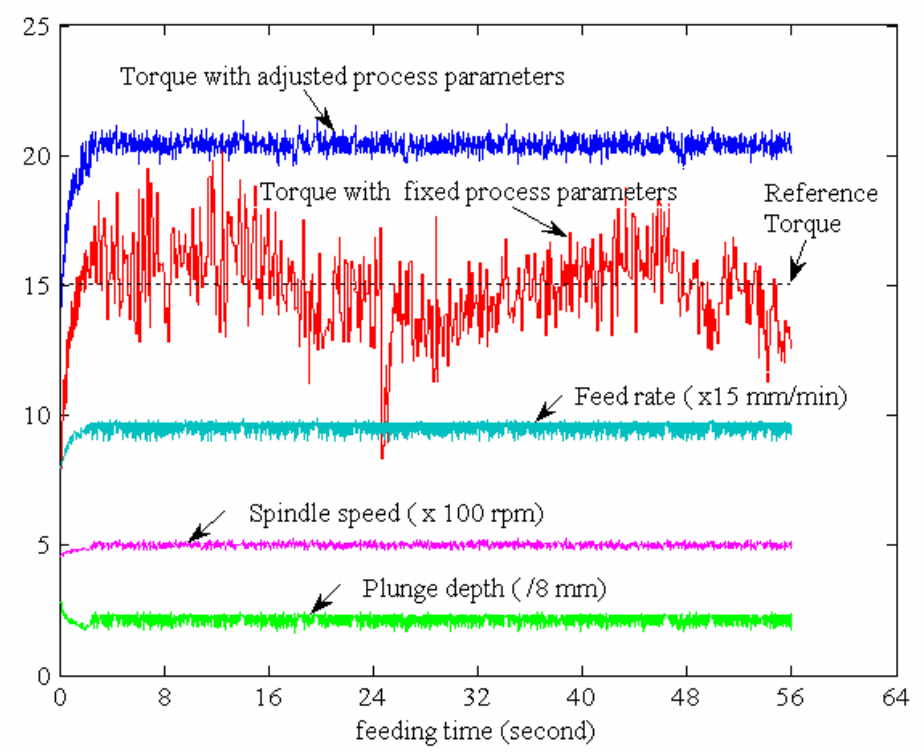

Figure 5.7: Comparison of (a) torque between sample weld and simulation results of Al 6061 round tube

(b)

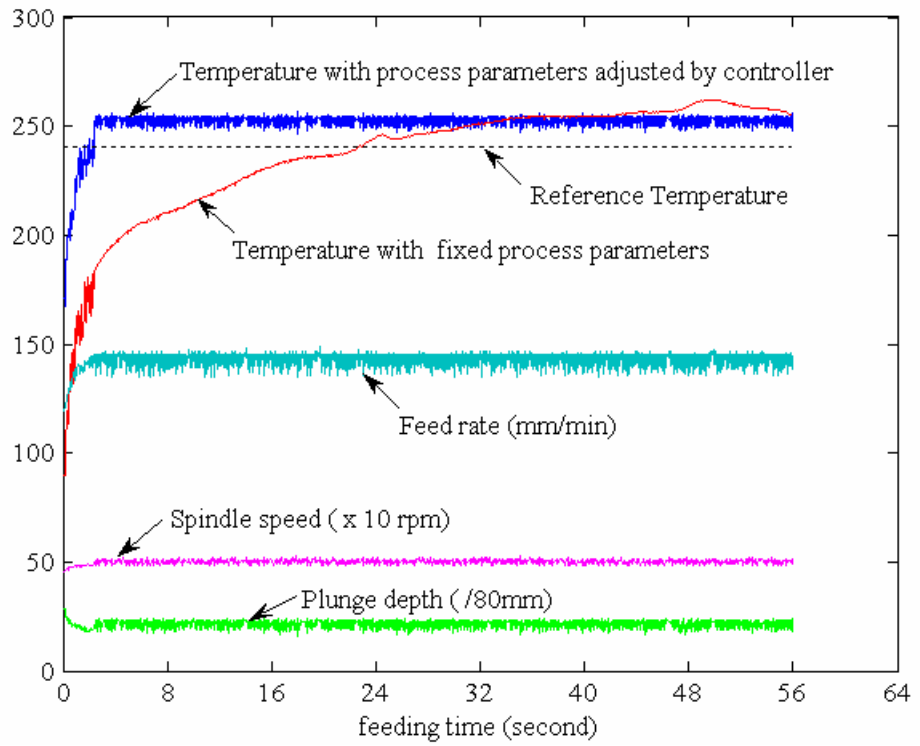

(c)

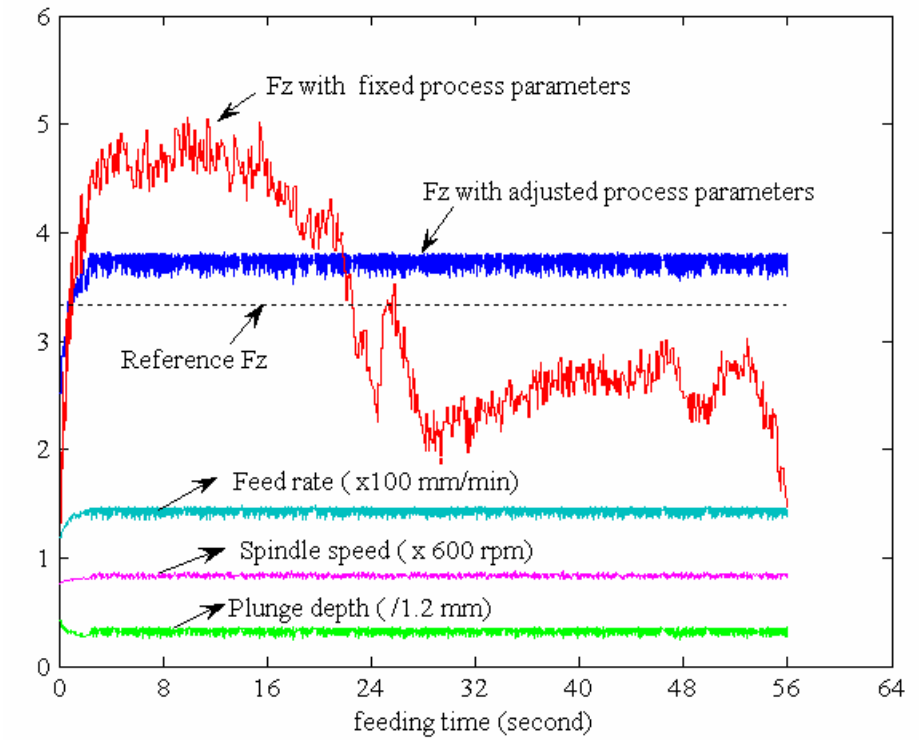

Figure 5.7 (cont): Comparison of (b) temperature, and (c) Fz between sample weld and simulation results of Al 6061 round tube

It can be seen that torque, temperature and Fz of the sample weld are not well controlled during welding with fixed process parameters. This can be explained mainly by the plunge depth. The sample was not actually welded with the expected constant plunge depth, as the workpiece rotating around the axis of the fixture is not perfectly 'round' due to the machining error of workpiece and fixture. This cause the tool/workpiece contact conditions to change during welding. However, with the neuro-fuzzy control scheme, on-line sensor data of torque, temperature, and Fz were analyzed to find out the reason for the deviation of sensor data from their reference values, and corresponding process parameter adjustments were made to maintain correct tool/workpiece contact and energy input. The simulation results of temperature and Fz are maintained much better towards the reference level than the sample welded on the old system, while torque is almost 33% higher than the reference value. This also comes from the error of the NN model used in simulation. It can be expected that with more samples used in OA experiments, a more accurate NN model and better simulation results can be achieved.

5.4.3 Workpieces with Changing Material

Fig.5.8 shows the comparison of torque and temperature between the experimental sample and neuro-fuzzy controller simulation results of flat plate with material changing from Al 6061 alloy to Al 5251 alloy. The sample was welded with fixed process parameters: feed rate 50mm/min, spindle speed 400 rpm, tilt angle 1 ° and plunge depth 0.2 mm for both materials. The trained NN, which maps the relationship between process conditions and parameters (material, feed, speed, tilt and plunge), and sensor data (torque and temperature), were used to derive the reference value of torque (24.25 Nm) and temperature (249.56 °C).

(a)

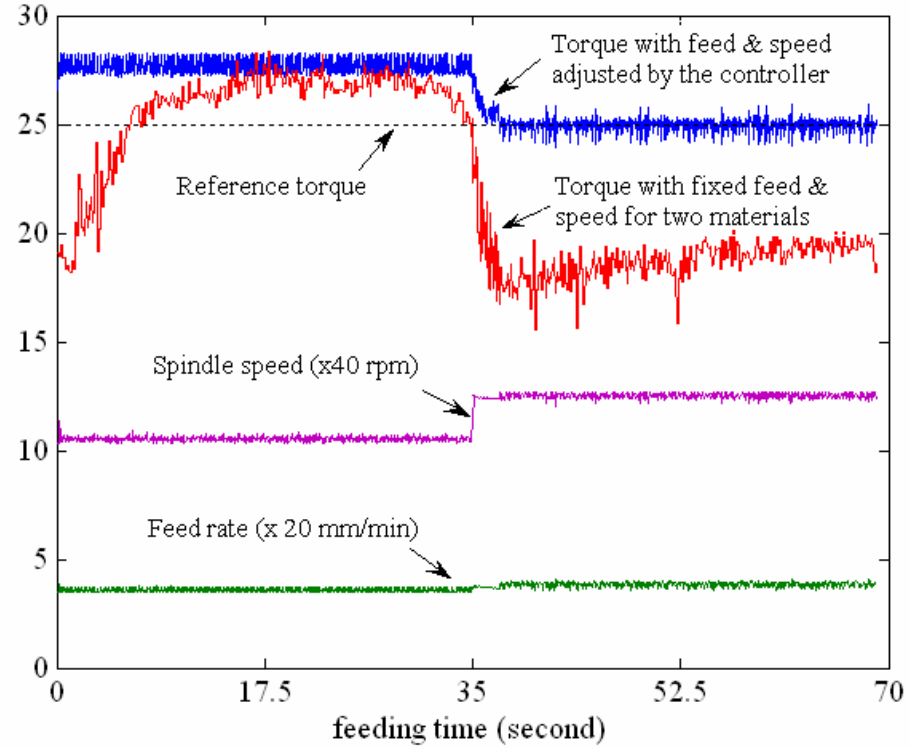

(b)

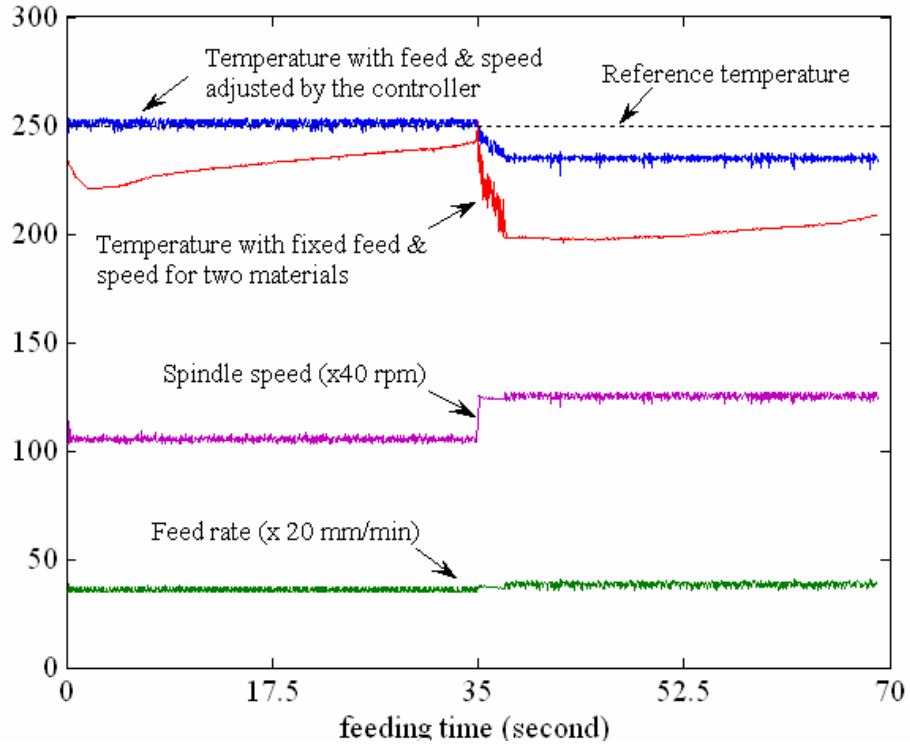

Figure 5.8: Comparison of (a) torque, and (b) temperature between sample weld and simulation results of workpieces with changing materials

During simulating, the same constant tilt angle and plunge depth were used, as they can be well maintained during flat plate welding. The feed rate and spindle speed were adjusted by the controller to maintain torque and temperature towards their reference value for the two materials. A trained NN, which maps the relationship between process parameters and sensor data (e.g. tilt angle, plunge depth, torque, and temperature), and material (‘0’ for Al 6061 and ‘1’ for Al 5251), was used for material detecting. When the tool moved from Al 6061 to Al 5251 alloy plate, the on-line sensor data of torque and temperature, together with process parameter tilt angle and plunge depth, were used to determine what kind of material it was welding, and thus the controller was able to use the material type and on-line sensor data to perform neuro-fuzzy control.

It can be seen that with fixed process parameters, considerable decrease in torque and temperature was observed in the data of the sample welded on the old system due to a material change. However, with the neuro-fuzzy controller, torque and temperature were much better maintained towards their reference values by adjusting feed rate and spindle speed on-line, although small deviations were still observed. This indicated that the proposed neuro-fuzzy control scheme has adaptability to material changes.

5.4.4 Workpieces with Changing Curvature

To test the adaptability of the proposed neuro-fuzzy control scheme to complex curvature, the welding process of workpiece with changing curvature was simulated and compared to the sample welded without the proposed neuro-fuzzy controller.

The curvature of the sample workpiece starts with a curvature radius of 35 mm, which is connected to a flat plate and ends with a curvature radius of 20mm, as shown in Figure

5.5 (d). The sample was welded with fixed process parameters: feed rate 100mm/min, spindle speed 500 rpm, tilt angle 1 ° and plunge depth 0.2 mm. The reference sensor values for torque, temperature and Fz for simulation were thus derived from the trained NN, which mapped the relationship between process conditions and parameters (curvature, feed, speed, tilt, and plunge), and sensor data (torque, temperature and Fz), as 15.08 Nm, 240.71 °C and 3.34 kN with the fixed process parameters and a curvature radius of 35 mm.

During simulating, the same constant tilt angle as the welded sample was used. The feed rate, spindle speed and plunge depth were adjusted by the controller to maintain torque, temperature and Fz towards their reference values. A trained NN mapping the relationship between process parameters and sensor data, and a curvature radius was used for curvature detecting. When the tool moved from one curvature to another, on-line sensor data of torque, temperature, Fz and process parameters were used to predict the curvature being welded. The controller used the predicted workpiece curvature and on-line sensor data to perform neuro-fuzzy control.

Figures 5.9 (a) to (c) show the comparison of control variables between a welded sample without the neuro-fuzzy controller and simulation results with the controller, as well as process parameter adjustments by the controller. The results show that in the data of the sample welded with fixed process parameters, large deviations of the three control variables from their reference values were observed for all the three different curvatures. It was also observed that large difference in torque, temperature and Fz existed between the three curvatures.

(a)

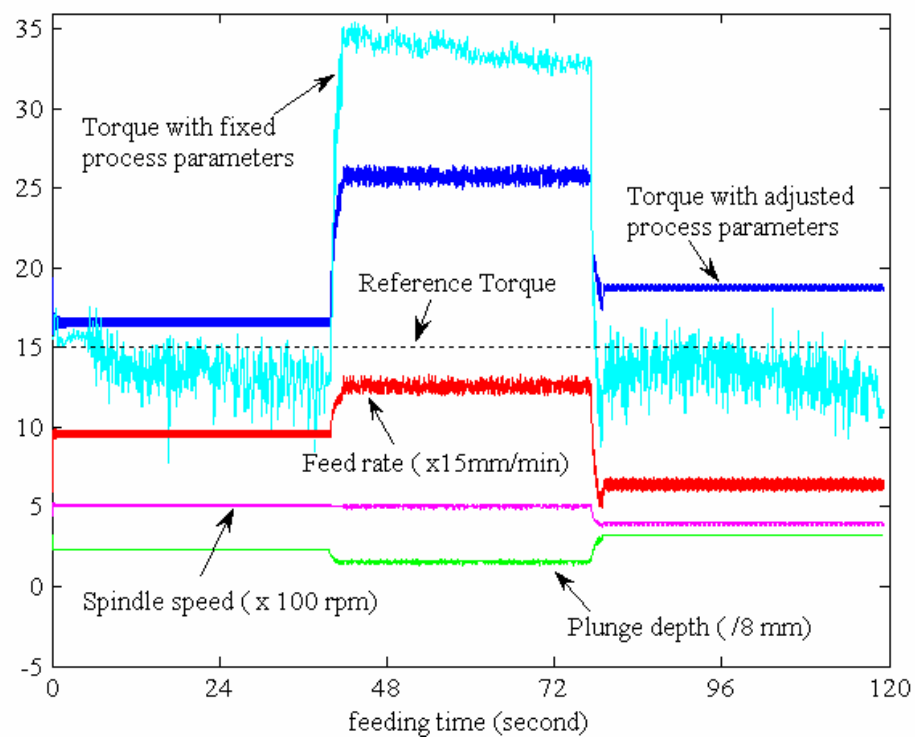

(b)

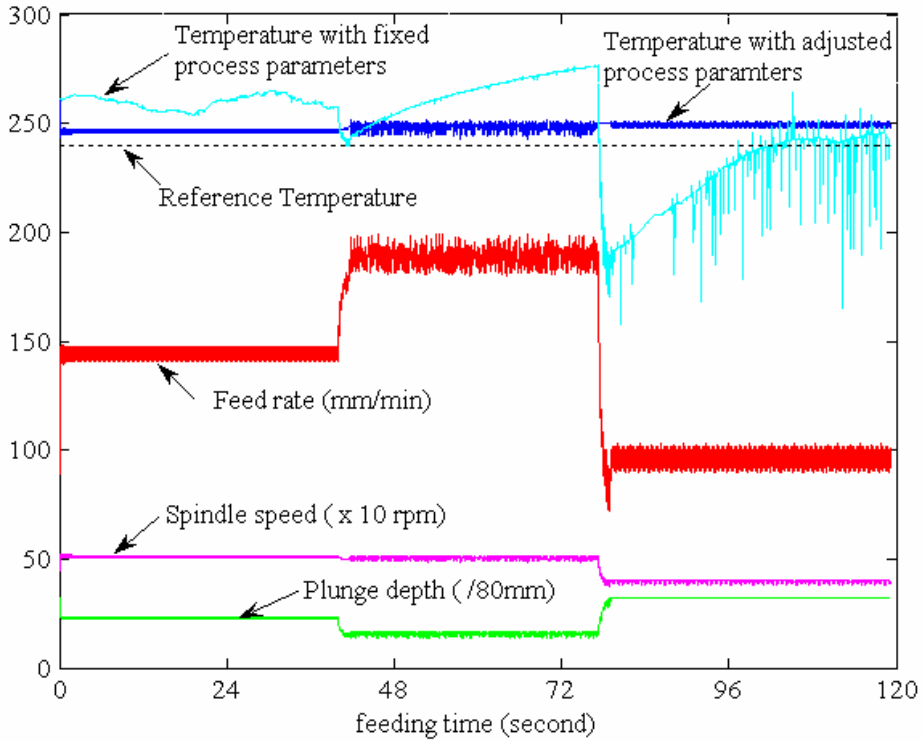

Figure 5.9: Comparison of (a) torque, (b) temperature between sample weld and simulation results of workpiece with changing curvature

(c)

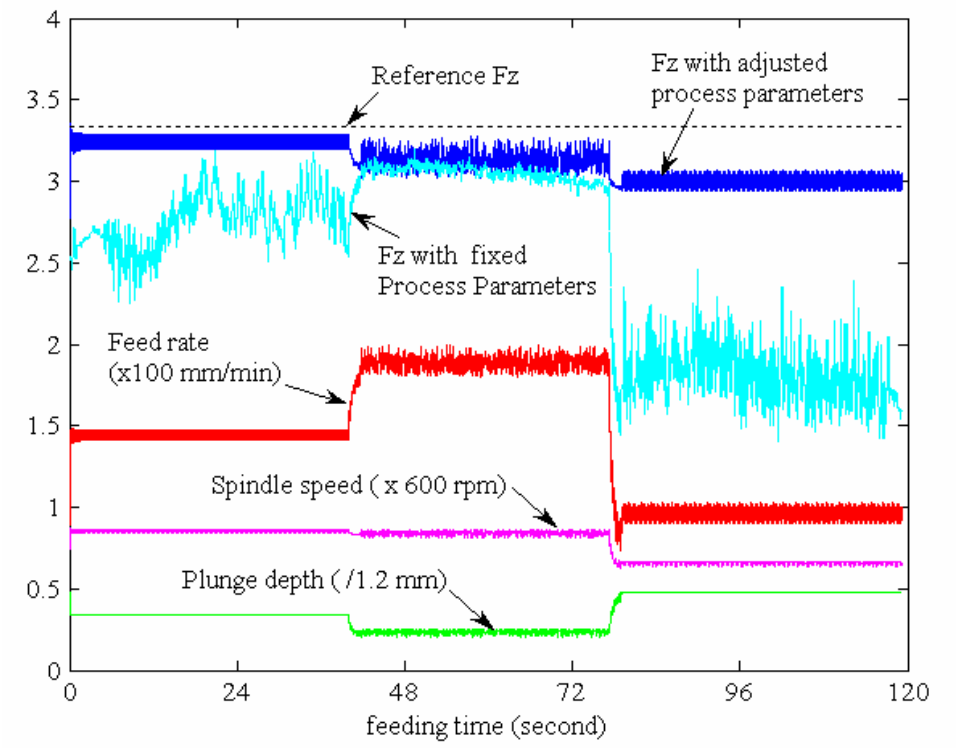

Figure 5.9 (cont): Comparison of (c) Fz between sample weld and simulation results of workpiece with changing curvature

However, with the neuro-fuzzy control scheme, torque, temperature and Fz were much better maintained towards their reference values than the welded sample by adjusting feed rate, spindle speed and plunge depth on-line. This indicated that the proposed neuro-fuzzy control scheme has good adaptability to curvature changing, and thus it is applicable for complex curvature FSW. Among the three control variables of the simulation results, temperature seems to have the least deviation from its reference value and the smallest change range; while torque shows the most deviation from its reference value and the largest change range. This suggests that sensor values are limited to different ranges for different workpiece curvatures; or in other words, for complex curvature FSW, some but not all of the control variables can be well maintained.

5.5 Discussion

FSW is a non-linear process which involves multiple variables of process parameter, process condition and process outputs. During complex curvature FSW, process condition such as workpiece curvature change diversely. Even for workpiece with uniform curvature, the slight machining error of the workpiece and the disturbance from the machine cause the deviation of the control variables from reference value, and results in unstable weld quality. To maintain tool/workpiece contact and energy input, which dominate the weld quality, the neuro-fuzzy control scheme is characterised by the ability of detecting the change of process condition and making on-line decision of process parameter adjustments to maintain control variables towards their reference value.

For flat plate welds, the sensor data of the weld sample show good stability. They were generally well maintained towards their reference value owing to the well controlled process parameters. It also shows small deviations of sensor data (e.g., torque and Fz) from their reference values in the sample welding. This can be explained by the non-uniformity of material. Even the slightest change of workpiece material thickness has influence on the sensor data. The sample was welded without adjusting process parameters in response of the changing of sensor data. However, using the neuro-fuzzy control scheme, the deviations of sensor data to their reference value were fed into the fuzzy controller. With the fuzzy rules generated with the trained NN which maps the relationship between process parameters and sensor data established during training, process parameters were on-line adjusted to maintain the control variables towards their

reference value. It can be seen in Figure 5.6 that the stability of sensor data from simulation results was improved compared to the data from the welded sample.

When welding workpiece of round tube, sensor data (torque, temperature and Fz) from the sample welded with unadjusted process parameters showed large deviation from their reference value, as shown in Figure 5.7. The sample was not really welded with the preset process parameters due to the weld trajectory fluctuation caused by machining error of workipece and clamping system. With the neuro-fuzzy controller, the real process parameters, especially the plunge depth, were derived with on-line sensor data by the trained NN. The difference between real value and preferred value of process parameters suggested the reason for the deviation of sensor data, and accordingly the fuzzy rules were on-line generated to update the basic FLCs. The tuning mechanism of the controller further strengthen or weaken the process parameter adjustments adapt to the accumulation and change trend of sensor data error. By on-line adjusting process parameters towards preferred value, the sensor data were maintained stable towards their reference value. However, it was also shown in Figure 5.7 that the torque of simulation results was maintained towards a stable value higher than the reference value (20 N.m to 15N.m); this can be explained by the training error of the NN model. The real relationship between process parameters and sensor data was not perfectly reflected by the NN model. This also indicated that with updated NN model, the control variables can be better maintained towards their reference value for round tube FSW.

The welding of workpieces with changing material and curvature were also demonstrated to test the adaptability of the neuro-fuzzy control scheme to process condition (e.g., material and curvature) changes. When the sample with changing material (or curvature)

was welded with fixed process parameters, the sensor data (torque, temperature and Fz) from the sample weld showed big fluctuation when the tool moved from one material (or curvature) to another. The difference of sensor data for different material was cause by different material properties such as formability and thermal conductivity, while the difference of sensor data for different curvature was mainly caused by tool/workpiece contact condition, as shown in Chapter 4 and 3 respectively. However, using the trained NN for material (or curvature) detecting, the difference of sensor data between different materials (or curvatures) was used to detect material (or curvature) change. With the detected material (or curvature), the preferred and instant process parameters were derived from the reference and on-line value of sensor data respectively. The error of sensor data were fed into the FLCs updated with on-line generated fuzzy rules for making process parameter adjustments. The same preferred process parameters were used during welding until another material (or curvature) was detected. As shown in Figure 5.8 and Figure 5.9, the simulation results of sensor data were much better maintained towards reference value compared to the sample weld data, and this indicates that the neuro-fuzzy controller has good adaptability to material (or curvature) change.

It was also shown in the simulation results that among the sensor signals, torque exhibited larger deviation from reference value than the other sensor signals. Even with the neuro-fuzzy control scheme, it was impossible to well maintain all of the sensor data towards their reference value during complex curvature FSW. This can be explained by the limitation of the process parameters and welding tool used in this project. Process parameters such as spindle speed were limited within certain ranges by the FSW machine, and the same tool was used in all tests. Therefore, for certain material (or curvature), only

limited range of sensor value can be achieved. To further improve the performance and adaptability of the neuro-fuzzy control scheme, the NN models used for material (curvature) detecting and fuzzy rule generating need to be updated with training data outside the selected range and weld tools of different geometries.

5.6 Summary

A neuro-fuzzy control scheme integrating AIs such as NN and FLC for solving MIMO system such as FSW process was presented. The proposed neuro-fuzzy control system consists of several trained NNs for detecting process condition changes and deriving instant process parameters, a rule-generating module for fuzzy rule generation using control variable errors, and process parameter errors between preferred values and derived instant values, a basic fuzzy controller with predefined input/output membership functions to generate primary command for process parameters adjustment, and a tuning module to strengthen or weaken control actions by tuning input and output scale factors in response of the dynamic process changing.

The proposed neuro-fuzzy control scheme for maintaining contact and energy input between tool and workpiece during complex curvature FSW was demonstrated. The simulation results of workpieces with changing process conditions such as material and curvature indicate that with the algorithms of input/output scale factor tuning and on-line fuzzy rule generating, the maintenance of tool/workpiece contact and energy input represented by control variables such as torque, temperature and Fz, can be greatly improved. The simulation results also indicated that the proposed neuro-fuzzy control scheme has good adaptability to process condition (e.g. material and curvature) changes.

It can also be observed from the simulation results and the welded samples that among the control variables of torque, temperature, and Fz, the deviation from reference values and the changing ranges are different with the same changing of process condition (e.g. material and curvature). This indicates that sensor values are limited to different ranges for different process condition (e.g. material and curvature); that is to say, for complex curvature FSW, not all of the control variables can be well maintained with changing process condition. By using different trained NNs, the proposed neuro-fuzzy control scheme also shows good flexibility to change its control variables for different requirements.

Further research on increasing NN model accuracy by investigating wider range of process condition and process parameters is needed in order to improve the performance of the proposed intelligent neuro-fuzzy control scheme for complex curvature FSW. The application of the proposed intelligent control scheme is also expected to be extended to dynamic processes other than FSW.

Chapter 6 Conclusion and Future Development

FSW is a relative new technique that has shown much promise and potential. Much research has been done on mechanical properties, monitoring, and control of FSW; however, most of the research into monitoring and control of FSW are mainly focused on straight welds. In addition, most of the conclusions have been qualitative and have been based largely on observation. Little documentation could be found on control and monitoring of complex curvature FSW.

Artificial intelligence is to describe and build an intelligent agent, which has the ability to sense the environment, to make decisions and to control action. The relative concepts of intelligent control and on-line monitoring, including sensitive feature selection, multi-sensor fusion, machine learning and adaptive control were introduced in this research project. In the establishment of the neuro-fuzzy control scheme proposed in this study, AI algorithms such as NN and FL were applied to monitoring and control complex curvature FSW to solve the non-linearity and uncertainty problems of the process.

The accomplishments and contributions of this study for the particular machine, tool and materials are summarized as follows:

- An adaptive neuro-fuzzy control scheme which integrates process condition sensing, on-line fuzzy rule generation, fuzzy inference and input/output tuning was implemented successfully for non-linear FSW process control.

- Hardware architecture and software components for a table-tilting multi-axis system providing large force and precise orientation and position control were

proposed and implemented to perform complex curvature FSW on the platform of the existing FSW machine for flat plate welding.

- OA experiments of Al 5251 and Al 6061 alloy FSW were carried out to obtain experimental data by varying process parameters (feed rate, spindle speed, tilt angle and plunge depth), and process conditions (parent material and curvature). The effects of process conditions and process parameters on sensor data were investigated.

- Statistical analysis and feed-forward back-propagation NNs were applied to perform sensor fusion. The feed-forward back-propagation NNs, which map the non-linear relationship between process conditions, process parameters and sensor data, were trained with selected sensitive features for process condition monitoring and on-line fuzzy rule generation.

- The uncertainty and non-linearity in complex curvature FSW makes it difficult to establish am accurate kinematic and dynamic model. Owing to its ability to model non-linear functions of arbitrary complexity, FL was integrated with NN to realize intelligent control of the MIMO FSW process. The tuning mechanism, which tuned input/output scale factors on-line in response of both the amount, and the trend of control variable deviations from their reference values, provide the FL control with adaptability to process changes.

- Simulations were conducted to test the performance of the intelligent nero-fuzzy control scheme during complex curvature FSW. Simulation results showed that the presented neuro-fuzzy control scheme has adaptability to process condition

such as parent material and curvature changes and that the control variables were well maintained.

Intelligent control and monitoring system is an advanced approach in manufacturing. Further development may enhance the performance and intelligence of the system. Future development may be summarized as follows:

- To investigate mechanical and thermal properties such as fatigue life, microstructure and temperature distribution of friction stir welds and take these factors into the monitoring and intelligent control system.

- To integrate other AIs such as GA and EC to enhance the learning and optimizing abilities of the neuro-fuzzy control scheme.

- To implement the neuro-fuzzy controller in a C program and integrate it into the real-time QNX operation system. GUI for monitoring and process simulation can be upgraded with visualised process animation.

- To explore more variables used in sensor fusion and fuzzy control such as spindle power, Fx and Fy. Using other variables as inputs for controlling outputs may add the intelligence of the neuro-fuzzy control scheme for complex curvature FSW.

- To perform additional testing and analysis for the creation of transient models which include both the steady-state and transient portion of the FSW process. More features are to be extracted from the sensor signals by additional signal processing and analysis methods such as power, kurtosis value and skew value in the time domain and Fast Fourier Transformation in frequency domain.

- To enhance the adaptability of the monitoring and control system by investigating process parameters outside the selected range for this study and new tool, material and workiece thickness.

- To extend the application of the presented neuro-fuzzy control scheme in other MIMO machining processes.

References

Akbarzadeh-T M.R., K. Kumbla, E. Tunstel and M. Jamshidi (2000). Soft computing for autonomous robotic systems. Computers and Electrical Engineering, **26 (1),** 5-32.

Aluminium City (Pty) Limited (1999). Engineering Division Handbook, pp. T8-T9.

Altintas, Y. (1994). Direct adaptive control of end milling process. International Journal of Machine Tools and Manufacture, **34 (4)**, 461–472.

Al-Habaibeh, A. and N. Gindy (1999). Rapid design of condition monitoring system for milling operations. Proceedings of the 15th International Conference on Computer-Aided Production Engineering, University of Durham.

Al-Habaibeh, A. and N. Gindy (2001). Self-Learning Algorithm for Automated Design of Condition Monitoring Systems for Milling Operations. The International Journal of Advanced Manufacturing Technology, **18**, 448–459.

Al-Habaibeh, A., F. Zorriassatine and N. Gindy (2002). Comprehensive experimental evaluation of a systematic approach for cost effective and rapid design of condition monitoring systems using Taguchi's method. Journal of Materials Processing Technology, **124**, 372~383.

Anderson, J.A. (1995). An Introduction to Neural Networks. ISBN 0-262-01144-1, MIT Press, Cambridge, MA.

Andrews, R. E. (1999). TWI project no 221166, progress report 1/11 1998- 19/2 1999.

Arbegast, W. and M. Skinner (2002). Multi-axis Friction Stir Welding and Intelligent Laser Processing at the Advanced Materials Processing Center, AEROMAT 2002 Conference, June 8-14.

Azouzi, R. and M. Guillot (1997). On-line prediction of surface finish and dimensional deviation in turning using neural network based sensor fusion. Int. Journal of Machine Tools and Manufacture, **37**, 1201-1217.

Axinte, D.A. and N. Gindy (2003). Tool condition monitoring in broaching. Wear, **254** 370–382.

Birla, S. K. (1980). Sensors for adaptive control and machine diagnostics. Proc. Machine Tool Task Force Conf., 4, Section 7-12.

Blignault, C. (2005). A Friction Stir Weld Tool-force and Response Surface Model Characterizing Tool Performance and Weld Joint Integrity. Thesis of Doctor Technologiae: Mechanical Engineering, Faculty of Engineering, Nelson Mandela Metropolitan University, Port Elizabeth, South Africa.

Bobrow, J.E. (1985). NC machine tool path generation from CSG representation. Comput-Aided Des, **17**:69–76.

Carvajal, J., G.R. Chen and H. Ogmen (2000). Fuzzy PID controller: Design, performance evaluation, and stability analysis. Information Sciences, **123**, 249-270.

Chang, D.S. and S.T. Jiang (2002). Assessing quality performance based on the on-line sensor measurements using neural networks. Computers & industrial engineering, **42**, 417~424.

CHAN, S. P (2003). A Robust Control Law with Estimated Perturbation Compensation for Robot Manipulators. Journal of Intelligent and Robotic Systems, **36**, 265–283.

Chen, C.H. (1996). Fuzzy Logic and Neural Network Handbook. ISBN 0-07-011189-8, McGraw-Hill, New York.

Chen, C.M. and R. Kovacevic (2003). Finite element modelling of friction stir welding—thermal and thermomechanical analysis. International Journal of Machine Tools & Manufacture **43**, 1319–1326.

Chen, C.M., R. Kovacevic and D. Jandgric (2003). Wavelet transform analysis of acoustic emission in monitoring friction stir welding of Al 6061 aluminum. International Journal of Machine Tools & Manufacture, **43**, 1383–1390.

Chiang, S.T., D.I. Liu, A.C. Lee and W.H. Chieng (1995). Adaptive control optimization in end milling using neural networks. International Journal of Machine Tools and Manufacture, **34 (5)**, 637–660.

Chittayil, K., S.R.T. Kumara, and P.H. Cohen (1992). Acoustic emission sensing for tool wear monitoring and process control in metal cutting. In R. C. Dorf & A. Kusiak, Handbook of design, manufacturing and automation, New York: Wiley.

Choi, B.K. and R.B. Jerard (1998). Sculptured surface machining. Dordrecht: Kluwer.

Chryssolouris, G. and M. Guillot (1990). A comparison of statistical and AI approaches to the selection of process parameters in intelligent machining. Trans. ASME, J, Engng Ind., 112-122.

Chung, K.T. and A. Geddam (2003). A multi-sensor approach to the monitoring of end milling operations. Journal of Materials Processing Technology, **139**, 15–20.

Colegrove, P.A. (2000). Three dimensional flow and thermal modelling of the friction stir welding process. Proceedings of the second International Symposium on Friction Stir Welding, Gothenburg , Sweden.

Dayhoff, J.E. (1990). Neural network architectures. New York: Van Nostrand Reinhold.

Dornfeld, D.A., W. Koenig and G. Kettle (1993). Present state of tool and process monitoring in cutting. Proceedings of the New Developments in Cutting, **VDI Berichte NR988**, pp. 363–375.

Dragomatz, D and S. Mann (1997). A classified bibliography of literature on NC milling path generation. Comput-Aided Des, **29**, 239–47.

D'Errico, G.E. (2001). Fuzzy control systems with application to machining processes. Journal of Materials Processing Technology, **109**, 38-43.

Elber, G. and E. Cohen (1994). Tool path generation from free-form surface models. Comput-Aided Des, **26**, 490–496.

Ericsson, M. and R. Sandström (2003). Influence of welding speed on the fatigue of friction stir welds,and comparison with MIG and TIG. International Journal of Fatigue, **25**, 1379–1387

Farouki, R.T., J. Manjunathaiah and G.F. Yuan (1998). Variable-feedrate interpolators for constant material removal rates along Pythagoreanhodograph curves. Comput-Aided Des, **30**, 631–40.

Feng, H.Y. and C.H. Menq (1994). The prediction of cutting forces in the ball-end milling process. I. Model formulation and model building procedure. International Journal of Machine Tools and Manufacture, **34(5)**, 697–710.

Fukuda, T. and N. Kubota (1997). Computational Intelligence in Robotics and Mechatronics. Proc. of the 23rd Int'l Conf. on Industrial Electronics, Control, and Instrumentation (IECON), **4 (4)**, 1517-1528.

Garrett JH (1994). Where and why artificial neural networks are applicable in civil engineering. ASCE, J Comp Civ Engng [special issue], **8(2)**, 129-30.

Guillot, M., R. Azouzi and M.C. Cote (1994). Process monitoring and control. In Artificial Neural Networks for Intelligent Manufacturing (edited by C. Dagli). Chapman and Hall, London.

Gunaratnam, D.J. and J.S. Gero (1994). Effect of representation on the performance of neural networks in structural engineering applications. Microcomput Civ Engng, **9**, 97-108.

Haagensen, P. J., O.T. Midling and M. Ranes (1995). Fatigue performance of friction stir butt welds in a 6000 series aluminium alloy, Computer Methods and Experimental Measurements for Surface Treatment Effects II, Computational Mechanics Publications, 225-237.

Haber, R.E, J.R. Alique, A. Alique, J. Herna´ndez and R. Uribe-Etxebarria (2003). Embedded fuzzy-control system for machining processes: Results of a case study. Computers in Industry, **50**, 353–366.

Haber, R.E, R.H. Haber, S. Ros, A. Alique and J.R. Alique (2002). Dynamic model of the machining process on the basis of neural networks: from simulation to real time application, Lecture Notes in Computer Science **2331**, 574–583.

Han, Z. and D.C.H. Yang (1999). Iso-phote based tool-path generation for machining free-form surfaces. Trans ASME J Manufact Sci Engng, **121**, 656–64.

Hoo, K.A., E.D. Sinzinger and M.J. Piovoso (2002). Improvements in the predictive capability of neural networks. Journal of Process Control, **12**, 193–202.

Hou, T.H., W.L. Liu and L. Lin (2003). Intelligent remote monitoring and diagnosis of manufacturing processes using an integrated approach of neural networks and rough sets. Journal of intelligent manufacturing, **14**, 239~253.

Hwang, Y.R. (2000). Cutting error analysis for table-tilting type four-axis NC machines. International journal of advanced manufacturing technology, **16**, 265-270.

James, M.N., D.G. Hattingh and G.R. Bradley (2003). Weld tool travel speed effects on fatigue life of friction stir welds in 5083 aluminium. International journal of fatigue, **25,** 1389-1398.

Jenkins WM (1997a). An introduction to neural computing for the structural engineer. The Struct Engng, **75(3)**, 38-41.

Jenkins WM (1997b). Approximate analysis of structural grillages using a neural network. Proc Instn Civil Engrs Structs Buildings, **122**, 355-63.

Jennings, A. D. and P. R. Drake (1994). Machine tool condition monitoring system for tool breakage monitoring in milling. International Journal of Machine Tools and Manufacture, **32(5)**, 641–649.

Jiaa, Ch. L. and D. A. Dornfeld (1998). Self-organising approach to the prediction and detection of tool wear. ISA Transactions, **37(4)**, 239–255.

Jin, Y.C. and B. Sendhoff (2003). Extracting Interpretable Fuzzy Rules from RBF Networks. Neural Processing Letters, **17,** 149-164.

Johnson, R. (2001). Forces in Friction Stir Welding of Aluminium Alloys. TWI Ltd.

Kallee, S. and D. Nicholas (2002). Friction Stir Welding at TWI. Paper available from www.twi.co.uk

Kang, M.C., J.S. Kim and J.H. Kim (2001). A monitoring technique using a multi-sensor in high speed machining. Journal of materials processing technology, **113**, 331~336.

Kasabov, N.K. (1996). Learning fuzzy rules and approximate reasoning in fuzzy neural networks and hybrid systems. Fuzzy Sets and Systems, **82**, 135-149.

Khandkar, M.Z.H., J.A. Khan and A.P. Reynolds (2003). Prediction of temperature distribution and thermal history during friction stir welding: input torque based model. Science and Technology of Welding and Joining, **8 (3)**, 165-174.

Kim, T.W. and J. Yuh (2002). Application of on-line neuro-fuzzy controller to AUVs. Information Sciences, **145**, 169–182.

Kima, Ill-S., J.S. Sona, S.H. Lee and P.K.D.V. Yarlagadda (2004). Optimal design of neural networks for control in robotic arc welding. Robotics and Computer-Integrated Manufacturing **20**, 57–63.

Kong, L.X. and S. Nahavandi (2002). On-line tool condition monitoring and control system in forging process. Journal of processing technology, 125-126 464~470

Koren, Y. (1997). Control of machine tools. Journal of manufacturing science and engineering, November, **119**, 749-755.

Koren, Y. and R.S. Lin (1997). Five-axis surface interpolators. Ann CIRP 1995, **44 (1)**, 379–82.

Kruger, G. (2003). Intelligent monitoring and control system for a friction stir welding process. M.TECH Dissertation, Port Elizabeth Technikon.

Kuo, R.J. (2000). Multi-sensor integration for on-line tool wear estimation through artificial neural networks and fuzzy neural network. Engineering Applications of Artificial Intelligence, **13**, 249-261.

Lau, H.C., T.T. Wong and A. Ning (2001). Incorporating machine intelligence in a prarmeter-based control system: a neural-fuzzy approach. Artificial intelligence in engineering, **15**, 253-264.

Lee, E.S, J.D. Kim and N.H. Kim (2003). Plunge grinding characteristics using the current signal of spindle motor. Journal of materials processing technology, **132**, 58~66.

Lee, Y.S. (1998). Mathematical modelling using different endmills and tool placement problem for 4- and 5-axis NC complex surface machining. Int J Prod Res, **36,** 785–814.

Leine and Linde (2002). Optical Encoder product datasheet, Siemens, Micromaster Encoder Module Operation Instructions, February, 610-632.

Lennox, B., G.A. Montague, A.M. Frith, C. Gent and V. Bevan (2001). Industrial application of neural networks – an investigation. Journal of process control, **11**, 497-507.

Lezanski, P. (2001). An intelligent system for grinding wheel condition monitoring. Journals of materials processing technology, **109**, 258-263.

Liang, M., T. Yeap, A. Hermansyah and S. Rahmati (2003). Fuzzy control of spindle torque for industrial CNC machining. International Journal of Machine Tools & Manufacture, **43**, 1497–1508.

Liang, M., T. Yeap, S. Rahmati and Z.X. Han (2002). Fuzzy control of spindle power in end milling processes, International Journal of Machine Tools & Manufacture **42**, 1487–1496.

Liang, S.Y., R.L. Hecker and R.G. Landers (2004). Machining process monitoring and control: the State-of-the-Art. Journal of Manufacturing Science and Engineering, **126**, 297-310.

Lin, L.C. and G.-Y. Lee (1999). Hierarchical fuzzy control for C-axis of CNC turning centers using genetic algorithms, Journal of Intelligent and Robotic Systems: Theory and Applications **25 (3)**, 255–275.

Lin, R. and Y. Koren (1996). Efficient tool path planning for machining free-form surfaces. ASME J Manufact Sci Engng, **118,** 20–28.

Lippmann, R.P. (1987). An introduction to computing with neural nets. IEEE ASSP Mag., April, 4.

Lisboa, P.G.J. (1992). Neural networks: current applications. London : Chapman & Hall.

Funahashi, K. (1989). One approach realization of continuous mapping by neural network. Neural Network, **2 (3)**, 183–192.

Liu, G., L.E. Murr, C.S. Niou, J.C. McClure and F.R. Vega (1997). Microstructural aspects of the Friction-Stir Welding of 6061-T6 Al, Scripta Materialia (1359-6462), **37 (3)**, 355-361.

Liu, Y. and C. Wang (1999). Neural networks based adaptive control and optimization in milling process. International Journal of Advanced Manufacturing Technology, **15**, 791–795.

Liu, Y., L. Zhuo and C. Wang (1999). Intelligent adaptive control in milling process. International Journal of Computer Integrated Manufacturing, **12 (5)**, 453–460.

Li, T.S., C.T. Su and T.L. Chiang (2003). Applying robust multi-response quality engineering for parameter selection using a novel neural–genetic algorithm. Computers in Industry, **50**, 113–122.

Lo, C.C. (1997). Feedback interpolator for CNC machine tool. ASME J Manufact Sci Engng, **119**, 587–592.

Lo, C.C. (1998). A new approach to CNC tool path generation. Comput-Aided Des, **30**, 49–55.

Lo, C.C. (1999). Real-time generation and control of cutter path for 5-axis CNC machining. Int J Mach Tool Manufact, **39**, 471–88.

Lu, T.F., G.C.I. Lin and J.R. HE (1997). Neural-network-based 3D force/torque sensor calibration for robot applications. Engng Applic. Artif. Intell, **10 (1),** 87-97.

Ma, X.W., X. Li and H. Qiao (2001). Fuzzy neural network-based real-time self-reaction of mobile robot in unknown environments. Mechatronics, **11,** 1039-1052.

MacKay, D. J. C. (1992). Bayesian interpolation. Neural Computation, **4 (3)**, 415-447.

Malan, SF. and AE Paterson (1987). Introduction to Aluminium, pp. 71-76. ISBN 062009219X, The Natal Witness (Pty) Ltd, Pietermaritzburg.

Mashimoto, M., E. Marui and S. Kato (1996). Experimental research on cutting force variation during regenerative chatter vibration in a plain milling operation. International Journal of Machine Tools and Manufacture, **36(10)**, 1073–1092.

Midling, O.T., E.J. Morley and A.O. Kluken (1994). Joining of Al Constructions by friction stir welding, Presented at The International Symposium on Advance Transportation Applications- Dedicated Conference on New and Alternative Materials for the Transportation Industries, ISATA 27, Aachen, Germany, November.

Miran, B., B. Joze and B. Zmago (2003). Emergence of intelligence in next-generation manufacturing systems. Robotics and Computer Integrated Manufacturing, **19**, 55–63.

Nakata, K., S. Inoki, Y. Nagano, T. Hashimoto, S. Johgan and M. Ushio (2001). Friction Stir Welding of AZ91D Thixomolded Sheet. Proceedings of 3rd international friction stir welding symposium.

Nicholas, E.D. and S.W. Kallee (2000). FRICTION STIR WELDING - A DECADE ON**.** IIW Asian Pacific International Congress, Sydney.

Noori-Khajavi, A. and R. Komanduri (1993). On multi-sensor approach to drill wear monitoring. CIRP Ann, **42 (1)**, 71–74.

North, T.H., G.J. Bendzsak and C. Smith (2000). Material Properties Relevant to 3-D FSW Modelling, Proceedings, 2nd International Symposium on FSW, Gothenburg, Sweden.

O'Donnell, G., P. Young, K. Kelly and G. Byrne (2001). Towards the Improvement of Tool Condition Monitoring Systems in Manufacturing Environment. J. Mater. Process. Technol., **119**, 133–139

Panos, A. (1993). Defining Intelligent Control, Report of the Task Force on Intellignent Control, IEEE Control Systems Society, December.

Peel, M., A. Steuwer, M. Preuss and P.J. Withers (2003). Microstructure, mechanical properties and residual stresses as a function of welding speed in aluminium AA5083 friction stir welds. Acta Materialia, **51**, 4791–4801

Qiu, H., K. Cheng and Y. Li (1997). Optimal circular arc interpolation for NC tool path generation in curve contour manufacturing. Comput-Aided Des, **29**, 751–60.

Rafalowicz, J., P. Lezanski, P. Lajmert, J. Teodorczyk and D.Wrabel (1998). Application of fuzzy set theory in grinding process diagnostics. Report for KBN, Politechnika Lodzka, Lodz.

Rafiq, M.Y., G. Bugmann and D.J. Easterbrook (2001). Neural network design for engineering applications. Computers and Structures, **79**, 1541-1552.

Rangwala, S. and D. Dornfeld (1987). Integration of sensors via neural networks for detection of tool wear states. In Intelligent and Integrated Manufacturing Analysis and Syndissertation (edited by C. R. Liu *et al*.), Winter Annual Meeting ASME, Boston, MA.

Rao, N., F. Ismail and S. Bedi (1997). Tool path planning for five-axis machining using the principal axis method. Int J Mach Tool Manufact, **37**, 1025–40.

Rao, S. B. (1986). Tool wear monitoring through the dynamics of stable turning. Journal of Engineering for Industry, 108-183.

Reynolds, A.P., W. Tang, T. Gnaupel-Herold and H. Prask (2003). Structure, properties, and residual stress of 304L stainless steel friction stir welds. Scripta Materialia, **48**, 1289–1294.

Ross, P.J. (1995). Taguchi Techniques for Quality Engineering. ISBN 0070539588, McGraw-Hill, 2 Edition, New York.

Rowe W.B., L. Yan, I. Inasaki and S. Malkin (1994). Applications of artificial intelligence in grinding. Ann. CIRP, **43 (2),** 521-531.

Sadeghi, B.H.M. (2000). A BP-neural network predictor model for plastic injection molding process. Journal of Materials Processing Technology, **103**, 411-416.

Sarma, R and A. Rao (2000). Discretizors and interpolators for five-axis CNC machines. ASME J Manufact Sci Engng, **122**, 191–197.

Sasiadek, J.Z. (2002). SENSOR FUSION. Annual Reviews in Control, **26**, 203-228

Satoshi, H., O. Kazutaka, A. Kinya, O. Hisanori, A. Yasuhisa and O. Tomio (2001). Development of 3 dimensional type friction stir welding equipment. 3rd International Symposium on Friction Stir Welding, Kobe Exhibition Hall, Kobe, Japan, 27&28 September.

Shinoda, T., H. Tokisue and M. Enomoto (2001). Recent Trends of Research and development of FSW Technology in Japan, Proceedings, 3rd International Conference on FSW, Japan.

Shiptalni M, Koren Y, Lo CC (1994). Real time curve interpolators. Comput- Aided Des, **28(11)**, 832–8.

Siemens (2001). MICROMASTER 440 Reference Manual.

Sommerville, I. (2001). Software Engineering: 6th edition. ISBN: 020139815X, Addison-Wesley Publishers.

Sokolowski, S. and J. Kosmol (1996). Intelligent monitoring system designer. Japan/USA Symposium on Flexible Automation, **vol. 2**, ASME.

Sokolowski, S., A. Kolka and J. Kosmol (1997). A new approach to aid designing of monitoring systems. 32nd International MATADOR Conference, Manchester, July.

Song, M. and R. Kovacevic (2003). Thermal modelling of friction stir welding in a moving coordinate system and its validation. International Journal of Machine Tools & Manufacture **43**, 605–615.

Stein, R. (1994). Selecting data for neural networks. AI Expert, **No.2**, 42-47.

Stephanopoulos, G. and C. Han (1996). INTELLIGENT SYSTEMS IN PROCESS ENGINEERING: A REVIEW. Computers chcm. Engng, **20 (617)**, 143-191.

Suh, I.H. and T.W. Kim (1994). Fuzzy membership function based neural networks with applications to the visual servoing of robot manipulators. IEEE Trans. Fuzzy Systems, **2 (3)**, 203–220.

Suh, I.H. and T.W. Kim (2000). A visual servoing algorithm using fuzzy logics and fuzzy-neu ral networks. Mechatronics, **10 (1)**, 1–18.

Sun, Z.Q. and Z.D. Deng (1996). A fuzzy neural network and its application to controls. Artificial Intelligence in Engineering, **10**, 311-315.

Swingler K (1996). Applying neural networks a practical guide. New York: Academic Press.

Tam, H.Y., H.Y. Xu and Z.D. Zhou (2002). Iso-planar interpolation for the machining of implicit surface. Comput-Aided Des, **34**, 125–36.

Tang, K. and J. Tang (1994). Design of screening procedure: A review. Journal of Quality Technology, **26(3)**, 209-226.

Tarng, S. and B. Y. Lee (1994). Use of model-based cutting simulation system for tool breakage monitoring in milling. International Journal of Machine Tools and Manufacture, **32(5)**, pp. 641–649.

Tarng, Y.S. and S.T. Cheng (1993). Fuzzy control of feed rate in end milling operations. International Journal of Machine Tools and Manufacture, **33 (4)**, 643–650.

Tarng, Y.S., S.T. Hwang and Y.S. Wang (1994). A neural network controller for constant turning force. International Journal of Machine Tools and Manufacture, **34 (4)**, 453–460.

The MathWorks (2004a). Fuzzy Logic Toolbox User's Guide. The MathWorks Inc, Natick, MA.

The MathWorks (2004b). Neural Network Toolbox User's Guide. The MathWorks Inc, Natick, MA.

The MathWorks (2004c). MATLAB: The Language of Technical Computing, version 7.

The MathWorks (2004d). Simulink: Simulation and Model-Based Design, version 6.

Thomas, W.M., E.D. Nicholas, J.C. Needham, M.G. Murch, P. Templesmith and C.J. Dawes (1991). Friction stir butt welding. International patent application no. PCT/GB92/02203 and GB patent application no. 9125978.8, 6,0 December.

Tomas M.W., E.D. Nicholas and S.D. Smith (2001). Friction Stir Welding tool developments. TWI Ltd.

Threadgill, P.L. (1997). Friction stir welds in aluminium alloys – preliminary microstructural assessment. TWI Bulletin, March/April.

Tseng, P.C. and A. Chou (2002). The intelligent on-line monitoring of end milling. International Journal of Machine Tools & Manufacture, **42**, 89–97.

Tseng, Y.J. and Y.D. Chen (2000). Three dimensional biarc approximation of freeform surfaces for machining tool path generation. Int J Prod Res, **38**, 739–63.

Ulsoy, A. and Y. Koren (1993). Control of machining processes. Transactions ASME Journal of Dynamic Systems Measurement and Control, 115.

Van Niekerk, T.I. (2001). Monitoring and diagnosis for control of an intelligent machining process. D.TECH Dissertation, Port Elizabeth Technikon.

Warkentin, A., F. Ismail and S. Bedi (2000). Comparison between multi-point and other 5-axis tool positioning strategies. Int J Mach Tool Manufactk, **40**, 185–208.

Xua, H.Y., H.Y. Tamb and J.J. Zhang (2003). Isophote interpolation. Computer-Aided Design, **35**, 1337–1344.

Xua, H.Y., Y.H. Zhoua and J.J. Zhang (2003). Angular interpolation of bi-parameter curves. Computer-Aided Design, **35**, 1211–1220.

Xu, H.Y. (2003). Linear and angular feedrate interpolation for planar implicit curves. Comput-Aided Des, **35(3)**, 301–17.

Xu, H.Y., H.Y. Tam, Z. Zhou and P.W.T. Tse (2001). Variable feedrate CNC interpolation for planar implicit curves. Int J Adv Manufact Technol, **18**, 794–800.

Yeh, S.S. and P.L. Hsu (2002). Adaptive-feedrate interpolation for parametric curves with a confined chord error. Computer-Aided Design, **34**, 229-237.

Yeung, M.Y. and D.J. Walton (1994). Curve fitting with arc splines for NC tool path generation. Comput-Aided Des, **26**, 845–849.

Zahedi, F (1991). An introduction to neural network and a comparison with artificial intelligence and expert systems. Interfaces, **21(2)**, 25-28.

Zhang, H.C. and S.H. Huang (1995). Applications of neural networks in manufacturing: a state-of-the-art survey. International Journal of Production Research, **33 (3),** 705–728.

Appendix A Experimental Data of FSW

Table A.1: Experimental data of Al 5251 alloy flat plate welding

Experiment 1: 3mm Al 5251 flat plates																
Exp number	**feed mm/min**	**speed rpm**	**tilt °**	**plunge mm**	**dwell s**	**Bend1 N**	**Torq Nm**	**Temp °C**	**Comp KN**	**Bend /Torq**	**Bend /Temp**	**Bend /Comp**	**Temp /Torq**	**Temp /Comp**	**Torq /Comp**	**GUI value**	**actual sequence**
1	50	300	2	0.1	10	*373.460*	*12.818*	*115.019*	*1.573*	*29.136*	*3.247*	*237.419*	*8.973*	*73.121*	*8.149*	*17.2*	**1**
2	50	400	1	0.2	10	*134.008*	*22.770*	*224.451*	*1.089*	*5.885*	*0.597*	*123.056*	*9.857*	*206.107*	*20.909*	*17.2*	**6**
3	50	500	0.5	0.3	10	*231.280*	*17.414*	*255.405*	*0.663*	*13.281*	*0.906*	*348.839*	*14.667*	*385.226*	*26.265*	*17.2*	**11**
4	50	600	0	0.4	10	*226.342*	*15.516*	*251.466*	*0.572*	*14.588*	*0.900*	*395.703*	*16.207*	*439.626*	*27.126*	*17.2*	**13**
5	100	300	1	0.3	10	*460.446*	*24.341*	*186.464*	*1.372*	*18.916*	*2.469*	*335.602*	*7.660*	*135.907*	*17.741*	*17.3*	**5**
6	100	400	2	0.4	10	*292.248*	*23.737*	*219.183*	*1.261*	*12.312*	*1.333*	*231.759*	*9.234*	*173.817*	*18.824*	*17.5*	**2**
7	100	500	0	0.1	10	*149.984*	*15.416*	*191.594*	*0.904*	*9.729*	*0.783*	*165.912*	*12.428*	*211.940*	*17.053*	*16.9*	**14**
8	100	600	0.5	0.2	10	*187.312*	*19.244*	*246.317*	*0.744*	*9.734*	*0.760*	*251.763*	*12.800*	*331.071*	*25.866*	*17.1*	**9**
9	150	300	0.5	0.4	10	*812.691*	*22.375*	*192.983*	*1.214*	*36.321*	*4.211*	*669.432*	*8.625*	*158.965*	*18.431*	*17.3*	**12**
10	150	400	0	0.3	10	*281.851*	*17.821*	*190.032*	*0.867*	*15.816*	*1.483*	*325.088*	*10.663*	*219.183*	*20.555*	*17.1*	**16**
11	150	500	2	0.2	10	*179.127*	*23.334*	*212.609*	*1.084*	*7.677*	*0.843*	*165.246*	*9.112*	*196.134*	*21.526*	*17.3*	**3**
12	150	600	1	0.1	10	*260.209*	*18.703*	*237.290*	*0.905*	*13.913*	*1.097*	*287.524*	*12.687*	*262.199*	*20.666*	*17.1*	**7**
13	200	300	0	0.2	10	*892.903*	*20.363*	*167.181*	*1.386*	*43.849*	*5.341*	*644.230*	*8.210*	*120.621*	*14.692*	*17.0*	**15**
14	200	400	0.5	0.1	10	*447.734*	*18.737*	*200.030*	*1.313*	*23.896*	*2.238*	*341.001*	*10.676*	*152.346*	*14.270*	*17.0*	**10**
15	200	500	1	0.4	10	*483.540*	*19.478*	*230.240*	*1.221*	*24.825*	*2.100*	*396.020*	*11.821*	*188.567*	*15.952*	*17.4*	**8**
16	200	600	2	0.3	10	*303.581*	*21.632*	*233.519*	*1.497*	*14.034*	*1.300*	*202.793*	*10.795*	*155.991*	*14.450*	*17.4*	**4**

Table A.2: Experimental data of Al 6061 alloy flat plate welding

OA Experiment 2: 3mm Al 6061 flat plates																	
Exp number	**feed mm/min**	**speed rpm**	**tilt °**	**plunge mm**	**dwell s**	**Bend1 N**	**Torq Nm**	**Temp °C**	**Comp KN**	**Bend /Torq**	**Bend /Temp**	**Bend /Comp**	**Temp /Torq**	**Temp /Comp**	**Torq /Comp**	**GUI value**	**actual sequence**
1	50	300	2	0.1	10	*1271.63*	*18.52*	*174.48*	*2.45*	*68.66*	*7.29*	*519.03*	*9.42*	*71.22*	*7.56*	*17.2*	**16**
2	50	400	1	0.2	10	*373.84*	*24.25*	*249.56*	*2.81*	*15.42*	*1.50*	*133.04*	*10.29*	*88.81*	*8.63*	*17.2*	**11**
3	50	500	0.5	0.3	10	*439.37*	*20.39*	*282.99*	*1.52*	*21.55*	*1.55*	*289.06*	*13.88*	*186.18*	*13.41*	*17.2*	**6**
4	50	600	0	0.4	10	*411.44*	*17.09*	*301.81*	*1.23*	*24.07*	*1.36*	*334.50*	*17.66*	*245.37*	*13.89*	*17.2*	**4**
5	100	300	1	0.3	10	*856.27*	*27.91*	*211.89*	*4.00*	*30.68*	*4.04*	*214.07*	*7.59*	*52.97*	*6.98*	*17.3*	**12**
6	100	400	2	0.4	10	*593.28*	*31.37*	*228.78*	*3.67*	*18.91*	*2.59*	*161.66*	*7.29*	*62.34*	*8.55*	*17.5*	**13**
7	100	500	0	0.1	10	*410.56*	*22.85*	*252.95*	*2.45*	*17.97*	*1.62*	*167.58*	*11.07*	*103.24*	*9.33*	*16.9*	**3**
8	100	600	0.5	0.2	10	*335.95*	*20.33*	*275.20*	*1.74*	*16.52*	*1.22*	*193.07*	*13.54*	*158.16*	*11.68*	*17.1*	**8**
9	150	300	0.5	0.4	10	*1468.24*	*32.55*	*232.88*	*4.20*	*45.11*	*6.30*	*349.58*	*7.15*	*55.45*	*7.75*	*17.3*	**5**
10	150	400	0	0.3	10	*949.51*	*29.18*	*256.72*	*3.03*	*32.54*	*3.70*	*313.37*	*8.80*	*84.73*	*9.63*	*17.1*	**1**
11	150	500	2	0.2	10	*709.56*	*20.71*	*222.82*	*2.49*	*34.26*	*3.18*	*284.96*	*10.76*	*89.49*	*8.32*	*17.3*	**15**
12	150	600	1	0.1	10	*408.91*	*25.24*	*260.16*	*2.28*	*16.20*	*1.57*	*179.35*	*10.31*	*114.11*	*11.07*	*17.1*	**10**
13	200	300	0	0.2	10	*1374.17*	*28.07*	*215.43*	*4.24*	*48.96*	*6.38*	*324.10*	*7.67*	*50.81*	*6.62*	*17.0*	**2**
14	200	400	0.5	0.1	10	*1069.28*	*26.57*	*232.57*	*3.60*	*40.24*	*4.60*	*297.02*	*8.75*	*64.60*	*7.38*	*17.0*	**7**
15	200	500	1	0.4	10	*854.07*	*26.73*	*251.53*	*3.41*	*31.95*	*3.40*	*250.46*	*9.41*	*73.76*	*7.84*	*17.4*	**9**
16	200	600	2	0.3	10	*466.99*	*23.82*	*237.90*	*2.66*	*19.60*	*1.96*	*175.56*	*9.99*	*89.44*	*8.95*	*17.4*	**14**

Table A.3: Experimental data of Al 6061 round tube welding

OA Experiment 3: 3mm Al 6061 round tubes																
Exp number	**feed mm/min**	**speed rpm**	**tilt °**	**plunge mm**	**Diameter mm**	**Bend1 N**	**Torq Nm**	**Temp °C**	**Fz KN**	**Bend /Torq**	**Bend /Temp**	**Bend /Fz**	**Temp /Torq**	**Temp /Fz**	**Torq /Fz**	**actual sequence**
exp1	50	400	2	0.1	40	*771.90*	*11.25*	*187.56*	*1.90*	*68.63*	*4.12*	*406.69*	*16.67*	*98.82*	*5.93*	**5**
exp2	50	500	1	0.2	70	*1207.93*	*12.88*	*256.72*	*1.18*	*93.78*	*4.71*	*1025.94*	*19.93*	*218.05*	*10.94*	**10**
exp3	50	600	0	0.4	95	*467.26*	*19.83*	*315.00*	*1.88*	*23.57*	*1.48*	*248.24*	*15.89*	*167.35*	*10.53*	**14**
exp4	100	400	2	0.2	95	*1660.01*	*17.49*	*206.70*	*3.24*	*94.94*	*8.03*	*512.64*	*11.82*	*63.83*	*5.40*	**18**
exp5	100	500	1	0.4	40	*269.46*	*20.93*	*269.40*	*2.31*	*12.88*	*1.00*	*116.41*	*12.87*	*116.39*	*9.04*	**4**
exp6	100	600	0	0.1	70	*1197.22*	*12.79*	*249.48*	*1.82*	*93.62*	*4.80*	*659.58*	*19.51*	*137.45*	*7.05*	**11**
exp7	200	400	1	0.1	70	*2473.22*	*18.06*	*207.10*	*3.80*	*136.95*	*11.94*	*650.00*	*11.47*	*54.43*	*4.75*	**9**
exp8	200	500	0	0.2	95	*2198.77*	*26.35*	*251.56*	*4.74*	*83.43*	*8.74*	*463.39*	*9.55*	*53.02*	*5.55*	**13**
exp9	200	600	2	0.4	40	*1380.90*	*11.62*	*235.30*	*2.00*	*118.81*	*5.87*	*690.41*	*20.25*	*117.64*	*5.81*	**6**
exp10	50	400	0	0.4	70	*715.99*	*16.22*	*268.09*	*2.53*	*44.14*	*2.67*	*283.24*	*16.53*	*106.05*	*6.42*	**12**
exp11	50	500	2	0.1	95	*1405.21*	*11.85*	*204.70*	*1.57*	*118.63*	*6.86*	*892.84*	*17.28*	*130.06*	*7.53*	**17**
exp12	50	600	1	0.2	40	*706.26*	*7.98*	*245.50*	*1.86*	*88.55*	*2.88*	*379.50*	*30.78*	*131.92*	*4.29*	**3**
exp13	100	400	1	0.4	95	*1913.16*	*20.39*	*256.07*	*3.13*	*93.85*	*7.47*	*611.57*	*12.56*	*81.86*	*6.52*	**16**
exp14	100	500	0	0.1	40	*1531.09*	*8.49*	*222.16*	*1.98*	*180.27*	*6.89*	*772.41*	*26.16*	*112.08*	*4.28*	**1**
exp15	100	600	2	0.2	70	*1441.68*	*11.54*	*237.13*	*1.72*	*124.97*	*6.08*	*836.40*	*20.55*	*137.57*	*6.69*	**7**
exp16	200	400	0	0.2	40	*2204.96*	*15.79*	*202.49*	*3.56*	*139.66*	*10.89*	*619.37*	*12.83*	*56.88*	*4.43*	**2**
exp17	200	500	2	0.4	70	*2676.80*	*18.81*	*217.83*	*4.42*	*142.27*	*12.29*	*605.90*	*11.58*	*49.31*	*4.26*	**8**
exp18	200	600	1	0.1	95	*2668.33*	*15.18*	*244.94*	*4.03*	*175.83*	*10.89*	*662.84*	*16.14*	*60.85*	*3.77*	**15**

Appendix B Fuzzy rules, M functions and Scripts

B.1: Linguistic Fuzzy Rules Generated for Tool/workipece Contact

```
>> showrule(fismat)
ans =

1. If (Temperature is PM) and (Temperature/Fz is NS) and (Torque/Fz is PS) then (Tilt is NM) (Plunge is PL) (1)
2. If (Temperature is PL) and (Temperature/Fz is NS) and (Torque/Fz is PS) then (Tilt is NM) (Plunge is PL) (1)
3. If (Temperature is PM) and (Temperature/Fz is ZE) and (Torque/Fz is PS) then (Tilt is NM) (Plunge is PL) (1)
4. If (Temperature is PL) and (Temperature/Fz is ZE) and (Torque/Fz is PS) then (Tilt is NM) (Plunge is PL) (1)
5. If (Temperature is PM) and (Temperature/Fz is NS) and (Torque/Fz is PM) then (Tilt is NM) (Plunge is PL) (1)
6. If (Temperature is PL) and (Temperature/Fz is NS) and (Torque/Fz is PM) then (Tilt is NM) (Plunge is PL) (1)
7. If (Temperature is PM) and (Temperature/Fz is ZE) and (Torque/Fz is PM) then (Tilt is NM) (Plunge is PL) (1)
8. If (Temperature is PL) and (Temperature/Fz is ZE) and (Torque/Fz is PM) then (Tilt is NM) (Plunge is PL) (1)
9. If (Temperature is PM) and (Temperature/Fz is NS) and (Torque/Fz is PS) then (Tilt is NS) (Plunge is PL) (1)
10. If (Temperature is PL) and (Temperature/Fz is NS) and (Torque/Fz is PS) then (Tilt is NS) (Plunge is PL) (1)
11. If (Temperature is PM) and (Temperature/Fz is ZE) and (Torque/Fz is PS) then (Tilt is NS) (Plunge is PL) (1)
12. If (Temperature is PL) and (Temperature/Fz is ZE) and (Torque/Fz is PS) then (Tilt is NS) (Plunge is PL) (1)
13. If (Temperature is PM) and (Temperature/Fz is NS) and (Torque/Fz is PM) then (Tilt is NS) (Plunge is PL) (1)
14. If (Temperature is PL) and (Temperature/Fz is NS) and (Torque/Fz is PM) then (Tilt is NS) (Plunge is PL) (1)
15. If (Temperature is PM) and (Temperature/Fz is ZE) and (Torque/Fz is PM) then (Tilt is NS) (Plunge is PL) (1)
16. If (Temperature is PL) and (Temperature/Fz is ZE) and (Torque/Fz is PM) then (Tilt is NS) (Plunge is PL) (1)
17. If (Temperature is PM) and (Temperature/Fz is NS) and (Torque/Fz is PS) then (Tilt is NM) (Plunge is PX) (1)
18. If (Temperature is PL) and (Temperature/Fz is NS) and (Torque/Fz is PS) then (Tilt is NM) (Plunge is PX) (1)
19. If (Temperature is PM) and (Temperature/Fz is ZE) and (Torque/Fz is PS) then (Tilt is NM) (Plunge is PX) (1)
20. If (Temperature is PL) and (Temperature/Fz is ZE) and (Torque/Fz is PS) then (Tilt is NM) (Plunge is PX) (1)
21. If (Temperature is PM) and (Temperature/Fz is NS) and (Torque/Fz is PM) then (Tilt is NM) (Plunge is PX) (1)
22. If (Temperature is PL) and (Temperature/Fz is NS) and (Torque/Fz is PM) then (Tilt is NM) (Plunge is PX) (1)
23. If (Temperature is PM) and (Temperature/Fz is ZE) and (Torque/Fz is PM) then (Tilt is NM) (Plunge is PX) (1)
24. If (Temperature is PL) and (Temperature/Fz is ZE) and (Torque/Fz is PM) then (Tilt is NM) (Plunge is PX) (1)
25. If (Temperature is PM) and (Temperature/Fz is NS) and (Torque/Fz is PS) then (Tilt is NS) (Plunge is PX) (1)
26. If (Temperature is PL) and (Temperature/Fz is NS) and (Torque/Fz is PS) then (Tilt is NS) (Plunge is PX) (1)
27. If (Temperature is PM) and (Temperature/Fz is ZE) and (Torque/Fz is PS) then (Tilt is NS) (Plunge is PX) (1)
28. If (Temperature is PL) and (Temperature/Fz is ZE) and (Torque/Fz is PS) then (Tilt is NS) (Plunge is PX) (1)
29. If (Temperature is PM) and (Temperature/Fz is NS) and (Torque/Fz is PM) then (Tilt is NS) (Plunge is PX) (1)
30. If (Temperature is PL) and (Temperature/Fz is NS) and (Torque/Fz is PM) then (Tilt is NS) (Plunge is PX) (1)
31. If (Temperature is PM) and (Temperature/Fz is ZE) and (Torque/Fz is PM) then (Tilt is NS) (Plunge is PX) (1)
32. If (Temperature is PL) and (Temperature/Fz is ZE) and (Torque/Fz is PM) then (Tilt is NS) (Plunge is PX) (1)
```

B.2: Linguistic Fuzzy Rules Generated for Tool/workipece Energy Input

```
>> showrule(fismat)
ans =
1. If (err_Fz is PS) and (err_Temp2Torq is NM) and (err_Torq2Fz is PS) then (adjust_feed is PL)(adjust_speed is PL) (1)
2. If (err_Fz is PM) and (err_Temp2Torq is NM) and (err_Torq2Fz is PS) then (adjust_feed is PL)(adjust_speed is PL) (1)
3. If (err_Fz is PS) and (err_Temp2Torq is NS) and (err_Torq2Fz is PS) then (adjust_feed is PL)(adjust_speed is PL) (1)
4. If (err_Fz is PM) and (err_Temp2Torq is NS) and (err_Torq2Fz is PS) then (adjust_feed is PL)(adjust_speed is PL) (1)
5. If (err_Fz is PS) and (err_Temp2Torq is NM) and (err_Torq2Fz is PM) then (adjust_feed is PL)(adjust_speed is PL) (1)
6. If (err_Fz is PM) and (err_Temp2Torq is NM) and (err_Torq2Fz is PM) then (adjust_feed is PL)(adjust_speed is PL) (1)
7. If (err_Fz is PS) and (err_Temp2Torq is NS) and (err_Torq2Fz is PM) then (adjust_feed is PL)(adjust_speed is PL) (1)
8. If (err_Fz is PM) and (err_Temp2Torq is NS) and (err_Torq2Fz is PM) then (adjust_feed is PL)(adjust_speed is PL) (1)
9. If (err_Fz is PS) and (err_Temp2Torq is NM) and (err_Torq2Fz is PS) then (adjust_feed is PX)(adjust_speed is PL) (1)
10. If (err_Fz is PM) and (err_Temp2Torq is NM) and (err_Torq2Fz is PS) then (adjust_feed is PX)(adjust_speed is PL) (1)
11. If (err_Fz is PS) and (err_Temp2Torq is NS) and (err_Torq2Fz is PS) then (adjust_feed is PX)(adjust_speed is PL) (1)
12. If (err_Fz is PM) and (err_Temp2Torq is NS) and (err_Torq2Fz is PS) then (adjust_feed is PX)(adjust_speed is PL) (1)
13. If (err_Fz is PS) and (err_Temp2Torq is NM) and (err_Torq2Fz is PM) then (adjust_feed is PX)(adjust_speed is PL) (1)
14. If (err_Fz is PM) and (err_Temp2Torq is NM) and (err_Torq2Fz is PM) then (adjust_feed is PX)(adjust_speed is PL) (1)
15. If (err_Fz is PS) and (err_Temp2Torq is NS) and (err_Torq2Fz is PM) then (adjust_feed is PX)(adjust_speed is PL) (1)
16. If (err_Fz is PM) and (err_Temp2Torq is NS) and (err_Torq2Fz is PM) then (adjust_feed is PX)(adjust_speed is PL) (1)
17. If (err_Fz is PS) and (err_Temp2Torq is NM) and (err_Torq2Fz is PS) then (adjust_feed is PL)(adjust_speed is PX) (1)
18. If (err_Fz is PM) and (err_Temp2Torq is NM) and (err_Torq2Fz is PS) then (adjust_feed is PL)(adjust_speed is PX) (1)
19. If (err_Fz is PS) and (err_Temp2Torq is NS) and (err_Torq2Fz is PS) then (adjust_feed is PL)(adjust_speed is PX) (1)
20. If (err_Fz is PM) and (err_Temp2Torq is NS) and (err_Torq2Fz is PS) then (adjust_feed is PL)(adjust_speed is PX) (1)
21. If (err_Fz is PS) and (err_Temp2Torq is NM) and (err_Torq2Fz is PM) then (adjust_feed is PL)(adjust_speed is PX) (1)
22. If (err_Fz is PM) and (err_Temp2Torq is NM) and (err_Torq2Fz is PM) then (adjust_feed is PL)(adjust_speed is PX) (1)
23. If (err_Fz is PS) and (err_Temp2Torq is NS) and (err_Torq2Fz is PM) then (adjust_feed is PL)(adjust_speed is PX) (1)
24. If (err_Fz is PM) and (err_Temp2Torq is NS) and (err_Torq2Fz is PM) then (adjust_feed is PL)(adjust_speed is PX) (1)
25. If (err_Fz is PS) and (err_Temp2Torq is NM) and (err_Torq2Fz is PS) then (adjust_feed is PX)(adjust_speed is PX) (1)
26. If (err_Fz is PM) and (err_Temp2Torq is NM) and (err_Torq2Fz is PS) then (adjust_feed is PX)(adjust_speed is PX) (1)
27. If (err_Fz is PS) and (err_Temp2Torq is NS) and (err_Torq2Fz is PS) then (adjust_feed is PX)(adjust_speed is PX) (1)
28. If (err_Fz is PM) and (err_Temp2Torq is NS) and (err_Torq2Fz is PS) then (adjust_feed is PX)(adjust_speed is PX) (1)
29. If (err_Fz is PS) and (err_Temp2Torq is NM) and (err_Torq2Fz is PM) then (adjust_feed is PX)(adjust_speed is PX) (1)
30. If (err_Fz is PM) and (err_Temp2Torq is NM) and (err_Torq2Fz is PM) then (adjust_feed is PX)(adjust_speed is PX) (1)
31. If (err_Fz is PS) and (err_Temp2Torq is NS) and (err_Torq2Fz is PM) then (adjust_feed is PX)(adjust_speed is PX) (1)
32. If (err_Fz is PM) and (err_Temp2Torq is NS) and (err_Torq2Fz is PM) then (adjust_feed is PX)(adjust_speed is PX) (1)
```

B.3: Visualised On-line Fuzzy Rules and Primary Fuzzy Outputs for Tool/workipece Contact Condition

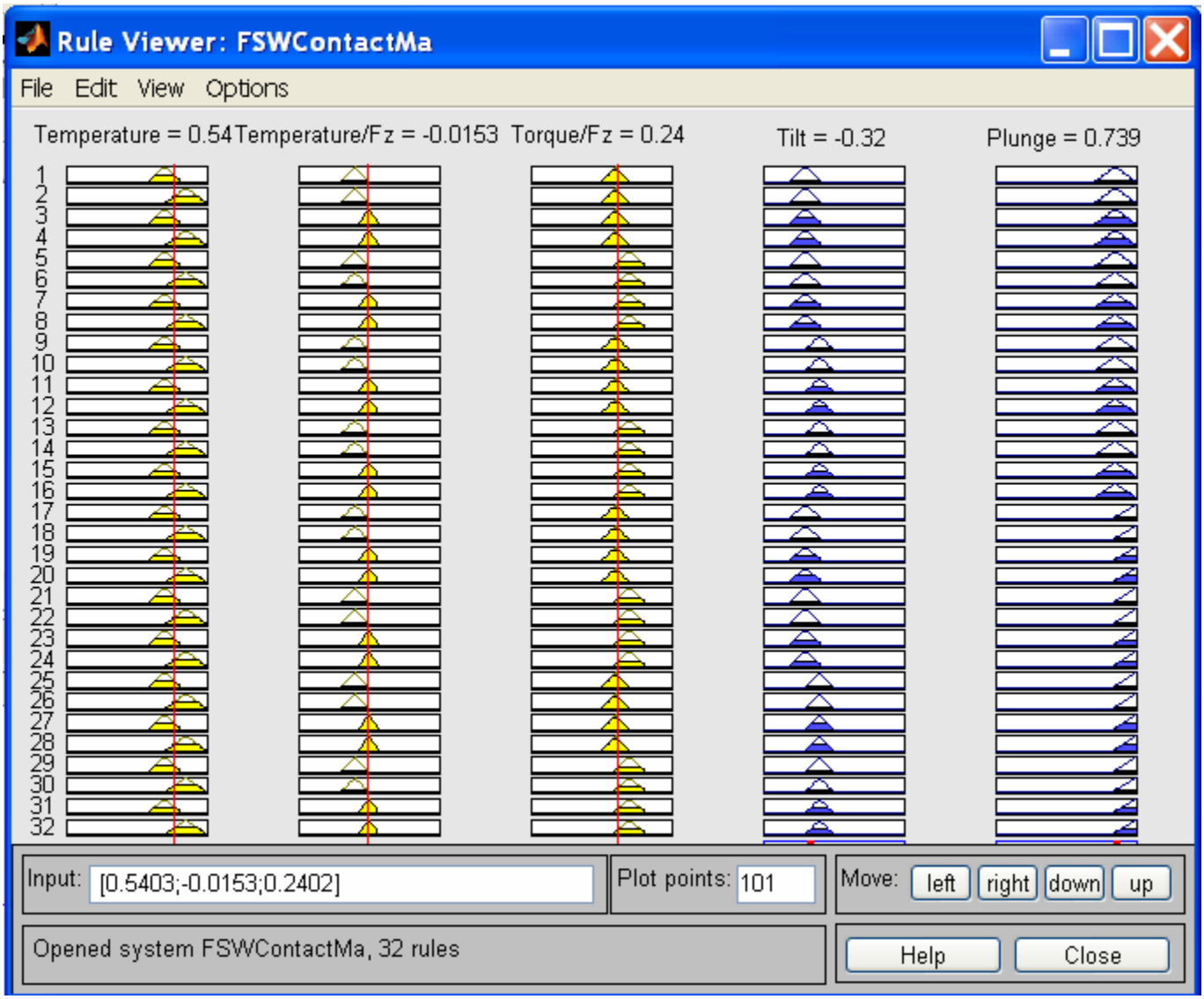

B.4: Visualised On-line Fuzzy Rules and Primary Fuzzy Outputs for Tool/workipece Energy Input

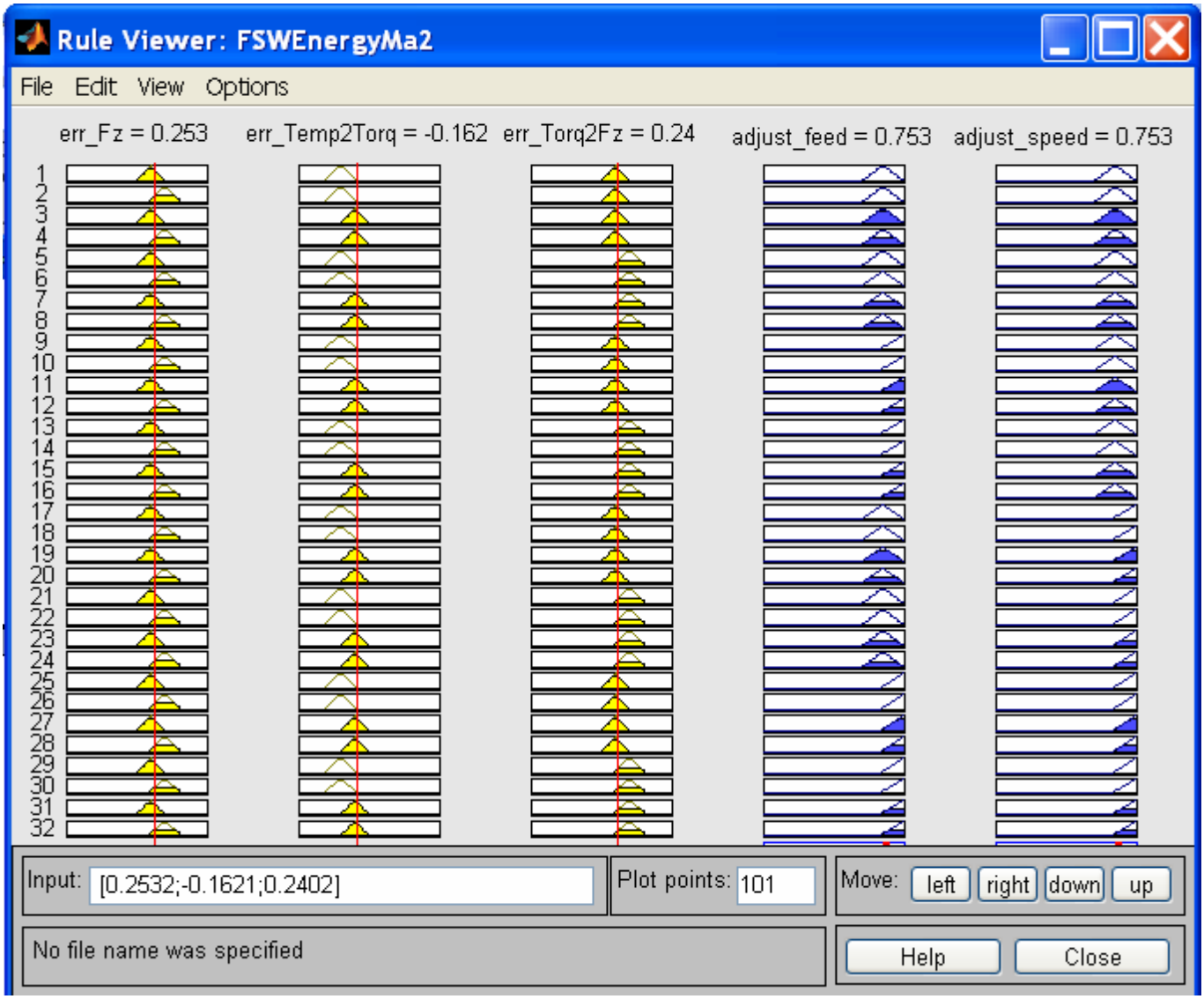

B.5: M Script for NN Training for Al 6061 Alloy Changing Curvature

```
% load the data including 6061 flat plate and round tube into workspace
Data6061flat = load('3mm6061FlatPlatesData.dat');
Data6061flat = [Data6061flat(:,1:4) zeros(16,1) Data6061flat(:,5:8)];
Data_extraflat = load('6061flat_extraWeld.dat')';
Data6061tube = load('sens_param_6061Tube.dat');
Data6061tube(:,5) = 2./Data6061tube(:,5); %change tube diameter to curvature
Data6061 = [Data6061flat;Data6061tube(:,1:9);Data_extraflat];

% ************************************************************************
% NN training for deriving sensor data from process parameter and condition
% inputs of the NN: feed,speed,tilt,plunge, curvature
% outputs of the NN: torq, temp, Fz
% ************************************************************************
P = Data6061(:,1:5)';
T = Data6061(:,7:9)';
 [PN,minp_para2sens_6061complex,maxp_para2sens_6061complex,...
   TN,mint_para2sens_6061complex,maxt_para2sens_6061complex] = premnmx(P,T);

nn_para2sens_6061complex = newff(minmax(PN),[7,3],{'tansig','purelin'},'trainbr');
nn_para2sens_6061complex.trainParam.show = 10;
nn_para2sens_6061complex.trainParam.epochs = 200;
randn('seed',192736);
nn_para2sens_6061complex = init(nn_para2sens_6061complex);
[nn_para2sens_6061complex,tr_para2sens]=train(nn_para2sens_6061complex,PN,TN);
gensim(nn_para2sens_6061complex);
save nn_para2sens_6061complex.mat nn_para2sens_6061complex;

% ************************************************************************
% NN training for process parameter from sensor data and condition
% inputs of the NN: curvature, torq, temp, Fz
% outputs of the NN: feed,speed,tilt,plunge.
% ************************************************************************
T = Data6061(:,1:4)';
P = Data6061(:,[5 7 8 9])';
% normalize input/output into [-1 1]
[PN,minp_sens2para_6061complex,maxp_sens2para_6061complex,...
   TN,mint_sens2para_6061complex, maxt_sens2para_6061complex] = premnmx(P,T);
% nn_sens2para=newff(minmax(PN),[9,4],{'tansig','purelin'},'trainbr');
nn_sens2para_6061complex=newff(minmax(PN),[9,4],{'tansig','purelin'},'trainlm');
nn_sens2para_6061complex.trainParam.show = 10;
nn_sens2para_6061complex.trainParam.epochs = 200;
randn('seed',192736);
nn_sens2para_6061complex = init(nn_sens2para_6061complex);
[nn_sens2para_6061complex,tr_sens2para]=train(nn_sens2para_6061complex,PN,TN);
gensim(nn_sens2para_6061complex);
save nn_sens2para_6061complex.mat nn_sens2para_6061complex;
% ************************************************************************
% NN training for process condition from sensor data
% inputs of the NN: torq, temp, Fz
% outputs of the NN:curvature
% ************************************************************************
T = Data6061(:,5)';
P = Data6061(:,[7 8 9])';
% normalize input/output into [-1 1]
[PN,minp_sens2curv_6061complex,maxp_sens2curv_6061complex,...
   TN,mint_sens2curv_6061complex,maxt_sens2curv_6061complex] = premnmx(P,T);
nn_sens2curv_6061complex=newff(minmax(PN),[6,1],{'tansig','purelin'},'trainlm');
nn_sens2curv_6061complex.trainParam.show = 5;
nn_sens2curv_6061complex.trainParam.epochs = 50;
nn_sens2curv_6061complex.trainParam.goal = 1e-2;
randn('seed',192736);
nn_sens2curv_6061complex = init(nn_sens2curv_6061complex);
[nn_sens2curv_6061complex,tr_sens2curv]=train(nn_sens2curv_6061complex,PN,TN);
gensim(nn_sens2curv_6061complex);
save nn_sens2curv_6061complex.mat nn_sens2curv_6061complex;
```

B.6: M Function for Tuning Fuzzy Output Scale Factor

```
function [Kout_tilt,Kout_plunge] = scaleOutContact(Err_new,Err_old,Dev_new,Dev_old)
% Err: error of sensor data to reference value     % Dev: the change of error
% $ Author: TAO Date: 2005

co_tilt = [0.54;0.33;0.31];   % use the correlation analysis result
co_plunge = [0.29;0.15;0.15];
ScaleMat_con = zeros(3,1); % calculate coefficient for each sensory signal
ScaleMat_con = ScaleMat(Err_new,Err_old,Dev_new,Dev_old);
Kout_tilt = MSE(co_tilt,ScaleMat_con); % compute final scale factor for feed and speed
adjustment
Kout_plunge = MSE(co_plunge,ScaleMat_con);

% ***************************************************
function coMat = ScaleMat(E_new,E_old,C_new,C_old)
% ***************************************************
[R,C] = size(E_new);
coMat = zeros(R,1);
for i = 1:R
   coMat(i) = Scale(E_new(i),E_old(i),C_new(i),C_old(i));
end

% ***************************************************
function MeanVal = MSE(CoeMat,InputMat)
% ***************************************************
[R,Q] = size(CoeMat);
PowInput = power(InputMat,2);
MeanVal = 0;
for i = 1:Q
   MeanVal = MeanVal + PowInput(i)*CoeMat(i);
end
MeanVal = MeanVal/(sum(CoeMat));
MeanVal = sqrt(MeanVal);

% ***************************************************
function Kout = Scale(Err0,Err1,Change0,Change1)
% ***************************************************
if Change0*Change1 < 0
   if (abs(Err0)>abs(Err1)) && (abs(Change0)/(abs(Change1)+0.00001) > 1) && (Err0*Err1>0)
      Kout = power(abs(Change0)/(abs(Change1)+0.00001),0.1);
   elseif (abs(Err0)<abs(Err1)) && ((abs(Change0)/(abs(Change1)+0.00001)) > 1) &&
(Err0*Err1>0)
      Kout = power(abs(Change1)/(abs(Change0)+0.00001),0.1);
   else
      Kout = 1;
   end
 elseif  abs(Change0)/(abs(Change1)+0.00001) > 1
   if abs(Err0)>abs(Err1)
      Kout = power(abs(Change0)/(abs(Change1)+0.00001),0.1);

   else
      Kout = power(abs(Change1)/(abs(Change0)+0.00001),0.1);
   end
else
   Kout = 1;
end
```

B.7: M Function for Fuzzy Rule Generation

```
function RuleList = RuleCreate(fis_name,input,output)
% INPUTS:        fisname: variable in the workspace which a FIS structure was assigned to
%                inputVec: vector which is normalized as FIS input
%                outputVec: vector which is normalized as FIS output
% OUTPUTS:   RULELIST: rule list created for the initial non-rule FIS
% CREATED BY TAO 2005,SEPTEMBER

[inMat outMat]=fuzzifyInOut(fis_name,input,output);
[inMfList outMfList]=MfComb(inMat,outMat);
[rowInList colInlist]=size(inMfList);
A=ones(rowInList,1);
RuleList=[inMfList outMfList A A];

 % ************************************************************************
function [inMfCell outMfCell]= fuzzifyInOut(fis_name,vecInput,vecOutput)
% ************************************************************************
% FUZZIFY: fuzzify inputs&outputs for a FLC, deduce the fuzzy rules

% find out how many membership functions for each input, normally this
% is a mxn vector, where m is the number of inputs, and n is the number of
% membership functions for each input
[rowIn,numInput]=size(fis_name.input);
inMfCell=cell(numInput,1);  %  suppose the crisp input number is the same as the FL input

for i = 1:numInput
   [row_i NumMf_i] = size(fis_name.input(i).mf);
   inMfCell{i} = zeros(NumMf_i,2);  % initial matrix for storing number&value
    for j = 1:NumMf_i  % find out type, and parameter of each MF
       type_in = fis_name.input(i).mf(j).type;
       param_in = fis_name.input(i).mf(j).params;
       MfValue_in = evalmf(vecInput(i),param_in,type_in);
       inMfCell{i}(j,:)=[j MfValue_in];
    end
    indexMat_in=find(inMfCell{i}<=0.005); % find out which MF to be fired
    [rowZero_in colZero_in]=ind2sub(size(inMfCell{i}),indexMat_in);
    inMfCell{i}(rowZero_in,:)=[];     % delete the rows with membership <= 0.05
end

% find out fuzzified MFs for each output
[rowOut,numOutput]=size(fis_name.output);
outMfCell=cell(numOutput,1);
for i = 1:numOutput
    [row_o NumMf_o] = size(fis_name.output(i).mf);
    outMfCell{i} = zeros(NumMf_o,2);
    for j = 1:NumMf_o
       type_out = fis_name.output(i).mf(j).type;
       param_out = fis_name.output(i).mf(j).params;
       MfValue_out = evalmf(vecOutput(i),param_out,type_out);
       outMfCell{i}(j,:)=[j MfValue_out];
    end
    indexMat_out=find(outMfCell{i}<=0.005);
    [rowZero_out colZero_out]=ind2sub(size(outMfCell{i}),indexMat_out);
    outMfCell{i}(rowZero_out,:)=[];
end
```

B.7 continue

```
% ************************************************************************
function [inMfList outMfList] = MfComb (InMfCell, OutMfCell)
% ************************************************************************
numInput = max(size(InMfCell));
numOutput = max(size(OutMfCell));

inMfLevel = zeros(1,numInput);
for i = 1:numInput  % calculate how many rows of MemFcnComb
   [numMfIn colMfIn] = size(InMfCell{i});
   inMfLevel(i) = numMfIn;
end
outMfLevel = zeros(1,numOutput);
for j = 1:numOutput
   [numMfOut colMfOut] = size(OutMfCell{j});
   outMfLevel(j) = numMfOut;
end
MfLevelIO = [inMfLevel, outMfLevel];  % concatenate the two vectors into one
CombMat = fullComb(MfLevelIO); % calculate all the possible MF level combinations
 [totalRow, totalCol] = size(CombMat); % substitute each variable with MF number

for k = 1:numInput % for input variables
   for l = 1:totalRow
      CombMat(l,k) = InMfCell{k}(CombMat(l,k),1);
   end
end
for m = (numInput + 1):totalCol % for output variables
   for n = 1:totalRow
      CombMat(n,m) = OutMfCell{m-numInput}(CombMat(n,m),1);
   end
end
inMfList = CombMat(:,1:numInput); % divide CombMat into input MF list and output MF list
outMfList = CombMat(:,(numInput + 1):totalCol);

% ************************************************************************
function MfCombMat = fullComb(numMfVec)
% ************************************************************************
%FULLCOMB full combinations of membership functions of fuzzified variable.
 [row,col] = size(numMfVec);
rowLength = prod(numMfVec);
ncycles = rowLength;
cols = max(row,col);
MfCombMat = zeros(rowLength,cols);  % initialize a ZEROS matrix
for k = 1:cols
   if numMfVec(k) == 1
       MfCombMat(:,k) = ones(rowLength,1);
   else
      settings = (1:numMfVec(k));
      ncycles = ncycles./numMfVec(k);
      nreps = rowLength./(ncycles*numMfVec(k));
      settings = settings(ones(1,nreps),:);
      settings = settings(:);
      settings = settings(:,ones(1,ncycles));
      MfCombMat(:,k) = settings(:);
   end
end
```

Appendix C Mechanical Designs for Experimental Setup

Drawing List:

- FSW Device Assembly
- Shaft Clamping Sub Assembly
- Supporting Sub Assembly
- Shaft
- Coupler
- Complex Curvature Backing Piece
- Dia95 Circular Backing
- Dia70 Circular Backing
- Dia60 Circular Backing
- Dia40 Circular Backing
- Flat Backing Plate
- Complex Curvature Workpiece
- Dia95 Round Workpiece
- Dia70 Round Workpiece
- Dia40 Round Workpiece
- Flat Plate Workpiece
- Grooved Tool 3 m

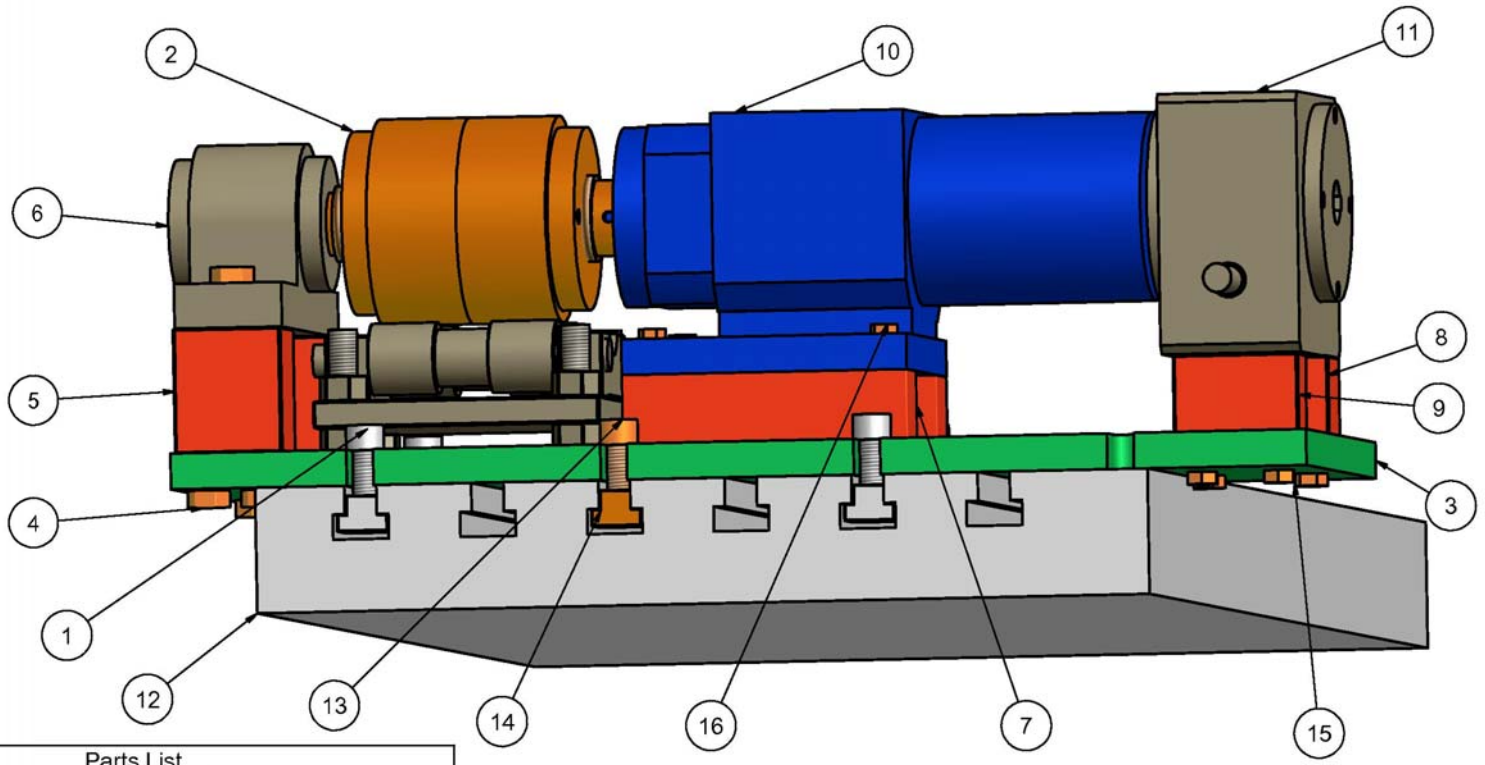

Parts List			
ITEM	QTY	PART NUMBER	DESCRIPTION
16	4	part-111	M8bolt_gearbox
15	4	part-110	M10bolt_reducer
14	6	part-114	T_nut
13	6	part-113	M14HexSocketBolt
12	1	part-112	worktable
11	1	part-106	speed reducer
10	1	part-105	gearbox
9	1	part-108	seating_reducer_s
8	1	part-109	seating_reducer_l
7	2	part-107	seating_gearbox
6	1	part-102	bearing-SN508
5	2	part-101	seating_bearing
4	6	part-104	M14bolt_bearing
3	1	part-100	base_worktable
2	1	assembly-001	shaftPipeAssembly
1	1	assembly-002	Roller Assembly

Designed by	Checked by	Approved by - date		Date	
Tao				2004/03/11	

PE TECHNIKON

PIPE FSW DEVICE

assembly-000 | Edition | Sheet 1 / 1

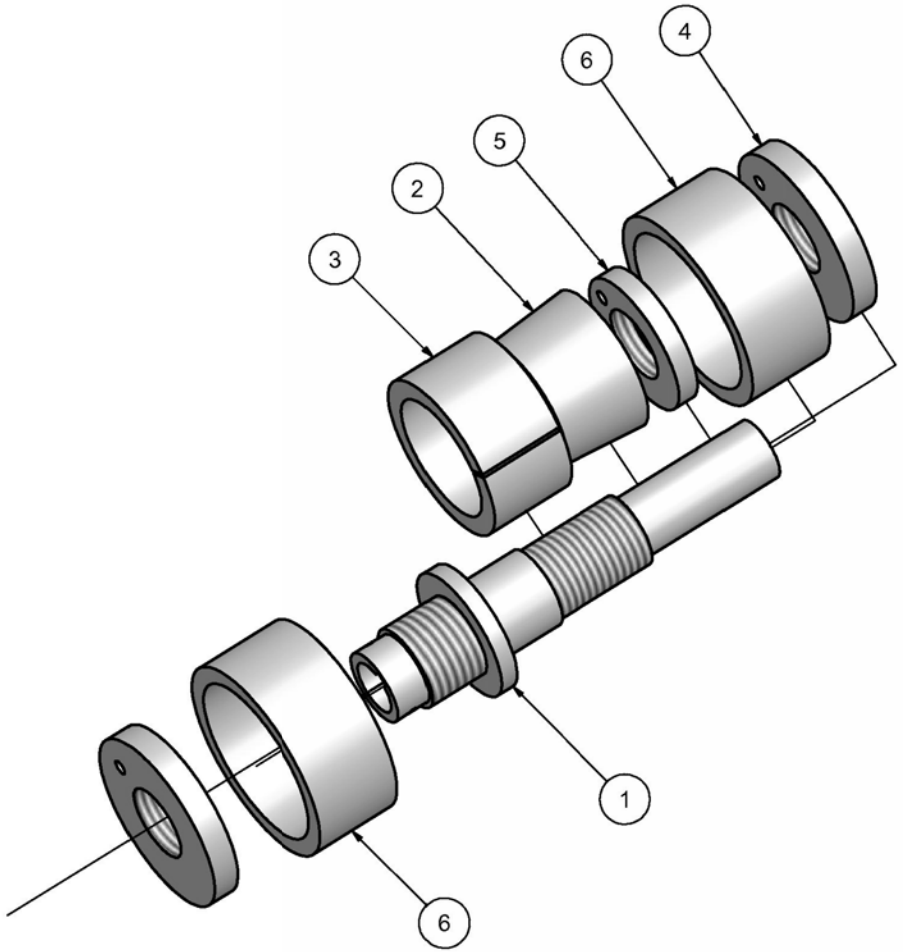

Exploded View

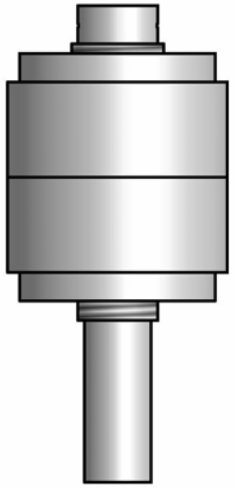

Assembled

Parts List			
ITEM	QTY	PART NUMBER	DESCRIPTION
1	1	A101	shaft
2	1	A102	tapering Bushing
3	1	A103	tapering Collet
4	2	A104	pipe lock nut
5	1	A105	bushing lock nut
6	2	A106	workpiece_pipe

Designed by	Checked by	Approved by - date		Date	
Tao				2/24/2004	

PE TECHNIKON	PIPE SUB ASSEMBLY		
	Design30-1	Edition A	Sheet 1 / 1

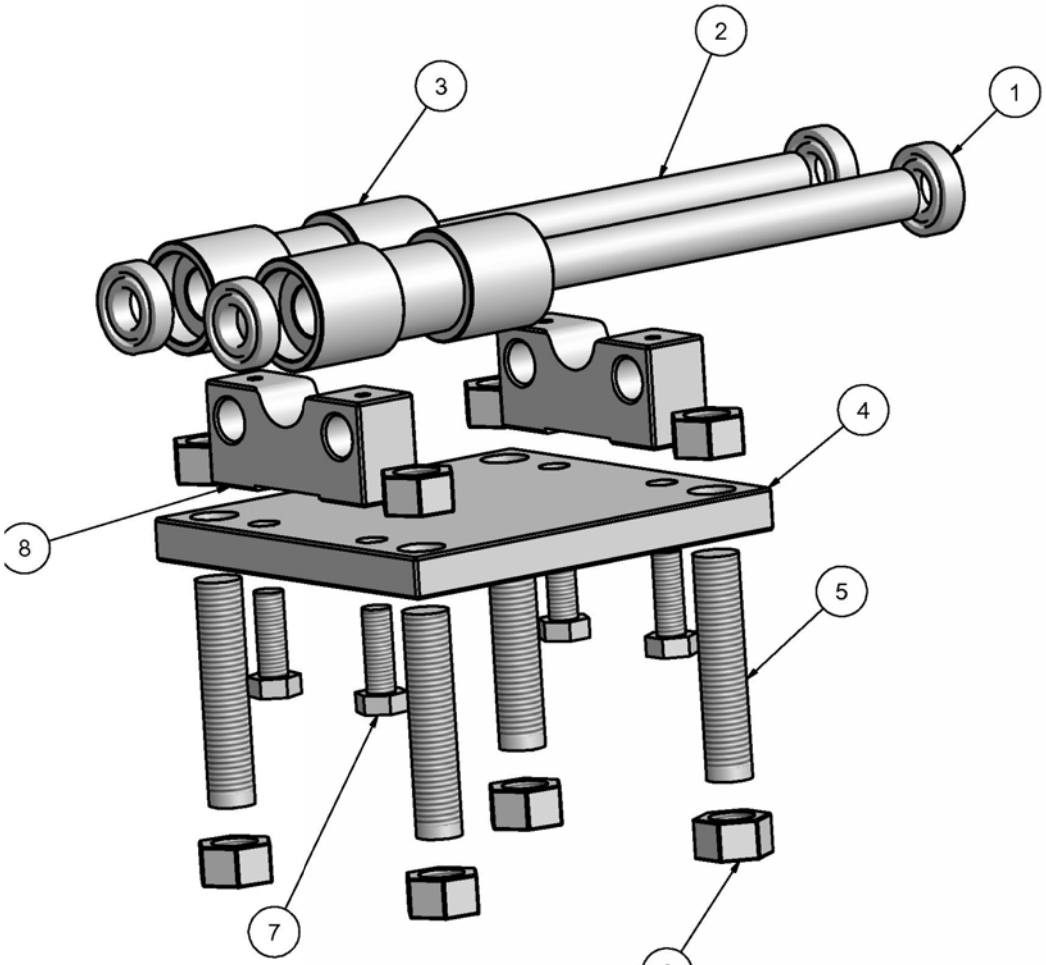

exploded

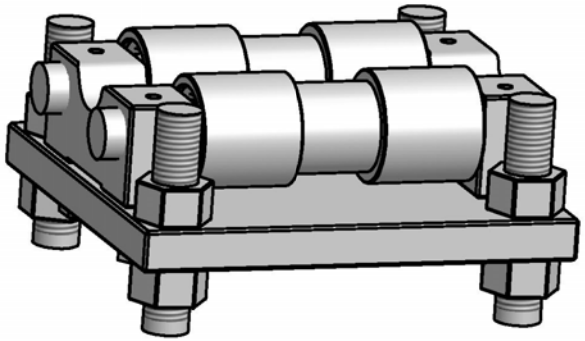

assembled

Parts List			
ITEM	QTY	PART NUMBER	DESCRIPTION
8	2	B101	roller housing
7	4	B105	M14bolt
6	8	B107	M14nut
5	4	B106	M14screw
4	1	B100	plate
3	2	B104	roller
2	2	B103	shaft_roller
1	4	B102	bearing_16002

Designed by	Checked by	Approved by - date		Date	
Tao				3/1/2004	

PE TECHNIKON	Roller Assembly		
	assembly-002	Edition A	Sheet 1 / 1

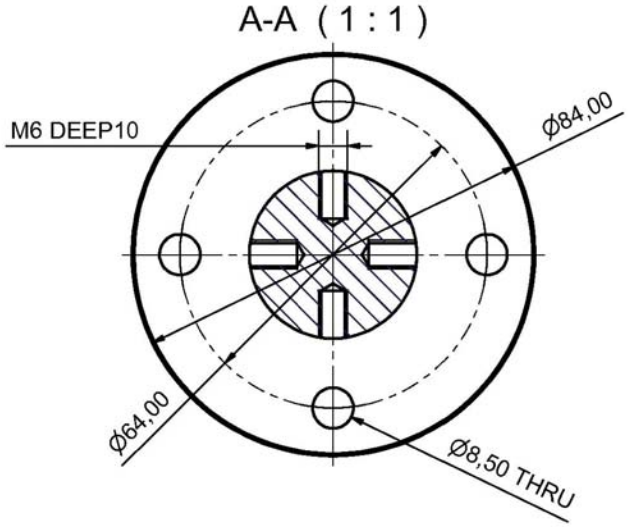

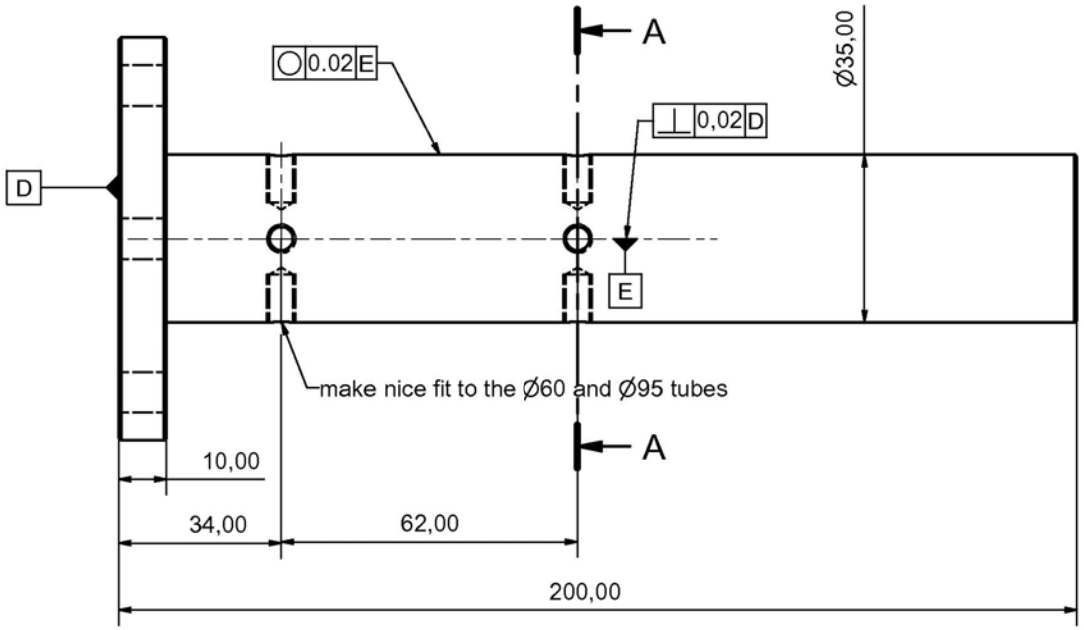

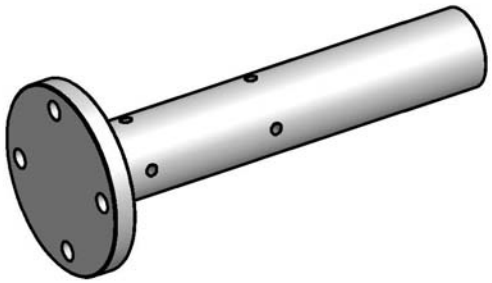

material: BMS
quantity: 1
all chamfer: 0.5X45°

Designed by	Checked by	Approved by - date		Date	
Tao				2004/10/07	

PE TECHNIKON	Shaft_CircularWorkpiece		
	TAO-01-004	Edition	Sheet 1 / 1

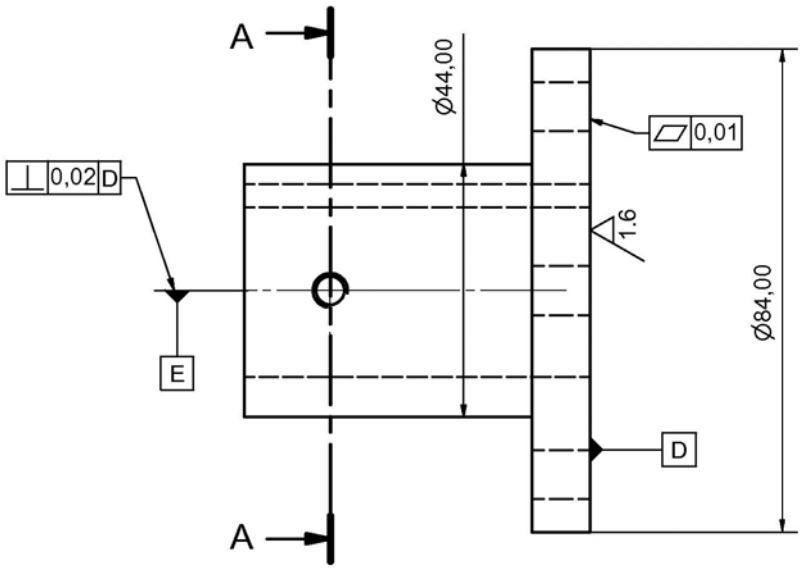

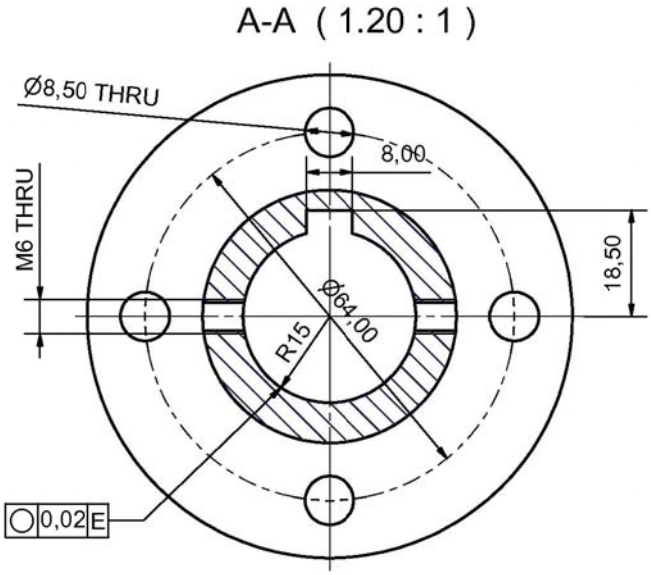

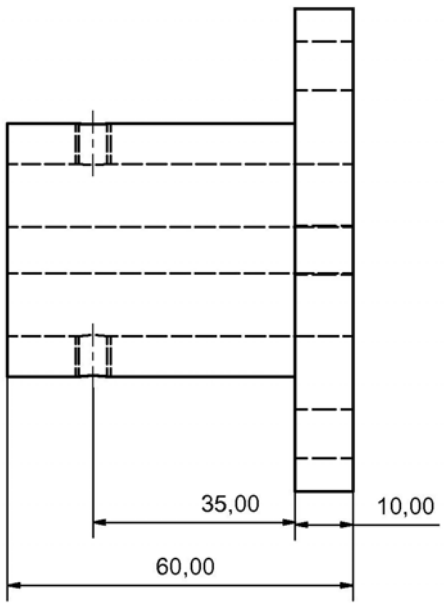

material: BMS
quantity: 1

all chamfer: 0.5X45°

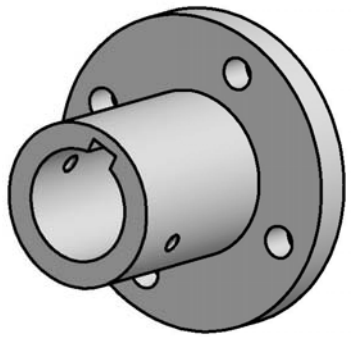

Designed by	Checked by	Approved by - date		Date	
Tao				2004/10/07	

PE TECHNIKON	Coupler_CircularWorkpiece		
	s110	Edition	Sheet 1 / 1

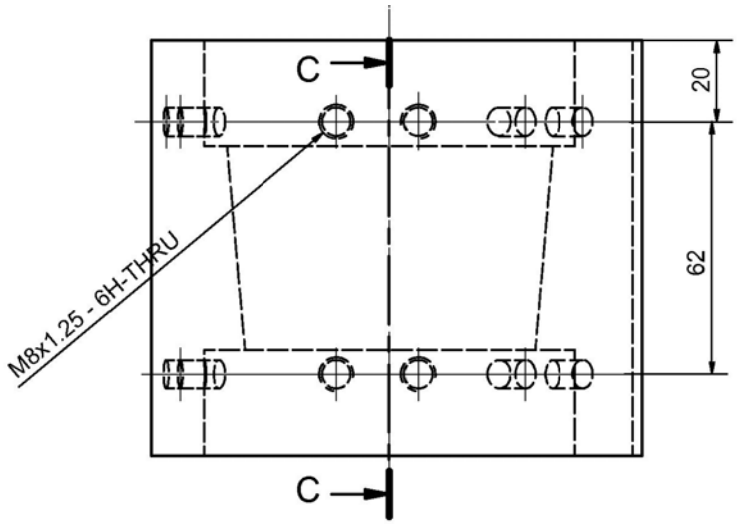

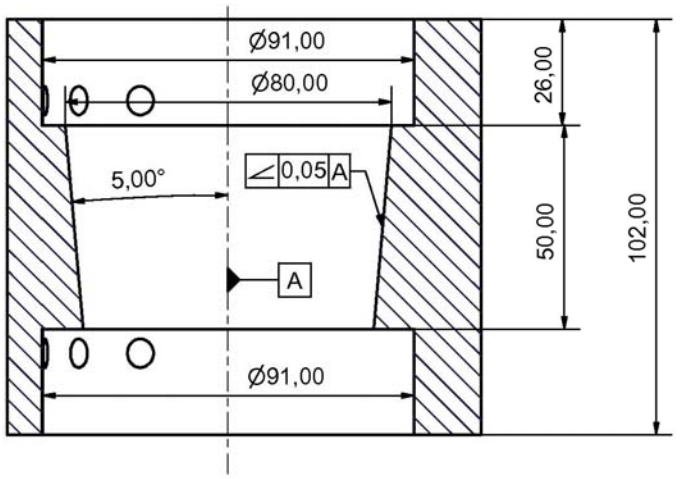

C-C (0.85 : 1)

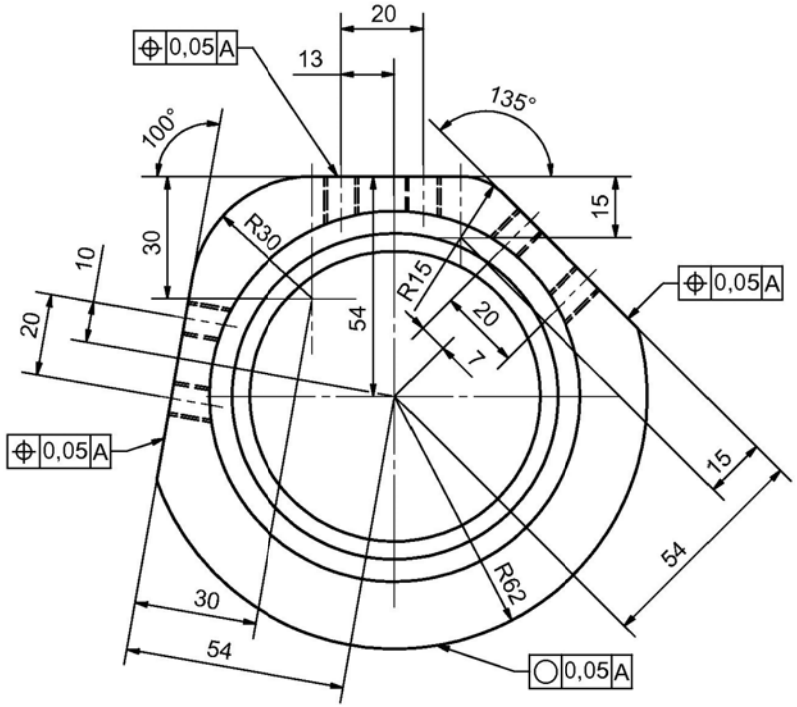

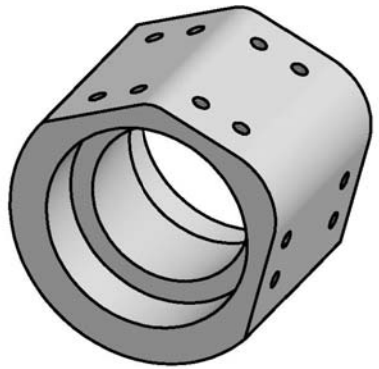

Designed by	Checked by	Approved by - date		Date	
Tao				2004/09/03	
PE TECHNIKON		Backing_ComplexCurvature			
		A103-1		Edition	Sheet 1 / 1

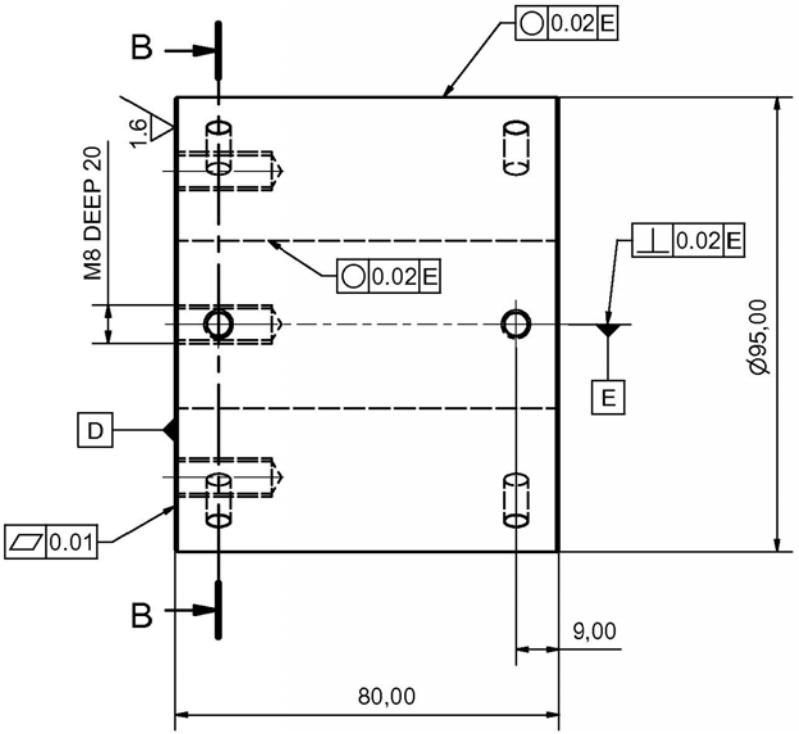

B-B (1 : 1)

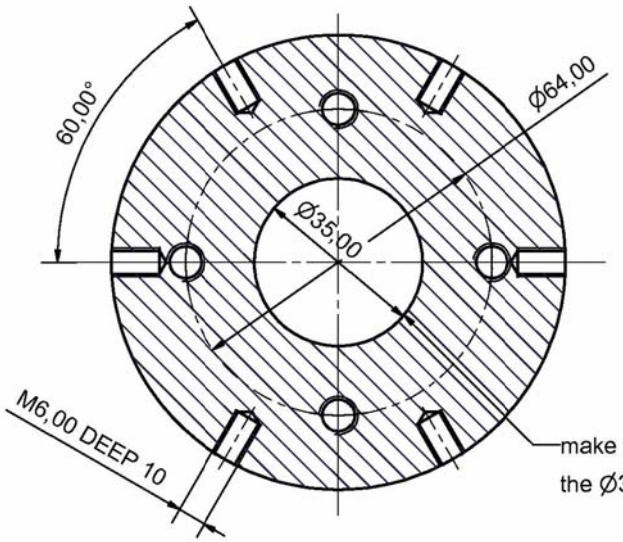

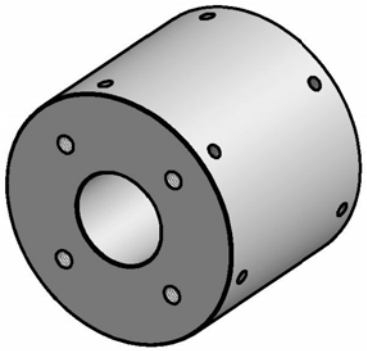

material: BMS
quantity: 1

all chamfer: 0.5X45°

Designed by	Checked by	Approved by - date		Date	
Tao				2004/10/07	

PE TECHNIKON	Backing_CircularDia95		
	TAO-01-005	Edition	Sheet 1 / 1

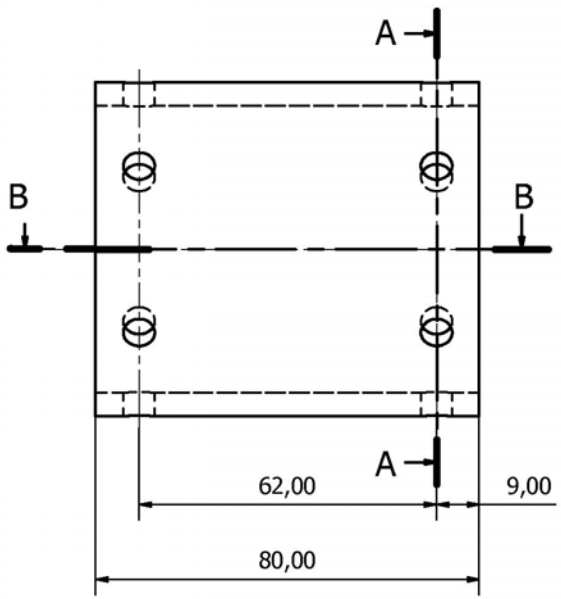

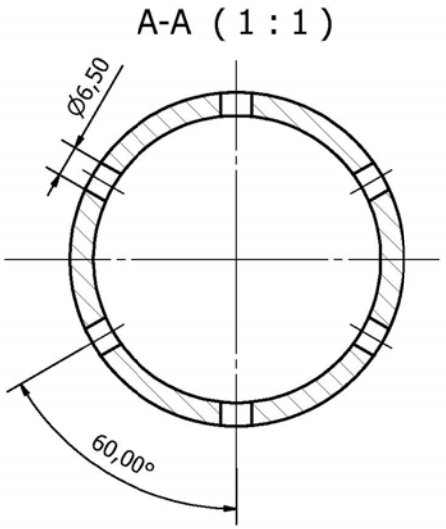

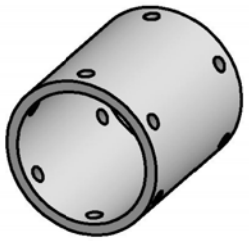

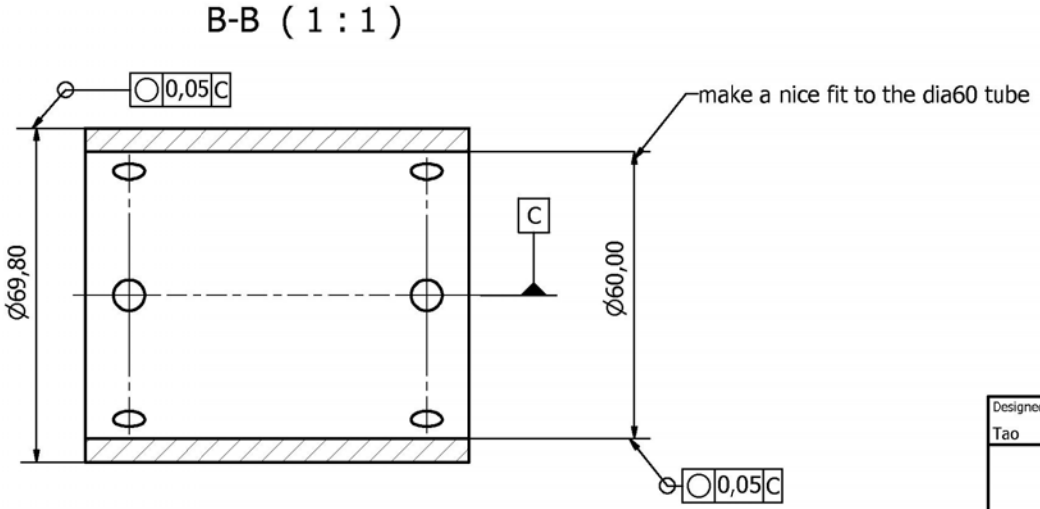

material: BMS
quantity: 1
all chamfer: 0.5X45°

Designed by	Checked by	Approved by	Date		Date	
Tao					2005/06/07	

PE TECHNIKON	Backing_CircularDia70		
	TAO-01-001	Edition	Sheet 1 / 1

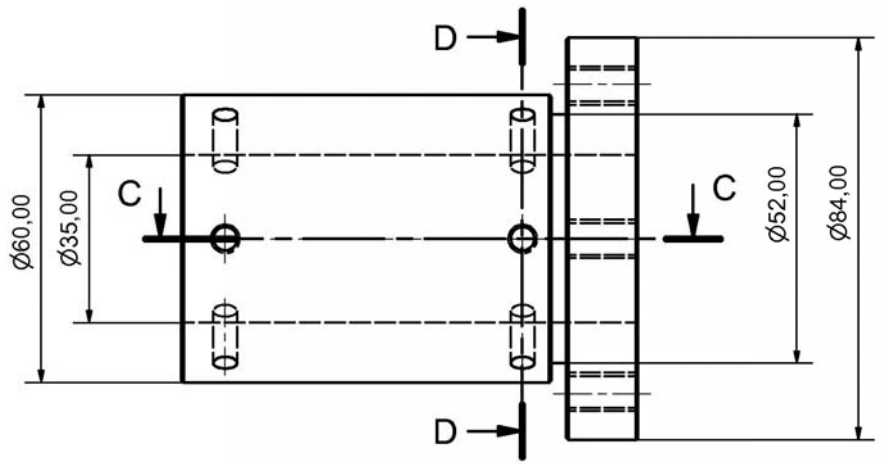

D-D (1 : 1)

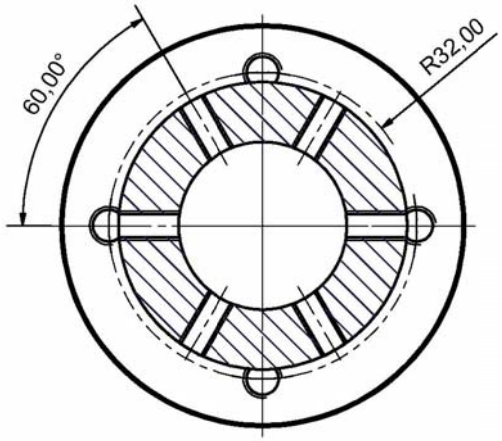

C-C (1 : 1)

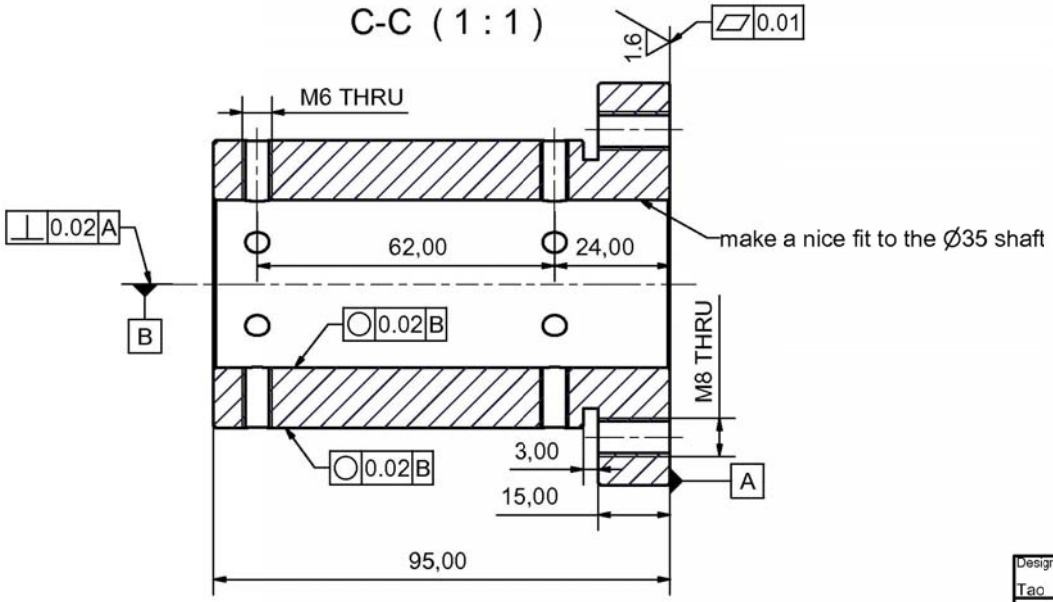

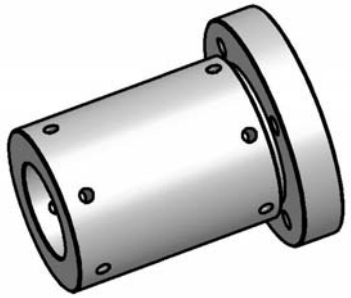

material: BMS
quantity: 1

all chamfer: 0.5X45°

Designed by	Checked by	Approved by - date		Date	
Tao				2004/10/07	

PE TECHNIKON	Backing_CircularDia60		
	TAO-01-003	Edition	Sheet 1 / 1

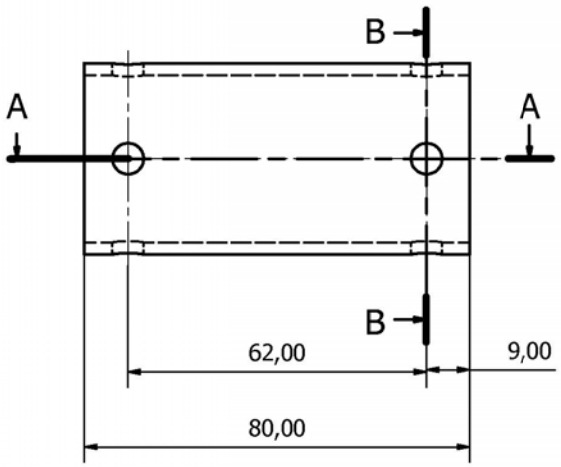

B-B (1 : 1)

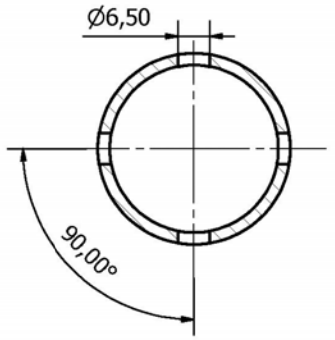

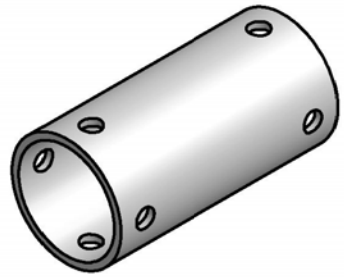

A-A (1 : 1)

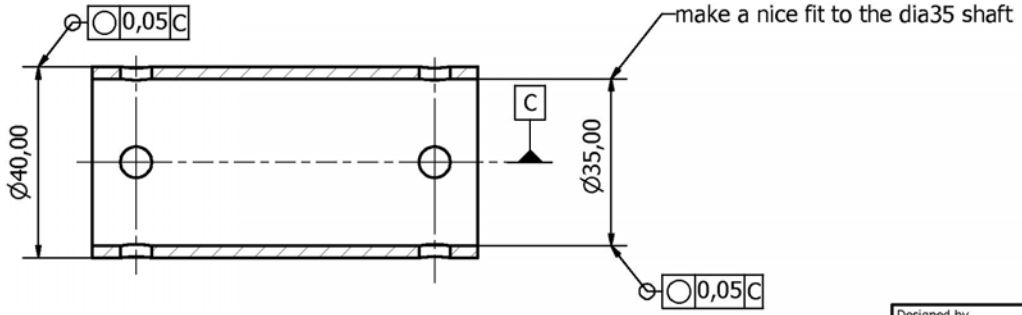

material: BMS
quantity: 1

all chamfer: 0.5X45°

Designed by	Checked by	Approved by	Date		Date	
Tao					2005/06/07	

PE TECHNIKON	Backing_CircularDia40		
	TAO-01-002	Edition	Sheet 1 / 1

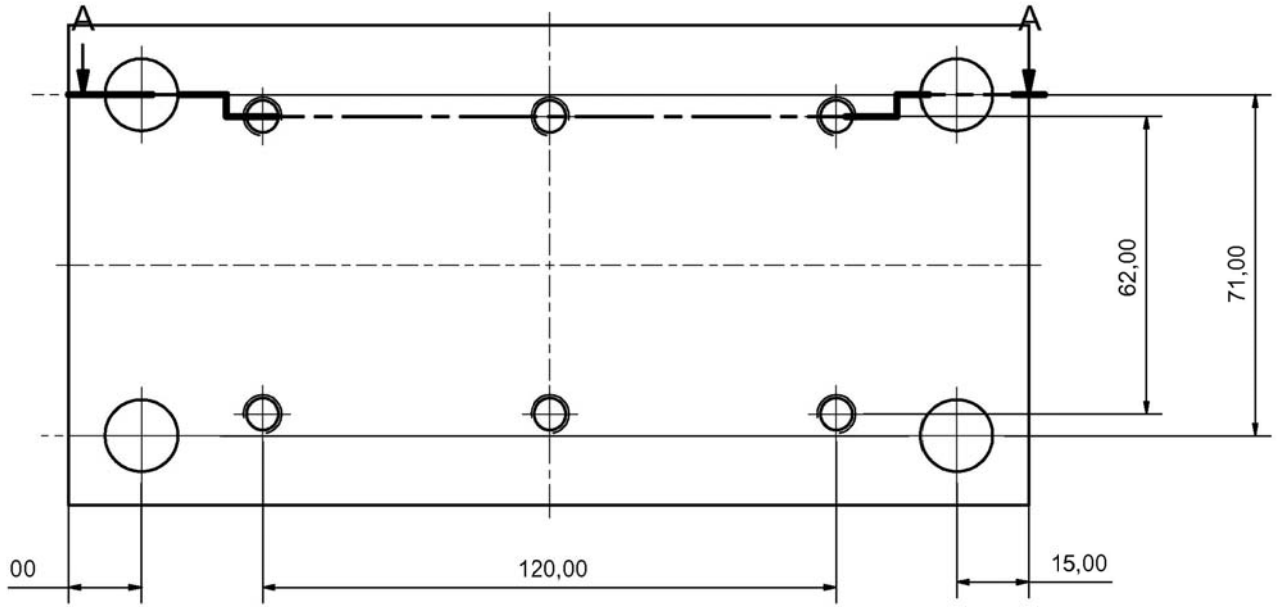

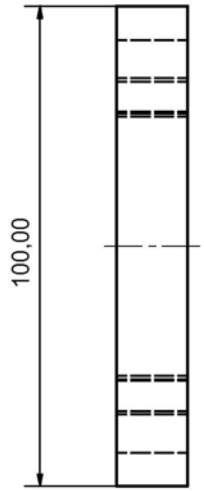

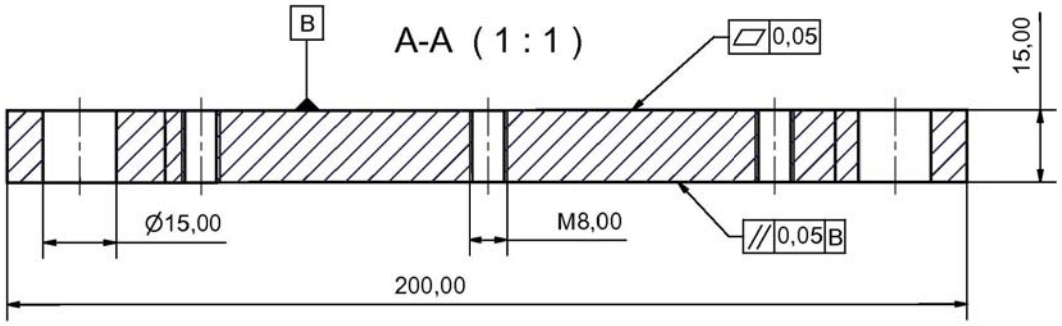

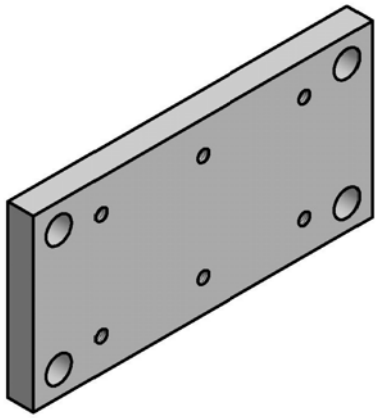

Designed by	Checked by	Approved by - date		Date	
Tao				2004/09/08	

PE TECHNIKON	Backing_FlatPlate		
	back_plate	Edition	Sheet 1 / 1

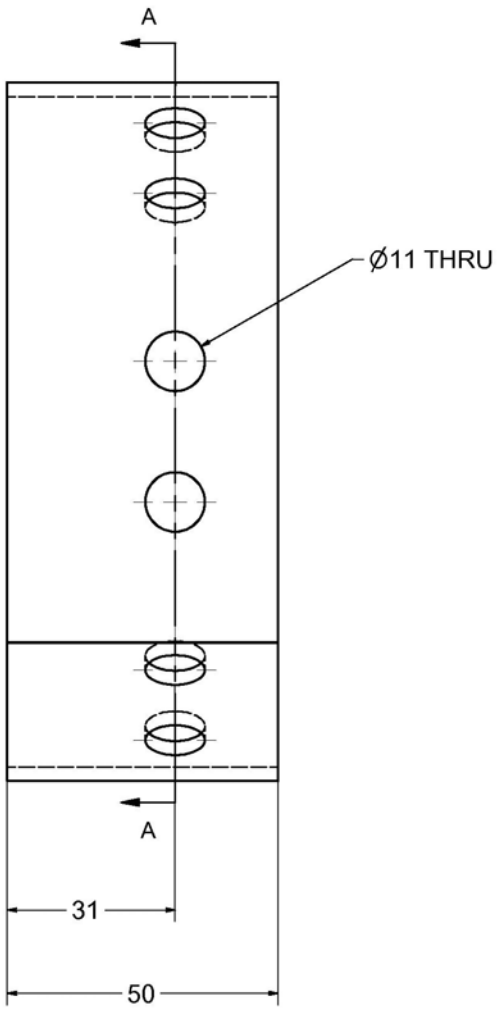

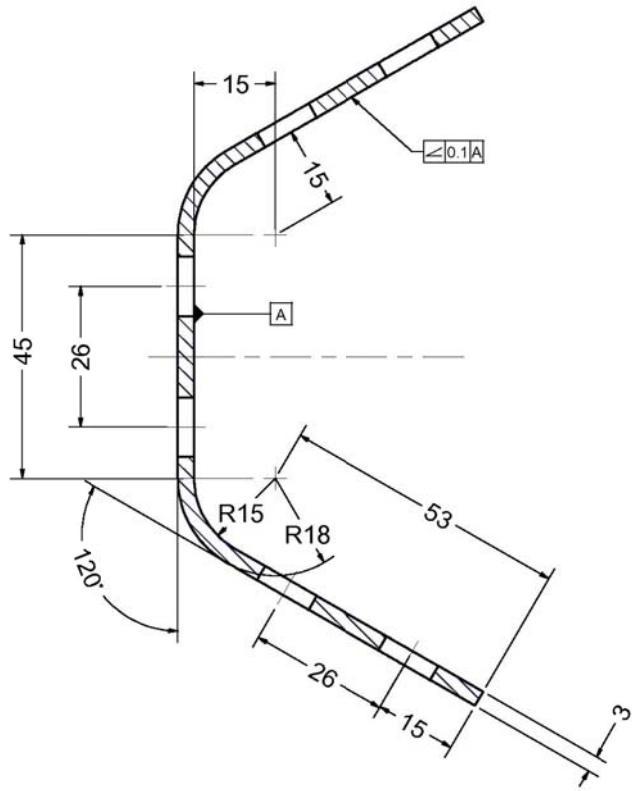

SECTION A-A
SCALE 1.50 : 1

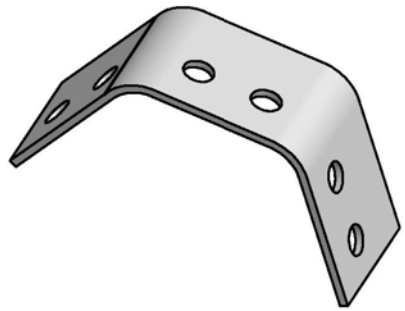

DRAWN Tao	2004/08/30	PE TECHNIKON	
CHECKED		TITLE	
QA		workpiece_ComplexCurvature	
MFG			
APPROVED		SIZE C	DWG NO corner_workpiece_3mm REV
		SCALE	SHEET 1 OF 1

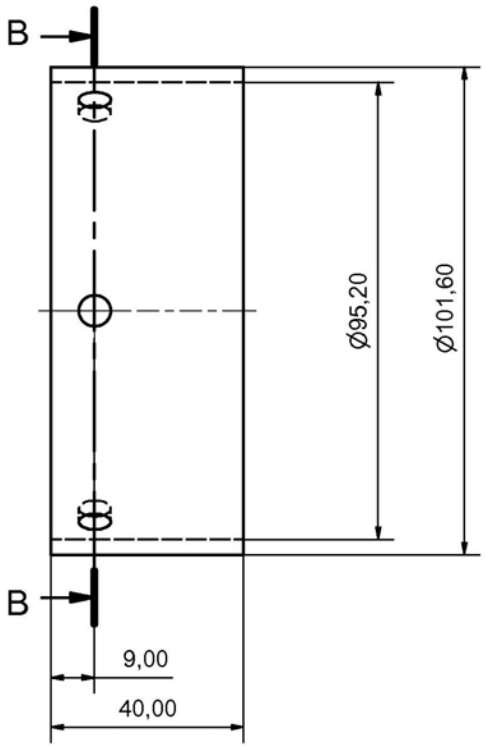

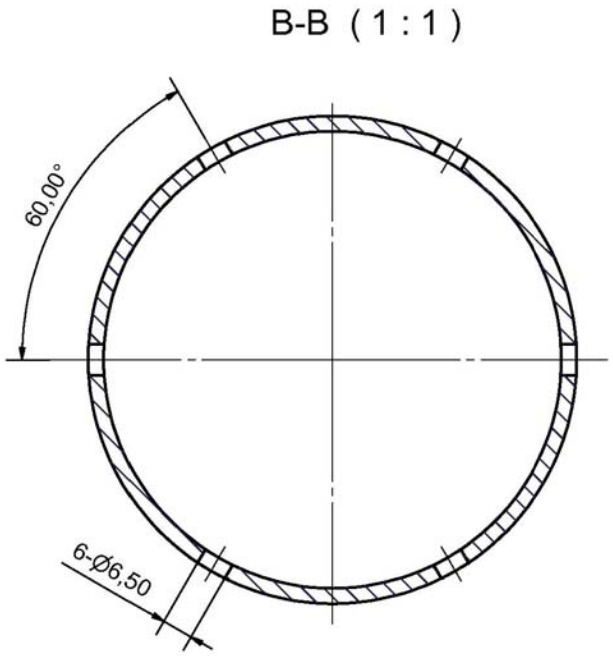

material: aluminium 6061T6
quantity: 20

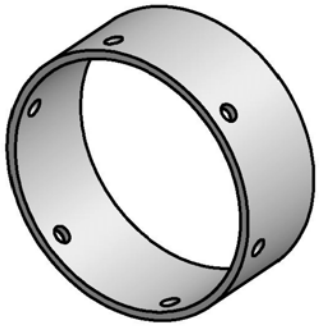

Designed by	Checked by	Approved by - date		Date	
Tao				2004/10/07	

PE TECHNIKON	Workpiece_RoundDia95		
	TAO-01-005	Edition	Sheet 1 / 1

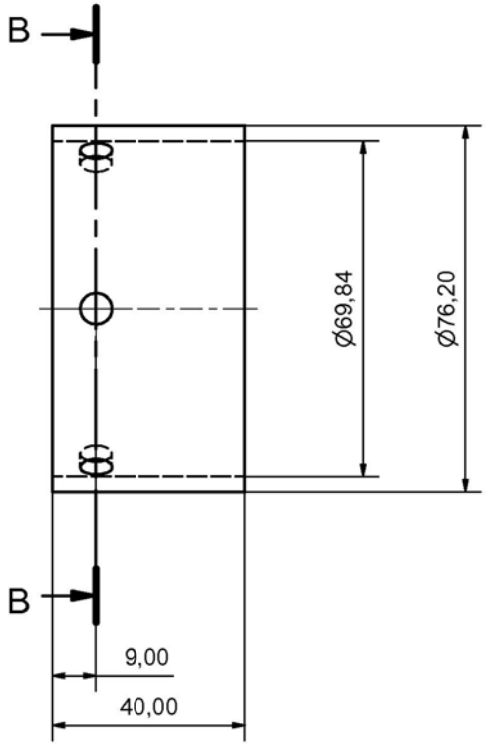

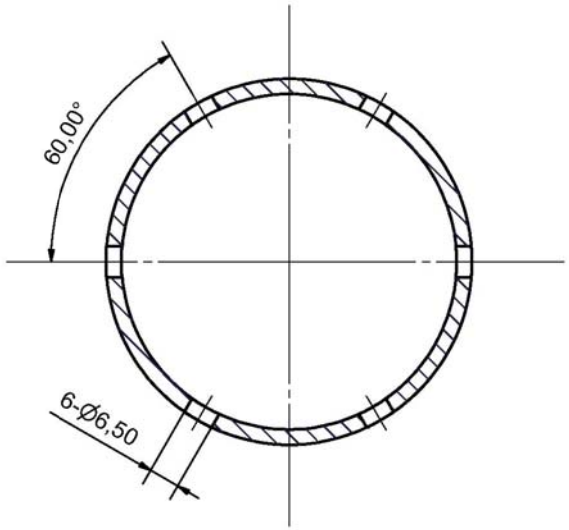

material: aluminium 6061T6
quantity: 20

Designed by	Checked by	Approved by - date		Date	
Tao				2004/10/07	

PE TECHNIKON	Workpiece_RoundDia70		
	TAO-01-005	Edition	Sheet 1 / 1

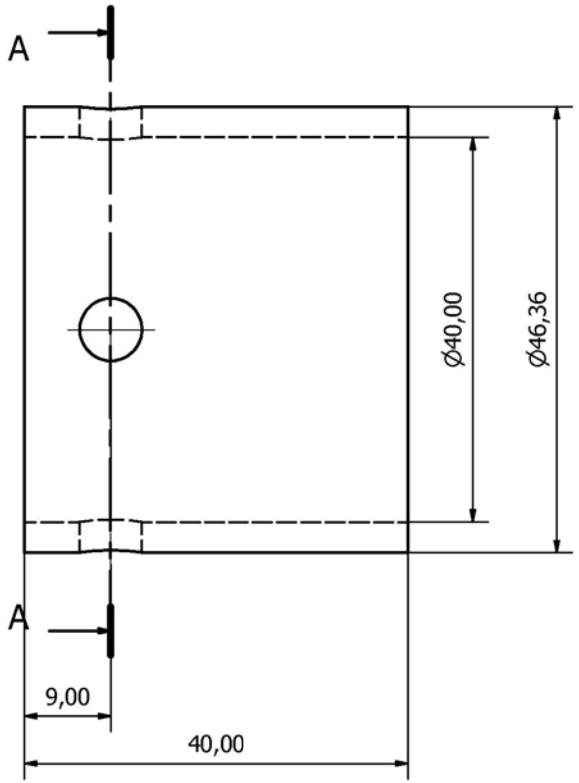

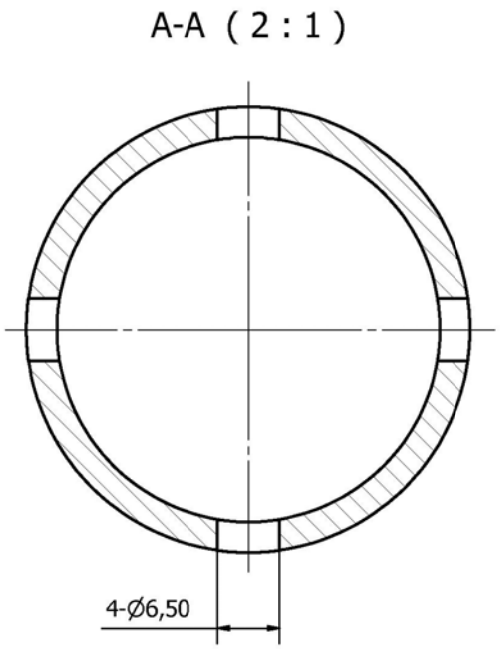

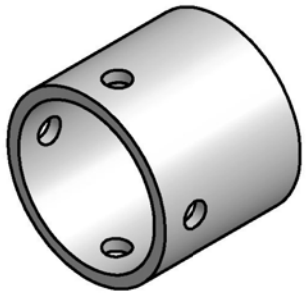

material: aluminium 6061T6
quantity: 20

Designed by	Checked by	Approved by	Date		Date	
Tao					2005/06/28	

PE TECHNIKON	Workpiece_RoundDia40		
	TAO-WP-002	Edition	Sheet 1 / 1

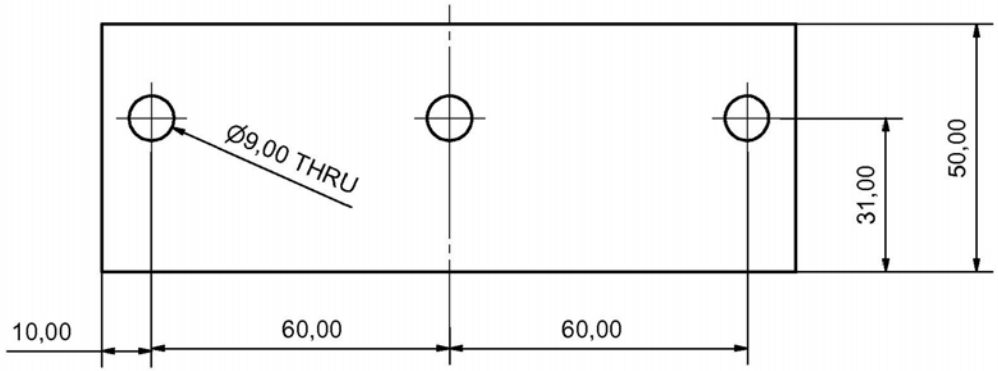

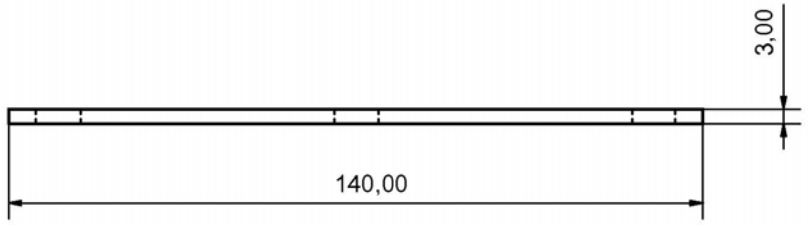

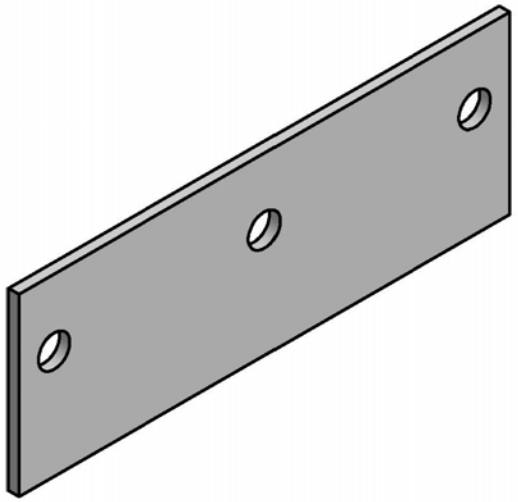

Designed by	Checked by	Approved by - date		Date	
Tao				2004/09/08	

PE TECHNIKON	Workpiece_3mmFlat		
	TAO-WP-001	Edition	Sheet 1 / 1

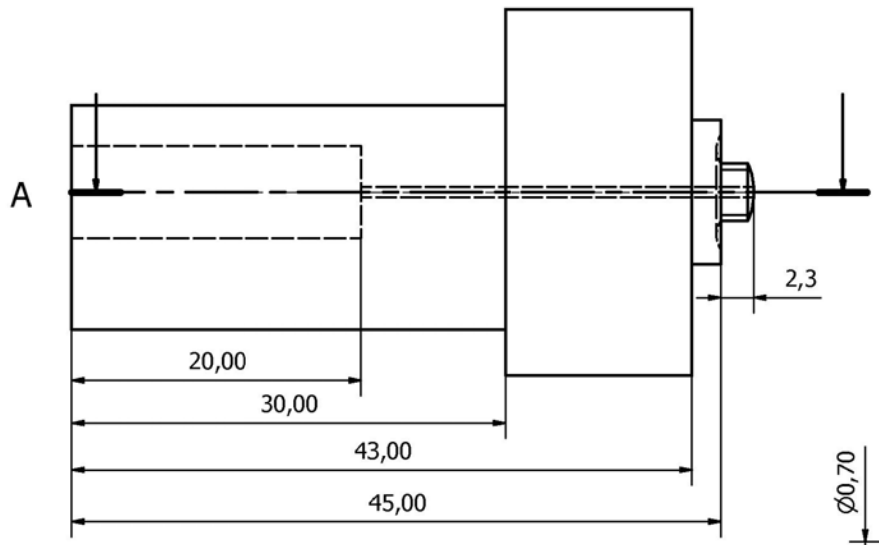

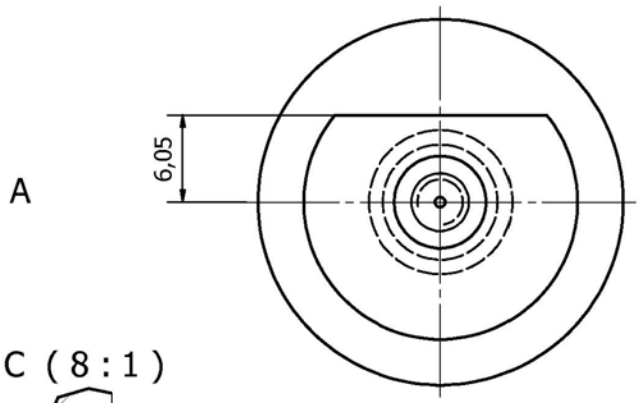

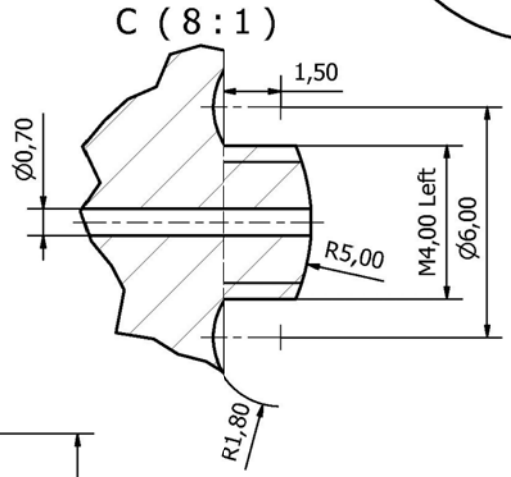

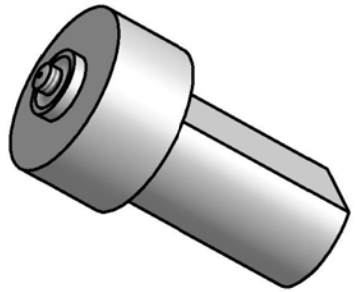

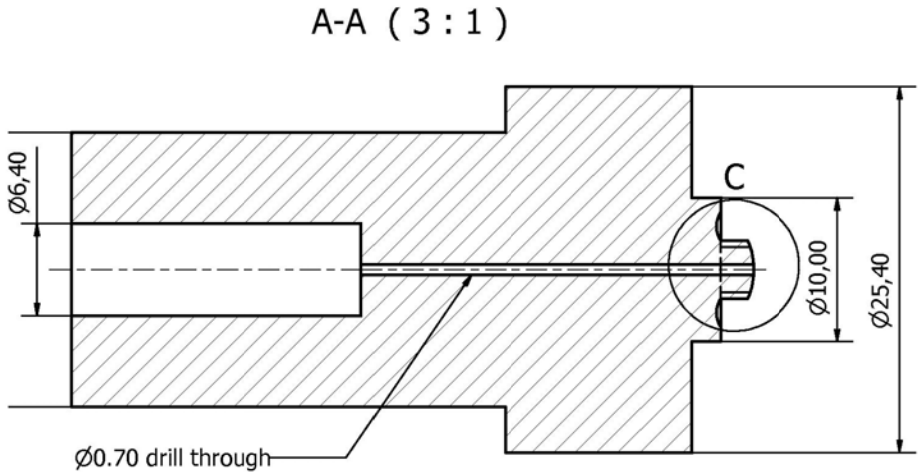

MTR: W302 (H13) tool steel: Heat treat RHc ± 54

All fillets R0.5
Surface roughness

Designed by	Checked by	Approved by	Date		Date	
Tao					2005/05/30	

PE TECHNIKON	3mm tool grooved		
	tool for 3mm plate	Edition	Sheet 1 / 1

Appendix D Publications

Paper 1: A Neuro-fuzzy Scheme for Process Control during Complex Curvature Friction Stir Welding FSW (Approved: 12th International Federation of Automatic Control Symposium on Control Problems in Manufacturing)

Paper 2: Experimental Implementation of Complex Curvature Friction Stir Welding (Submitted: R & D Journal)

Paper 3: Monitoring and Intelligent Control for Complex Curvature Friction Stir Welding (Submitted: Journal of Engineering Manufacture)

A NEURO-FUZZY SCHEME FOR PROCESS CONTROL DURING COMPLEX CURVATURE FRICTION STIR WELDING

T.I. van Niekerk, T. Hua, D.G. Hattingh
theo.vanniekerk@nmmu.ac.za

Faculty of Engineering, Nelson Mandela Metropolitan University,
Port Elizabeth, 6031, South Africa

Abstract: This paper presents a neuro-fuzzy control scheme for the nonlinear process of complex curvature Friction Stir Welding with multi-input-multi-output parameters. The proposed scheme consists of integrated sensor monitoring, fuzzy logic controller with basic membership functions, a trained back-propagation feed-forward neural network used to generate on-line fuzzy rules, and an input/output scale tuning system used to improve output response to process changes. To validate the feasibility of the neuro-fuzzy controller, simulations have been conducted with the objective to maintain tool/workpiece contact during complex curvature FSW. The simulation results show that the control variables were well maintained within limited ranges from reference values.

Keywords: Neural network, fuzzy logic, on-line monitoring, intelligent control, friction stir welding.

1. INTRODUCTION

Friction Stir Welding (FSW) is a joining technique developed by TWI in 1991 (Thomas*, et al.,* 1991). In FSW, a cylindrical tool consisting of a profiled pin under a wider shoulder rotates about its own axis and the pin is slowly plunged into the joint of the workpieces. Material in the joint is plasticized by frictional heating between the tool and the workpieces. The welding tool moves along the weld joint when the material has been sufficiently plasticized. The plasticized material is transported about the rotating pin and is pressed together, forming a solid joint on cooling. The tool is extracted from the workpieces when required weld length is finished. The process schematic of FSW is shown in Fig. 1.

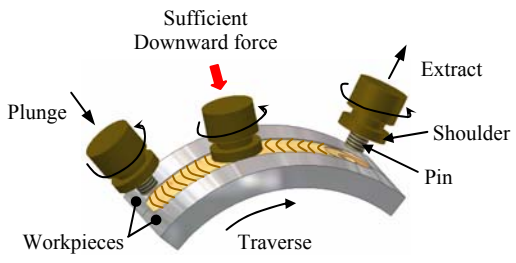

Fig. 1. Process of Friction Stir Welding

Currently, the research of monitoring and control of FSW is mainly focused on straight welds. Effects of process parameters such as feed rate, spindle speed and tool size on fatigue life, tensile strength, weld crack and residual stress of FSW welds have been investigated (James, *et al.*, 2003; Reynolds, *et al.*, 2003; NAKATA, *et al.*, 2001; Ericsson and Sandström, 2003). Khandkar *et al.* (2003) introduced an input torque based model of temperature distribution and thermal history prediction. Chen *et al.* (2003) presented a monitoring system using wavelet transform analysis of acoustic emission for aluminium 6061 FSW.

To machine parts with complex geometry which involves multi-input-multi-outputs (MIMO), fuzzy logic is an ideal tool for process control due to its tolerance of imprecise data and ability to model nonlinear functions of arbitrary complexity. It can also be blended with conventional control techniques (The MathWorks, 2004a). Liang et al. (2003) presented a tuning mechanism, including an input scale factor tuned with the integration of torque error and an output scale factor tuned by the change of torque error, to strengthen or weaken the fuzzy control of CNC machine spindle torque by adjusting spindle speed and feed rate.

The fuzzy rules of most fuzzy controllers are set based on past experience. However, when facing a complex MIMO process involving nonlinear relationship between inputs and outputs, a more efficient fuzzy rule generating method is needed. Neural network (NN), which has the ability to learn relationships among input and output data sets through a training process, is able to 'induce' output data if a new set of input data is made available (The MathWorks, 2004b). This can be utilized to solve the 'bottleneck' problem of fuzzy rule extracting. Sun and Deng (1996) presented a fuzzy NN control structure which is composed of an antecedent NN to match fuzzy rule premises, and a consequent NN to

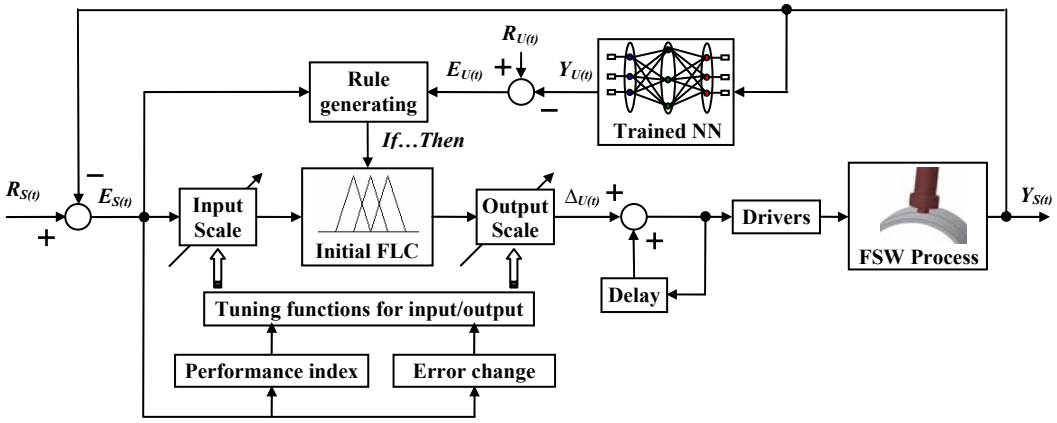

Fig. 2. Structure of the proposed neuro-fuzzy scheme for process control.

implement fuzzy rule consequences. Lau et al. (2001) proposed an integrated neural-fuzzy model using NN to generate 'If-Then' fuzzy rule.

The MIMO and nonlinear FSW process makes the intelligent technologies fuzzy logic and NN feasible control strategies. A neuro-fuzzy control scheme incorporating the advantages of NN and fuzzy logic, together with an input/output tuning mechanism, is proposed in this paper for tool/workpiece contact control during complex curvature FSW.

2. SYSTEM STURCTURE

Fig. 2 shows the overall structure of the proposed neuro-fuzzy control scheme. Inputs $E_{S(t)}$ to the control system are the errors of on-line control variables $Y_{S(t)}$ to their reference value $R_{S(t)}$, and outputs from the control system are proposed process parameter adjustments $\Delta_{U(t)}$. The main part of the control scheme consists of a trained NN for deriving instant process parameters $Y_{U(t)}$, a rule-generating module for fuzzy rule generation using control variable errors $E_{S(t)}$ and process parameter errors $E_{U(t)}$ of derived instant value $Y_{U(t)}$ to preset value $R_{U(t)}$, an fuzzy controller with predefined input/output membership functions to generate primary command for process parameters adjustment, and a tuning module to strengthen or weaken control actions by tuning input and output scale factors in response of the dynamic process changing. The design details and simulation results are described in following sections.

3. IMPLIMENTATION OF THE NEURO-FUZZY CONTROL SCHEME

Tool/workpiece contact condition plays a critical role in thermal input between tool and workpiece, which dominates weld properties (Peel, *et al.,* 2003; Chen and Kovacevic, 2003). Plunge depth and tilt angle of welding tool to workpieces co-operate to determine tool/workipiece contact condition. During complex curvature FSW, tilt angle and plunge depth need to be adaptive to changing curvature. Even for uniform curvature workpieces, the well pre-planned tilt angle and plunge depth may be not maintained due to process disturbance. Fig.3 shows the incorrect tool/workpiece contact due to incorrect tilt angle, incorrect plunge depth, and changing curvature. Thus the proposed neuro-fuzzy control scheme is used to adjust tilt angle and plunge depth for maintaining tool/workpiece contact adapting to the changing process condition.

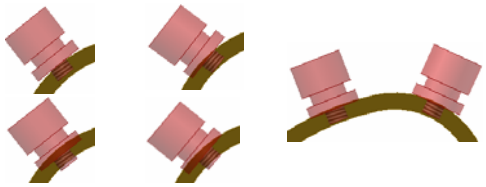

Fig. 3. Incorrect tool/workpiece contact due to (a) incorrect plunge depth, (b) incorrect tilt angle, and (c) changing curvature.

3.1 Sensor fusion

To on-line monitor tool/workpiece contact condition, sensor fusion is used to establish tool/workpiece contact model. Sensitive features with higher sensitivity to tilt angle and plunge depth are selected from sensor signals and process parameters as control variables. NN is trained to map the relationship between tilt angle, plunge depth and the selected sensitive features (Azouzi and Guillot, 1997).

Experiment design. Orthogonal arrays developed by Taguchi (Ross, 1988) was used in experiment design due to its capabilities of minimizing test number and representing all factors equally. Process parameters were used as experimental factors to investigate their effects on sensor signals. L16_4_5 factor-level table is selected for orthogonal experiment of aluminium 6061 T6 plates, as shown in Table 1.

Table 1 Process parameters and their levels

level	*Feed rate mm/min*	*Spindle speed RPM*	*Tilt angle °*	*Plunge depth mm*
1	50	300	2	0.1
2	100	400	1	0.2
3	150	500	0.5	0.3
4	200	600	0	0.4

Sensor feature selection. Table 2 shows the correlation coefficients of each sensor signal to tilt angle (*Co_tilt*) and plunge depth (*Co_plunge*). It can be seen from Table 2 that signals of temperature,

temperature/Fz, and torque/Fz have larger absolute sum of correlation coefficients to tilt angle and plunge depth, and were thus selected as the control variables for fuzzy control of tool/workpiece contact.

Table 2 Correlation coefficients of sensor signals to tilt angle and plunge depth

Sensor signal	*Co_tilt*	*Co_plunge*	*Absolute sum*
bending (N)	-0.0596	0.0315	0.0911
torque (N.m)	-0.0623	0.3279	0.3902
temperature (˚C)	-0.5382	0.2932	**0.8314**
Fz (KN)	0.0479	0.1582	0.2061
bending/torque	0.0974	-0.1559	0.2533
bending/temperature	0.0728	-0.0772	0.1500
bending/Fz	-0.0350	-0.0421	0.0771
temperature/torque	-0.2789	0.0400	0.3189
temperature/Fz	-0.3322	0.1486	**0.4808**
torque/Fz	-0.3074	0.1546	**0.4620**

NN training. A 5-8-2 back-propagation feed-forward NN is trained to map the relationship between inputs and outputs. Three sensor signals: torque, temperature, and Fz, and two process parameters: feed rate and spindle speed, are selected as inputs for network training. Structure of the trained NN is shown in Fig. 4.

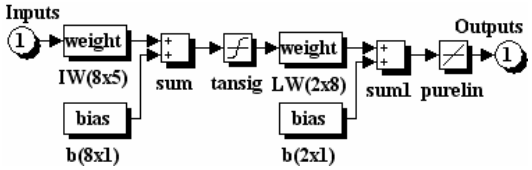

Fig. 4. Structure of the trained neural network.

Fig. 5 shows the comparison of NN output to target values for plunge depth, similar results was obtained for tilt angle.

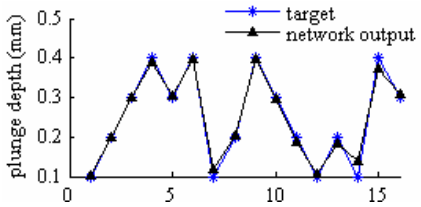

Fig. 5. NN output Vs target value for plunge depth.

3.2 Basic structure of initial fuzzy logic controller

The initial Mamdani type fuzzy controller consists of a fuzzifier, a fuzzy inference engine, a defuzzifier, and membership functions (MFs). The fuzzy rules were however not preset for the controller in this study. The on-line generating of fuzzy rules is described in Section 3.4.

Inputs and normalizing. Each of the three sensitive features selected in sensor fusion was compared to a reference value, and the error was used as an input to the fuzzy controller. At each sampling time *i*, the three errors were respectively calculated as:

$$ERR_{Temp}(i) = Temp_{ref} - Temp(i) \quad (1)$$

$$ERR_{Temp/Fz}(i) = \frac{Temp_{ref}}{Fz_{ref}} - \frac{Temp(i)}{Fz(i)} \quad (2)$$

$$ERR_{Torq/Fz}(i) = \frac{Torq_{ref}}{Fz_{ref}} - \frac{Torq(i)}{Fz(i)} \quad (3)$$

Each of the errors was normalized into [-1, 1] before fed into the controller by multiplying corresponding normalizing coefficient (Liang et al., 2003).

$$err_{Temp}(i) = ERR_{Temp}(i) \times K_{Temp}(i) \quad (4)$$

$$err_{Torq/Fz}(i) = ERR_{Torq/Fz}(i) \times K_{Torq/Fz}(i) \quad (5)$$

$$err_{Temp/Fz}(i) = ERR_{Temp/Fz}(i) \times K_{Temp/Fz}(i) \quad (6)$$

The input normalizing coefficient was separately considered in the zones above and below the reference value to ensure that both sides from the reference value (zero error point) have the same membership functions. The normalizing coefficient for temperature error was calculated as follows. The same rule was applied for the other inputs.

If $Temp(i) \geq Temp_{ref}$

$$K_{Temp}(i) = 1/(Temp_{\max} - Temp_{ref})$$

Else $K_{Temp}(i) = 1/(Temp_{ref} - Temp_{\min})$

Where $K_{Temp}(i)$ is temperature normalizing coefficient, $Temp_{max}$ maximum temperature, and $Temp_{min}$ minimum temperature.

Membership functions. In this paper, all the inputs and outputs of the fuzzy controller used the same triangular membership functions due to its computation efficiency. In order to regulate the system output to a desired output, more accurate control actions were taken near the reference value (Kim and Yuh, 2002). Therefore, finer fuzzy sets were placed near the reference value.

3.3 Tuning mechanism

Three parts of a fuzzy controller including membership functions, fuzzy rules and inputs/outputs can be tuned to make the fuzzy controller adaptable. In this study, the membership functions were predefined, and the fuzzy rules were generated on-line. Thus to enhance control actions, fuzzy inputs and outputs were tuned with corresponding scale factors.

Performance index and input scale factors. Performance index was used to evaluate process quality using current and delayed control variable errors. The performance index of temperature was given as follows. The algorithm applied to the other two inputs.

$$Perform_{Temp}(i) = \sqrt{\frac{\Sigma_{i-2}^{i}(err_{Temp}(i))^2}{3}} \quad (7)$$

To adaptively strengthen or weaken control actions in response to on-line signals, the performance index was used for tuning input scale factor. The scale factor for temperature error was calculated as follows. The same algorithm applies to the other two fuzzy inputs (Liang et al., 2003).

$$Kin_{Temp}(i) = \left| \frac{Perform_{Temp}(i)}{\varepsilon_{Temp}} \right|^{0.16} \quad (8)$$

where ε_{Temp} is the bandwidth of tolerance zone, $Kin_{Temp}(i)$ temperature error scale factor at time i.

The final input of temperature error to the fuzzy controller was:

$$err_{Temp}(i) = err_{Temp}(i) \times Kin_{Temp}(i) \qquad (9)$$

Output scale factors. Outputs from fuzzy controller are primary adjustments of tilt angle Δ_{tilt} and plunge depth Δ_{plunge}. Output scale factor for each output was calculated by taking into account the correlation coefficients of the three control variable to tilt angle and plunge depth. The algorithm for calculating scale factor of tilt angle adjustment was given:

$$Kout_{Tilt} = \sqrt{\frac{\Sigma_{i=1}^{3}(|Co_{Tilt}(i)| \times (K_{Tilt}(i))^2)}{\Sigma_{i=1}^{3}|Co_{Tilt}(i)|}} \qquad (10)$$

The algorithm for calculating the output scale factor from the first fuzzy input temperature error is shown as follows (Liang et al., 2003). The same rule applies to the other two fuzzy input temperature/Fz error and torque/Fz error.

$$\text{If} \quad \frac{\delta_{Temp}(i)}{\delta_{Temp}(i-1)} < 0 \quad \&\& \quad \left|\frac{\delta_{Temp}(i)}{\delta_{Temp}(i-1)}\right| > 1$$

$$\text{If} \quad \frac{ERR_{Temp}(i)}{ERR_{Temp}(i-1)} > 1, \qquad K_{Tilt}(1) = \left|\frac{\delta_{Temp}(i)}{\delta_{Temp}(i-1)}\right|^{\alpha};$$

$$\text{If} \quad 0 < \frac{ERR_{Temp}(i)}{ERR_{Temp}(i-1)} < 1, K_{Tilt}(1) = \left|\frac{\delta_{Temp}(i-1)}{\delta_{Temp}(i)}\right|^{\alpha};$$

$$\text{If} \quad \frac{\delta_{Temp}(i)}{\delta_{Temp}(i-1)} > 0 \quad \&\& \quad \left|\frac{\delta_{Temp}(i)}{\delta_{Temp}(i-1)}\right| > 1$$

$$\text{If} \quad \left|\frac{ERR_{Temp}(i)}{ERR_{Temp}(i-1)}\right| > 1, \quad K_{Tilt}(1) = \left|\frac{\delta_{Temp}(i)}{\delta_{Temp}(i-1)}\right|^{\alpha};$$

$$\text{If} \quad \left|\frac{ERR_{Temp}(i)}{ERR_{Temp}(i-1)}\right| < 1, \quad K_{Tilt}(1) = \left|\frac{\delta_{Temp}(i-1)}{\delta_{Temp}(i)}\right|^{\alpha};$$

$$\text{Else} \quad K_{Tilt}(1) = 1$$

With the output scale factors and adjustment steps, final tilt angle adjustment Δ_{tilt} and plunge depth adjustment Δ_{plunge} from the fuzzy controller are given:

$$\Delta_{tilt} = Fuzzyout_{tilt} \times Kout_{Tilt} \times 1 \quad (^{\circ}) \qquad (11)$$

$$\Delta_{plunge} = Fuzzyout_{plunge} \times Kout_{Plunge} \times 0.2 \ (mm) \qquad (12)$$

3.4 Fuzzy rule generation

The rule base for the initial fuzzy controller was on-line generated using signals of control variables and the trained neural network. The on-line generation of fuzzy rules are described in following procedure (Lau et al. 2001).

NN mapping. With new inputs of torque, temperature, Fz, feed rate and spindle speed, the trained NN generates instant tilt angle and plunge depth. Examples shown in Table 3 are reference and instant value of tilt angle and plunge depth derived from reference NN inputs and on-line NN inputs respectively.

Table 3 On-line sensor signal and reference values; instant process parameters and preset value

Sensor signal & process parameter		*Reference value*	*On-line value*
NN INPUTS	Torque	20.33	15
	Temperature	275.20	235
	Fz (KN)	1.74	2.2
	Feed	100	100
	Speed	600	600
NN OUTPUTS	Tilt	0.5	1.6390
	Plunge	0.2	0.1300

The difference between reference value and on-line value of both NN inputs and outputs suggests that the deviation of tilt angle and plunge depth from reference value cause the deviation of torque, temperature, and Fz from reference value.

Fuzzify inputs. Errors of the three control variables to their reference value are normalized into [-1 1] with equations (4), (5) and (6) as crisp value of fuzzy inputs. Using the example data in Table 3, error of control variable to its reference value and the normalized crisp value is given in Table 4:

Table 4 control variable error and normalized value

Control variable	*Temperature*	*Temperature /Fz*	*Torque/Fz*
Reference value	275.20	158.16	11.68
On-line value	235	106.82	6.82
Error	40.20	51.34	4.86
Crisp input value	0.3991	0.4783	0.9609
Fuzzy input MFs	PS, PM	PM, PL	PL, PX

Each crisp input value is then fuzzified by mapping it into the predefined fuzzy input membership functions to acquire the name and value of the membership function it falls in. Fig. 6 shows the fuzzified membership function names and value for temperature error: *PS* (0.0045) and *PM* (0.9964). The names of fuzzy membership functions for the three crisp input values can be seen in Table 4.

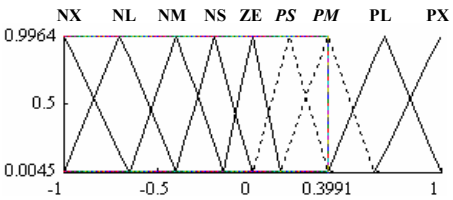

Fig. 6. Membership function name and value of Error of temperature fuzzified input.

Fuzzify output Using the example data in Table 3 and the normalizing algorithm, the errors of tilt angle and plunge depth to their reference values and their normalized crisp values are given in Table 5.

Table 5 Error and normalized value of tilt angle and plunge depth

Process parameter	*Tilt angle*	*Plunge depth*
Reference value	0.5	0.2
On-line value	1.6390	0.1300
Error	-1.139	0.07
Crisp output value	-0.76	0.70
Fuzzy output MFs	NX, NL	PL, PX

Each normalized crisp output value is fuzzified with predefined output MFs. Fig. 7 shows the fuzzifed membership function name and value of tilt angle adjustment. The fuzzified membership function names of the two outputs can be seen in Table 5.

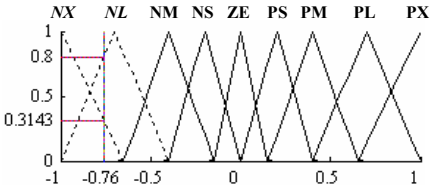

Fig. 7. Tilt angle adjustment fuzzified output

Rule generating. The fuzzified membership function names from previous steps for inputs and outputs are used as fuzzy rule antecedents and consequents, respectively. Fuzzy rule antecedents and consequents from the example data are shown in Table 6.

Table 6 Fuzzy rule antecedents and consequents

Fuzzy rule Antecedents & consequents		*Membership function*
ANTECEDENTS	Temperature error	*PS, PM*
	Temperature/Fz error	*PM, PL*
	Torque/Fz error	*PL, PX*
CONSEQUENTS	Tilt angle adjustment	*NX, NL*
	Plunge depth adjustment	*PL, PX*

The 32 on-line fuzzy rules are thus generated from the full combination of the antecedents and consequents. Linguistic expression of rule 1 is given:

IF error of temperature is positive small (PS) && error of temperature/Fz is positive middle (PM) && error of torque/Fz is positive large (PL),
THEN tilt angle adjust is extra negative (NX) && plunge depth adjust is positive large (PL);

With this algorithm, when each set of on-line sensor data is fed back from the welding process, the rule generation module automatically generates the on-line 'if-then' rules for fuzzy inference.

4. SIMULATION RESULTS

To test the performance of the proposed neuro-fuzzy control scheme, a simulation model was built with MATLAB, SIMULINK, neural network and fuzzy logic toolboxes (The MathWorks, 2004c). An experiment of Al 6061 round tube (diameter 95mm and thickness 3mm) was carried out with process parameters: feed rate 100 mm/min, spindle speed 500 rpm, tilt angle 1°, and plunge depth 0.2mm. A simulation was conducted with the reference sensor value: torque 15 N.m, temperature 240 °C, and Fz 3.34 kN. The reference value was calculated from the multi-regression model with process parameters used in the experiment. Fig. 8 and 9 show the comparison of process parameters and sensor value between recorded experimental data and simulation results from the neuro-fuzzy controller.

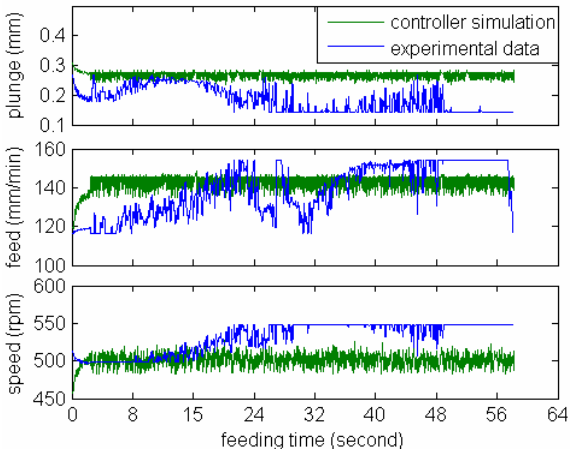

Fig.8. Comparison of process parameters between simulation results and experimental data.

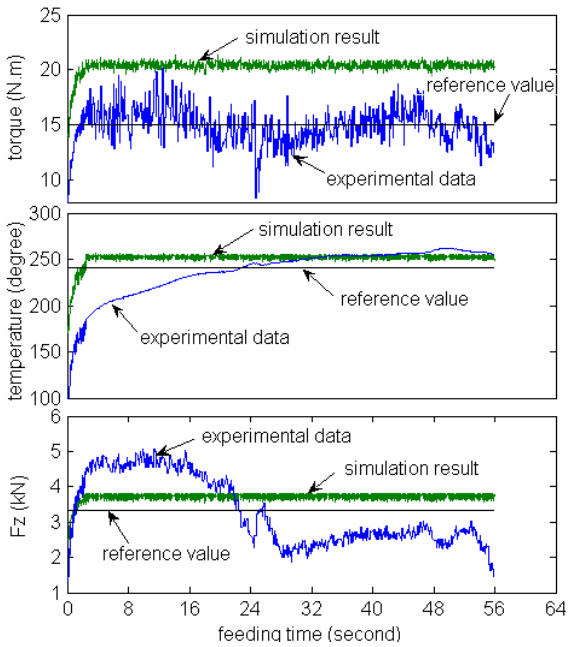

Fig. 9. Comparison of control variable status between simulation results and experimental data.

During the experiment and simulation, tilt angle was considered as constant as it changes very little during welding once the workpiece was firmly clamped. It can be observed in Fig.8 that all three parameters, which were derived from trained NN with recorded experimental sensor data, deviated from their preset value. This can be explained by the machining error of workpiece and fixture, which significantly influence the real plunge depth, and the fluctuation of the feed rate and spindle due to mechatronic error. Tool/workpiece contact was not well maintained due to plunge depth error. However, with the neuro-fuzzy controller, the three parameters were on-line adjusted according to the error of on-line sensor value to their

reference value. Therefore, the three process parameters were well controlled, and stable tool/workpiece contact condition was maintained.

From Fig. 9, it can be seen that torque, temperature and Fz of the experimental sample were not well controlled. The experimental sample was not actually welded with the expected perfect 'round' trajectory due to aforementioned reason for process parameter deviation. However, with the neuro-fuzzy controller, online sensor data of torque, temperature, and Fz were analyzed to find out the reason for the deviation of sensor data from their reference values, and corresponding process parameter adjustments were made to maintain correct tool/workpiece contact and energy input. The simulation results of temperature and Fz are maintained much better towards the reference level, while torque is almost 33% higher than the reference value. This possibly comes from the error of the NN model used in simulation. It can be expected that with more samples used in OA experiments, a more accurate NN model and better simulation results can be achieved.

5. CONCULSION

A neuro-fuzzy control scheme integrating NN and fuzzy logic algorithms for solving MIMO system has been presented in this paper. The implementation of the neuro-fuzzy control scheme for maintaining tool/workpiece contact during complex curvature FSW is demonstrated. Further research on improving NN training and configuring the control scheme for different curvature, material and tool is needed in order to enhance the feasibility of the scheme.

ACKNOWLEDGEMENTS

The authors wish to express their thanks to South African National Research Foundation for providing funding towards this research.

REFERENCE

Azouzi, R. and M. Guillot (1997). On-line prediction of surface finish and dimensional deviation in turning using neural network based sensor fusion. *Int. J. Mach. Tools Manufact*, **37**, 1201-1217.

Blignault, C. (2002). Design, development and analysis of the friction stir welding process. *Master Thesis*, Port Elizabeth Technikon.

Chen, C.M. and R. Kovacevic (2003). Finite element modeling of friction stir welding—thermal and thermomechanical analysis. *International Journal of Machine Tools & Manufacture,* **43**, 1319–1326.

Chen, C.M., R. Kovacevic and D. Jandgric (2003). Wavelet transform analysis of acoustic emission in monitoring friction stir welding of 6061 aluminum. *International Journal of Machine Tools & Manufacture,* **43**, 1383–1390.

Ericsson, M. and R. Sandstro¨m (2003). Influence of welding speed on the fatigue of friction stir welds and comparison with MIG and TIG. *International Journal of Fatigue,* **25**, 1379–1387.

James, M.N., D.G. Hattingh and G.R. Bradley (2003). Weld tool travel speed effects on fatigue life of friction stir welds in 5083 aluminium. *International journal of fatigue*, **25,** 1389-1398.

Khandkar, M.Z.H., J.A. Khan and A.P. Reynolds (2003). Prediction of temperature distribution and thermal history during friction stir welding: input torque based model. *Science and Technology of Welding and Joining*. **Vol. 8**, No. 3.

Kim, T.W. and J. Yuh (2002). Application of on-line neuro-fuzzy controller to AUVs. *Information Sciences*, **145**, 169–182.

Kruger, G. (2003). Intelligent monitoring and control system for a friction stir welding process. *Master Thesis*, Port Elizabeth Technikon.

Lau, H.C, T.T. Wong and A. Ning (2001). Incorporating machine intelligence in a parameter-based control system: a neural-fuzzy approach. *Artificial intelligence in engineering*, **15**, 253-264.

Liang, M., T. Yeap, A. Hermansyah and S. Rahmati (2003). Fuzzy control of spindle torque for industrial CNC machining. *International Journal of Machine Tools & Manufacture*, **43**, 1497–1508.

Liu, Y. and C. Wang (1999). Neural networks based adaptive control and optimization in milling process. *International Journal of Advanced Manufacturing Technology*, **15,** 791–795.

NAKATA, K., S. INOKI, Y. NAGANO, T. HASHIMOTO, S. JOHGAN, and M. USHIO (2001). Friction Stir Welding of AZ91D Thixomolded Sheet. *Proceedings of 3rd international friction stir welding symposium*, **Session 1**: Process Development 1.

Peel, M., A. Steuwer, M. Preuss and P.J. Withers (2003). Microstructure, mechanical properties and residual stresses as a function of welding speed in aluminium AA5083 friction stir welds. *Acta Materialia*. **51**, 4791–4801.

Reynolds, A.P., W. Tang, T. Gnaupel-Herold and H. Prask (2003). Structure, properties, and residual stress of 304L stainless steel friction stir welds, *Scripta Materialia*, **48**, 1289–1294.

Ross, P.J. (1988). Taguchi Techniques for Quality Engineering. McGraw-Hill New York.

Sun Z.Q and Z.D. Deng (1996). A fuzzy neural network and its application to controls. *Artificial intelligence in engineering*, **10**, 311-315.

The MathWorks (2004a). Fuzzy Logic Toolbox User's Guide. *The MathWorks Inc,* Natick, MA.

The MathWorks (2004b). Neural Network Toolbox User's Guide. *The MathWorks Inc,* Natick, MA.

The MathWorks (2004c). Simulink: Simulation and Model-Based Design. *The MathWorks Inc,* Natick, MA.

Thomas W. M., E.D. Nicholas, J.C. Needham and M.G. Murch, Temple, P. Smith and Dawes (TWI) (1991). Improvements relating to friction welding. *European Patent specification,* **0 615 480**, B1.

Experimental Implementation of Complex Curvature Friction Stir Welding

T.I. van Niekerk[1], T. Hua[2] and D.G. Hattingh[1]

This paper presents the experimental set-up for complex curvature friction stir welding. By adding an extra rotation axis to the existing three translation axes and clamping system, a table-tilting multi-axis system was implemented to perform complex curvature friction stir welding. Orthogonal array experiments and statistical analyses were carried out to investigate the relationship between sensor data, process parameters and process conditions with multi-sensor and telemetry system.

NOMENCLATURE

ANOVA	Analysis of variance
FSW	Friction stir welding
OA	Orthogonal array

Introduction

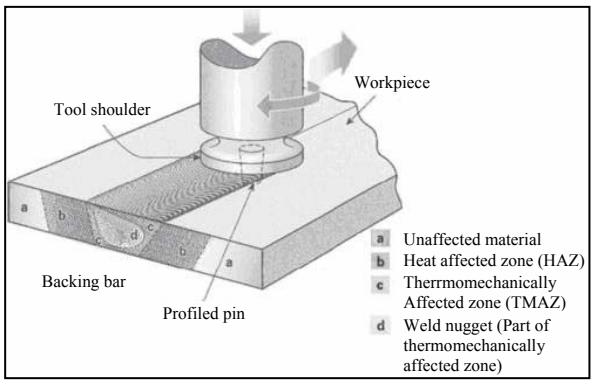

Figure 1: Process of Friction Stir Welding.

Friction Stir Welding (FSW) is a joining technique developed by TWI in 1991[1]. In FSW, a cylindrical tool consisting of a profiled pin under a wider shoulder rotates about its own axis and the pin is slowly plunged into the joint of the workpieces. Material in the joint is plasticized by frictional heating between the tool and the workpieces. The welding tool moves along the weld joint when the material has been sufficiently plasticized. The plasticized material is transported about the rotating pin and is pressed together, forming a solid joint on cooling. The tool is extracted from the workpieces when required weld length is finished. The process schematic of FSW is shown in Figure 1.

Currently, the research of monitoring and control of FSW is mainly focused on straight welds. Effects of process parameters such as feed rate, spindle speed and tool size on fatigue life, tensile strength, weld crack and residual stress of FSW have been presented by many researchers[2,3,4,5]. Except for process parameters, process conditions such as workpiece curvature also play a critical role in weld quality during complex curvature FSW. This paper describes the experimental setup for complex curvature FSW and the investigation of the relationship between sensor data, process parameters and process conditions.

Complex curvature FSW

Due to the hardware limitation of the existing FSW machine, the complex curvature in this project is defined as the connection of a series of simple curvatures such as straight line and circular arc, as shown in Figure 2.

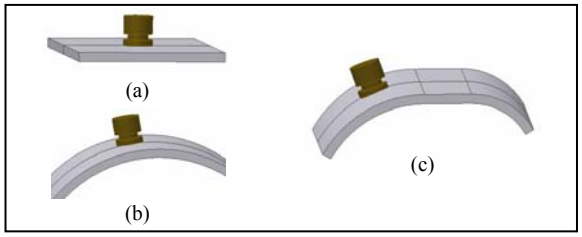

Figure 2: Workpieces curvature: (a) straight line, (b) circular arc, and (c) complex curvature.

[1]Professor, Manufacturing Technology Research Centre, Faculty of Engineering, the Built Environment and Information Technology, Nelson Mandela Metropolitan University, Private Bag X6011, Port Elizabeth, South Africa.
[2]Faculty of Engineering, Nelson Mandela Metropolitan University.

System setup

To perform complex curvature FSW, a multi-axis or robotic system is needed to provide mechanical stiffness and precise orientation/position control. Multi-axis is preferred due to the large force involved in the welding process for complex curvature workpieces[6]. Therefore, an extra rotation axis was added to the existing three translation axes to form a table-tilting multi-axis system. A Renold motor with rating power 0.37kw and full speed 1390rpm was used to provide output torque. Siemens Micromaster 440 inverter and CoreTech DRS 1440 incremental encoder were used to control motor operation and provide feedback from the motor. Workpiece fixture was also designed for locating and holding the workpieces to bear the large involved force. Figure 2 shows the multi-axis FSW machine used in this project.

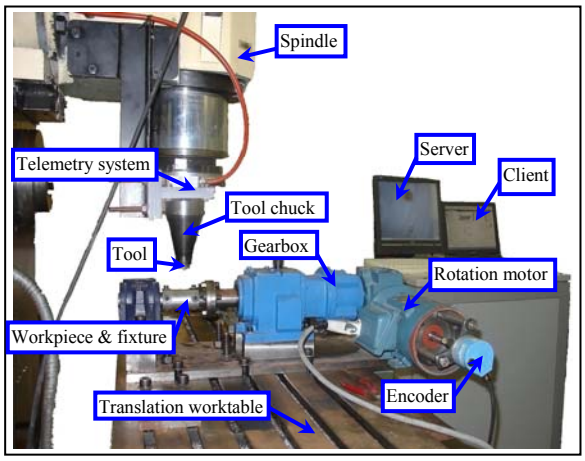

Figure 3: FSW machine with additional rotation axis implemented for this project

Experiment results and discussion

Experiments of aluminium flat plates and round tubes were conducted to acquire sensor data with the telemetry system. Different process conditions and various process parameters were used in the experiments to record on-line sensor data of bending force, torque, Fz and temperature. Figure 4 shows the welding cause-effect diagram.

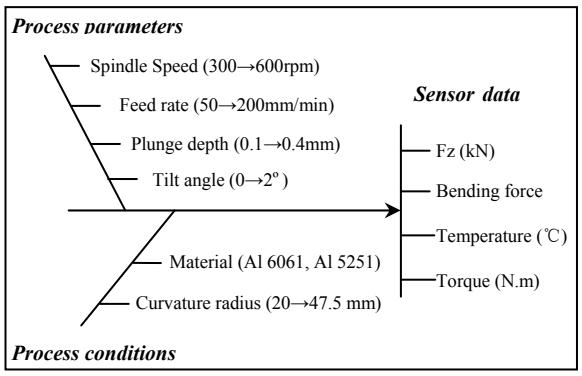

Figure 4: Cause-effect diagram of FSW

Orthogonal array experiment

Orthogonal arrays (OAs) developed by Taguchi was used in experiment design due to its capabilities of minimizing test number and representing all factors equally[7]. L16_4_5 and L18_3_7 OA experiments were chosen for FSW of flat plates (Al 5251 and Al 6061) and round tubes (Al 6061) respectively. The factor-level table for flat plate and round tube FSW is shown in Table 1.

Table 1: Factor-level table for FSW experiment

Factor & level		Feed (mm/min)	Speed (rpm)	Tilt (°)	Plunge (mm)	Diameter (mm)
Flat	Level 1	50	300	0	0.1	
	Level 2	100	400	0.5	0.2	
	Level 3	150	500	1	0.3	
	Level 4	200	600	2	0.4	
Round	Level 1	50	400	0	0.1	40
	Level 2	100	500	1	0.2	70
	Level 3	200	600	2	0.4	95

Figure 5 shows the experimental samples welded at NMMU.

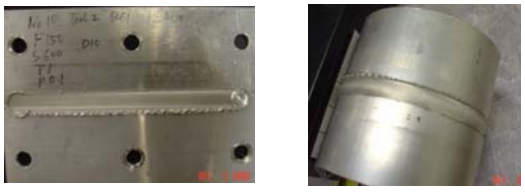

(a) Flat plate (b) Round tube

Figure 5: Aluminium flat plate and round tube welded at NMMU

Average effect of factor level

In OA experiment, effects of experiment factors and their levels on state variable measurements are calculated as the average of all observations under that factor level.

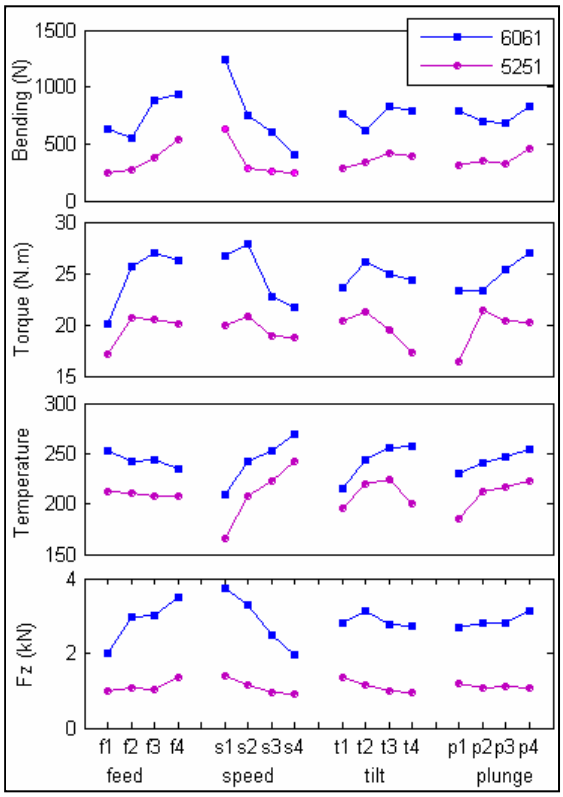

Figure 6: Effects of process parameters on sensor measurements of flat plate FSW

Figure 6 shows the average effect of each factor level on sensor measurements with the data obtained from 3 mm Al 6061 and Al 5251 flat plate welds. It can be concluded that all the sensor data are affected at different degrees by each process parameter. Temperature seems to be more sensitive to process parameter changes. In the process parameters, spindle speed seems to have stronger influence on sensor data than the other parameters. It also shows that for Al 6061 and Al 5251 alloy, most of the sensor measurements have the same changing trend with process parameter changes, while the averages bending force, torque, temperature and Fz from each factor level of Al 5251 alloy are significantly lower than Al 6061 alloy. This can be explained by their mechanical properties: Al 5251 is a softer material with better formability, thus lower force is caused during welding using the same process parameters, while Al 6061 has better thermal conductivity. More heat is propagated from tool/workpiece contact area to the area to be welded whilst higher temperature is generated.

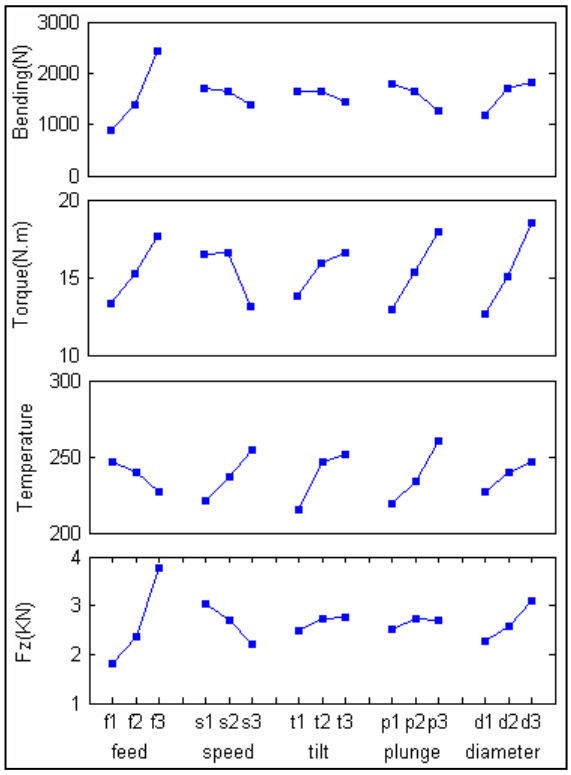

Figure 7: Effects of process parameters on sensor measurements of round tube friction stir welds

Figure 7 shows the average effect of each factor level on sensor measurements with the data from 3 mm Al 6061 round tube welding. From the figure, it can be concluded that besides process parameters of feed, speed, tilt and plunge, the process condition of curvature radius also significantly affects sensor data. It also shows that temperature and all the forces increase with curvature diameter. This can be explained by the tool/workpiece contact condition: with smaller curvature radius, less tool/workpiece contact is obtained, and thus less force and

temperature are generated due to less friction between tool and workpieces during welding.

Variance percentage contribution

The percentage contribution, which reflects the portion of the total variation observed in the experiment attributed to a factor. A factor with higher percentage contribution to a state variable indicates that the state variable is more sensitive to that factor. The calculation of percentage contribution of a factor is given as[7]:

$$P_F = \frac{SS_F - V_e v_F}{SS_T} \times 100 \quad (1)$$

SSF and SST are given as:

$$SS_F = \sum_{i=1}^{K_F} \frac{Fi^2}{n_{Fi}} - \frac{T^2}{N} \quad (2)$$

$$SS_T = \sum_{i=1}^{N} y_i^2 - \frac{T^2}{N} \quad (3)$$

V_e is the variance due to the error and is given as:

$$V_e = \frac{SS_T - \sum_F SS_F}{N - 1 - \sum_F v_F} \quad (4)$$

Where v_F is degree of freedom; K_F is number of levels for the factor; n_{Fi} is number of observations under level i of the factor; T is sum of all observations; N is total number of observations; and Fi is sum of observations under ith level of factor.

Using analysis of variance (ANOVA) of the OA experiment, the percentage contribution of each factor to each state variable variance was calculated. Table 4.4 shows the percentage contribution of each process parameter (feed, speed, tilt and plunge) on sensor measurements of data collected from the OA experiments of Al 6061 and Al 5251 plate welds.

Table 2: Variance percentage contribution of Al6061 and Al5251 flat plate welds

Factors & percentage		Bending force	Torque	Temperature	Fz
Al6061	Feed	20.11%	38.50%	4.56%	35.05%
	Speed	69.46%	35.80%	55.05%	56.55%
	Tilt	4.29%	4.13%	30.85%	2.93%
	Plunge	2.93%	11.89%	8.75%	3.17%
	error	3.22%	9.68%	0.79%	2.29%
Al5251	Feed	28.10%	20.27%	0.22%	25.86%
	Speed	56.23%	6.41%	64.74%	38.06%
	Tilt	5.57%	21.69%	12.22%	31.81%
	Plunge	7.19%	34.77%	16.39%	2.06%
	error	2.91%	16.86%	6.42%	2.20%

Table 3 shows the percentage contribution of process parameters (feed, speed, tilt and plunge) and process condition (curvature) on sensor measurements from the data of Al6061 round tube welds.

Table 3: Variance percentage contribution of Al6061 round tube welds

Factors & percentage	Bending force	Torque	Temperature	Fz
Feed	71.42%	16.61%	7.79%	68.52%
Speed	3.18%	13.69%	21.09%	11.34%
Tilt	1.58%	7.76%	30.16%	1.57%
Plunge	8.24%	22.67%	33.08%	0.89%
Curvature	14.10%	30.88%	7.38%	12.07%
error	1.48%	8.39%	0.50%	5.61%

It can be seen from Table 2 and Table 3 that temperature is the most sensitive signal to spindle speed, tilt angle, and plunge depth. Fz has a higher sensitivity to feed and speed than plunge and tilt. Torque is more sensitive to plunge depth and tilt angle than the other sensor signals. Both the flat plate and round tube experimental data show that the error contributions associated with sensor signals are acceptable (less than 8%). This implies that the most important process conditions and parameters that influence these characteristics were included in the experiment[8].

Correlation analysis

Correlation coefficient, a normalized measure of the strength of the linear relationship between two variables, is used in this study to investigate the dependency of a sensor signal on a process parameter[9]. The correlation efficient *r(x, y)* of variable *y* to variable *x* is calculated as:

$$r(x,y) = \frac{\sum (x_i - \bar{x})(y_i - \bar{y})}{\sqrt{\sum (x_i - \bar{x})^2}\sqrt{\sum (y_i - \bar{y})^2}} \qquad (5)$$

Where x_i is the *i*th element of variable x; $\bar{x}$ is the mean value of variable x; y_i is the *i*th element of variable y; and $\bar{y}$ is the mean value of variable y.

Table 4 shows the correlation coefficients of sensor measurements to process parameters of Al6061 and Al5251 flat plate welds. It shows that all sensor measurements have high correlation to feed and speed; while torque and temperature show higher correlation to plunge and tilt than the other two sensor measurements.

Table 4: Correlation coefficients of sensor measurements to process parameters

Correlation coefficient		*Bending force*	*torque*	*temperature*	*Fz*
feed	Al6061	0.3875	0.5084	-0.1984	0.5512
	Al5251	0.5117	0.3002	-0.0453	0.4164
speed	Al6061	-0.7994	-0.5234	0.7202	-0.7471
	Al5251	-0.6244	-0.1895	0.7794	-0.5878
tilt	Al6061	-0.0596	-0.0623	-0.5382	0.0479
	Al5251	-0.2076	0.3343	-0.1160	0.5580
plunge	Al6061	0.0315	0.3279	0.2932	0.1582
	Al5251	0.2127	0.3629	0.3707	-0.1135

Conclusion

A table-tilting multi-axis system consisting of three translational axes and one rotation axis was implemented to perform complex curvature FSW. Process parameters (feed, speed, tilt and plunge) and process condition (material and curvature) were used as experiment factors in OA experiments to acquire sensor measurements (force, torque and tool temperature) with multi-sensor and telemetry system. The average effect and variance percentage contribution of each factor level on sensor measurements were analysed. Correlations of sensor measurements to process parameters were also used to investigate the relationship between process parameters, process conditions and sensor data during complex curvature FSW. Further research on sensor fusion and intelligent process control is needed in order to establish the on-line monitoring and control system for the nonlinear process of complex curvature FSW.

Acknowledgements

The authors wish to express their thanks to South African National Research Foundation for providing funding towards this research.

Reference

1. Thomas, W.M., E.D. Nicholas, J.C. Needham, M.G. Murch, P. Templesmith and C.J. Dawes (1991). Friction stir butt welding. International patent application no. PCT/GB92/02203 and GB patent application no. 9125978.8, 6,0 December.

2. James, M.N., D.G. Hattingh and G.R. Bradley (2003). Weld tool travel speed effects on fatigue life of friction stir welds in 5083 aluminium. International journal of fatigue, ***25,*** *1389-1398.*

3. Reynolds, A.P., W. Tang, T. Gnaupel-Herold and H. Prask (2003). Structure, properties, and residual stress of 304L stainless steel friction stir welds, Scripta Materialia, ***48****, 1289–1294.*

4. NAKATA, K., S. INOKI, Y. NAGANO, T. HASHIMOTO, S. JOHGAN, and M. USHIO (2001). Friction Stir Welding of AZ91D Thixomolded Sheet. Proceedings of 3rd international friction stir welding symposium, ***Session 1****: Process Development 1.*

5. Ericsson, M. and R. Sandstro¨m (2003). Influence of welding speed on the fatigue of friction stir welds

and comparison with MIG and TIG. International Journal of Fatigue, ***25****, 1379–1387.*

6. Satoshi, H., O. Kazutaka, A. Kinya, O. Hisanori, A. Yasuhisa and O. Tomio (2001). Development of 3 dimensional type friction stir welding equipment. 3rd International Symposium on Friction Stir Welding, Kobe Exhibition Hall, Kobe, Japan, 27&28 September.

7. Ross, P.J. (1995). Taguchi Techniques for Quality Engineering. ISBN 0070539588, McGraw-Hill, 2 Edition, New York.

8. Azouzi, R. and M. Guillot (1997). On-line prediction of surface finish and dimensional deviation in turning using neural network based sensor fusion. Int. Journal of Machine Tools and Manufacture, 37, 1201-1217.

9. The MathWorks (2004). MATLAB: The Language of Technical Computing, version 7.

Monitoring and intelligent control for complex curvature friction stir welding

T.I. van Niekerk[1*], T. Hua[1] and D.G. Hattingh[1]

[1]Faculty of Engineering, the Built Environment and Information Technology, Nelson Mandela Metropolitan University, Port Elizabeth, South Africa

Abstract: This paper presents the implementation of sensor fusion and intelligent control for multi-input-multi-output process. Based on the telemetry sensory system, orthogonal array experiments and statistical analysis were used to select sensitive sensor features as process control variables. Feed-forward back-propagation neural networks were used in sensor fusion to investigate the relationship between process parameters, process conditions and sensor data. A neuro-fuzzy control scheme consists of fuzzy logic controller with basic membership functions, on-line fuzzy rule generation module using trained neural networks, and an input/output scale factor tuning system used to improve output response to process changes. To validate the performance and feasibility of the neuro-fuzzy controller, simulations of FSW for workpieces with changing material and curvature were conducted. The simulation results show that the control variables were well maintained within limited ranges from reference values. The proposed neuro-fuzzy control scheme also exhibits good adaptability to process condition changes such as workpiece material and curvature changes.

Keywords

Friction stir welding, neural network, fuzzy logic, on-line monitoring, intelligent control

1 INTRODUCTION

Friction Stir Welding (FSW) is a joining technique developed by TWI in 1991[1]. In FSW, a cylindrical tool consisting of a profiled pin under a wider shoulder rotates about its own axis and the pin is slowly plunged into the joint of the workpieces. Material in the joint is plasticized by frictional heating between the tool and the workpieces. The welding tool moves along the weld joint when the material has been sufficiently plasticized. The plasticized material is transported about the rotating pin and is pressed together, forming a solid joint on cooling. The tool is extracted from the workpieces when required weld length is finished. The process schematic of FSW is shown in Fig. 1.

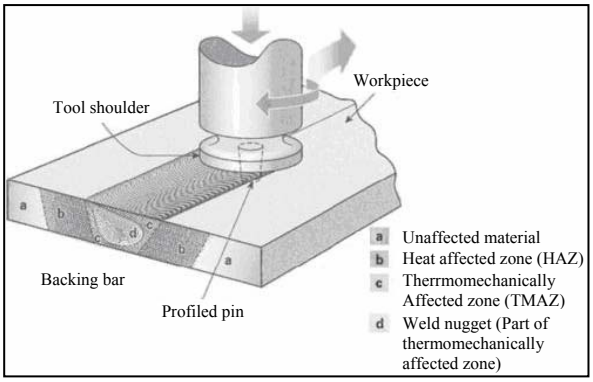

Figure 1: Process of friction stir welding

Corresponding author: Faculty of Engineering, the Built Environment and Information Technology, Nelson Mandela Metropolitan University, Private Bag X6011, Port Elizabeth, South Africa.

A broad spectrum of on-line sensors, signal processing schemes and various model-based calculations have been proposed to retrieve information relevant to machining process conditions. Sensor signals such as force, torque, temperature, power and vibrations etc., have been successfully applied in indirect sensing[2, 3, 4]. Sensor fusion is a method of integrating signals from multiple sources to provide a robust prediction of one or more machining attributes with a fusion model[5, 6]. Sensor fusion mainly consists of two components: selecting sensitive signals as good candidates and establishing proper relationships between the sensed variables and the investigated features[4]. An exhaustive analysis with statistical tools to determine the most sensitive process parameters and sensor signals for predicting the surface roughness and diameter error in machining was presented by Azouzi and Guillot[4]. Various techniques such as multiple regression, the group method of data handling or neural networks are implemented in building sensor fusion models[3, 4].

Fuzzy logic is an ideal tool for multi-input-multi-output (MIMO) process control due to its tolerance of imprecise data and ability to model nonlinear functions of arbitrary complexity[7]. Liang[8] et al. presented a tuning mechanism, including an input scale factor tuned with the integration of torque error and an output scale factor tuned by the change of torque error, to strengthen or weaken the fuzzy control of CNC machine spindle torque by adjusting spindle speed and feed rate. The fuzzy rules of most fuzzy controllers are set based on past experience. However, when facing a complex MIMO process involving nonlinear relationship between inputs and outputs, a more efficient fuzzy rule generating

method is needed. Neural network (NN), which has the ability to learn relationships among input and output data sets through a training process, is able to 'induce' output data if a new set of input data is made available[9]. This can be utilized to solve the 'bottleneck' problem of fuzzy rule extracting. Sun and Deng[10] presented a fuzzy NN control structure which is composed of an antecedent NN to match fuzzy rule premises, and a consequent NN to implement fuzzy rule consequences. Lau[11] et al. proposed an integrated neural-fuzzy model using NN to generate 'If-Then' fuzzy rule.

The MIMO and nonlinear FSW process makes the intelligent technologies fuzzy logic and NN feasible monitoring and control strategies. A systematic multi-sensor fusion method and neuro-fuzzy control scheme for complex curvature FSW is presented in this paper.

2 EXPERIMENTAL SETUP

(a)

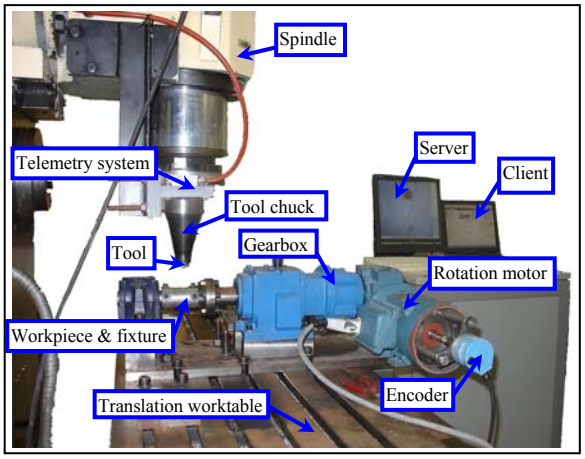

(b)

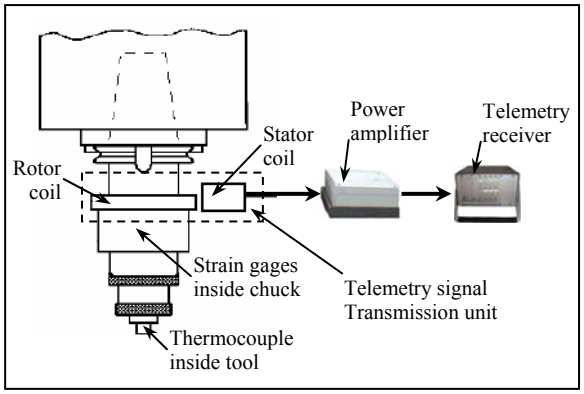

Fig. 2 Experimental setup for FSW: (a) multi-axis system; (b) telemetry sensory system

The FSW machine was converted from a conventional 3-axis milling machine. Three translational axes for bed movements, one spindle axis for tool rotation and one rotational axis (R) for workpieces rotation were driven by three-phase induction motors. Clamping system was designed for orientating and locating the workpieces on the machine worktable. Strain gauges and thermocouple were fitted on the chuck and tool to detect horizontal forces, vertical force, torque exerted on the tool and the tool's pin temperature. Electrical power is transferred to the chuck using induction and the sampled data is sent off the chuck in digital form using a capacitive technique with the annular stator coil and pickup rotor coil. The telemetry receiver receives the transmitted measurement data, demodulates the signals and outputs filtered and amplified signals. The signals and from telemetry system and encoders were connected to computer through PCI730 data acquisition card[12, 13]. Fig. 2 shows experimental setup of the multi-axis FSW machine and telemetry sensory system.

Based on the FSW system, experiments of aluminium flat plates and round tubes of different curvature were conducted to acquire sufficient information for sensitive feature selection and sensor fusion. Efficient experimental method Orthogonal arrays (OAs) developed by Taguchi was chosen to minimize the number of tests[14]. Under different process conditions (material and curvature), various process parameters (feed rate, spindle speed, plunge depth and tilt angle) were used to record on-line sensor data of torque, bending force, Fz and temperature. L16_4_5 and L18_3_7 OA experiments were chosen for flat plates of Al5251 and Al6061 and round tubes of Al6061 respectively. Fig. 3 shows the welding cause-effect diagram with factor-level range of process parameters and conditions.

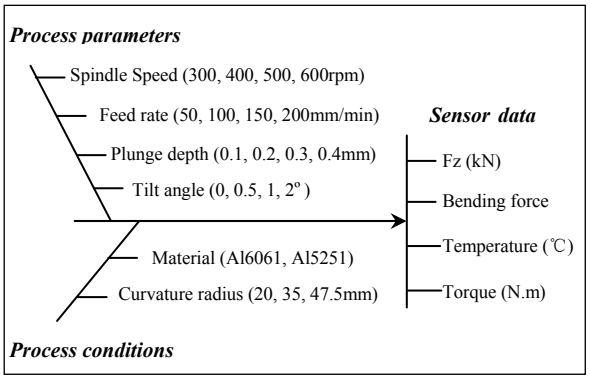

Fig.3 Cause-effect diagram and factor levels

3 SENSOR FUSION

This section describes the statistical analysis and NN modelling used to select sensors and build a fusion model for on-line monitoring of complex curvature FSW.

3.1 Statistical analysis

Data from OA experiments were analysed with statistical method to investigate relationships between process parameter and sensor data. Correlation coefficient, a normalized measure of the strength of the linear relationship between two variables, was used to investigate the dependency of a sensor signal, or the ratio of two sensor signals, on a process parameter[15]. The correlation efficient $r(x, y)$ of variable y to variable x is calculated as:

Table 1 Correlation coefficients of sensor signals to process parameters of Al6061 and Al5251 flat plate welds

material	Al6061						Al5251					
Correlation coefficient	***Co_tilt***	***Co_plunge***	***Absolute sum***	***Co_feed***	***Co_speed***	***Absolute sum***	***Co_tilt***	***Co_plunge***	***Absolute sum***	***Co_feed***	***Co_speed***	***Absolute sum***
bending force (N)	-0.0596	0.0315	0.0911	0.3875	-0.7994	1.1869	-0.2076	0.2127	0.4203	0.5117	-0.6244	**1.1361**
torque (Nm)	-0.0623	0.3279	0.3902	0.5084	-0.5234	1.0318	0.3343	0.3629	**0.6972**	0.3002	-0.1895	0.4897
temperature (˚C)	-0.5382	0.2932	**0.8314**	-0.1984	0.7202	0.9186	-0.1160	0.3707	0.4867	-0.0453	0.7794	0.8247
Fz (kN)	0.0479	0.1582	0.2061	0.5512	-0.7471	**1.2983**	0.5580	-0.1135	0.6715	0.4164	-0.5878	1.0042
bending/torque	0.0974	-0.1559	0.2533	0.1506	-0.6877	0.8383	-0.2106	0.0787	0.2893	0.4179	-0.6241	1.0420
bending/temperature	0.0728	-0.0772	0.1500	0.2787	-0.8179	1.0966	-0.1361	0.0453	0.1814	0.3842	-0.7285	**1.1127**
bending/Fz	-0.0350	-0.0421	0.0771	-0.0865	-0.4362	0.5227	-0.4835	0.3743	**0.8578**	0.3535	-0.4079	0.7614
temperature/torque	-0.2789	0.0400	0.3189	-0.5024	0.7109	**1.2133**	-0.3998	0.0864	0.4862	-0.3089	0.7789	1.0878
temperature/Fz	-0.3322	0.1486	**0.4808**	-0.5208	0.6870	1.2078	-0.4277	0.2437	0.6714	-0.4352	0.6874	**1.1226**
torque/Fz	-0.3074	0.1546	**0.4620**	-0.4966	0.7180	**1.2146**	-0.3679	0.3266	**0.6945**	-0.3898	0.5396	0.9294

$$r(x,y)=\frac{\sum(x_i-\bar{x})(y_i-\bar{y})}{\sqrt{\sum(x_i-\bar{x})^2}\sqrt{\sum(y_i-\bar{y})^2}} \quad (1)$$

Where x_i is the ith element of variable x; $\bar{x}$ is the mean value of variable x; y_i is the ith element of variable y; and $\bar{y}$ is the mean value of variable y.

Table 1 shows the correlation coefficients of sensor data to process parameters for Al6061 and Al5251 flat plate welds. It can be seen that sensor signals of temperature, the ratio of temperature to Fz, and the ratio of torque to Fz, have larger correlation coefficients to tilt angle and plunge depth for Al6061 welds. Therefore, they were chosen as the control variables for tool/workpiece contact condition, which is dominated by tilt angle and plunge depth, for Al6061 flat welds. Fz, the ratio of temperature to torque, and the ratio of torque to Fz were chosen as control variables of tool/workpiece energy input, which is dominated by feed rate and spindle speed, for Al6061 flat plate as they have larger absolute sum of correlation coefficients to feed rate and spindle speed. Similarly, Torque, the ratio of bending force to Fz, and the ratio of torque to Fz have the larger correlation coefficient absolute sum to tilt angle and plunge depth, and were thus chosen as the control variables for tool/workpiece contact of Al 5251 flat weld. It can also be seen that bending force, the ratio of bending force to temperature, and the ratio of temperature to Fz, have larger correlation coefficient absolute sum to feed and speed, and were thus selected as control variables for tool/workpiece energy input for Al5251 flat plate welds.

To develop an intelligent monitoring and control system for complex curvature FSW, relationships between sensor signals and different workpiece curvature radii is required to be investigated. Table 2 shows the correlation coefficients of process parameters and process condition curvature diameter to sensor signals of different diameter Al 6061 alloy round tube welds. It can be seen that torque and temperature were chosen as control variables for tool/workpiece contact, while bending force and Fz were selected as control variables for tool/workpiece energy input. The detailed description of tool/workpiece contact and energy input control is described in the following section.

3.2 Multi-sensor modelling

To establish the relationship between sensed variables and the investigated features, two distinct methods were used: theoretical and empirical. Theoretical techniques normally include a great deal of simplification because of the poor understanding of fundamental behavior of machining processes, which makes them difficult to implement in real

Table 2 Correlation coefficients of sensor signals to process parameters of Al 6061 flat plate and Al 6061 round tube

experiment	***Sensor signal***	***Co_tilt***	***Co_plunge***	***Absolute sum***	***Co_feed***	***Co_speed***	***Absolute sum***	***Co_curvature***
6061 tube	bending force (N)	0.16	-0.24	0.40	0.72	-0.22	**0.940**	**0.40**
	torque (Nm)	-0.22	0.41	**0.63**	0.38	-0.32	0.70	**0.47**
	temperature (˚C)	-0.51	0.52	**1.03**	-0.28	0.48	0.76	0.27
	Fz (kN)	-0.05	0.03	0.08	0.73	-0.38	**1.11**	0.35
6061 plate & tube	bending force (N)	0.11	-0.17	0.28	0.47	-0.15	0.62	**0.30**
	torque (Nm)	-0.13	0.28	**0.41**	0.33	-0.45	0.78	**-0.75**
	temperature (˚C)	-0.52	0.42	**0.94**	-0.24	0.56	**0.80**	-0.17
	Fz (kN)	-0.02	0.09	0.11	0.66	-0.55	**1.21**	-0.26

industrial environments. Empirical modelling uses experimental work to evaluate process performance[16, 17]. NN was chosen to perform sensor modelling owing to its ability to learn relationships among input and output data sets through a training process.

NN training for curvature detection In complex curvature FSW, process parameters of feed rate, spindle speed, tilt angle and plunge depth cooperate with workpiece curvature to determine the condition of tool/workpiece contact and energy input. To make correct decisions for process parameter adjustment, the changing of workpiece curvature radius needs to be detected from on-line sensor data. Using the data obtained in previous Al 6061 flat plate and round tube experiments, a 6-9-1 feed-forward back-propagation NN with 6 inputs (torque, temperature, Fz, feed, speed, and plunge) and 1 output (workpiece curvature) was trained with the fast training method Levenberg-Marquardt algorithm. The 16 Al6061 flat plate welds and 18 round tube welds from the OA experiments, together with another five additional round tube welds were used as training and checking data. The comparison of NN outputs to experimental data is shown in Fig. 4. The training result showed that good performance was achieved with a mean sum of squares of network errors (MSE) value 0.0153772 after training 50 epochs.

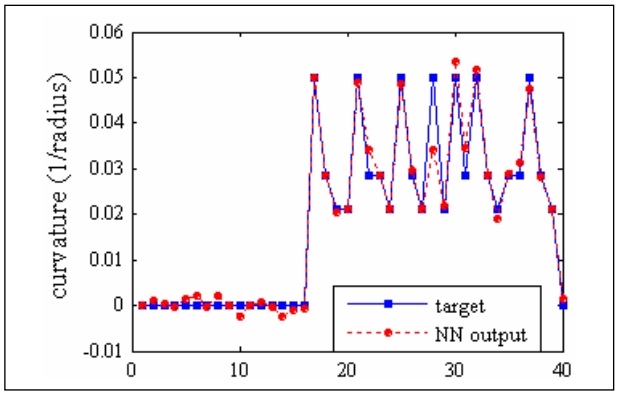

Fig. 4 NN output Vs target value for workpiece curvature

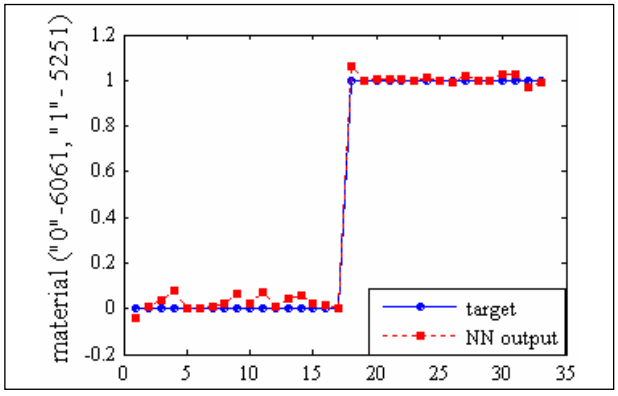

Fig. 5 NN output Vs target value for workpiece material

NN training for material detection When welding plates of different materials, different sensor data were obtained using the same process parameters. Thus the intelligent monitoring system must 'tell' what kind of material is being welded before making decision of process adjustments. In this study, the changing of material is limited in flat plates of Al 5251 and Al 6061 alloy. Using the data from the two OA experiment and additional test data, a 4-4-1 back-propagation NN with 4 inputs (tilt angle, plunge depth, torque and temperature) and 1 output (parent material) was trained with Levenberg-Marquardt algorithm. After training, the system can 'tell' whether the material being welded was '0' (for Al 6061 alloy) or '1' (for Al 5251 alloy). The training result shows good performance with MSE value 0.0874027 after 300 training epochs. The comparison of NN outputs to experimental data is shown in Fig. 5.

NN training for process parameter prediction To make control decisions with the detected parent material, workpiece curvature and on-line sensor data, a 4-9-4 NN with 4 inputs (curvature, torque, temperature and Fz) and 4 outputs (feed rate, spindle speed, tilt angle and plunge depth) was trained to map the relationship between sensor data, process condition and process parameters. Fig. 6 shows the comparison of NN outputs to experimental data of the trained NN for complex curvature FSW of Al 6061. The NN trained with the Levenberg-Marquardt algorithm training resulted in a MSE value of 0.0571601 after 200 training epochs. It can be used to derive instant process parameters given on-line sensor data and process conditions. The derived process parameters can be used for on-line fuzzy rule generating as described in following section.

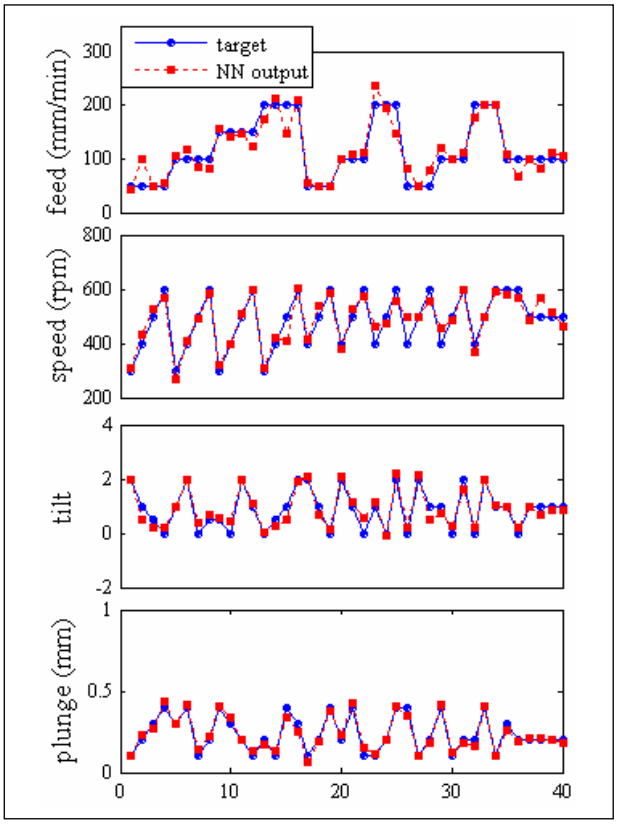

Fig. 6 Comparison of NN outputs to target values of process parameters

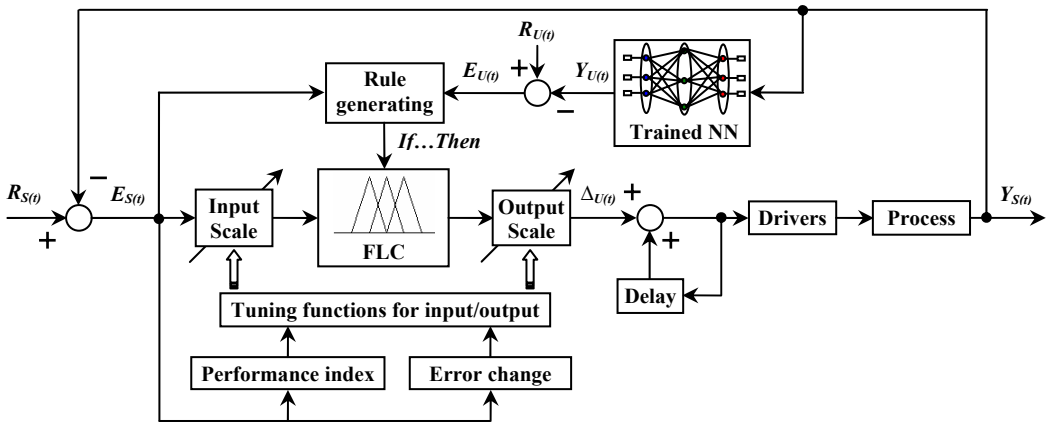

Fig. 7 Structure of the proposed neuro-fuzzy scheme for process control.

4 NEURAL-FUZZY PROCESS CONTROL

Fig. 7 shows the overall structure of the intelligent neuro-fuzzy control scheme for complex curvature FSW. Inputs $E_{S(t)}$ to the control system are the errors of on-line control variables $Y_{S(t)}$ to their reference value $R_{S(t)}$, and outputs from the control system are proposed process parameter adjustments $\Delta_{U(t)}$. The main part of the control scheme consists of a trained NN for deriving instant process parameters $Y_{U(t)}$, a rule-generating module for fuzzy rule generation using control variable errors $E_{S(t)}$ and process parameter errors $E_{U(t)}$ of derived instant value $Y_{U(t)}$ to preset value $R_{U(t)}$, an fuzzy controller with predefined input/output membership functions to generate primary command for process parameters adjustment, and a tuning module to strengthen or weaken control actions by tuning input and output scale factors in response of the dynamic process changing. The design details and simulation results are described in following sections.

The initial Mamdani type fuzzy controller consists of a fuzzifier, a fuzzy inference engine, a defuzzifier, and membership functions (MFs). The fuzzy rules were however not preset for the controller in this study. The on-line generating of fuzzy rules is described in Section 4.3.

4.1 Inputs and normalizing

Each of the three sensitive features selected in sensor fusion is compared to a reference value, and the error was used as an input to the fuzzy controller. At each sampling time *i*, the three errors were respectively calculated as:

$$ERR_{Temp}(i) = Temp_{ref} - Temp(i) \tag{2}$$

$$ERR_{Temp/Fz}(i) = \frac{Temp_{ref}}{Fz_{ref}} - \frac{Temp(i)}{Fz(i)} \tag{3}$$

$$ERR_{Torq/Fz}(i) = \frac{Torq_{ref}}{Fz_{ref}} - \frac{Torq(i)}{Fz(i)} \tag{4}$$

Each of the errors was normalized into [-1, 1] before fed into the controller by multiplying corresponding normalizing coefficient[8].

$$err_{Temp}(i) = ERR_{Temp}(i) \times K_{Temp}(i) \tag{5}$$

$$err_{Torq/Fz}(i) = ERR_{Torq/Fz}(i) \times K_{Torq/Fz}(i) \tag{6}$$

$$err_{Temp/Fz}(i) = ERR_{Temp/Fz}(i) \times K_{Temp/Fz}(i) \tag{7}$$

The input normalizing coefficient was separately considered in the zones above and below the reference value to ensure that both sides from the reference value (zero error point) have the same membership functions. The normalizing coefficient for temperature error was calculated as follows. The same rule was applied for the other inputs.

If $Temp(i) \geq Temp_{ref}$

$$K_{Temp}(i) = 1/(Temp_{\max} - Temp_{ref})$$

Else $K_{Temp}(i) = 1/(Temp_{ref} - Temp_{\min})$

Where $K_{Temp}(i)$ is temperature normalizing coefficient, $Temp_{max}$ maximum temperature, and $Temp_{min}$ minimum temperature.

All the inputs and outputs of the fuzzy controller use the same triangular membership function due to its computation efficiency. Each fuzzy input or output has nine MFs: NX (extra negative), NL (negative large), NM (negative middle), NS (negative small), ZE (zero error), PS (positive small), PM (positive middle), PL (positive large), and PX (extra positive). In order to regulate the system output to a desired output, more accurate control actions are taken near the reference value[18]. Therefore, finer fuzzy sets are placed near the reference value, that is to say, fuzzy values are dense when near zero but sparse when far from zero.

4.2 Tuning mechanism

Three parts of a fuzzy controller including membership functions, fuzzy rules and inputs/outputs can be tuned to make the fuzzy controller adaptable. In this study, the membership functions were predefined, and the fuzzy rules were generated on-line. Thus to enhance control actions,

fuzzy inputs and outputs were tuned with corresponding scale factors.

Performance index and input scale factors. Performance index was used to evaluate process quality using current and delayed control variable errors. The performance index of temperature was given as follows. The algorithm applied to the other two inputs.

$$Perform_{Temp}(i) = \sqrt{\frac{\Sigma_{i-2}^{i}(err_{Temp}(i))^2}{3}} \tag{8}$$

To adaptively strengthen or weaken control actions in response to on-line signals, the performance index was used for tuning input scale factor. The scale factor for temperature error was calculated as follows. The same algorithm applies to the other two fuzzy inputs[8].

$$Kin_{Temp}(i) = \left| \frac{Perform_{Temp}(i)}{\varepsilon_{Temp}} \right|^{0.16} \tag{9}$$

where ε_{Temp} is the bandwidth of tolerance zone, $Kin_{Temp}(i)$ temperature error scale factor at time i.

The final input of temperature error to the fuzzy controller was:

$$err_{Temp}(i) = err_{Temp}(i) \times Kin_{Temp}(i) \tag{10}$$

Output scale factors. Outputs from fuzzy controller are primary adjustments of tilt angle Δ_{tilt} and plunge depth Δ_{plunge}. Output scale factor for each output was calculated by taking into account the correlation coefficients of the three control variable to tilt angle and plunge depth. The algorithm for calculating scale factor of tilt angle adjustment was given:

$$Kout_{Tilt} = \sqrt{\frac{\Sigma_{i=1}^{3}(|Co_{Tilt}(i)| \times (K_{Tilt}(i))^2)}{\Sigma_{i=1}^{3}|Co_{Tilt}(i)|}} \tag{11}$$

The algorithm for calculating the output scale factor from the first fuzzy input temperature error is shown as follows[8]. The same rule applies to the other two fuzzy input temperature/Fz error and torque/Fz error.

If $\frac{\delta_{Temp}(i)}{\delta_{Temp}(i-1)} < 0$ && $\left|\frac{\delta_{Temp}(i)}{\delta_{Temp}(i-1)}\right| > 1$

If $\frac{ERR_{Temp}(i)}{ERR_{Temp}(i-1)} > 1$, $K_{Tilt}(1) = \left|\frac{\delta_{Temp}(i)}{\delta_{Temp}(i-1)}\right|^{\alpha}$;

If $0 < \frac{ERR_{Temp}(i)}{ERR_{Temp}(i-1)} < 1$, $K_{Tilt}(1) = \left|\frac{\delta_{Temp}(i-1)}{\delta_{Temp}(i)}\right|^{\alpha}$;

If $\frac{\delta_{Temp}(i)}{\delta_{Temp}(i-1)} > 0$ && $\left|\frac{\delta_{Temp}(i)}{\delta_{Temp}(i-1)}\right| > 1$

If $\left|\frac{ERR_{Temp}(i)}{ERR_{Temp}(i-1)}\right| > 1$, $K_{Tilt}(1) = \left|\frac{\delta_{Temp}(i)}{\delta_{Temp}(i-1)}\right|^{\alpha}$;

If $\left|\frac{ERR_{Temp}(i)}{ERR_{Temp}(i-1)}\right| < 1$, $K_{Tilt}(1) = \left|\frac{\delta_{Temp}(i-1)}{\delta_{Temp}(i)}\right|^{\alpha}$;

Else $K_{Tilt}(1) = 1$

Where,

$K_{Tilt}(1)$ Output scale factor for tilt angle from the first input temperature error.

α Constant in [-1 1]. In this study it was chosen as 0.1 through simulation.

$$\nabla_{Temp}(i) = ERR_{Temp}(i) - ERR_{Temp}(i-1) \tag{12}$$

$$\nabla_{Temp}(i-1) = ERR_{Temp}(i-1) - ERR_{Temp}(i-2) \tag{13}$$

With the output scale factors and adjustment steps, final tilt angle adjustment Δ_{tilt} and plunge depth adjustment Δ_{plunge} from the fuzzy controller are given:

$$\Delta_{tilt} = Fuzzyout_{tilt} \times Kout_{Tilt} \times 1 \quad (^{\circ}) \tag{14}$$

$$\Delta_{plunge} = Fuzzyout_{plunge} \times Kout_{Plunge} \times 0.2 \ (mm) \tag{15}$$

4.3 Fuzzy rule generation

The rule base for the initial fuzzy controller was on-line generated using signals of control variables and the trained neural network. The on-line generation of fuzzy rules are described in following procedure.

Recalling trained NN Technically, for FSW with the same process condition (material, curvature, tool, etc.), if the predefined process parameters are well maintained during welding, there should not be big changes in the sensor signal. In reality, there can be many reasons for process parameters and sensor signals changing. The trained NNs were used to detect process conditions and derive the instant process parameters from the on-line sensor signals, using the relationships established during training. With new inputs of bending force, torque, temperature and Fz, the process conditions can be detected first for FSW with changing process condition. Using the detected process condition, together with on-line sensor data, instant values of process parameters can be derived. Similarly, given reference values of sensor signals and original process conditions, the desired process parameters can be derived and used as preferred values at the start of the process. The preset and instant tilt angle, plunge depth, feed rate and spindle speed derived from

the NN with the original process conditions (material Al 6061) are shown in Table 3.

Table 3 On-line sensorgnal and reference values, instant process parameters and preset values

Sensor signal & process parameter		Reference value	On-line value
NN inputs	Bending force (N)	1070	980
	Torque (Nm)	27	20
	Temperature (°C)	230	200
	Fz (kN)	3.6	3
NN outputs	Feed rate (mm/min)	191.41	77.613
	Spindle Speed (rpm)	398.56	323.91
	Tilt angle (°)	0.55472	0.83998
	Plunge depth (mm)	0.17666	0.10163

The difference between on-line process parameters derived from NN and preferred process parameters suggests that the deviations of tilt angle, plunge depth, feed rate and spindle speed from their preferred values cause the deviation of sensor signals from their reference values. It also indicates to what extend the sensor signals and process parameters have deviated from their reference and preferred values.

Fuzzify inputs. Errors of the three control variables to their reference value are normalized into [-1 1] with equations (4), (5) and (6) as crisp value of fuzzy inputs. Using the example data in Table 3, error of control variable to its reference value and the normalized crisp value is given in Table 4:

Table 4 Errors and normalized values of control variables

Control variable	Reference value	On-line value	Error	Normalized value
Temperature	230	200	30	0.5403
Fz	3.6	3	0.6	0.2532
Temperature/Fz	63.89	66.67	-2.78	-0.0153
Torque/Fz	7.5	6.67	0.83	0.2402
Temperature/Torque	8.52	10	-1.48	-0.1621

Each crisp input value is then fuzzified by mapping it into the predefined fuzzy input membership functions to acquire the name and value of the membership function it falls in. Fig. 6 shows the fuzzified membership function names and value for temperature error. The fuzzy membership function names for the three crisp input values can be seen in Table 4.

Fuzzify output Using the example data in Table 3 and the normalizing algorithm, the errors of tilt angle and plunge depth to their reference values and their normalized crisp values are given in Table 5.

Table 5 Errors and normalized values of process parameters

Process parameter	Preferred value	On-line value	Error	Normalized value
Feed rate	191.41	77.613	113.897	0.8047
Spindle speed	398.56	323.91	74.650	0.7574
Tilt angle	0.55472	0.83998	-0.285	-0.1974
Plunge depth	0.17666	0.10163	0.075	0.9787

Each normalized crisp output value is fuzzified with predefined output MFs. Fig. 7 shows the fuzzifed membership function name and value of tilt angle adjustment. The fuzzified membership function names of the two outputs can be seen in Table 5.

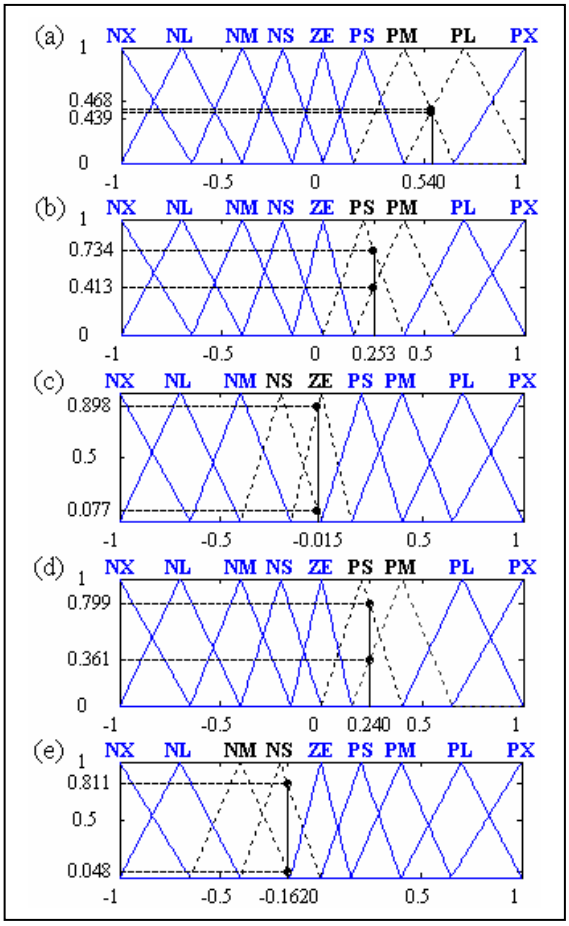

Fig. 6 Membership function name and value of fuzzified input: (a) error of temperature, (b) error of Fz, (c) error of temperature/Fz, (d) error of torque/Fz, and (e) error of temperature/torque

Rule generating. The fuzzified membership function names from previous steps for inputs and outputs are used as fuzzy rule antecedents and consequents, respectively. Fuzzy rule antecedents and consequents from the example data are shown in Table 6.

Table 6 Fuzzy rule antecedents and consequents

Fuzzy rule antecedents & consequents			Membership function
Tool/workpiece contact FLC	Antecedents	err_{Temp}	*PM, PL*
		$err_{Temp/Fz}$	*NS, ZE*
		$err_{Torq/Fz}$	*PS, PM*
	Consequents	Δ_{Tilt}	*NM, NS*
		Δ_{Plunge}	*PL, PX*
Tool/workpiece energy input FLC	Antecedents	err_{Fz}	*PS, PM*
		$err_{Temp/Torq}$	*NM, NS*
		$err_{Torq/Fz}$	*PS, PM*
	Consequents	Δ_{Feed}	*PL, PX*
		Δ_{Speed}	*PL, PX*

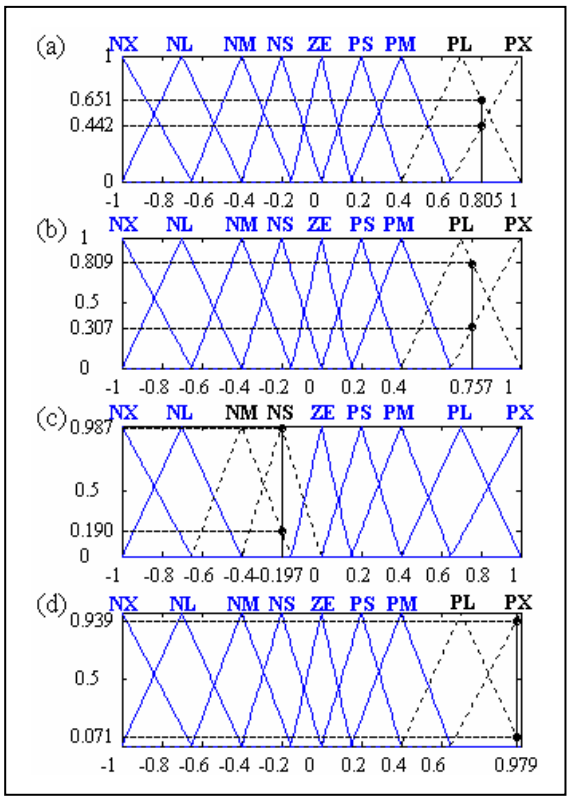

Fig 7 Membership function name and value of fuzzified outputs: (a) feed adjustment, (b) speed adjustment, (c) tilt adjustment, and (d) plunge adjustment

The on-line fuzzy rule is thus generated from the full combination of the antecedents and consequents. For this example, there are 2x2x2x2x2 = 32 fuzzy rules generated on-line for the tool/workpiece contact FLC, and 2x2x2x2x2 = 32 fuzzy rules generated on-line for the tool/workpiece energy input FLC respectively. The linguistic expression of the first fuzzy rule for the tool/workpiece contact FLC is shown as follows:

IF error of temperature is PM && error of temperature/Fz is NS && error of torque/Fz is PS,

THEN tilt angle adjustment is NM && plunge depth adjustment is PL.

The linguistic expression of the 32 fuzzy rules for the tool/workpiece energy input FLC can be seen in Appendix B.2. The first rule is listed as follows:

IF error of Fz is PS && error of temperature/torque is NM && error of torque/Fz is PS,

THEN feed rate adjustment is PL && spindle speed adjustment is PL.

With this algorithm, when each set of on-line sensor data is fed back from the welding process, the rule generation module automatically generates the on-line 'if-then' rules for fuzzy inference. The two basic FLCs are then updated with the fuzzy rules and perform fuzzy inference.

5 SIMULATION RESULTS

To test the performance and adaptability of the proposed neuro-fuzzy control scheme, a simulation model was built with MATLAB, SIMULINK, neural network and fuzzy logic toolboxes (The MathWorks, 2004d). Two examples were demonstrated: (1) 3mm flat plate with material changing from Al6061 to Al5251, and (2) 3mm thickness Al6061 alloy with curvature changing from a diameter of 70mm to flat and a diameter of 40mm. The simulation results were compared to the data recorded from experiments performed without the proposed controller. Fig. 8 shows the workpieces to be welded in the two demonstrations.

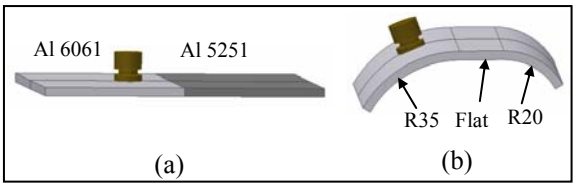

Fig.8 FSW workpieces of (a) flat plate with changing material and (b) Al 6061 plate with changing curvature.

Fig. 9 shows the comparison of feed rate and spindle speed between the neuro-fuzzy controller simulation results and preset value of flat plate weld with material changing from Al6061 to Al5251. Fig.10 shows the comparison of torque and temperature between simulation results and experimental data recorded without the proposed controller. The sample was welded with fixed process parameters: feed rate 50mm/min, spindle speed 400 rpm, tilt angle 1 ° and plunge depth 0.2 mm for both materials. The trained NN, which maps the relationship between process conditions and parameters (material, feed, speed, tilt and plunge), and sensor data (torque and temperature), were used to derive the reference value of torque (24.25 Nm) and temperature (249.56 °C).

During simulating, the same constant tilt angle and plunge depth were used, as they can be well maintained during flat plate welding. The feed rate and spindle speed were adjusted by the controller to maintain torque and temperature towards their reference value for the two materials. A trained NN, which maps the relationship between process parameters and sensor data (e.g. tilt angle, plunge depth, torque, and temperature), and material ('0' for Al 6061 and '1' for Al 5251), was used for material detecting. When the tool moved from Al 6061 to Al 5251 alloy plate, the on-line sensor data of torque and temperature, together with process parameter tilt angle and plunge depth, were used to determine what kind of material it was welding, and thus the controller was able to use the material type and on-line sensor data to perform neuro-fuzzy control.

It can be seen that with fixed process parameters, considerable decrease in torque and temperature was observed in the data of the sample welded on the old system due to a material change. However, with the neuro-fuzzy controller, torque and temperature were much better maintained towards their reference values by adjusting feed rate and spindle speed on-line, although small deviations

were still observed. This indicated that the proposed neuro-fuzzy control scheme has adaptability to material changes.

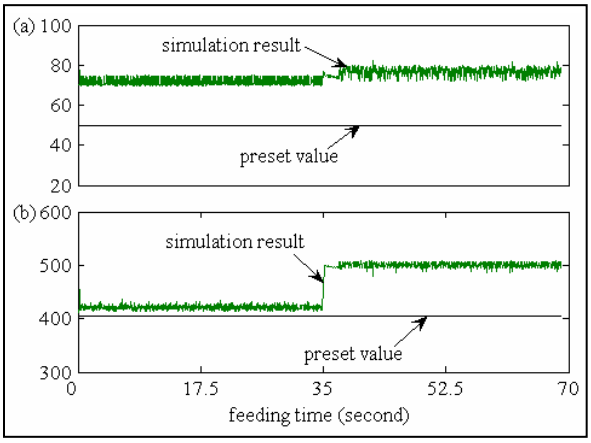

Fig. 9 Comparison of (a) feed rate (mm/min), and (b) spindle speed (rpm) between preset value and simulation results of workpieces with changing materials

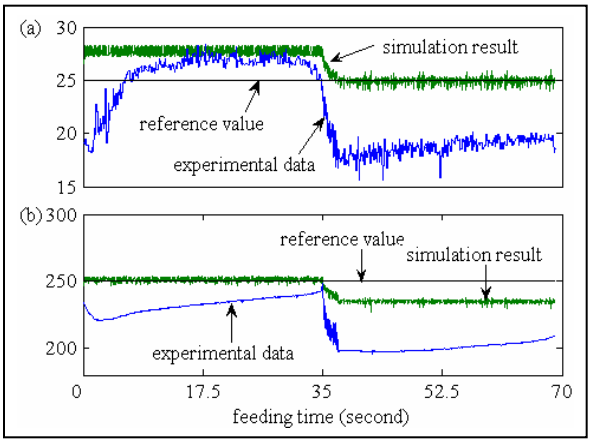

Fig. 10 Comparison of (a) torque, and (b) temperature between sample weld and simulation results of workpieces with changing materials

Fig. 11 and Fig. 12 show the comparison of process parameters and sensor data of workpiece with changing curvature between controller simulation results and experimental data respectively. The curvature of the complex shape workpiece starts with a curvature radius of 35 mm, which is connected to a flat plate and ends with a curvature radius of 20mm, as shown in Fig. 8 (b). The sample was welded with fixed process parameters: feed rate 100mm/min, spindle speed 500 rpm, tilt angle 1 ° and plunge depth 0.2 mm. The reference sensor values for torque, temperature and Fz for simulation were thus derived from the trained NN, which mapped the relationship between process conditions and parameters (curvature, feed, speed, tilt, and plunge), and sensor data (torque, temperature and Fz), as 15.08 Nm, 240.71 °C and 3.34 kN with the fixed process parameters and a curvature radius of 35 mm.

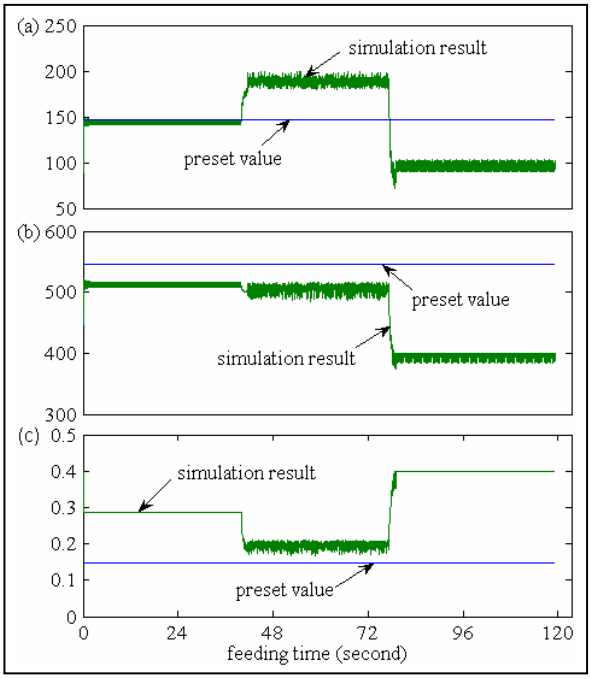

Fig. 11 Comparison of (a) feed rate (mm/min), (b) spindle speed (rpm), and (c) plunge depth (mm) between preset value and simulation results of workpiece with changing curvature

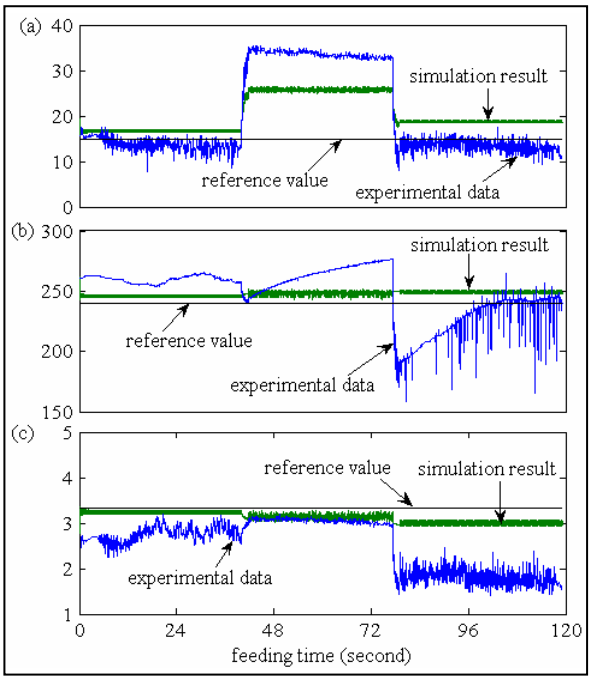

Fig. 12 Comparison of (a) torque (N.m), (b) temperature (˚C), and (c) Fz (kN) between sample weld and simulation results of workpiece with changing curvature

During simulating, the same constant tilt angle as the welded sample was used. The feed rate, spindle speed and plunge depth were adjusted by the controller to maintain torque, temperature and Fz towards their reference values. A trained NN mapping the relationship between process parameters and sensor data, and a curvature radius was used for

curvature detecting. When the tool moved from one curvature to another, on-line sensor data of torque, temperature, Fz and process parameters were used to predict the curvature being welded. The controller used the predicted workpiece curvature and on-line sensor data to perform neuro-fuzzy control.

Fig. 12 (a) to (c) show the comparison of control variables between a welded sample without the neuro-fuzzy controller and simulation results with the controller. The results show that in the data of the sample welded with fixed process parameters, large deviations of the three control variables from their reference values were observed for all the three different curvatures. It was also observed that large difference in torque, temperature and Fz existed between the three curvatures. However, with the neuro-fuzzy control scheme, torque, temperature and Fz were much better maintained towards their reference values than the welded sample by adjusting feed rate, spindle speed and plunge depth on-line. This indicated that the proposed neuro-fuzzy control scheme has good adaptability to curvature changing, and thus it is applicable for complex curvature FSW. Among the three control variables of the simulation results, temperature seems to have the least deviation from its reference value and the smallest change range; while torque shows the most deviation from its reference value and the largest change range. This suggests that sensor values are limited to different ranges for different workpiece curvatures; or in other words, for complex curvature FSW, some but not all of the control variables can be well maintained.

6 CONCLUSION

Based on the multi-axis FSW machine and telemetry sensory system, OA experiment, statistical tools and NNs were used in experimental data acquisition, sensitive feature selection and sensor fusion. OA experiments were conducted by varying process parameters (feed rate, spindle speed, tilts angle and plunge depth) and process conditions (parent material and curvature) to acquire sensor data of bending force, torque, temperature and Fz. Correlation analysis was used to select sensitive sensor features as candidates for NN training and control variables for intelligent system control. Feed-forward back-propagation NNs were trained to perform sensor fusion for process condition detecting, tool/workpiece contact and energy input monitoring. Different inputs and outputs were designed for different NNs with a specific modelling target. All the simulation results showed that the errors of NN outputs to target values were well controlled within a limited range after NN training. Using the trained NNs, the intelligent system can detect curvature and material changes during complex curvature FSW of Al 5251 and Al 6061. The trained NNs can be also used to generate on-line 'if-then' fuzzy rules.

A neuro-fuzzy control scheme integrating AIs such as NN and FLC for solving MIMO system such as FSW process was presented. The proposed neuro-fuzzy control scheme consists of several trained NNs for detecting process condition changes and deriving instant process parameters, a rule-generating module for fuzzy rule generation with the trained NNs, a basic fuzzy controller with predefined input/output membership functions to generate primary command for process parameters adjustment, and a tuning module to strengthen or weaken control actions by tuning input and output scale factors in response of the dynamic process changing. To test the performance and adaptability of the proposed neuro-fuzzy control scheme, simulations of workpiece with changing material and curvature were demonstrated. The simulation results show that the maintenance of the control variables such as torque, temperature and Fz, can be greatly improved. The simulation results also indicated that the proposed neuro-fuzzy control scheme has good adaptability to process condition (e.g. material and curvature) changes. By using different trained NNs, the proposed neuro-fuzzy control scheme also shows good flexibility to change its control variables for different requirements.

Further research on increasing NN model accuracy by investigating wider range of process condition and process parameters is needed in order to improve the performance of the proposed intelligent neuro-fuzzy control scheme for complex curvature FSW. The application of the proposed intelligent control scheme is also expected to be extended to dynamic processes other than FSW.

Acknowledgements

The authors wish to express their thanks to South African National Research Foundation for providing funding towards this research.

Reference

1 Thomas W. M., E.D. Nicholas, J.C. Needham and M.G. Murch, Temple, P. Smith and Dawes (TWI) (1991). Improvements relating to friction welding. *European Patent specification,* **0 615 480**, B1.t

2 Van Niekerk, T.I. (2001). Monitoring and diagnosis for control of an intelligent machining process. D.TECH Dissertation, Port Elizabeth Technikon.

3 Liang, S.Y., R.L. Hecker and R.G. Landers (2004). Machining process monitoring and control: the State-of-the-Art. Journal of Manufacturing Science and Engineering, **126**, 297-310.

4 Azouzi, R. and M. Guillot (1997). On-line prediction of surface finish and dimensional deviation in turning using neural network based sensor fusion. *Int. J. Mach. Tools Manufact*, **37**, 1201-1217.

5 Sasiadek, J.Z. (2002). SENSOR FUSION. Annual Reviews in Control, **26**, 203-228.

6 Guillot, M., R. Azouzi and M.C. Cote (1994). Process monitoring and control. In Artificial Neural Networks for Intelligent Manufacturing (edited by C. Dagli). Chapman and Hall, London.

7 The MathWorks (2004a). Fuzzy Logic Toolbox User's Guide. *The MathWorks Inc,* Natick, MA.

8 Liang, M., T. Yeap, A. Hermansyah and S. Rahmati (2003). Fuzzy control of spindle torque for industrial CNC machining. *International Journal of Machine Tools & Manufacture*, **43**, 1497–1508.

9 The MathWorks (2004b). Neural Network Toolbox User's Guide. *The MathWorks Inc,* Natick, MA.

10 Sun Z.Q and Z.D. Deng (1996). A fuzzy neural network and its application to controls. *Artificial intelligence in engineering*, **10**, 311-315.

11 Lau, H.C, T.T. Wong and A. Ning (2001). Incorporating machine intelligence in a parameter-based control system: a neural-fuzzy approach. *Artificial intelligence in engineering*, **15**, 253-264.

12 Blignault, C. (2002). Design, development and analysis of the friction stir welding process. *Master Thesis*, Port Elizabeth Technikon.

13 Kruger, G. (2003). Intelligent monitoring and control system for a friction stir welding process. *Master Thesis*, Port Elizabeth Technikon.

14 Ross, P.J. (1995). Taguchi Techniques for Quality Engineering. ISBN 0070539588, McGraw-Hill, 2 Edition, New York.

15 The MathWorks (2004c). MATLAB: The Language of Technical Computing, version 7.

16 Ulsoy, A. and Y. Koren (1993). Control of machining processes. Transactions ASME Journal of Dynamic Systems Measurement and Control, 115.

17 Mashimoto, M., E. Marui and S. Kato (1996). Experimental research on cutting force variation during regenerative chatter vibration in a plain milling operation. International Journal of Machine Tools and Manufacture, **36(10)**, 1073–1092.

18 Kim, T.W. and J. Yuh (2002). Application of on-line neuro-fuzzy controller to AUVs. *Information Sciences*, **145**, 169–182.